This electronic thesis or dissertation has been downloaded from the King's Research Portal at https://kclpure.kcl.ac.uk/portal/

Exploring the Exact Spectrum in Gauge/String Dualities

Levkovich-Maslyuk, Fedor

Awarding institution:
King's College London

The copyright of this thesis rests with the author and no quotation from it or information derived from it may be published without proper acknowledgement.

END USER LICENCE AGREEMENT

This work is licensed under a Creative Commons Attribution-NonCommercial-NoDerivatives 4.0 International licence. https://creativecommons.org/licenses/by-nc-nd/4.0/

You are free to:

- Share: to copy, distribute and transmit the work

Under the following conditions:

- Attribution: You must attribute the work in the manner specified by the author (but not in any way that suggests that they endorse you or your use of the work).
- Non Commercial: You may not use this work for commercial purposes.
- No Derivative Works - You may not alter, transform, or build upon this work.

Any of these conditions can be waived if you receive permission from the author. Your fair dealings and other rights are in no way affected by the above.

Take down policy

If you believe that this document breaches copyright please contact librarypure@kcl.ac.uk providing details, and we will remove access to the work immediately and investigate your claim.

Download date: 06. Nov. 2017

KING'S College LONDON

Exploring the Exact Spectrum in Gauge/String Dualities

Fedor Levkovich-Maslyuk

Department of Mathematics, King's College London,
The Strand, London WC2R 2LS, United Kingdom

Thesis supervisor Dr. Nikolay Gromov

Thesis submitted in partial fulfilment of the requirements
of the Degree of Doctor of Philosophy

April 2016

Был язык мой правдив, как спектральный анализ...

Арсений Тарковский[1]

[1] "My tongue was true, like a spectral analysis...", Arseny Tarkovsky, Russian poet (1907–1989); translation by Philip Metres and Dimitri Psurtsev.

Abstract

Understanding the dynamics of strongly coupled gauge theories is one of the greatest challenges in modern theoretical physics. A new hope in attacking this problem was brought by the surprising discovery of *integrability* in a special four-dimensional gauge theory – the $\mathcal{N} = 4$ supersymmetric Yang-Mills theory (SYM) in the limit of large number of colors. Quantum integrability manifests itself as a powerful hidden symmetry which allows to explore the theory far beyond the conventional perturbative regime, and may even lead to its exact solution. Integrability should also shed light on the striking gauge/string duality, which holographically relates $\mathcal{N} = 4$ SYM with a string theory in curved geometry.

In this thesis we focus on one of the key quantities in the $\mathcal{N} = 4$ SYM theory – its spectrum of conformal dimensions, which correspond to string state energies. The study of integrability has culminated in reformulation of the spectral problem as a compact set of Riemann-Hilbert type equations known as the Quantum Spectral Curve (QSC). We demonstrate the power of this framework by applying it to study the spectrum in a wide variety of settings. The new methods which we present allow to explore previously unreachable regimes. We first discuss an all-loop solution in a near-BPS limit, leading also to new strong coupling predictions. Next we describe an efficient numerical algorithm which allows to compute the finite-coupling spectrum with nearly unlimited precision (e.g. 60 digits in some important cases). We also present a universal analytic iterative method, which in particular allows to solve a longstanding open problem related to the BFKL limit in which $\mathcal{N} = 4$ SYM develops close links with QCD. Finally we propose the extension of the QSC to the deformed case corresponding to a cusped Wilson line, uncovering new algebraic features of the construction. This allows to systematically study the generalized quark-antiquark potential and generate numerous new results.

Acknowledgements

I am deeply grateful to my supervisor Nikolay Gromov for his invaluable guidance and mentorship. I also thank my fellow students and collaborators Grisha Sizov and Saulius Valatka for the fun and intensive work we've done together.

I thank many people at ITEP in Moscow who created an exceptional and uniquely inspiring environment, and particularly A. Gorsky, A. Losev, V. Losyakov, A. Mironov, Al. Morozov, M. Olshanetsky and A. Zotov. My gratitude also goes to many professors and researchers at Moscow State University, especially N. Goncharova, D. Levkov, A. Ovchinnikov, V. Rubakov, G. Rubtsov, S. Sibiryakov and S. Troitsky, and of course also to my classmates.

I am grateful to A. Tseytlin for his excellent guidance during my time at Imperial College London, and to M. Beccaria and G. Macorini for joint work on several projects.

And finally, for insightful and enjoyable discussions I thank M. Alfimov, B. Basso, A. Belavin, L. Bork, J. Bourdier, J. Caetano, A. Cavaglia, N. Drukker, B. Hoare, V. Kazakov, I. Kostov, A. Krikun, C. Marboe, And. Morozov, A. Petrovskij, S. Schafer-Nameki, V. Schomerus, D. Serban, A. Sfondrini, E. Sobko, A. Stepanchuk, J. Teschner, S. van Tongeren, D. Volin, K. Zarembo, A. Zayakin, Y. Zenkevich and A. Zhiboedov.

The research leading to these results has received funding from the People Programme (Marie Curie Actions) of the European Union's Seventh Framework Programme FP7/2007-2013/ under REA Grant Agreement No 317089 (GATIS). My work was also supported in part by grants RFBR-12-02-00351-a, PICS-12-02-91052, and by Russian Ministry of Science and Education under the grant 2012-1.1-12-000-1011-016 (contract number 8410).

Contents

List of Figures

List of Tables

Part I

Introduction

1 Overview

1.1 Integrability and gauge/string dualities

One of the most fascinating and difficult problems in modern theoretical physics is solving strongly interacting quantum field theories. These theories are of paramount importance in physics as they describe a wide array of phenomena ranging from condensed matter systems to interactions of elementary particles. Yet their behaviour is difficult to study outside of the weak coupling regime. In particular, it has long been the dream of many physicists to understand the behavior of quantum chromodynamics (QCD) – the part of the Standard Model of particle physics describing the strong nuclear force, which is one of the four fundamental types of interactions in our world alongside gravity, electromagnetism and the weak force. Traditional field theory methods have limited usefulness in studying QCD, as they are based on a perturbative expansion in the theory's coupling constant which in QCD is not small except at very high energies.

Some non-perturbative methods to handle strongly coupled theories were becoming available already in the 1980s, as exact solutions were found for conformal theories in two dimensions, and a number of remarkable results were obtained also in the more realistic 3 and 4 dimensional cases. More recently, other powerful approaches have been developed with guidance coming from *string theory*. While string theory may allow us to combine the Standard Model with gravity and obtain a unified description of all interactions, it also offers an entirely new perspective on the Standard Model itself. Namely, there is a hope that any conventional gauge theory should have another, completely different but *equivalent*, description as a string theory on a higher-dimensional spacetime. This type of duality is known as the AdS/CFT correspondence or gauge/string duality, and its first concrete example [1, 2, 3] was proposed in 1997, relating $\mathcal{N} = 4$ supersymmetric Yang-Mills (SYM) theory in 4d (in the planar limit when the num,ber of colors is large) with a string theory on $AdS_5 \times \mathrm{S}^5$. This duality is also called "holographic", as the 4d gauge theory may be understood as living on the four-dimensional boundary of the Anti-de Sitter space AdS_5, while string theory is defined in the bulk of the whole $AdS_5 \times \mathrm{S}^5$ manifold.

The isometries of AdS are identified with the symmetries of the 4d theory suggesting that it should be a conformal field theory (CFT), i.e. possess invariance under conformal transformations of spacetime. In addition to this already constraining symmetry, the Yang-Mills theory appearing in this example also has supersymmetry – that is, invariance under field transformations which relate bosons to fermions. Despite the high amount of symmetry, the $\mathcal{N} = 4$ SYM theory is in many ways similar to QCD and is still a highly nontrivial theory. It is therefore very remarkable that the AdS/CFT duality allows us to glimpse the behavior of this theory at strong coupling. Namely, the non-perturbative regime in the gauge theory is mapped to the weakly coupled, perturbative regime in string theory which is tractable by standard methods. Conversely, the AdS/CFT duality also sheds light on quantum gravity as modelled by string theory, as the strongly interacting string theory is described by traditional techniques in weakly coupled gauge theory.

The AdS/CFT duality remains a conjecture which has not been proven rigorously even in this most-studied example. A great body of evidence leaves little doubt for the validity of this gauge/string correspondence, but its mathematical origins remain to a large extent mysterious [4]. However, in 2002 a fascinating discovery was made [5], opening a whole new direction of research which should bring us closer to understanding the nature of AdS/CFT. This approach is based on *integrability* which was found on both sides of the duality between $\mathcal{N} = 4$ SYM and superstring theory on $AdS_5 \times S^5$ (for a review see [6]). Integrable systems have been known in mathematics for a long time[2], and are characterized by the presence of a complete set of conservation laws/symmetries whose presence leads to the exact solution of the model (see e.g. [7]). In quantum field theories integrability was observed for various models (CFTs, sigma models, sine-Gordon theory, ...) defined in two dimensions, and later in supersymmetry-protected sectors of higher dimensional gauge theories [8, 9, 10]. In fact after appropriate gauge fixing the string action defines an 2d integrable theory on the worldsheet, to solve which one can apply (modulo various complications of course) the well-developed methods based on the S-matrix bootstrap, similarly to solutions of such renowned 2d models as the sine-Gordon theory. What is truly remarkable is that this rather conventional integrability on the string side translates, via AdS/CFT, into integrability on the gauge theory side – providing a rare case of integrable structures in four, instead of two, spacetime dimensions. The emergence of integrability for a full, non-protected set of observables in a 4d theory – even if only in the large N_c limit – was a completely novel phenomenon and gives a hope to reach, for the first time

[2]Best-known examples are models in classical mechanics such as the Kepler problem or spinning tops, and integrable PDEs such as the Korteveg-de Vries equation.

ever, the complete solution of an interacting 4d gauge theory.

Integrability is also one of the very few methods which allow to verify and test the AdS/CFT correspondence on a non-perturbative level. An extra interest in the subject stems from the fact that the integrable system arising here is of a novel type, in particular the corresponding R-matrix has nontrivial branch points and is related to a new type of quantum group.

As $\mathcal{N} = 4$ SYM is a conformal theory, a key observable to study is the spectrum of conformal dimensions, which on the string theory side corresponds to string energy levels. Integrability has proven to be especially powerful in application to the spectral problem, and more than a decade's efforts have led to a strikingly simple set of equations which are expected to describe the full spectrum (for local operators) at any coupling. These equations are known as the Quantum Spectral Curve (QSC) and are based on deep algebraic structures such as the QQ-relations. As the QSC encodes the exact Q-functions of the model which are linked to wavefunctions in separated variables, it is also expected to have applications for computing 3-point correlation functions in addition to the spectrum.

The main focus of the work presented in this thesis is exploring the spectrum using this novel Quantum Spectral Curve framework. We will see the QSC in action in a wide variety of settings, uncovering key features of solutions to the QSC equations in different regimes and obtaining valuable data for the spectrum at the same time. The applications range from exceptionally precise numerical calculations to high-order analytic expansions and several all-loop results. We will show how using this approach it is possible to attack several previously untractable problems, including next-to-next-to-leading order calculations in the BFKL limit which links the $\mathcal{N}$=4 theory to realistic QCD. In addition, while the original QSC describes local operators, we will show how to extend it to a cusped Wilson line setup. This opens the way to deeply study another important observable – the generalized quark-antiquark potential, for which we will be able to obtain numerous new results as well as uncovering surprising new structures in the QSC. All these solutions also allow us to obtain Q-functions in different regimes, which we hope will help to develop applications of the QSC to computation of 3-point correlators.

1.2 Thesis structure

The results described in this thesis were originally presented in six of my papers (with co-authors) which are listed in the next section. The thesis contains eight parts: the

first part provides an introduction and overview, in parts II - VII the main results are presented, and the final part contains conclusions and appendices with technical details. A more detailed summary of the content is given below.

- **Part I**

  In this introductory part we first give an overview of gauge/string dualities and the appearance of integrability in this context. We present the structure of the thesis and list the author's publications. Then we discuss in more detail the $\mathcal{N} = 4$ SYM theory and the dual string theory and describe the historical development of the integrability program. We also specifically focus on the key Quantum Spectral Curve (QSC) framework, which is the basis for most of the results presented in the thesis.

- **Part II**

  In this part we describe the solution of the QSC at any coupling in the small spin limit. We compute the first two orders of the near-BPS expansion to all loops and show that this data also provides new strong coupling predictions for much-studied observables such as the Konishi anomalous dimension and the BFKL intercept.

- **Part III**

  Here we present a highly efficient numerical algorithm for solving the QSC for an arbitrary state/operator. It allows to generate extremely precise data for the non-perturbative spectrum at finite coupling. Moreover we show how to implement analytic continuation in the spin away from integer values, and deeply explore the rich analytic structure of the spectrum for twist two operators.

- **Part IV**

  We present in this part a new analytic iterative method for solving the QSC perturbatively, which by now has found many diverse applications. We show that in particular it allows to compute for the first time the NNLO correction to the BFKL eigenvalue, resolving a longstanding problem open for more than 10 years. The regime we study resums all orders of usual perturbation theory. We verify the result with 60 digits precision using the numerical method discussed in part III. We also achieve a further simplification of the QSC by eliminating several auxiliary functions.

- **Part V**

  Having discussed the spectrum of local operators, in the parts V-VII we switch

to the generalized cusp anomalous dimension, associated to a cusped Wilson line. In this part we present the analytic solution of the TBA equations (which are the predecessor of the QSC) to all loops in a near-BPS limit. The calculation reproduces localization-based predictions and reveals a curious matrix model structure of the result. It also provides guidance for extending the QSC to this case.

- **Part VI**

  In this part we propose the Quantum Spectral Curve formulation for the angle-dependent cusp anomalous dimension at all values of the parameters and the coupling. This opens the way to study this observable systematically and apply the powerful methods developed for local operators. The proposal is checked extensively and leads to new analytic as well as numerical predictions. In particular, we analytically compute the next term in the near-BPS expansion to all loops.

- **Part VII**

  Here we show that the QSC proposed in the previous part leads to a finite closed set of equations for the flat space quark-antiquark potential – a key observable in AdS/CFT which is nearly inaccessible by previous integrability-based methods. It corresponds to a singular limit in which the QSC develops qualitatively new features. We calculate the first 7 nontrivial orders of the weak coupling expansion, going far beyond the reach of other methods. We also compute the potential numerically in a wide range of the coupling, reproducing the celebrated string theory results with high accuracy. Finally we demonstrate how the Schrodinger equation resumming all ladder diagrams in a double scaling limit is encoded in the QSC.

- **Part VIII**

  We present concluding remarks and discuss directions for future research. This part also contains appendices which supplement the main text.

1.3 The author's publication list

A list of all my publications is given below. The papers (1)–(6) form the basis for this thesis. The papers (7)–(11) are on closely related subjects, while papers (12), (13) are on completely different topics. In the bibliography these papers are listed as [11] – [23].

(1) N. Gromov and F. Levkovich-Maslyuk, "Quark–anti-quark potential in $\mathcal{N} = 4$ SYM," arXiv:1601.05679 [hep-th].

(2) N. Gromov and F. Levkovich-Maslyuk, "Quantum Spectral Curve for a Cusped Wilson Line in $\mathcal{N} = 4$ SYM,"

arXiv:1510.02098 [hep-th] (to appear in JHEP).

(3) N. Gromov, F. Levkovich-Maslyuk and G. Sizov, "Pomeron Eigenvalue at Three Loops in $\mathcal{N} = 4$ Supersymmetric Yang-Mills Theory,"

Phys. Rev. Lett. **115** (2015) 25, 251601 [arXiv:1507.04010 [hep-th]].

(4) N. Gromov, F. Levkovich-Maslyuk and G. Sizov, "Quantum Spectral Curve and the Numerical Solution of the Spectral Problem in AdS5/CFT4,"

arXiv:1504.06640 [hep-th].

(5) N. Gromov, F. Levkovich-Maslyuk, G. Sizov and S. Valatka, "Quantum spectral curve at work: from small spin to strong coupling in $\mathcal{N} = 4$ SYM,"

JHEP **1407** (2014) 156 [arXiv:1402.0871 [hep-th]].

(6) N. Gromov, F. Levkovich-Maslyuk and G. Sizov, "Analytic Solution of Bremsstrahlung TBA II: Turning on the Sphere Angle,"

JHEP **1310** (2013) 036 [arXiv:1305.1944 [hep-th]].

(7) M. Beccaria, F. Levkovich-Maslyuk, G. Macorini and A. A. Tseytlin, "Quantum corrections to spinning superstrings in $AdS_3 \times S^3 \times M^4$: determining the dressing phase,"

JHEP **1304** (2013) 006 [arXiv:1211.6090 [hep-th]].

(8) F. Levkovich-Maslyuk, "Numerical results for the exact spectrum of planar AdS4/CFT3,"

JHEP **1205** (2012) 142 [arXiv:1110.5869 [hep-th]].

(9) M. Beccaria, F. Levkovich-Maslyuk and G. Macorini, "On wrapping corrections to GKP-like operators,"

JHEP **1103** (2011) 001 [arXiv:1012.2054 [hep-th]].

(10) N. Gromov and F. Levkovich-Maslyuk, "Y-system and β-deformed $\mathcal{N} = 4$ Super-Yang-Mills,"

J. Phys. A **44** (2011) 015402 [arXiv:1006.5438 [hep-th]].

(11) N. Gromov and F. Levkovich-Maslyuk, "Y-system, TBA and Quasi-Classical strings in AdS(4) x CP3,"

JHEP **1006** (2010) 088 [arXiv:0912.4911 [hep-th]].

(12) N. Tulyakov, F. Levkovich-Maslyuk, V. Samoilov, "Analytical Calculation of Atom Ejection from the Ni (111), Ni (001), and Au (001) Surfaces in Frames of a Three-Dimensional Model",

Journal of Surface Investigation. X-ray, Synchrotron and Neutron Techniques, 2011, Vol. **5**, p. 335.

(13) F. Levkovich-Maslyuk, "Two destructive effects of decoherence on Bell inequality violation",

Phys. Rev. A **79**, 054101 (2009) [arXiv:0812.3736 [quant-ph]]

Let us also mention that in part II we mostly present results from paper (5), in part III from paper (4), in part IV from paper (3), in part V from paper (6), in part VI from paper (2), and in part VII from paper (1).

1.4 Frequently used notation

For the reader's convenience we present here some frequently used notation.

- The coupling constant of planar $\mathcal{N}=4$ SYM is defined as

$$g = \frac{\sqrt{\lambda}}{4\pi}, \tag{1.1}$$

  where $\lambda = g_{YM}^2 N_c$ is the 't Hooft coupling (with $N_c \to \infty$).

- For a function $f(u)$ we denote

$$f^{\pm} = f\left(u \pm \frac{i}{2}\right) \quad f^{[n]} = f\left(u + \frac{in}{2}\right) \tag{1.2}$$

- We widely use the Zhukovsky variable $x(u)$ defined by

$$x + \frac{1}{x} = \frac{u}{g}, \tag{1.3}$$

  choosing the solution with $|x| > 1$ (in part V we use another solution in some cases, which is discussed explicitly). This parameterisation resolves the branch cut $u \in [-2g, 2g]$ which many functions discussed below have.

2 $\mathcal{N} = 4$ super Yang-Mills and strings on $AdS_5 \times \mathrm{S}^5$

In this section we will describe both sides of the AdS/CFT duality discussed above, and make more precise their relation with each other.

On the gauge theory side we have $\mathcal{N} = 4$ SYM with gauge group $SU(N_c)$ which is the maximally supersymmetric gauge theory in 4d (for a review see [24]). Its field content is a non-abelian gauge field A_μ, six real scalars Φ_a $(a = 1, \ldots, 6)$ and fermionic fields $\psi_\alpha, \psi_{\dot{\alpha}}$. All fields are in the adjoint representation of the gauge group. The action reads

$$S = \frac{1}{2g_{YM}^2} \int d^4x \mathrm{Tr} \left[-\frac{1}{2} (F_{\mu\nu})^2 + D_\mu \Phi_a D^\mu \Phi^a - \sum_{a<b} [\Phi_a, \Phi_b]^2 + fermions \right] \tag{2.1}$$

The beta function for the coupling is zero and this theory is conformally invariant at the quantum level [25], with the corresponding symmetry group being $SO(4, 2)$. There is also an $SU(4)$ R-symmetry, under which the fermions transform in the (anti)fundamental representation, and the scalars in the 6-dimensional irrep. Together with supersymmetry transformations, the global symmetries of the theory form the supergroup $PSU(2, 2|4)$.

We will be interested in the planar limit when the number of colors N_c goes to infinity while the combination

$$\lambda = g_{YM}^2 N_c, \tag{2.2}$$

which is known as the 't Hooft coupling, stays fixed. While this limit may seem an extra complication it in fact offers a great simplification, with reduction of the number of relevant Feynman diagrams and most importantly the emergence of integrability.

Let us now turn to the string side of the duality, which is type IIB superstring theory on the $AdS_5 \times \mathrm{S}^5$ space. A useful formulation of this theory which highlights the symmetries is the sigma model action [26] (for a discussion and review see [27, 28]). This Metsaev-Tseytlin action can be written as

$$S = \frac{\sqrt{\lambda}}{4\pi} \int \mathrm{STr} \left(J^{(2)} \wedge *J^{(2)} - J^{(1)} \wedge J^{(3)} \right) \tag{2.3}$$

where J is the current constructed from the supergroup element $g \in PSU(2, 2|4)$ as

$$J = -g^{-1} dg = \sum_{i=1}^{4} J^{(i)}. \tag{2.4}$$

The action is written in terms of the components $J^{(i)}$ which give the decomposition of the current under the $\mathbb{Z}_4$ grading which is important for integrability.

The global symmetry of this action is given by the supergroup $PSU(2, 2|4)$, matching the symmetries of $\mathcal{N} = 4$ SYM. The parameter λ which defines the string tension in the action is identified with gauge theory 't Hooft coupling. This already shows the weak/strong

nature of the AdS/CFT correspondence: the gauge theory perturbative regime of small λ is mapped to the highly interacting regime in the string theory. Conversely, the semiclassical and tractable regime of large λ on the string side is mapped to the fully quantum gauge theory.

Let us mention that the string coupling constant is set to zero (in the limit $N_c \to \infty$), so the action (2.3) describes the propagation of a single string whose worldsheet is a cylinder, but of course the model is still highly nontrivial as the string is moving in a curved space. The AdS/CFT duality is conjectured to extend for the finite N_c case as well with $g_s \sim \lambda/N_c$. We will always discuss the large N_c regime.

The main statement of AdS/CFT is that gauge theory observables are directly related to those of string theory. A particularly important class of observables are the scaling dimensions $\Delta(\lambda)$ of local gauge-invariant single trace operators in gauge theory,

$$\mathcal{O}(x) = \mathrm{Tr}(\Phi_1(x)\Phi_2(x)\dots). \tag{2.5}$$

The scaling dimensions are very nontrivial functions of λ which determine the form of 2-point correlators

$$\langle \mathcal{O}(x)\bar{\mathcal{O}}(y)\rangle = \frac{1}{|x-y|^{2\Delta}} \tag{2.6}$$

and also fix the coordinate dependence of 3-point functions

$$\langle \mathcal{O}_1(x)\mathcal{O}_2(y)\mathcal{O}_3(z)\rangle = \frac{C_{123}}{|x-y|^{\Delta_1+\Delta_2-\Delta_3}|x-z|^{\Delta_1+\Delta_3-\Delta_2}|y-z|^{\Delta_2+\Delta_3-\Delta_1}} \tag{2.7}$$

(here the coefficients C_{123} are called the 3-point structure constants). The conformal dimensions are conjectured to be equal to the energies of string states, i.e. their Noether charge E with respect to translations in the AdS global time. In the commonly used lightcone gauge [28] this AdS energy is also simply related to the worldsheet energy of the state,

$$E_{ws} = E - J \tag{2.8}$$

where J is one of the R-charges. Thus the problem of computing scaling dimensions in gauge theory is reformulated as computing the worldsheet spectrum in finite volume for a nontrivial sigma model.

3 Integrable structures in AdS/CFT

In this section we will summarize the development of integrability methods in gauge/string dualities.

Exploration of integrability started with the discovery that the dilatation operator in $\mathcal{N} = 4$ SYM, whose eigenvalues are the scaling dimensions, coincides at 1 loop in the scalar sector with the Hamiltonian of an integrable spin chain [5]. This nearest-neighbor spin chain is solvable by beautiful Bethe ansatz techniques (see [24] for an introduction) providing immediate access to the spectrum. Integrability was later extended to more generic sectors and to higher orders in the 't Hooft coupling.

On the string side, classical integrability stems from the construction of a connection which is flat on equations of motion and includes an additional complex variable called the spectral parameter [29, 30]. The monodromy of this flat connection around the worldsheet then generates infinitely many conserved charges when expanded as a series in the spectral parameter. This construction is typical for sigma models on coset spaces. All the conserved charges are encoded in the classical spectral curve of the theory [30] which also provides a framework to compute 1-loop quantum corrections [31].

While integrable structures on the gauge theory side played a crucial role in the subject, the complete all-loop solution for the spectrum was guided mostly by logic originating from the string side of the duality. The reason for this is that after appropriate lightcone gauge-fixing, the string action defines the worldsheet model which is a 2d integrable field theory solvable by the bootstrap and related methods, which have been extensively developed for simpler models like the sine-Gordon or principal chiral field models. These methods were adapted to conjecture the exact S-matrix for string excitations as reviewed in [32]. Its structure is to a large extent fixed by the Yang-Baxter equation, although an overall prefactor called the dressing phase required a special effort to determine [33]. An important complication compared to more conventional models is that the dispersion relation for excitations is non-relativistic.

These developments finally led to the asymptotic Bethe ansatz (ABA) equations at any coupling that were formulated in [34]. They descibe the exact spectrum for operators containing an asymptotically large number of fields, and interpolate between the gauge and string theory predictions. The number of fields L in the operator corresponds to the spatial volume in which the 1+1 dimensional worldsheet theory is defined. Thus as usual in massive integrable QFTs, the ABA does not capture the corrections to the energy which are exponentially small in the volume L.

More precisely, for length L operators the ABA equations describe the spectrum up to order g^{2L}, and they miss finite-size wrapping corrections that appear at higher orders [35, 36]. At first several orders these effects can be studied using Luscher formulas. To

fully take into account the wrapping effects, it was necessary to apply the Thermodynamic Bethe ansatz (TBA) approach in which the energy levels of an integrable QFT in finite volume are related to the asymptotic spectrum [37]. This led to the formulation of an infinite set of functional Y-system relations [38] or integral TBA equations [39, 40, 41] that are expected to capture the full spectrum with all finite-size contributions. Schematically, the TBA equations have the following form:

$$\log Y_{as}(u) = \Phi_{as}(u) + \sum_{a',s'} \int_{-\infty}^{\infty} dv K_{as}^{a's'}(u,v) \log(1 + Y_{a's'}(v)) \tag{3.1}$$

where $Y_{as}(u)$ are the unknown functions while $K_{as}^{a's'}$ and Φ_{as} are known explicitly. The indices (a, s) of the Y-functions belong to a T-shaped domain of the integer lattice. Once these equations are solved the energy can be extracted from the Y-functions. One of the problems of this approach is that the explicit form of the equations requires case-by-case study and is not known in general except for a few explicit examples such as Konishi [42, 43]. They, however, allowed for a detailed numerical study of these simplest operators [42, 44, 45, 46] and led to a prediction for string theory which was confirmed in [47, 48, 49].

While the TBA can be reliably applied only to a certain subset of states, the Y-system equations are universal and have algebraic origins[3]. Their relation with the Hirota bilinear equations allowed to get a set of extra conditions that impose on the Y-functions correct analyticity properties dictated by TBA [50]. These developments led to a reduction of the spectral equations to a finite set of nonlinear integral equations (FiNLIE) [51]. Finally, an immense simplification of the spectral problem was achieved in [52] (see full details in [53]) with the reformulation of TBA as Quantum Spectral Curve (QSC) equations. These are a finite set of equations of Riemann-Hilbert type, which in contrast to FiNLIE have a transparent analytic structure and are deeply connected with the $PSU(2,2|4)$ symmetry of the problem. The QSC equations provide perhaps the ultimate solution of the spectral problem, and are expected to apply for arbitrary operators/string states. In addition, in this framework the finite-zize corrections and the asymptotic part of the spectrum are treated on equal footing. In fact, these equations capture not only the spectrum but also the exact Q-functions of the model, which should correspond to wavefunctions in Sklyanin's separated variables [54, 194]. As 3-point correlators are closely related to overlaps of wavefunctions, it is widely believed the QSC should play an important role in computing various correlators as well. In the next subsection we will describe the QSC in

[3]However, analyticity properties of Y-functions may differ from state to state, thus it is still highly difficult to single out the physical solutions for generic states

more detail.

Integrability is also being developed for other observables, such as correlation functions and scattering amplitudes though a complete and simple description for these quantities is yet to be found (for recent advances see e.g. [55, 56], [57], [58]). In addition, following the success of integrability in the most studied duality, other integrable cases of AdS/CFT have been found. Some of them are deformations of the original theory [59, 203, 204, 60], while others concern dualities in different number of dimensions, such as the by now well-studied ABJM theory [61], or AdS_3/CFT_2 (see the review [62]) where a lot of open questions still remain. Let us also mention that one can consider not just the local operators but also highly interesting boundary problems related e.g. to Wilson lines with insertions, where integrability methods are powerful as well (see in particular [63, 64, 65]).

4 The Quantum Spectral Curve of AdS/CFT

The Quantum Spectral Curve equations are the central object discussed in this thesis. In this section we will give an overview of the QSC framework.

4.1 Motivation and the XXX chain

Let us first discuss some general features of the construction and provide motivation for it. As stated above, the QSC for states in some subsector can be derived from the Thermodynamic Bethe Anstaz, but in general stands as a conjecture motivated by compelling arguments and a multitude of tests. Impressive confirmations of the correctness of the proposed QSC equations were supplied already in the original papers [52, 53]. In particular it was shown that the QSC encodes the all-loop asymptotic Bethe ansatz equations which have played a seminal role in the development of AdS/CFT integrability.

The name "Quantum Spectral Curve" suggests that the construction may be viewed as a quantum version of the classical spectral curve. Indeed, as shown in [53], in the classical limit it reduces to the classical AdS/CFT spectral curve. Moreover, in general it is known at least for some examples (such as the XXX chain) that from the characteristic equation defining the classical spectral curve one can obtain (promoting the spectral parameter and the eigenvalue to operators) functional equations describing the corresponding quantum integrable model (see e.g. [66] and references therein). These take the form of difference equations on Q-functions of the model, which can be usually written in the form of

canonical QQ-relations. The set of these equations is thus sometimes called the quantum spectral curve of the model. In AdS/CFT due to various complications this quantization program has not been carried out directly, but the equations of the QSC are indeed precisely the QQ-relations (supplemented with additional constraints), which is another reason for giving the construction this name[4].

The QQ-relations can be easily illustrated on the example of the $SU(2)$ XXX Heisenberg quantum spin chain. This quantum integrable model is defined by the Hamiltonian

$$\hat{H} = \frac{1}{2}\sum_{k=1}^{L}\left(1 - \hat{P}_{k,k+1}\right) \tag{4.1}$$

acting on the tensor product of L copies of $\mathbb{C}^2$. Here $\hat{P}_{k,k+1}$ is the permutation operator acting on the product of the k-th and $(k+1)$-th site (and $k = L+1$ is identified with $k = 1$). This system can be solved by Bethe ansatz techniques which lead to equations for the Bethe roots u_j,

$$\left(\frac{u_j + i/2}{u_j - i/2}\right)^L = -\prod_{k=1}^{N}\frac{u_j - u_k + i}{u_j - u_k - i}\ ,\ j = 1, \dots, N\ . \tag{4.2}$$

In terms of solutions to these equations, the energy levels of the Hamiltonian are given by

$$E = \sum_{j=1}^{N}\frac{1}{u_j^2 + 1/4}\ . \tag{4.3}$$

We see that the Bethe roots are key quantities which encode the spectrum of the Hamiltonian. It is convenient to assemble the roots into the Baxter Q-function $Q_1(u)$ defined as

$$Q_1(u) = \prod_{k=1}^{N}(u - u_k) \tag{4.4}$$

Remarkably, the Bethe ansatz equations (4.2) can be obtained from a simple functional equation on $Q_1(u)$. Namely, we require that there exists another polynomial $Q_2(u)$ such that

$$Q_1(u + i/2)Q_2(u - i/2) - Q_1(u - i/2)Q_2(u + i/2) = u^L\ . \tag{4.5}$$

This equation is known as the QQ-relation for this simple model. Now let us instead start from this QQ-relation and *define* the parameters u_k as zeros of $Q_1(u)$. Then using (4.5) evaluated at $u = u_j + i/2$ and $u = u_j - i/2$ we see that Q_2 drops out and we find

$$\left(\frac{u_j + i/2}{u_j - i/2}\right)^L = -\frac{Q_1(u_j + i)}{Q_1(u_j - i)} \tag{4.6}$$

[4] A quantization of the classical curve in one or another sense also arises in other contexts, e.g. in relation to topological recursion in matrix models [67, 68].

which are precisely the Bethe equations (4.2)! Thus solely from the QQ-relation (supplemented by the condition that Q_1, Q_2 are polynomials) we have obtained the key Bethe ansatz equations, which determine the spectrum via (4.3).[5] In fact one can derive the same Bethe equations for the roots of $Q_2(u)$. They are known as dual Bethe roots and give an equivalent description of the same energy levels. To write the QQ-relation in a more canonical form let us introduce

$$Q_{12}(u) = u^L, \quad Q_{\emptyset}(u) = 1 \tag{4.7}$$

then we have

$$Q_1(u+i/2)Q_2(u-i/2) - Q_1(u-i/2)Q_2(u+i/2) = Q_{12}(u)Q_{\emptyset}(u) \ . \tag{4.8}$$

This is the standard bilinear form of the QQ-relation for models with $SU(2)$ symmetry. For integrable systems with higher rank symmetries one introduces more Q-functions, which for spin chains encode Bethe roots on different levels of the nested Bethe ansatz. The QQ-relations are then bilinear equations similar to those above, and their structure is dictated by the symmetry group.

4.2 The QSC for gauge/string duality: equations and analyticity

As the spectral problem in AdS/CFT is expected to give rise to a quantum integrable system, we should also have a set of Q-functions satisfying the canonical QQ-relations based on $PSU(2,2|4)$ symmetry. In general the Q-system of $\mathcal{N}=4$ SYM is composed of 2^8 Q-functions. They are labelled as $Q_{a_1,\ldots,a_k|b_1,\ldots,b_n}$ where k and n range from 1 to 4, and each of the indices a_i, b_j takes values from 1 to 4 as well. In other words, we have Q-functions with up to eight indices in total, some examples being $Q_{a_1|b_1}$, $Q_{a_1a_2|\emptyset}$, $Q_{a_1a_2a_3a_4|b_1b_2}$. The indices a_i are often called "bosonic" while b_i are called "fermionic". The Q-functions are moreover antisymmetric in all the a indices and in all the b indices. In this notation the QQ-relations have the following form:

$$Q_{A|I}Q_{Aab|I} = Q^+_{Aa|I}Q^-_{Ab|I} - Q^+_{Ab|I}Q^-_{Aa|I} \tag{4.9}$$

$$Q_{A|I}Q_{A|Iij} = Q^+_{A|Ii}Q^-_{A|Ij} - Q^+_{A|Ij}Q^-_{A|Ii} \tag{4.10}$$

$$Q_{Aa|I}Q_{A|Ii} = Q^+_{Aa|Ii}Q^-_{A|I} - Q^+_{A|I}Q^-_{Aa|Ii} \tag{4.11}$$

[5] The formula for the energy (4.3) is an extra input which supplements the QQ-relation in this case, but there are many models, including AdS/CFT, where such extra information is not needed, instead one specifies how the energy is encoded in the asymptotics of Q-functions.

Here A and I stand for some sets of indices. We see that the $SU(2)$ QQ-relation (4.8) is just a particular case of (4.9) with $A = I = \emptyset$, $a = 1$, $b = 2$. The Q-functions can be neatly assembled into a Hasse diagram (see [53] and references therein) where each node corresponds to a Q-function and each face with four vertices corresponds to a QQ-relation, see Fig. 4.2.

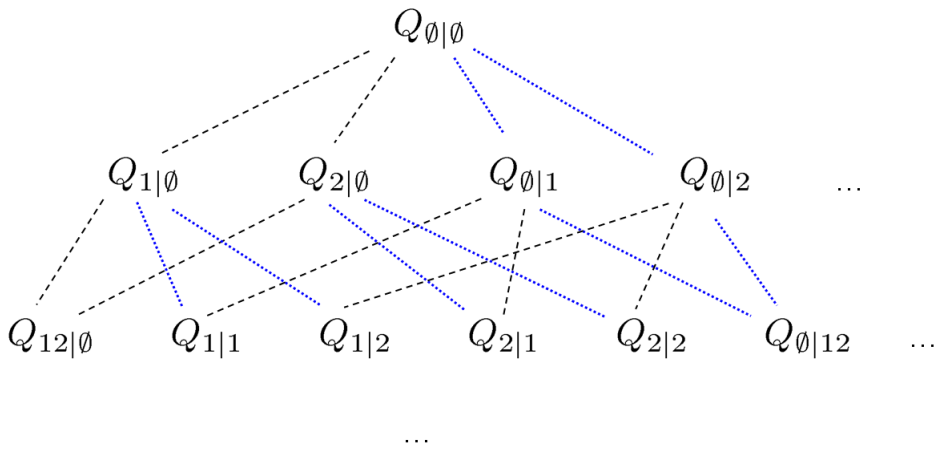

Figure 1: A part of the Hasse diagram describing the Q-system for the $PSU(2,2|4)$ group. Each black dashed link corresponds to adding a "bosonic" index, and each blue dotted link to adding a "fermionic" index. Rectangular facets in the diagram correspond to QQ-relations, e.g. the facet containing $Q_{\emptyset|\emptyset}, Q_{1|\emptyset}, Q_{2|\emptyset}$ and $Q_{12|\emptyset}$ gives rise to the QQ-relation (4.8). The part of the diagram shown here corresponds to an $SU(2|2)$ subgroup inside the whole symmetry group.

For spin chains the QQ-relations together with requiring polynomiality of the Q-functions essentially lead to the solution of the model. However the main complication in the AdS/CFT integrable system is that the Q-functions are not polynomials, instead they have a complicated analytic structure with branch points whose position depends on the 't Hooft coupling. However we still require the Q-functions to be free of any singularities except these branch points. The branch points are inherited from the dispersion relation of the excitations, which is written in terms of the Zhukovsky variable $x(u)$ defined by

$$x + \frac{1}{x} = \frac{u}{g} \,, \tag{4.12}$$

where we take the solution with $|x| > 1$ and we introduced

$$g = \frac{\sqrt{\lambda}}{4\pi} \tag{4.13}$$

where λ is the 't Hooft coupling. Then using also the notation

$$f^{\pm} \equiv f(u \pm i/2), \quad f^{[+a]} \equiv f(u + ia/2) \tag{4.14}$$

we can parameterize the energy and momentum of excitations as

$$e^{ip} = \frac{x^+}{x^-}, \quad E = 2ig\left(\frac{1}{x^+} - \frac{1}{x^-}\right) . \tag{4.15}$$

We see that as functions of the spectral parameter u, the energy and momentum have branch points at the ends of the cut $[-2g \pm i/2, 2g \pm i/2]$. Similar branch cuts are also present in the S-matrix of the theory and eventually appear in the Q-functions. In the limit when λ is small the system reduces to the usual $\mathfrak{psu}(2,2|4)$ Heisenberg spin chain.

Because of the branch points, the QQ-relations should be supplemented by extra analyticity conditions which are the key element of the construction. Let us descrbe all the QSC equations in detail (we also refer the reader to [53] where the QSC is covered in full depth).

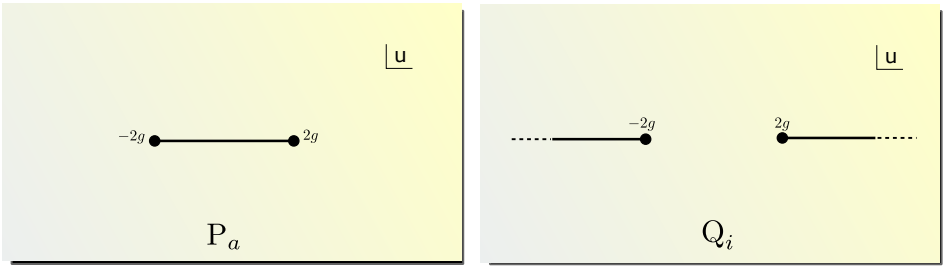

Figure 2: $\mathbf{P}_a$ and $\mathbf{Q}_i$ have one cut on the real axis in the representations with short and long cuts respectively. The ellipse shows the region of convergence of the series (4.19)

Importantly, the algebraic relations between the Q-functions allow one to choose a much smaller subset, which will be complete in the sense that the rest of Q-functions can be generated from the selected ones algebraically. A convenient choice for such a subset consists of $4+4$ functions $\mathbf{P}_a(u)$ and $\mathbf{Q}_i(u)$ $(a, i = 1, \ldots, 4)$. One can say that $\mathbf{P}_a$ describe the S^5 degrees of freedom whereas $\mathbf{Q}_i$ correspond to the AdS_5 part. In the notation of (4.9) they correspond to $\mathbf{P}_a = Q_{a|\emptyset}$, $\mathbf{Q}_i = Q_{\emptyset|i}$. A particularly nice property of $\mathbf{P}$'s is that they have only two branch points at $\pm 2g$ when they are connected by a "short" cut $[-2g; 2g]$ (see Fig. 4.2). This means that there are more branch points on the next sheet, but for this choice of the cut they do not appear on the first sheet. As most Q-functions have infinitely many cuts, the fact that on some Riemann sheet the $\mathbf{P}_a$ have only one cut is far from trivial and can be viewed as somewhat miraculous. Very similarly $\mathbf{Q}$'s have

only two branch point on the main sheet if the cut is taken to go through infinity. In a sense this reflects the non-compactness of the AdS_5 part of the space.

Whereas the coupling determines the position of the branch points, the quantum numbers of the state are specified through the large u asymptotics of Q-functions. The $\mathbf{P}_a$ encode the compact bosonic subgroup $SO(6)$ quantum numbers (J_1, J_2, J_3), while $\mathbf{Q}_i$ gives the $SO(4,2)$ charges (Δ, S_1, S_2), which include the conformal dimension of the state Δ. Explicitly

$$\mathbf{P}_a \sim A_a u^{-\tilde{M}_a}, \quad \mathbf{Q}_i \sim B_i u^{\hat{M}_i - 1}, \ \mathbf{P}^a \sim A^a u^{\tilde{M}_a - 1}, \ \mathbf{Q}^i \sim B^i u^{-\hat{M}_i} \tag{4.16}$$

where

$$\tilde{M}_a = \left\{ \frac{J_1 + J_2 - J_3 + 2}{2}, \frac{J_1 - J_2 + J_3}{2}, \frac{-J_1 + J_2 + J_3 + 2}{2}, \frac{-J_1 - J_2 - J_3}{2} \right\} , \tag{4.17}$$

$$\hat{M}_i = \left\{ \frac{\Delta - S_1 - S_2 + 2}{2}, \frac{\Delta + S_1 + S_2}{2}, \frac{-\Delta - S_1 + S_2 + 2}{2}, \frac{-\Delta + S_1 - S_2}{2} \right\} . \tag{4.18}$$

Note that often the $\mathbf{P}_a$ are easier to deal with, as they can be expressed as a series in the Zhukovsky variable $x(u)$,

$$\mathbf{P}_a(u) = \sum_{n=\tilde{M}_a}^{\infty} \frac{c_{a,n}}{x^n(u)} . \tag{4.19}$$

This series is convergent everywhere on the upper sheet and also in an elliptic region around the cut on the next sheet (see Fig. 4.2). A similar parametrization for $\mathbf{Q}_a$ will not cover even the upper sheet. Fortunately, in the whole set of 2^8 Q-functions there are other 4 functions with one single cut, which are denoted as $\mathbf{P}^a(u)$, $a = 1, \ldots, 4$. Together with $\mathbf{P}_a(u)$ they also form a complete set of Q-functions. In particular, one can reconstruct $\mathbf{Q}_i$ from them. The procedure for this, which will be important in many applications discussed below, is the following:

- Find a set of 16 functions $\mathcal{Q}_{a|i}$, satisfying

$$\mathcal{Q}_{a|i}(u + \tfrac{i}{2}) - \mathcal{Q}_{a|i}(u - \tfrac{i}{2}) = -\mathbf{P}_a(u)\mathbf{P}^b(u)\mathcal{Q}_{b|i}(u + \tfrac{i}{2}) \ . \tag{4.20}$$

  Note that this is a 4-th order finite difference equation, which entangles all $\mathcal{Q}_{a|i}$ with fixed i. Different values of i label the 4 linearly independent solutions of this equation. One could also equivalently use $\mathcal{Q}_{b|i}(u - \frac{i}{2})$ in place of $\mathcal{Q}_{b|i}(u + \frac{i}{2})$ in the r.h.s., due to the constraint [53]

$$\mathbf{P}_a \mathbf{P}^a = 0 . \tag{4.21}$$

  Importantly, we also need to choose the solutions of (4.20) to be analytic in the upper half plane. In fact for all Q-functions one can ensure that they only have cuts in the lower half-plane.

- The matrix $\mathcal{Q}_{a|i}$ can then be used to pass to $\mathbf{Q}_i$ from $\mathbf{P}^a$'s,

$$\mathbf{Q}_i(u) = -\mathbf{P}^a(u)\ \mathcal{Q}_{a|i}(u+i/2)\ . \tag{4.22}$$

The equations (4.20) and (4.22) are simply two of the QQ-relations as explained in [53]. Let us notice that combining this equation with (4.20) we find a neat relation

$$\mathcal{Q}_{a|i}(u+i/2) - \mathcal{Q}_{a|i}(u-+i/2) = \mathbf{P}_a(u)\mathbf{Q}_i(u) \tag{4.23}$$

which is also one of the usual QQ-relations.

We also introduce a matrix $\mathcal{Q}^{a|i}$ such that $\mathcal{Q}^{a|i}\mathcal{Q}_{a|j} = -\delta^i_j$ and use it to define $\mathbf{Q}$'s with an upper index:

$$\mathbf{Q}^i(u) = +\mathbf{P}_a(u)\ \mathcal{Q}^{a|i}(u+i/2)\ . \tag{4.24}$$

Note that since $\mathcal{Q}_{a|i}(u)$ is analytic in the upper-half-plane we can also analytically continue these relations around the branch point at $u = 2g$ to get

$$\tilde{\mathbf{Q}}_i(u) = -\tilde{\mathbf{P}}^a(u)\ \mathcal{Q}_{a|i}(u+i/2) \tag{4.25}$$

$$\tilde{\mathbf{Q}}^i(u) = +\tilde{\mathbf{P}}_a(u)\ \mathcal{Q}^{a|i}(u+i/2) \tag{4.26}$$

where the tilde denotes analytic continuation to the next sheet.

Since $\mathbf{Q}_i$ can now be recovered from $\mathbf{P}_a$ and $\mathbf{P}^a$ it is not surprising that actually all information we needed, in particular all the charges (including those in AdS_5), are encoded in $\mathbf{P}$'s alone, through

$$\mathbf{P}_a \sim A_a u^{-\tilde{M}_a},\ \mathbf{P}^a \sim A^a u^{\tilde{M}_a - 1},\quad A^{a_0}A_{a_0} = i\frac{\prod_j(\tilde{M}_{a_0} - \hat{M}_j)}{\prod_{b\neq a_0}(\tilde{M}_{a_0} - \tilde{M}_b)}, \tag{4.27}$$

where $\hat{M}_j$ and $\tilde{M}_a$ are defined in (4.17), (4.18) and there is no summation over a_0 in l.h.s. In particular, one can extract Δ from the last equation.

The coefficients $c_{a,n}$ and corresponding coefficients $c^{a,n}$ of the expansion of $\mathbf{P}^a(u)$ need to be found. The constraint (4.21) fixes some of them (for example, we can use it to fix all $c_{1,n}$). The condition (4.27) gives the leading coefficients $c_{a,\tilde{M}_a}$. The remaining coefficients should be fixed from the analyticity constraints on $\mathbf{P}$'s as prescribed by QSC. Let us describe these constraints. The analytic continuation of $\mathbf{P}_a$ to the second sheet, which we denote by $\tilde{\mathbf{P}}_a$, in terms of our ansatz (4.19) becomes simply

$$\tilde{\mathbf{P}}_a(u) = \sum_{n=\tilde{M}_a}^{\infty} c_{a,n}x^n(u)\ . \tag{4.28}$$

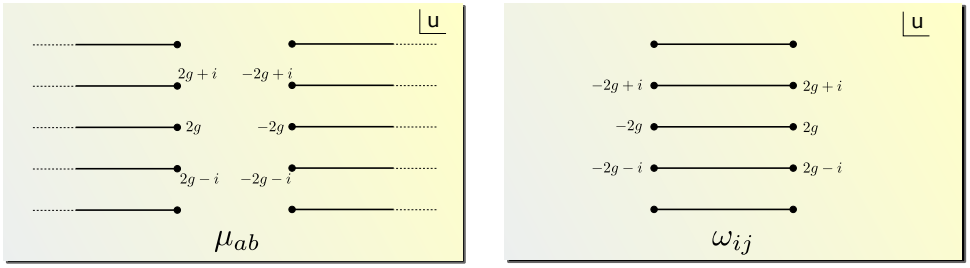

Figure 3: μ_{ab} is periodic as a function with long cuts, and ω_{ij} as a function with short cuts.

According to [53] this analytic continuation can be written in terms of auxiliary functions $\mu_{ab}(u)$ via

$$\tilde{\mathbf{P}}_a(u) = \mu_{ab}(u)\mathbf{P}^b \ , \ \ \tilde{\mathbf{P}}^a(u) = \mu^{ab}(u)\mathbf{P}_b(u) \tag{4.29}$$

where $\mu_{ab}(u)$ is an antisymmetric matrix with unit Pfaffian, i-periodic as a function with long cuts, with the discontinuity fixed in terms of $\mathbf{P}_a$

$$\tilde{\mu}_{ab}(u) - \mu_{ab}(u) = \mathbf{P}_a\tilde{\mathbf{P}}_b - \tilde{\mathbf{P}}_a\mathbf{P}_b \ . \tag{4.30}$$

The matrix μ^{ab} with upper indices is the inverse matrix to μ_{ab}. Let us also note that if we define μ's as functions with short cuts, we would have instead of i-periodicity the following condition:

$$\tilde{\mu}_{ab}(u) = \mu_{ab}(u + i) \tag{4.31}$$

Note also that μ_{ab} are not themselves Q-functions.[6]

At this stage one can already present a closed system of equations which allow to fix the energy Δ. In fact the equations (4.29), (4.30), (4.31) together with the requirement $\mathbf{P}^a\mathbf{P}_a = 0$ are already constraining enough to fix the spectrum [52]. One should only supplement them with asymptotics of the $\mathbf{P}$'s from (4.16), the relations (4.27) and the asymptotics of μ's which e.g. in the $sl(2)$ subsector with $J_2 = S_2 = 0$ take the form

$$(\mu_{12},\ \mu_{13},\ \mu_{14},\ \mu_{23},\ \mu_{24},\ \mu_{34}) \sim \left(u^{\Delta-J},\ u^{\Delta+1},\ u^{\Delta},\ u^{\Delta},\ u^{\Delta-1},\ u^{\Delta+J}\right) \ . \tag{4.32}$$

Finally we also require that $\mathbf{P}$'s and μ's should have no singularities apart from the branch points. This formulation, which is known as the $\mathbf{P}\mu$ system, does not use the $\mathbf{Q}_i$ functions at all.

The $\mathbf{P}\mu$ formulation of the QSC is certainly powerful and has led to many new results for the spectrum. However, we found that in many cases it is much more advantageous

[6] The matrix μ_{ab} can be interpreted as a rotation which transforms the Q-functions analytic in the upper half plane into Q-functions analytic in the lower half-plane, see [53] for details.

to close the analyticity conditions at the level of $\mathbf{Q}_i$, which obey very similar equations. The rule is quite simple – one has to interchange short and long cuts. That is, we have to introduce an i-periodic with *short* cuts function $\omega_{ij}(u)$ such that

$$\tilde{\mathbf{Q}}_i = \omega_{ij}\mathbf{Q}^j \ , \ \tilde{\mathbf{Q}}^i = \omega^{ij}\mathbf{Q}_j \ , \ \tilde{\omega}_{ij} - \omega_{ij} = \tilde{\mathbf{Q}}_i\mathbf{Q}_j - \mathbf{Q}_i\tilde{\mathbf{Q}}_j \ . \tag{4.33}$$

with Pf $\omega = 1$. At $u \to +\infty$ the set of ω_{ij} becomes a constant matrix. These equations represent another equivalent formulation of the QSC, known as the $\mathbf{Q}\omega$ system.

One can also relate μ's and ω's with the help of Q-functions with four indices $Q_{ab|ij}$ defined as a determinant,

$$Q_{ab|ij} = \begin{vmatrix} Q_{a|i} & Q_{a|j} \\ Q_{b|i} & Q_{b|j} \end{vmatrix} \ . \tag{4.34}$$

Then we have

$$\mu_{ab} = \frac{1}{2} Q^-_{ab|ij}\omega^{ij} \ . \tag{4.35}$$

Let us finally note that after the formulation of the original QSC in [52, 53], it was understood in [13] that one can avoid computing the auxiliary functions μ and ω altogether. The equations can be closed using Q-functions only[7], and e.g. in the $sl(2)$ sector it is enough to impose

$$\tilde{\mathbf{Q}}_1(u) = \text{const} \cdot \mathbf{Q}_3(-u) \ . \tag{4.36}$$

In addition to being conceptually important, this simplification increases the efficiency of the QSC even further, and in particular made it possible to reach the high-order results presented in [13], [12], [11] which will be discussed below.

4.3 The QSC in the $sl(2)$ sector

The anomalous dimensions of twist operators in the $sl(2)$ sector of $\mathcal{N} = 4$ SYM are one of the most interesting parts of the theory's spectrum, exhibiting rich structires in perturbation theory and being related to multicolor QCD in some limits [69]. These operators are built from sclaras and covariant derivatives, and they form the subsector known as the $sl(2)$ sector. Explicitly they have the form

$$\mathcal{O} = \text{Tr}\left(Z^{J-1}\,\mathcal{D}^S Z\right) + \dots \tag{4.37}$$

[7] This has been checked explicitly in some subsectors but it should be possible to derive similar relations for generic states.

where Z denotes one of the scalars of the theory[8], $\mathcal{D}$ is a lightcone covariant derivative and the dots stand for permutations. The number of derivatives S is called the spin of the operator, while J is called the twist. Below we will study them intensively in various regimes. We will focus on the symmetric case, corresponding to a distribution of the Bethe roots which is invariant under $u \to -u$.

For such states the QSC enjoys several simplifications. First, quantities with upper and lower indices are now related to each other: indices can be raised or lowered using a simple matrix

$$\chi = \begin{pmatrix} 0 & 0 & 0 & -1 \\ 0 & 0 & 1 & 0 \\ 0 & -1 & 0 & 0 \\ 1 & 0 & 0 & 0 \end{pmatrix}, \tag{4.38}$$

for example,

$$\mathbf{Q}^i = \chi^{ij}\mathbf{Q}_j, \ \mathbf{P}^a = \chi^{ab}\mathbf{P}_b. \tag{4.39}$$

It is also easy to show that in this sector ω_{ij} should satisfy $\omega_{14} = \omega_{23}$ in addition to antisymmetry, and similaraly $\mu_{14} = \mu_{23}$. Also, the $\mathbf{P}$ and $\mathbf{Q}$-functions have now definite parity in u.

The matrix $Q_{a|i}$ can be normalized in this case such that it preserves the χ^{ab} matrix,

$$\chi Q \chi Q^T = 1 \tag{4.40}$$

and should have unit determinant [53],

$$\det_{1\leq a,i\leq 4} Q_{a|i} = 1 \ . \tag{4.41}$$

4.4 The QSC in action: results obtained so far

Here we will summarize the applications of the QSC that have been explored so far.

One of the first impressive demonstrations of the efficiency of this approach was the calculation of the Konishi anomalous dimension to 10 loops in perturbation theory [70], supplemented later by more perturbative results in the $sl(2)$ sector [70, 71]. The QSC allows to prove general statements about the types of multiple zeta values that can appear as coefficients in the expansion, establishing a curious link to deep algebra and perhaps number theory. High-order weak coupling expansion for generic operators should also soon be available.

[8] Written in terms of two real scalars as $Z = \Phi_1 + i\Phi_2$.

The QSC was also proven to be powerful in application to expansion around BPS configurations. A great simplification comes from the fact that **P**-functions typically become suppressed in this case. In [15] the first two nontrivial orders in the small spin expansion of twist operator anomalous dimensions were computed at all loops. The leading order matches the known result encoded in ABA, while the next order is new and leads to novel analytic predictions at strong coupling for Konishi-type operators and for the BFKL intercept. The QSC also served as a guidance for the near-BPS solution of the TBA describing the generalized cusp with arbitrary angle θ [16].

The calculation of [15] led to a prescription in the QSC for analytic continuation of anomalous dimensions away from integer spin values. The regime of non-integer spin was further explored in [72] where the famous BFKL limit $S \to -1,\ g \to 0, \frac{g^2}{S+1} = \text{fixed}$ was studied. This limit has played an important role in explorations of integrability in $\mathcal{N} = 4$ SYM and the theory develops close links to QCD in this case. In fact even long before the formulation of AdS/CFT integrability was observed for 4d multicolor QCD. The leading order anomalous dimension in this regime resums all orders of usual perturbation theory. In [72] the leading order result was fully reproduced from integrability for the first time and the LO solution of the QSC was constructed. The next challenge was to reach higher orders in the expansion. It was overcome in [13] where the NNLO term was computed for the first time, using an iterative analytic method which is also applicable in many other situations.

Furthemore, an efficient numerical algorithm which allows to solve the QSC for any state/operator was proposed in [14]. In particular it provided a check for the NNLO result with at least 60 digits of precision.

In [12] it was proposed how to extend the QSC to calculation of the generalized cusp anomalous dimension associated to a nonlocal operator (a cusped Wilson line). The versatile methods developed before were adapted to this case, leading to many new results, both analytical and numerical. Furthemore, it was understood in [11] how the singular limit corresponding to the flat space $q\bar{q}$ potential is implemented in the QSC. This allowed to deeply study this quantity at weak coupling, numerically and also in the double scaling limit resumming all perturbative orders.

A setup similar to the cusped Wilson line was considered in [73] where deformations of the QSC were described and in particular the QSC was formulated for $\gamma-$deformed $\mathcal{N} = 4$ SYM. Extension of the QSC to other defomations (e.g. q-deformations) remains to be carried out.

The QSC has also been formulated for the ABJM duality [74] in which the ABA and TBA/Y-system have been proposed earlier [75, 76, 77, 21, 78, 79]. The all-loop computation of [80] followed and led to the resolution of a longstanding problem by allowing to fix an interpolation function $h(\lambda)$ that enters all integrability-based results in this model and was previously studied intensively at weak and strong coupling [81, 82, 83, 84, 85, 86, 87]. The QSC was also applied to high-order weak coupling calculations [88]. Finally let us mention that the QSC is also known for the Hubbard model which has several common features with the AdS/CFT integrable system [89].

Part II

All-loop results at small spin

In this part we will describe the application of the QSC to studying the small spin near-BPS limit in the $sl(2)$ sector of $\mathcal{N}=4$ SYM, based on the paper [15]. To preserve the same notation as in that paper, in this part we chose to relabel the $\mathbf{P}_a$ functions compared to the discussion above, with

$$\mathbf{P}_1^{here}=\mathbf{P}_2,\ \mathbf{P}_2^{here}=\mathbf{P}_1,\ \mathbf{P}_3^{here}=\mathbf{P}_4,\ \mathbf{P}_4^{here}=\mathbf{P}_3\ . \tag{4.42}$$

5 Introduction

The small spin limit for operators in the $sl(2)$ sector has attracted significant attention since it is posible to obtain all-loop results in this regime. We will consider a two-cut configuration with a symmetric distribution of Bethe roots, thus for physical states S is even. For small spin, the scaling dimension of these operators can be written as

$$\Delta=J+S+\gamma(g),\qquad g=\sqrt{\lambda}/(4\pi) \tag{5.1}$$

with the anomalous dimension $\gamma(g)$ given as an expansion

$$\gamma(g)=\gamma^{(1)}(g)S+\gamma^{(2)}(g)S^2+\mathcal{O}(S^3). \tag{5.2}$$

The first term, $\gamma^{(1)}(g)$, is called the slope function. Remarkably, it can be found exactly at any value of the coupling [90]

$$\gamma^{(1)}(g)=\frac{4\pi g I_{J+1}(4\pi g)}{J I_J(4\pi g)}\ . \tag{5.3}$$

This expression was later derived from the asymptotic Bethe ansatz (ABA) equations in two different ways [91, 92] and further studied and extended in [93, 94, 95, 96, 97]. This quantity is protected from finite-size wrapping corrections and thus the ABA prediction is exact. It is also not sensitive to the dressing phase of the ABA, which contributes only starting from order S^2.

Our key observation is that in the small S regime the $\mathbf{P}\mu$-system can be solved iteratively order by order in the spin. We will first solve it at leading order and reproduce the slope function (5.3). Then we compute the coefficient of the S^2 term in the expansion, i.e. the function $\gamma^{(2)}(g)$ which we call the *curvature function*. For twist $J=2,3,4$ we obtain

closed exact expressions for it in the form of a double integral. Unlike the slope function, $\gamma^{(2)}(g)$ is affected by the dressing phase in the ABA and by wrapping corrections, all of which are incorporated in the exact $\mathbf{P}\mu$-system.

Furthermore, we will use the strong coupling expansion of our result to find the value of a new coefficient in the Konishi operator (i.e. $\mathrm{Tr}\left(\mathcal{D}^2 Z^2\right)$) anomalous dimension at strong coupling. Our result for the Konishi dimension reads

$$\Delta_{konishi} = 2\,\lambda^{1/4} + \frac{2}{\lambda^{1/4}} + \frac{-3\,\zeta_3 + \frac{1}{2}}{\lambda^{3/4}} + \frac{\frac{15\,\zeta_5}{2} + 6\,\zeta_3 + \frac{1}{2}}{\lambda^{5/4}} + \dots \ . \tag{5.4}$$

We have also obtained two new terms in the strong coupling expansion of the BFKL pomeron intercept,

$$\begin{aligned} j_0 = 2 + S(\Delta)|_{\Delta=0} \ &= \ 2 - \frac{2}{\lambda^{1/2}} - \frac{1}{\lambda} + \frac{1}{4\,\lambda^{3/2}} + (6\,\zeta_3 + 2)\,\frac{1}{\lambda^2} \\ &+ \ \left(18\,\zeta_3 + \frac{361}{64}\right)\frac{1}{\lambda^{5/2}} + \left(39\,\zeta_3 + \frac{511}{32}\right)\frac{1}{\lambda^3} + \mathcal{O}\left(\frac{1}{\lambda^{7/2}}\right), \end{aligned} \tag{5.5}$$

where the new terms are in the second line. In addition we have checked our results against available results in literature at weak and strong coupling, and found full agreement.

This part is organized as follows. We first write out some of the $\mathbf{P}\mu$ system equations more explicitly. In section 7 we demonstrate the usefulness of the QSC by rederiving the exact slope function of $\mathcal{N} = 4$ found in [90]. In section 8 we push the calculation further and find the exact expression for the next coefficient in the small spin expansion, i.e. the curvature function. In sections 9 and 10 we discuss the weak and strong coupling expansions of our result. We then use our results to calculate the previously unknown three loop strong coupling coefficient of the Konishi anomalous dimension in subsection 10.3 and two new coefficients for the BFKL intercept at strong coupling in subsection 10.4. We finish with conclusions.

6 Pμ-system – an overview

The $\mathbf{P}\mu$-system, already discussed above, is a nonlinear system of functional equations for a four-vector $\mathbf{P}_a(u)$ and a 4×4 antisymmetric matrix $\mu_{ab}(u)$ depending on the spectral parameter u. The functions μ_{ab} are also constrained by the relations

$$\mu_{12}\mu_{34} - \mu_{13}\mu_{24} + \mu_{14}^2 \ = \ 1\ , \tag{6.1}$$

$$\mu_{14} = \mu_{23}\ , \tag{6.2}$$

the first of which states that the Pfaffian of the matrix μ_{ab} is equal to 1. Let us also write the equations (4.29) explicitly:

$$\tilde{\mathbf{P}}_1 = -\mathbf{P}_3\mu_{12} + \mathbf{P}_2\mu_{13} - \mathbf{P}_1\mu_{14} \tag{6.3}$$

$$\tilde{\mathbf{P}}_2 = -\mathbf{P}_4\mu_{12} + \mathbf{P}_2\mu_{14} - \mathbf{P}_1\mu_{24} \tag{6.4}$$

$$\tilde{\mathbf{P}}_3 = -\mathbf{P}_4\mu_{13} + \mathbf{P}_3\mu_{14} - \mathbf{P}_1\mu_{34} \tag{6.5}$$

$$\tilde{\mathbf{P}}_4 = -\mathbf{P}_4\mu_{14} + \mathbf{P}_3\mu_{24} - \mathbf{P}_2\mu_{34}\ . \tag{6.6}$$

The above equations ensure that the branch points of $\mathbf{P}_a$ and μ_{ab} are of the square root type, i.e. $\tilde{\tilde{\mathbf{P}}}_a = \mathbf{P}_a$ and $\tilde{\tilde{\mu}}_{ab} = \mu_{ab}$.

Finally, we require that $\mathbf{P}_a$ and μ_{ab} do not have any singularities except these branch points[9].

The quantum numbers and the energy of the state are encoded in the asymptotics of the functions $\mathbf{P}_a$ and μ_{ab} at large real u. In the $sl(2)$ sector the relations read [52]

$$\mathbf{P}_a \sim (A_1 u^{-J/2}, A_2 u^{-J/2-1}, A_3 u^{J/2}, A_4 u^{J/2-1}) \tag{6.7}$$

$$(\mu_{12},\ \mu_{13},\ \mu_{14},\ \mu_{24},\ \mu_{34}) \sim \left(u^{\Delta-J},\ u^{\Delta+1},\ u^{\Delta},\ u^{\Delta-1},\ u^{\Delta+J}\right) \tag{6.8}$$

where J is the twist of the gauge theory operator, and Δ is its conformal dimension. Lastly, the spin S of the operator is related [52] to the leading coefficients A_a of the $\mathbf{P}_a$ functions (see (6.7)):

$$A_1 A_4 = \frac{\left((J+S-2)^2-\Delta^2\right)\left((J-S)^2-\Delta^2\right)}{16iJ(J-1)} \tag{6.9}$$

$$A_2 A_3 = \frac{\left((J-S+2)^2-\Delta^2\right)\left((J+S)^2-\Delta^2\right)}{16iJ(J+1)}\ . \tag{6.10}$$

6.1 Symmetries

The $\mathbf{P}\mu$-system enjoys a symmetry preserving all of its essential features. It has the form of a linear transformation of $\mathbf{P}_a$ and μ_{ab} which leaves the system (4.29)-(6.2) and the asymptotics (6.7), (6.8) invariant. Indeed, consider a general linear transformation $\mathbf{P}'_a = R_a{}^b\mathbf{P}_b$ with a non-degenerate constant matrix R. In order to preserve the system (4.29), μ should at the same time be transformed as

$$\mu' = -R\mu\chi R^{-1}\chi. \tag{6.11}$$

[9]For odd values of J the functions $\mathbf{P}_a$ may have an additional branch point at infinity. However, it should cancel in any product of two $\mathbf{P}_a$'s, and therefore it will not appear in any physically relevant quantity (see [52], [53]). We will discuss some explicit examples in the text.

Such a transformation also preserves the form of (4.30) if

$$R^T \chi R \chi = -1 \ , \tag{6.12}$$

which also automatically ensures antisymmetry of μ_{ab} and (6.1), (6.2). In general, this transformation will spoil the asymptotics of $\mathbf{P}_a$. These asymptotics are ordered as $|\mathbf{P}_2| < |\mathbf{P}_1| < |\mathbf{P}_4| < |\mathbf{P}_3|$, which implies that the matrix R must have the following structure[10]

$$R = \begin{pmatrix} * & * & 0 & 0 \\ 0 & * & 0 & 0 \\ * & * & * & * \\ * & * & 0 & * \end{pmatrix} . \tag{6.13}$$

The general form of R which satisfies (6.12) and does not spoil the asymptotics generates a 6-parametric transformation, which we will call a γ-transformation. The simplest γ-transformation is the following rescaling:

$$\mathbf{P}_1 \to \alpha \mathbf{P}_1 \ , \ \ \mathbf{P}_2 \to \beta \mathbf{P}_2 \ , \ \ \mathbf{P}_3 \to 1/\beta \mathbf{P}_3 \ , \ \ \mathbf{P}_4 \to 1/\alpha \mathbf{P}_4 \ , \tag{6.14}$$

$$\mu_{12} \to \alpha\beta\mu_{12} \ , \ \ \mu_{13} \to \frac{\alpha}{\beta}\mu_{13} \ , \ \ \mu_{14} \to \mu_{14} \ , \ \ \mu_{24} \to \frac{\beta}{\alpha}\mu_{24} \ , \ \ \mu_{34} \to \frac{1}{\alpha\beta}\mu_{34} \ , \tag{6.15}$$

with α, β being constants.

In all the solutions we consider in this part all functions $\mathbf{P}_a$ turn out to be functions of definite parity, so it makes sense to consider γ-transformations which preserve parity. $\mathbf{P}_1$ and $\mathbf{P}_2$ always have opposite parity (as one can see from from (6.7)) and thus should not mix under such transformations; the same is true about $\mathbf{P}_3$ and $\mathbf{P}_4$. Thus, depending on parity of J the parity-preserving γ-transformations are either

$$\begin{gathered} \mathbf{P}_3 \to \mathbf{P}_3 + \gamma_3 \mathbf{P}_2, \ \mathbf{P}_4 \to \mathbf{P}_4 + \gamma_2 \mathbf{P}_1, \\ \mu_{13} \to \mu_{13} + \gamma_3 \mu_{12}, \ \mu_{24} \to \mu_{24} - \gamma_2 \mu_{12}, \ \mu_{34} \to \mu_{34} + \gamma_3 \mu_{24} - \gamma_2 \mu_{13} - \gamma_2 \gamma_3 \mu_{12} \end{gathered} \tag{6.16}$$

for odd J or

$$\begin{gathered} \mathbf{P}_3 \to \mathbf{P}_3 + \gamma_1 \mathbf{P}_1, \ \mathbf{P}_4 \to \mathbf{P}_4 - \gamma_1 \mathbf{P}_2, \\ \mu_{14} \to \mu_{14} - \gamma_1 \mu_{12}, \ \mu_{34} \to \mu_{34} + 2\gamma_1 \mu_{14} - \gamma_1^2 \mu_{12} \ , \end{gathered} \tag{6.17}$$

for even J.

[10] This matrix would of course be lower triangular if we ordered $\mathbf{P}_a$ by their asymptotics.

7 Exact slope function from the Pμ-system

In this section we will find the solution of the $\mathbf{P}\mu$-system (4.29)-(6.2) corresponding to the $sl(2)$ sector operators at leading order in small S. Based on this solution we will compute the slope function $\gamma^{(1)}(g)$ for any value of the coupling.

7.1 Solving the Pμ-system in LO

The solution of the $\mathbf{P}\mu$-system is a little simpler for even J, because for odd J extra branch points at infinity will appear in $\mathbf{P}_a$ due to the asymptotics (6.7). Let us first consider the even J case.

The description of the $\mathbf{P}\mu$-system above was done for physical operators. Our goal is to take some peculiar limit when the (integer) number of covariant derivatives S goes to zero. As we will see this requires some extension of the asymptotic requirement for μ functions. In this section we will be guided by principles of naturalness and simplicity to deduce these modifications. The details of the prescription for the analytic continuation are discussed in [15], and we do not cover them here for the sake of brevity. The prescription was later understood to amount to allowing exponential asymptotics in one of the ω_{ij} functions (see the part of the thesis discussing the numerical solution for more details).

We will start by finding μ_{ab}. Recalling that $\Delta = J + \mathcal{O}(S)$, from (6.9), (6.10) we see that A_1A_4 and A_2A_3 are of order S for small S, so we can take the functions $\mathbf{P}_a$ to be of order $\sqrt{S}$. This is a key simplification, because now (4.30) indicates that the discontinuities of μ_{ab} on the cut are small when S goes to zero. Thus at leading order in S all μ_{ab} are just periodic entire functions without cuts. For power-like asymptotics of μ_{ab} like in (6.8) the only possibility is that they are all constants. However, we found that in this case there is only a trivial solution, i.e. $\mathbf{P}_a$ can only be zero. The reason for this is that for physical states S must be integer and thus cannot be arbitrarily small, nevertheless, it is a sensible question how to define an analytical continuation from integer values of S.[11]

Thus we have to relax the requirement of power-like behavior at infinity. The first possibility is to allow for $e^{2\pi u}$ asymptotics at $u \to +\infty$. We should, however, remember about the constraints (6.1) and (6.2) which restrict our choice and the fact that we can also use γ-symmetry. Let us show that by allowing μ_{24} to have exponential behavior and

[11] Restricting the large positive S behavior one can achieve uniqueness of the continuation.

setting it to $\mu_{24} = C\sinh(2\pi u)$, with other μ_{ab} being constant, we arrive to the correct result. This choice is dictated by our assumptions concerning the analytic continuation of μ_{ab} to non-integer values of S, and this point is discussed in detail in [15]. It is also shown therethat by using the γ-transformation (described in section 6.1) and the constraint (6.1) we can set the constant C to 1 and also $\mu_{12} = 1,\ \mu_{13} = 0,\ \mu_{14} = -1,\ \mu_{34} = 0$.

Having fixed all μ's at leading order we get the following system of equations[12] for $\mathbf{P}_a$:

$$\tilde{\mathbf{P}}_1 = -\mathbf{P}_3 + \mathbf{P}_1, \tag{7.1}$$

$$\tilde{\mathbf{P}}_2 = -\mathbf{P}_4 - \mathbf{P}_2 - \mathbf{P}_1\sinh(2\pi u), \tag{7.2}$$

$$\tilde{\mathbf{P}}_3 = \quad -\mathbf{P}_3, \tag{7.3}$$

$$\tilde{\mathbf{P}}_4 = \quad +\mathbf{P}_4 + \mathbf{P}_3\sinh(2\pi u). \tag{7.4}$$

Recalling that the functions $\mathbf{P}_a$ only have a single short cut, we see from these equations that $\tilde{\mathbf{P}}_a$ also have only this cut! This means that we can take all $\mathbf{P}_a$ to be infinite Laurent series in the Zhukovsky variable $x(u)$, which rationalizes the Riemann surface with two sheets and one cut. It is defined as

$$x + \frac{1}{x} = \frac{u}{g} \tag{7.5}$$

where we pick the solution with a short cut, i.e.

$$x(u) = \frac{1}{2}\left(\frac{u}{g} + \sqrt{\frac{u}{g} - 2}\,\sqrt{\frac{u}{g} + 2}\right) \quad . \tag{7.6}$$

Solving the equation (7.3) with the asymptotics (6.7) we find

$$\mathbf{P}_3 = \epsilon\left(x^{-J/2} - x^{+J/2}\right) + \sum_{k=1}^{J/2-1} c_k\left(x^{-k} - x^{k}\right) \tag{7.7}$$

where ϵ and c_k are constants. Now it is useful to rewrite the equation for $\mathbf{P}_1$ (i.e. (7.1)) in the form $\tilde{\mathbf{P}}_1 - \mathbf{P}_1 = -\mathbf{P}_3$, and we see that due to asymptotics of $\mathbf{P}_1$ both sides of this equation must have a gap in the powers of x from $x^{-J/2+1}$ to $x^{J/2-1}$. This means that all coefficients c_k in (7.7) must vanish and we find

$$\mathbf{P}_1 = \epsilon x^{-J/2}\ , \tag{7.8}$$

so we are left with one unfixed constant ϵ (we expect it to be proportional to $\sqrt{S}$).

[12] In this section we only consider the leading order of $\mathbf{P}$'s at small S, so the equations involving them are understood to hold at leading order in S. In section 4 we will study the next-to-leading order and elaborate the notation for contributions of different orders.

Thus the equations (7.2) and (7.4) become

$$\tilde{\mathbf{P}}_2 + \mathbf{P}_2 = -\mathbf{P}_4 - \epsilon x^{-J/2} \sinh(2\pi u) \,, \tag{7.9}$$

$$\tilde{\mathbf{P}}_4 - \mathbf{P}_4 = \epsilon(x^{-J/2} - x^{+J/2}) \sinh(2\pi u) \,. \tag{7.10}$$

We will first solve the second equation. It is useful to introduce operations $[f(x)]_+$ and $[f(x)]_-$, which take parts of Laurent series with positive and negative powers of x respectively. Taking into account that

$$\sinh(2\pi u) = \sum_{n=-\infty}^{\infty} I_{2n+1} x^{2n+1}, \tag{7.11}$$

where $I_k \equiv I_k(4\pi g)$ is the modified Bessel function of the first kind, we can write $\sinh(2\pi u)$ as

$$\sinh(2\pi u) = \sinh_+ + \sinh_-, \tag{7.12}$$

where explicitly

$$\sinh_+ = [\sinh(2\pi u)]_+ = \sum_{n=1}^{\infty} I_{2n-1} x^{2n-1} \tag{7.13}$$

$$\sinh_- = [\sinh(2\pi u)]_- = \sum_{n=1}^{\infty} I_{2n-1} x^{-2n+1} \,. \tag{7.14}$$

In this notation the general solution of Eq. (7.10) with asymptotics at infinity $\mathbf{P}_4 \sim u^{J/2-1}$ can be written as

$$\mathbf{P}_4 = \epsilon(x^{J/2} - x^{-J/2}) \sinh_- + Q_{J/2-1}(u), \tag{7.15}$$

where $Q_{J/2-1}$ is a polynomial of degree $J/2-1$ in u. The polynomial $Q_{J/2-1}$ can be fixed from the equation (7.9) for $\mathbf{P}_2$. Indeed, from the asymptotics of $\mathbf{P}_2$ we see that the lhs of (7.9) does not have powers of x from $-J/2+1$ to $J/2-1$. This fixes

$$Q_{J/2-1}(x) = -\epsilon \sum_{k=1}^{J/2} I_{2k-1} \left(x^{\frac{J}{2}-2k+1} + x^{-\frac{J}{2}+2k-1} \right). \tag{7.16}$$

Once $Q_{J/2-1}$ is found, we set $\mathbf{P}_2$ to be the part of the right hand side of (7.9) with powers of x less than $-J/2$, which gives

$$\mathbf{P}_2 = -\epsilon x^{+J/2} \sum_{n=\frac{J}{2}+1}^{\infty} I_{2n-1} x^{1-2n}. \tag{7.17}$$

Thus (for even J) we have uniquely fixed all $\mathbf{P}_a$ with the only unknown parameter being

ϵ. We summarize the solution below:

$$\mu_{12}=1,\ \mu_{13}=0,\ \mu_{14}=-1,\ \mu_{24}=\sinh(2\pi u),\ \mu_{34}=0, \tag{7.18}$$

$$\mathbf{P}_1=\epsilon x^{-J/2} \tag{7.19}$$

$$\mathbf{P}_2=-\epsilon x^{+J/2}\sum_{n=J/2+1}^{\infty} I_{2n-1}x^{1-2n} \tag{7.20}$$

$$\mathbf{P}_3=\epsilon\left(x^{-J/2}-x^{+J/2}\right) \tag{7.21}$$

$$\mathbf{P}_4=\epsilon\left(x^{J/2}-x^{-J/2}\right)\sinh_- -\epsilon\sum_{n=1}^{J/2} I_{2n-1}\left(x^{\frac{J}{2}-2n+1}+x^{-\frac{J}{2}+2n-1}\right)\ . \tag{7.22}$$

In the next section we fix the remaining parameter ϵ of the solution in terms of S and find the energy, but now let us briefly discuss the solution for odd J. As we mentioned above the main difference is that the functions $\mathbf{P}_a$ now have a branch point at $u=\infty$, which is dictated by the asymptotics (6.7). In addition, the parity of μ_{ab} is different according to the asymptotics of these functions (6.8). The solution is still very similar to the even J case and is discussed in detail in [15]. Let us present the result here:

$$\mu_{12}=1,\ \mu_{13}=0,\ \mu_{14}=0,\ \mu_{24}=\cosh(2\pi u),\ \mu_{34}=1 \tag{7.23}$$

$$\mathbf{P}_1=\epsilon x^{-J/2}, \tag{7.24}$$

$$\mathbf{P}_2=-\epsilon x^{J/2}\sum_{k=-\infty}^{-\frac{J+1}{2}} I_{2k}x^{2k}, \tag{7.25}$$

$$\mathbf{P}_3=-\epsilon x^{J/2}, \tag{7.26}$$

$$\mathbf{P}_4=\epsilon x^{-J/2}\cosh_- -\epsilon x^{-J/2}\sum_{k=1}^{\frac{J-1}{2}} I_{2k}x^{2k}-\epsilon I_0 x^{-J/2}. \tag{7.27}$$

Note that now $\mathbf{P}_a$ include half-integer powers of x.

Fixing the global charges of the solution. To fix our solution completely we have to find the value of ϵ and find the energy in terms of the spin using (6.9) and (6.10). For this we first extract the coefficients A_a of the leading terms for all $\mathbf{P}_a$ (see the asymptotics (6.7)). From (7.19)-(7.22) or (7.24)-(7.27) we get

$$A_1=g^{J/2}\epsilon, \tag{7.28}$$

$$A_2=-g^{J/2+1}\epsilon I_{J+1}, \tag{7.29}$$

$$A_3=-g^{-J/2}\epsilon, \tag{7.30}$$

$$A_4=-g^{-J/2+1}\epsilon I_{J-1}. \tag{7.31}$$

Expanding (6.9), (6.10) at small S with $\Delta = J + S + \gamma$, where $\gamma = \mathcal{O}(S)$, we find at linear order

$$\gamma = i(A_1 A_4 - A_2 A_3) \tag{7.32}$$

$$S = i(A_1 A_4 + A_2 A_3)\ . \tag{7.33}$$

Plugging in the coefficients (7.28)-(7.31) we find that

$$\epsilon = \sqrt{\frac{2\pi i S}{J I_J(\sqrt{\lambda})}} \tag{7.34}$$

and we obtain the anomalous dimension at leading order,

$$\gamma = \frac{\sqrt{\lambda} I_{J+1}(\sqrt{\lambda})}{J I_J(\sqrt{\lambda})} S + \mathcal{O}(S^2), \tag{7.35}$$

which is precisely the slope function of Basso [90].

In summary, we have shown how the $\mathbf{P}\mu$-system correctly computes the energy at linear order in S. In section 8 we will compute the next, S^2 term in the anomalous dimension.

8 Exact curvature function

In this section we use the $\mathbf{P}\mu$-system to compute the S^2 correction to the anomalous dimension, which we call the curvature function $\gamma^{(2)}(g)$. First we will discuss the case $J = 2$ in detail and then describe the modifications of the solution for the cases $J = 3$ and $J = 4$, more details on which can be found in [15].

8.1 Iterative procedure for the small S expansion of the $\mathbf{P}\mu$-system

For convenience let us repeat the leading order solution of the $\mathbf{P}\mu$-system for $J = 2$ (see (7.18)-(7.22))

$$\mathbf{P}_1^{(0)} = \epsilon \frac{1}{x} \quad , \quad \mathbf{P}_2^{(0)} = +\epsilon I_1 - \epsilon x [\sinh(2\pi u)]_- \ , \tag{8.1}$$

$$\mathbf{P}_3^{(0)} = \epsilon \left(\frac{1}{x} - x\right) \quad , \quad \mathbf{P}_4^{(0)} = -2\epsilon I_1 - \epsilon \left(\frac{1}{x} - x\right) [\sinh(2\pi u)]_- . \tag{8.2}$$

Here ϵ is a small parameter, proportional to $\sqrt{S}$ (see (7.34)), and by $\mathbf{P}_a^{(0)}$ we denote the $\mathbf{P}_a$ functions at leading order in ϵ.

The key observation is that the $\mathbf{P}\mu$-system can be solved iteratively order by order in ϵ. Let us write $\mathbf{P}_a$ and μ_{ab} as an expansion in this small parameter:

$$\mathbf{P}_a = \mathbf{P}_a^{(0)} + \mathbf{P}_a^{(1)} + \mathbf{P}_a^{(2)} + \dots \tag{8.3}$$

$$\mu_{ab} = \mu_{ab}^{(0)} + \mu_{ab}^{(1)} + \mu_{ab}^{(2)} + \ldots \ . \tag{8.4}$$

where $\mathbf{P}_a^{(0)} = \mathcal{O}(\epsilon)$, $\mathbf{P}_a^{(1)} = \mathcal{O}(\epsilon^3)$, $\mathbf{P}_a^{(2)} = \mathcal{O}(\epsilon^5)$, $\ldots$, and $\mu_{ab}^{(0)} = \mathcal{O}(\epsilon^0)$, $\mu_{ab}^{(1)} = \mathcal{O}(\epsilon^2)$, $\mu_{ab}^{(2)} = \mathcal{O}(\epsilon^4)$, etc. This structure of the expansion is dictated by the equations (4.29), (4.30) of the $\mathbf{P}\mu$-system (as we will soon see explicitly). Since the leading order $\mathbf{P}_a$ are of order ϵ, equation (4.30) implies that the discontinuity of μ_{ab} on the cut is of order ϵ^2. Thus to find μ_{ab} in the next to leading order (NLO) we only need the functions $\mathbf{P}_a$ at leading order. After this, we can find the NLO correction to $\mathbf{P}_a$ from equations (4.30). This will be done below, and having thus the full solution of the $\mathbf{P}\mu$-system at NLO we will find the energy at order S^2.

8.2 Correcting $\mu_{ab}\ldots$

In this subsection we find the NLO corrections $\mu_{ab}^{(1)}$ to μ_{ab}. As follows from (4.30) and (4.31), they should satisfy the equation

$$\mu_{ab}^{(1)}(u+i) - \mu_{ab}^{(1)}(u) = \mathbf{P}_a^{(0)}\tilde{\mathbf{P}}_b^{(0)} - \mathbf{P}_b^{(0)}\tilde{\mathbf{P}}_a^{(0)}, \tag{8.5}$$

in which the right hand is known explicitly. For that reason let us define an apparatus for solving equations of this type, i.e.

$$f(u+i) - f(u) = h(u). \tag{8.6}$$

More precisely, we consider functions $f(u)$ and $h(u)$ with one cut in u between $-2g$ and $2g$, and no poles. Such functions can be represented as infinite Laurent series in the Zhukovsky variable $x(u)$, and we additionally restrict ourselves to the case where for $h(u)$ this expansion does not have a constant term[13].

One can see that the general solution of (8.6) has a form of a particular solution plus an arbitrary i-periodic function, which we also call a zero mode. First we will describe the construction of the particular solution and later deal with zero modes. The linear operator which gives the particular solution of (8.6) described below will be denoted as Σ.

Notice that given the explicit form (8.2) of $\mathbf{P}_a^{(0)}$, the right hand side of (8.5) can be represented in a form

$$\alpha(x)\sinh(2\pi u) + \beta(x), \tag{8.7}$$

[13]The r.h.s. of (8.5) has the form $F(u) - \tilde{F}(u)$ and therefore indeed does not have a constant term in its expansion, as the constant in F would cancel in the difference $F(u) - \tilde{F}(u)$.

where $\alpha(x), \beta(x)$ are power series in x growing at infinity not faster than polynomially. Thus for such α and β we define

$$\Sigma \cdot [\alpha(x)\sinh(2\pi u) + \beta(x)] \equiv \sinh(2\pi u)\Sigma \cdot \alpha(x) + \Sigma \cdot \beta(x). \tag{8.8}$$

We also define $\Sigma \cdot x^{-n} = \Gamma' \cdot x^{-n}$ for $n > 0$, where the integral operator Γ' defined as

$$\left(\Gamma' \cdot h\right)(u) \equiv \oint_{-2g}^{2g} \frac{dv}{4\pi i} \partial_u \log \frac{\Gamma[i(u-v)+1]}{\Gamma[-i(u-v)]} h(v). \tag{8.9}$$

This requirement is consistent because of the following relation [14]

$$\left(\Gamma' \cdot h\right)(u+i) - \left(\Gamma' \cdot h\right)(u) = -\frac{1}{2\pi i} \oint_{-2g}^{2g} \frac{h(v)}{u-v} dv = h_-(u) - \widetilde{h_+}(u). \tag{8.10}$$

What is left is to define Σ on positive powers of x. We do it by requiring

$$\frac{1}{2}\Sigma \cdot [x^a + 1/x^a] \equiv p'_a(u) \tag{8.11}$$

where $p'_a(u)$ is a polynomial in u of degree $a+1$, which is a solution of

$$p'_a(u+i) - p'_a(u) = \frac{1}{2}\left(x^a + 1/x^a\right) \tag{8.12}$$

and satisfies the following additional properties: $p'_a(0) = 0$ for odd a and $p'_a(i/2) = 0$ for even a. One can check that this definition is consistent and defines of $p'_a(u)$ uniquely.

From this definition of Σ one can see that the result of its action on expressions of the form (8.7) can again be represented in this form - what is important for us is that no exponential functions other than $\sinh(2\pi u)$ appear in the result.

As an example we present the particular solution for two components of μ_{ab} (below we will argue that π_{12} and π_{13} can be chosen to be zero, see (8.17))

$$\mu^{(1)}_{13} - \pi_{13} = \Sigma \cdot \left(\mathbf{P}_1\tilde{\mathbf{P}}_3 - \mathbf{P}_3\tilde{\mathbf{P}}_1\right) = \epsilon^2 \Sigma \cdot \left(x^2 - \frac{1}{x^2}\right) = \epsilon^2 \quad \left(\Gamma' \cdot x^2 + p'_2(u)\right) \tag{8.13}$$

$$\mu^{(1)}_{12} - \pi_{12} = \Sigma \cdot \left(\mathbf{P}_1\tilde{\mathbf{P}}_2 - \mathbf{P}_2\tilde{\mathbf{P}}_1\right) =$$
$$= -\epsilon^2 \left[2I_1\Gamma' \cdot x - \sinh(2\pi u)\,\Gamma' \cdot x^2 - \Gamma' \cdot \left(\sinh_- \left(x^2 + \frac{1}{x^2}\right)\right)\right]. \tag{8.14}$$

Now let us apply Σ defined above to (8.5), writing that its general solution is

$$\mu^{(1)}_{ab} = \Sigma \cdot (\mathbf{P}^{(0)}_a \tilde{\mathbf{P}}^{(0)}_b - \mathbf{P}^{(0)}_b \tilde{\mathbf{P}}^{(0)}_a) + \pi_{ab}, \tag{8.15}$$

where the zero mode π_{ab} is an arbitrary i-periodic entire function, which can be written similarly to the leading order as $c_{1,ab}\cosh 2\pi u + c_{2,ab}\sinh 2\pi u + c_{3,ab}$. Omitting a rather

[14] We remind that f_+ and f_- stand for the part of the Laurent expansion with, respectively, positive and negative powers of x, while $\tilde{f}$ is the analytic continuation around the branch point at $u = 2g$ (which amounts to replacing $x \to \frac{1}{x}$)

technical argument (discussed in detail in [15]) we find that the final form of the zero mode in (8.15) is

$$\pi_{12}=0,\ \pi_{13}=0,\ \pi_{14}=0, \tag{8.16}$$

$$\pi_{24}=c_{1,24}\cosh 2\pi u,\ \pi_{34}=0. \tag{8.17}$$

In this way, using the particular solution given by Σ and the form of zero modes (8.17) we have computed all the functions $\mu^{(1)}_{ab}$. The details and the results of the calculation can be found in appendix A.2.1.

8.3 Correcting $\mathbf{P}_a\ldots$

In the previous section we found the NLO part of μ_{ab}. Now, according to the iterative procedure described in section 8.1, we can use it to write a closed system of equations for $\mathbf{P}^{(1)}_a$. Indeed, expanding the system (6.6) to NLO we get

$$\tilde{\mathbf{P}}^{(1)}_1-\mathbf{P}^{(1)}_1=-\mathbf{P}^{(1)}_3+r_1, \tag{8.18}$$

$$\tilde{\mathbf{P}}^{(1)}_2+\mathbf{P}^{(1)}_2=-\mathbf{P}^{(1)}_4-\mathbf{P}^{(1)}_1\sinh(2\pi u)+r_2, \tag{8.19}$$

$$\tilde{\mathbf{P}}^{(1)}_3+\mathbf{P}^{(1)}_3=r_3, \tag{8.20}$$

$$\tilde{\mathbf{P}}^{(1)}_4-\mathbf{P}^{(1)}_4=\mathbf{P}^{(1)}_3\sinh(2\pi u)+r_4, \tag{8.21}$$

where the free terms are given by

$$r_a=-\mu^{(1)}_{ab}\chi^{bc}\mathbf{P}^{(0)}_c. \tag{8.22}$$

Notice that r_a does not change if we add a matrix proportional to $\mathbf{P}^{(0)}_a\tilde{\mathbf{P}}^{(0)}_b-\mathbf{P}^{(0)}_b\tilde{\mathbf{P}}^{(0)}_a$ to $\mu^{(1)}_{ab}$, due to the relations

$$\mathbf{P}_a\chi^{ab}\mathbf{P}_b=0,\ \mathbf{P}_a\chi^{ab}\tilde{\mathbf{P}}_b=0, \tag{8.23}$$

which follow from the $\mathbf{P}\mu$-system equations. In particular we can use this property to replace $\mu^{(1)}_{ab}$ in (8.22) by $\mu^{(1)}_{ab}+\frac{1}{2}\left(\mathbf{P}^{(0)}_a\tilde{\mathbf{P}}^{(0)}_b-\mathbf{P}^{(0)}_b\tilde{\mathbf{P}}^{(0)}_a\right)$. This will be convenient for us, since in expressions for $\mu^{(1)}_{ab}$ in terms of p_a and Γ (see (8.13), (8.14) and appendix A.2.1) this change amounts to simply replacing Γ' by a convolution with a more symmetric kernel:

$$\Gamma'\to\Gamma, \tag{8.24}$$

$$(\Gamma\cdot h)(u)\equiv\oint_{-2g}^{2g}\frac{dv}{4\pi i}\partial_u\log\frac{\Gamma[i(u-v)+1]}{\Gamma[-i(u-v)+1]}h(v), \tag{8.25}$$

while at the same time replacing

$$p'_a(u)\to p_a(u), \tag{8.26}$$

$$p_a(u) = p'_a(u) + \frac{1}{2}\left(x^a(u) + x^{-a}(u)\right). \tag{8.27}$$

Having made this comment, we will now develop tools for solving the equations (8.18) - (8.21). Notice first that if we solve them in the order (8.20), (8.18), (8.21), (8.19), substituting into each subsequent equation the solution of all the previous, then at each step the problem we have to solve has a form

$$\tilde{f} + f = h \;\text{ or }\; \tilde{f} - f = h \;\;, \tag{8.28}$$

where h is known, f is unknown and both the right hand side and the left hand side are power series in x. It is obvious that equations (8.28) have solutions only for h such that $h = \tilde{h}$ and $h = -\tilde{h}$ respectively. On the class of such h a particular solution for f can be written as

$$f = [h]_- + [h]_0/2 \equiv H \cdot h \;\;\Rightarrow\;\; \tilde{f} + f = h \tag{8.29}$$

and

$$f = -[h]_- \equiv K \cdot h \;\;\Rightarrow\;\; \tilde{f} - f = h, \tag{8.30}$$

where $[h]_0$ is the constant part of Laurent expansion of h (it does not appear in the second equation, because h such that $h = -\tilde{h}$ does not have a constant part). The operators K and H introduced here can be also defined by their integral kernels

$$H(u,v) = -\frac{1}{4\pi i}\frac{\sqrt{u-2g}\sqrt{u+2g}}{\sqrt{v-2g}\sqrt{v+2g}}\frac{1}{u-v}dv, \tag{8.31}$$

$$K(u,v) = +\frac{1}{4\pi i}\frac{1}{u-v}dv. \tag{8.32}$$

which are equivalent to (8.29),(8.30) of the classes of h such that $h = \tilde{h}$ and $h = -\tilde{h}$ respectively[15]. The particular solution $f = H \cdot h$ of the equation $\tilde{f} + f = h$ is unique in the class of functions f decaying at infinity, and the solution $f = K \cdot h$ of $\tilde{f} - f = h$ is unique for non-growing f. In all other cases the general solution will include zero modes, which, in our case are fixed by asymptotics of $\mathbf{P}_a$.

[15] We denote e.g. $K \cdot h = \oint_{-2g}^{2g} K(u,v)h(v)dv$ where the integral is around the branch cut between $-2g$ and $2g$.

Now it is easy to write the explicit solution of the equations (8.18)-(8.21):

$$\begin{aligned}
\mathbf{P}_3^{(1)} &= H \cdot r_3, && (8.33)\\
\mathbf{P}_1^{(1)} &= \frac{1}{2}\mathbf{P}_3^{(1)} + K \cdot \left(r_1 - \frac{1}{2} r_3\right), && (8.34)\\
\mathbf{P}_4^{(1)} &= K \cdot \left(-\frac{1}{2}\left(\tilde{\mathbf{P}}_3^{(1)} - \mathbf{P}_3^{(1)}\right)\sinh(2\pi u) + \frac{2r_4 + r_3 \sinh(2\pi u)}{2}\right) - 2\delta, && (8.35)\\
\mathbf{P}_2^{(1)} &= H \cdot \left(-\frac{1}{2}\left(\mathbf{P}_4^{(1)} + \sinh(2\pi u)\mathbf{P}_1^{(1)} + \tilde{\mathbf{P}}_4^{(1)} + \sinh(2\pi u)\tilde{\mathbf{P}}_1^{(1)}\right) + \right. && (8.36)\\
&\quad \left. + \frac{r_4 + \sinh(2\pi u) r_1 + 2r_2}{2}\right) + \delta,
\end{aligned}$$

where δ is a constant fixed uniquely by requiring $\mathcal{O}(1/u^2)$ asymptotics for $\mathbf{P}_2$. This asymptotic also sets the last coefficient $c_{1,24}$ left in π_{12} to zero. Thus in the class of functions with asymptotics (6.7) the solution for μ_{ab} and $\mathbf{P}_a$ is unique up to a γ-transformation.

8.4 Result for $J = 2$

In order to obtain the result for the anomalous dimension, we again use the formulas (6.9), (6.10) which connect the leading coefficients of $\mathbf{P}_a$ with Δ, J and S. After plugging in A_i which we find from our solution, we obtain the result for the S^2 correction to the anomalous dimension:

$$\begin{aligned}
\gamma^{(2)}_{J=2} &= \frac{\pi}{g^2(I_1 - I_3)^3} \oint \frac{du_x}{2\pi i} \oint \frac{du_y}{2\pi i} \left[\frac{8 I_1^2 (I_1 + I_3)\left(x^3 - \left(x^2+1\right) y\right)}{(x^3 - x)\, y^2} \right. && (8.37)\\
&\quad + \frac{8 \mathrm{sh}^x_- \mathrm{sh}^y_- \left(x^2 y^2 - 1\right)\left(I_1(x^4 y^2 + 1) - I_3 x^2 (y^2+1)\right)}{x^2 \left(x^2 - 1\right) y^2}\\
&\quad - \frac{4 (\mathrm{sh}^y_-)^2 x^2 \left(y^4 - 1\right)\left(I_1(2x^2 - 1) - I_3\right)}{\left(x^2 - 1\right) y^2}\\
&\quad + \frac{8 I_1^2 \mathrm{sh}^y_- x \left(2\left(x^3 - x\right)\left(y^3 + y\right) - 2x^2\left(y^4 + y^2 + 1\right) + y^4 + 4y^2 + 1\right)}{\left(x^2 - 1\right) y^2}\\
&\quad - \frac{8 (I_1 - I_3) I_1 \mathrm{sh}^y_- x (x - y)(xy - 1)}{\left(x^2 - 1\right) y}\\
&\quad \left. - \frac{4 (I_1 - I_3)(\mathrm{sh}^x_-)^2 \left(x^2 + 1\right) y^2}{\left(x^2 - 1\right)} \right] \frac{1}{4\pi i} \partial_u \log \frac{\Gamma(i u_x - i u_y + 1)}{\Gamma(1 - i u_x + i u_y)}\,.
\end{aligned}$$

Here the integration contour goes around the branch cut at $(-2g, 2g)$. We also denote $\mathrm{sh}^x_- = \sinh_-(x)$, $\mathrm{sh}^y_- = \sinh_-(y)$ (recall that $\sinh_-$ was defined in (7.14)). This is our final result for the curvature function at any coupling.

It is interesting to note that our result contains the combination $\log \frac{\Gamma(iu_x - iu_y + 1)}{\Gamma(1 - iu_x + iu_y)}$ which plays an essential role in the construction of the BES dressing phase. We will use this

identification in section 10.3 to compute the integral in (8.37) numerically with high precision.

In the next subsections we will describe generalizations of the $J = 2$ result to operators with $J = 3$ and $J = 4$.

8.5 Results for higher J

Solving the $\mathbf{P}\mu$-system for $J = 3, 4$ is similar to the $J = 2$ case described above, except for several technical complications (mainly that $\mathbf{P}_a$ have a branch point at infinity for $J = 3$). For the sake of clarity, let us present only the final results here (full details can be found in [15]). For $J = 3$ we get

$$\begin{aligned}\gamma^{(2)}_{J=3} = \oint \frac{du_x}{2\pi i} \oint \frac{du_y}{2\pi i} i \frac{1}{g^2(I_2 - I_4)^3} \Bigg[& \frac{2\left(x^6-1\right) y (\mathrm{ch}^y_-)^2 (I_2 - I_4)}{x^3\left(y^2-1\right)} - \\ & - \frac{4\mathrm{ch}^x_- \mathrm{ch}^y_- \left(x^3y^3-1\right)\left(I_2 x^5 y^3 + I_2 - I_4 x^2\left(xy^3+1\right)\right)}{x^3\left(x^2-1\right)y^3} + \\ & + \frac{(y^2-1)(\mathrm{ch}^y_-)^2 I_2 \left(\left(x^8+1\right)\left(2y^4+3y^2+2\right) - \left(x^6+x^2\right)\left(y^2+1\right)^2\right)}{x^3\left(x^2-1\right)y^3} - \\ & - \frac{(y^2-1)(\mathrm{ch}^y_-)^2 I_4 \left(\left(x^8+1\right)y^2 + \left(x^6+x^2\right)\left(y^4+1\right)\right)}{x^3\left(x^2-1\right)y^3} - \\ & - \mathrm{ch}^y_- \frac{4 I_2 (x-y)(xy-1) F_1(x,y)}{x^3\left(x^2-1\right)y^3} - \\ & - \frac{I_2^2 (y^2-1)(x-y)(xy-1) F_2(x,y)}{x^3\left(x^2-1\right)y^3} \Bigg] \\ & \frac{1}{4\pi i} \partial_u \log \frac{\Gamma(iu_x - iu_y + 1)}{\Gamma(1 - iu_x + iu_y)}.\end{aligned} \tag{8.38}$$

with

$$F_1 = I_2\left(\left(x^6+1\right)\left(y^3+y\right) + \left(x^5+x\right)\left(y^4+y^2+1\right) - x^3\left(y^4+1\right)\right) + I_4 x^3 y^2 \tag{8.39}$$

$$F_2 = I_2\left(\left(x^6+x^4+x^2+1\right)y + 2x^3\left(y^2+1\right)\right) + I_4\left(x^5+x\right)\left(y^2+1\right) \tag{8.40}$$

We defined $\mathrm{ch}^x_- = \cosh_-(x)$ and $\mathrm{ch}^y_- = \cosh_-(y)$, where $\cosh_-(x)$ is the part of the Laurent expansion of $\cosh\left(g(x+1/x)\right)$ vanishing at infinity, i.e.

$$\cosh_-(x) = \sum_{k=1}^{\infty} I_{2k} x^{-2k}. \tag{8.41}$$

The result for $J = 4$ is given in appendix A.3.

9 Weak coupling tests and predictions

Our results for the curvature function $\gamma^{(2)}(g)$ at $J = 2, 3, 4$ (Eqs. (8.37), (8.38), (A.17)) are straightforward to expand at weak coupling. We give expansions to 10 loops for $J = 2$ in appendix A.4 (more data can be found in [15]). Let us start with the $J = 2$ case, for which we found

$$\begin{aligned}\gamma^{(2)}_{J=2} &= -8g^2\zeta_3 + g^4\left(140\zeta_5 - \frac{32\pi^2\zeta_3}{3}\right) + g^6\left(200\pi^2\zeta_5 - 2016\zeta_7\right) \\ &+ g^8\left(-\frac{16\pi^6\zeta_3}{45} - \frac{88\pi^4\zeta_5}{9} - \frac{9296\pi^2\zeta_7}{3} + 27720\zeta_9\right) \\ &+ g^{10}\left(\frac{208\pi^8\zeta_3}{405} + \frac{160\pi^6\zeta_5}{27} + 144\pi^4\zeta_7 + 45440\pi^2\zeta_9 - 377520\zeta_{11}\right) + \dots\end{aligned} \tag{9.1}$$

Remarkably, at each loop order all contributions have the same transcendentality, and only simple zeta values (i.e. ζ_n) appear. This is also true for the $J = 3$ and $J = 4$ cases.

We can check this expansion against known results, as the anomalous dimensions of twist two operators have been computed up to five loops for arbitrary spin [98, 99, 100, 101, 102, 103, 104, 105] (see also [106] and the review [69]). To three loops they can be found solely from the ABA equations, while at four and five loops wrapping corrections need to be taken into account which was done in [104, 105] by utilizing generalized Luscher formulas. All these results are given by linear combinations of harmonic sums

$$S_a(N) = \sum_{n=1}^{N} \frac{(\mathrm{sign}(a))^n}{n^{|a|}}, \quad S_{a_1,a_2,a_3,\dots}(N) = \sum_{n=1}^{N} \frac{(\mathrm{sign}(a_1))^n}{n^{|a_1|}} S_{a_2,a_3,\dots}(n) \tag{9.2}$$

with argument equal to the spin S. To make a comparison with our results we expanded these predictions in the $S \to 0$ limit. For this lengthy computation, as well as to simplify the final expressions, we used the `Mathematica` packages HPL [107], the package [108] provided with the paper [109], and the HarmonicSums package [110].

In this way we have confirmed the coefficients in (9.1) to four loops. Let us note that expansion of harmonic sums leads to multiple zeta values (MZVs), which however cancel in the final result leaving only ζ_n.

Importantly, the part of the four-loop coefficient which comes from the wrapping correction is essential for matching with our result. This is a strong confirmation that our calculation based on the $\mathbf{P}\mu$-system is valid beyond the ABA level. Additional evidence that our result incorporates all finite-size effects is found at strong coupling (see section 10).

For operators with $J = 3$, our prediction at weak coupling is

$$\begin{aligned}\gamma^{(2)}_{J=3} &= -2g^2\zeta_3 + g^4\left(12\zeta_5 - \frac{4\pi^2\zeta_3}{3}\right) + g^6\left(\frac{2\pi^4\zeta_3}{45} + 8\pi^2\zeta_5 - 28\zeta_7\right) \\ &+ g^8\left(-\frac{4\pi^6\zeta_3}{45} - \frac{4\pi^4\zeta_5}{15} - 528\zeta_9\right) + \dots\end{aligned} \tag{9.3}$$

The known results for any spin in this case are available at up to six loops, including the wrapping correction which first appears at five loops [111, 112, 113]. Expanding them at $S \to 0$ we have checked our calculation to four loops.

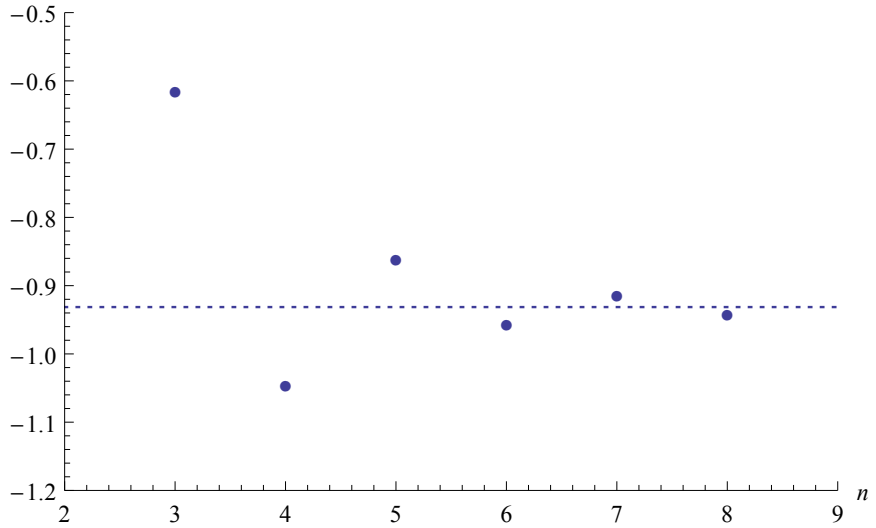

Figure 4: **One-loop energy at $J = 4$ from the Bethe ansatz.** The dashed line shows the result from the $\mathbf{P}\mu$-system for the coefficient of S^2 in the 1-loop energy at $J = 4$, i.e. $-\frac{14\zeta_3}{5} + \frac{48\zeta_5}{\pi^2} - \frac{252\zeta_7}{\pi^4} \approx -0.931$ (see (9.4)). The dots show the Bethe ansatz prediction (9.5) expanded to orders $1/J^3, 1/J^4, \dots, 1/J^8$ (the order of expansion n corresponds to the horizontal axis), and it appears to converge to the $\mathbf{P}\mu$-system result.

Let us now discuss the $J = 4$ case. The expansion of our result reads:

$$\begin{aligned}\gamma^{(2)}_{J=4} &= g^2\left(-\frac{14\zeta_3}{5} + \frac{48\zeta_5}{\pi^2} - \frac{252\zeta_7}{\pi^4}\right) \\ &+ g^4\left(-\frac{22\pi^2\zeta_3}{25} + \frac{474\zeta_5}{5} - \frac{8568\zeta_7}{5\pi^2} + \frac{8316\zeta_9}{\pi^4}\right) \\ &+ g^6\left(\frac{32\pi^4\zeta_3}{875} + \frac{3656\pi^2\zeta_5}{175} - \frac{56568\zeta_7}{25} + \frac{196128\zeta_9}{5\pi^2} - \frac{185328\zeta_{11}}{\pi^4}\right) \\ &+ g^8\left(-\frac{4\pi^6\zeta_3}{175} - \frac{68\pi^4\zeta_5}{75} - \frac{55312\pi^2\zeta_7}{125} + \frac{1113396\zeta_9}{25} - \frac{3763188\zeta_{11}}{5\pi^2}\right. \\ &\qquad \left. + \frac{3513510\zeta_{13}}{\pi^4}\right) + \dots\end{aligned} \tag{9.4}$$

Unlike for the $J = 2$ and $J = 3$ cases, we could not find a closed expression for the energy at any spin S in literature even at one loop, however there is another way to check our

result. One can expand the asymptotic Bethe ansatz equations at large J for fixed values of $S = 2, 4, 6, \dots$ and then extract the coefficients in the expansion which are polynomial in S. This was done in [93] (see appendix C there) where at one loop the expansion was found up to order $1/J^6$:

$$\gamma(S,J) \;=\; g^2\left(\frac{S}{2\,J^2}-\Big(\frac{S^2}{4}+\frac{S}{2}\Big)\frac{1}{J^3}+\Big[\frac{3S^3}{16}+\Big(\frac{1}{8}-\frac{\pi^2}{12}\Big)S^2+\frac{S}{2}\Big]\frac{1}{J^4}+\dots\right)+\mathcal{O}(g^4) \tag{9.5}$$

Now taking the part proportional to S^2 and substituting $J = 4$ one may expect to get a numerical approximation to the 1-loop coefficient in our result (9.4), i.e. $-\frac{14\zeta_3}{5}+\frac{48\zeta_5}{\pi^2}-\frac{252\zeta_7}{\pi^4}$. To increase the precision we extended the expansion in (9.5) to order $1/J^8$. Remarkably, in this way we confirmed the 1-loop part of the $\mathbf{P}\mu$ prediction (9.4) with about 1% accuracy! In Fig. 9 one can also see that the ABA result converges to our prediction when the order of expansion in $1/J$ is being increased. Later on our analytic prediction for $J = 4$ was confirmed in [114] where the curvature function at 1 loop was computed from the ABA for any J.

Also, in contrast to $J = 2$ and $J = 3$ cases we see that negative powers of π appear in (9.4) (although still all the contributions at a given loop order have the same transcendentality). It would be interesting to understand why this happens from the gauge theory perspective, especially since expansion of the leading S term (5.3) has the same structure for all J,

$$\gamma_J^{(1)} = \frac{8\pi^2 g^2}{J(J+1)} - \frac{32\pi^4 g^4}{J(J+1)^2(J+2)} + \frac{256\pi^6 g^6}{J(J+1)^3(J+2)(J+3)} + \dots \tag{9.6}$$

The change of structure at $J = 4$ might be related to the fact that for $J \geq 4$ the ground state anomalous dimension even at one loop is expected to be an irrational number for integer $S > 0$ (see [115], [116]), and thus cannot be written as a linear combination of harmonic sums with integer coefficients.

In the next section we will discuss tests and applications of our results at strong coupling.

10 Strong coupling tests and predictions

In this section we will present the strong coupling expansion of our results for the curvature function, and link these results to anomalous dimensions of short operators at strong coupling. We will also obtain new predictions for the BFKL pomeron intercept.

10.1 Expansion of the curvature function for $J = 2, 3, 4$

To obtain the strong coupling expansion of our exact results for the curvature function, we evaluated it numerically with high precision for a range of values of g and then made a fit to find the expansion coefficients. It would also be interesting to carry out the expansion analytically, and we leave this for the future.

For numerical study it is convenient to write our exact expressions (8.37), (8.38), (A.17) for $\gamma^{(2)}(g)$, which have the form

$$\gamma^{(2)}(g) = \oint du_x \oint du_y f(x,y) \partial_{u_x} \log \frac{\Gamma(iu_x - iu_y + 1)}{\Gamma(1 - iu_x + iu_y)} \tag{10.1}$$

where the integration goes around the branch cut between $-2g$ and $2g$, in a slightly different way (we remind that we use notation $x + \frac{1}{x} = \frac{u_x}{g}$ and $y + \frac{1}{y} = \frac{u_y}{g}$). Namely, by changing the variables of integration to x, y and integrating by parts one can write the result as

$$\gamma^{(2)}(g) = \oint dx \oint dy F(x,y) \log \frac{\Gamma(iu_x - iu_y + 1)}{\Gamma(iu_y - iu_x + 1)} \tag{10.2}$$

where $F(x,y)$ is some polynomial in the following variables: x, $1/x$, y, $1/y$, sh_-^x and sh_-^y (for $J = 3$ it includes ch_-^x, ch_-^y instead of the sh_- functions). The integral in (10.2) is over the unit circle. The advantage of this representation is that plugging in sh_-^x, sh_-^y as series expansions (truncated to some large order), we see that it only remains to compute integrals of the kind

$$C_{r,s} = \frac{1}{i} \oint \frac{dx}{2\pi} \oint \frac{dy}{2\pi} x^r y^s \log \frac{\Gamma(iu_x - iu_y + 1)}{\Gamma(iu_y - iu_x + 1)} \tag{10.3}$$

These are nothing but the coefficients of the BES dressing phase [117, 118, 119, 33]. They can be conveniently computed using the strong coupling expansion [117]

$$C_{r,s} = \sum_{n=0}^{\infty} \left[- \frac{2^{-n-1}(-\pi)^{-n} g^{1-n} \zeta_n \left(1 - (-1)^{r+s+4}\right) \Gamma\left(\frac{1}{2}(n - r + s - 1)\right) \Gamma\left(\frac{1}{2}(n + r + s + 1)\right)}{\Gamma(n-1) \Gamma\left(\frac{1}{2}(-n - r + s + 3)\right) \Gamma\left(\frac{1}{2}(-n + r + s + 5)\right)} \right] \tag{10.4}$$

However this expansion is only asymptotic and does not converge. For fixed g the terms will start growing with n when n is greater than some value N, and we only summed the terms up to $n = N$ which gives the value of $C_{r,s}$ with very good precision for large enough g.

Using this approach we computed the curvature function for a range of values of g (typically we took $7 \leq g \leq 30$) and then fitted the result as an expansion in $1/g$. This gave us only numerical values of the expansion coefficients, but in fact we found that with

very high precision the coefficients are as follows. For $J = 2$

$$\begin{aligned}\gamma^{(2)}_{J=2} &= -\pi^2 g^2 + \frac{\pi g}{4} + \frac{1}{8} - \frac{1}{\pi g}\left(\frac{3\zeta_3}{16} + \frac{3}{512}\right) - \frac{1}{\pi^2 g^2}\left(\frac{9\zeta_3}{128} + \frac{21}{512}\right) \\ &+ \frac{1}{\pi^3 g^3}\left(\frac{3\zeta_3}{2048} + \frac{15\zeta_5}{512} - \frac{3957}{131072}\right) + \dots ,\end{aligned} \tag{10.5}$$

then for $J = 3$

$$\begin{aligned}\gamma^{(2)}_{J=3} &= -\frac{8\pi^2 g^2}{27} + \frac{2\pi g}{27} + \frac{1}{12} - \frac{1}{\pi g}\left(\frac{1}{216} + \frac{\zeta_3}{8}\right) - \frac{1}{\pi^2 g^2}\left(\frac{3\zeta_3}{64} + \frac{743}{13824}\right) \\ &+ \frac{1}{\pi^3 g^3}\left(\frac{41\zeta_3}{1024} + \frac{35\zeta_5}{512} - \frac{5519}{147456}\right) + \dots ,\end{aligned} \tag{10.6}$$

and finally for $J = 4$

$$\begin{aligned}\gamma^{(2)}_{J=4} &= -\frac{\pi^2 g^2}{8} + \frac{\pi g}{32} + \frac{1}{16} - \frac{1}{\pi g}\left(\frac{3\zeta_3}{32} + \frac{15}{4096}\right) - \frac{0.01114622551913}{g^2} \\ &+ \frac{0.004697583899}{g^3} + \dots .\end{aligned} \tag{10.7}$$

To fix coefficients for the first four terms in the expansion we were guided by known analytic predictions which will be discussed below, and found that our numerical result matches these predictions with high precision. Then for $J = 2$ and $J = 3$ we extracted the numerical values obtained from the fit for the coefficients of $1/g^2$ and $1/g^3$, and plugging them into the online calculator EZFace [120] we obtained a prediction for their exact values as combinations of ζ_3 and ζ_5. Fitting again our numerical results with these exact values fixed, we found that the precision of the fit at the previous orders in $1/g$ increased. This is a highly nontrivial test for the proposed exact values of $1/g^2$ and $1/g^3$ terms. For $J = 2$ we confirmed the coefficients of these terms with absolute precision 10^{-17} and 10^{-15} at $1/g^2$ and $1/g^3$ respectively (at previous orders of the expansion the precision is even higher). For $J = 3$ the precision was correspondingly 10^{-15} and 10^{-13}.

For $J = 4$ we were not able to get a stable fit for the $1/g^2$ and $1/g^3$ coefficients from EZFace, so above we gave their numerical values (with uncertainty in the last digit). However below we will see that based on $J = 2$ and $J = 3$ results one can make a prediction for these coefficients, which we again confirmed by checking that precision of the fit at the previous orders in $1/g$ increases. The precision of the final fit at orders $1/g^2$ and $1/g^3$ is 10^{-16} and 10^{-14} respectively.

10.2 Generalization to any J

Here we will find an analytic expression for the strong coupling expansion of the curvature function which generalizes the formulas (10.5) and (10.6) to any J. To this end it will

be beneficial to consider the structure of classical expansions of the scaling dimension. A good entry point is considering the inverse relation $S(\Delta)$, frequently encountered in the context of BFKL. It satisfies a few basic properties, namely the curve $S(\Delta)$ goes through the points $(\pm J, 0)$ at any coupling, because at $S = 0$ the operator is BPS. At the same time for non-BPS states one should have $\Delta(\lambda) \propto \lambda^{1/4} \to \infty$ [2] which indicates that if Δ is fixed, S should go to zero, thus combining this with the knowledge of fixed points $(\pm J, 0)$ we conclude that at infinite coupling $S(\Delta)$ is simply the line $S = 0$. As the coupling becomes finite $S(\Delta)$ starts bending from the $S = 0$ line and starts looking like a parabola going through the points $\pm J$, see fig. 10.4. Based on this qualitative picture and the scaling $\Delta(\lambda) \propto \lambda^{1/4}$ at $\lambda \to \infty$ and fixed J and S, one can write down the following ansatz,

$$\begin{aligned} S(\Delta) &= \left(\Delta^2 - J^2\right)\Big(\alpha_1 \frac{1}{\lambda^{1/2}} + \alpha_2 \frac{1}{\lambda} + (\alpha_3 + \beta_3\Delta^2)\frac{1}{\lambda^{3/2}} + (\alpha_4 + \beta_4\Delta^2)\frac{1}{\lambda^2} \\ &+ (\alpha_5 + \beta_5\Delta^2 + \gamma_5\Delta^4)\frac{1}{\lambda^{5/2}} + (\alpha_6 + \beta_6\Delta^2 + \gamma_6\Delta^4)\frac{1}{\lambda^3} + \dots\Big). \end{aligned} \tag{10.8}$$

We omit odd powers of the scaling dimension from the ansatz, as only the square of Δ enters the $\mathbf{P}\mu$-system. We can now invert the relation and express Δ in terms of S at strong coupling, which gives

$$\Delta^2 = J^2 + S\left(A_1\sqrt{\lambda} + A_2 + \dots\right) + S^2\left(B_1 + \frac{B_2}{\sqrt{\lambda}} + \dots\right) + S^3\left(\frac{C_1}{\lambda^{1/2}} + \frac{C_2}{\lambda} + \dots\right) + \mathcal{O}(S^4)\,, \tag{10.9}$$

where the coefficients A_i, B_i, C_i are some functions of J. There exists a one-to-one mapping between the coefficients α_i, β_i, etc. and A_i, B_i etc, which is rather complicated but easy to find. We note that this structure of Δ^2 coincides with Basso's conjecture in [90] for mode number $n = 1$ [16]. The pattern in (10.9) continues to higher orders in S with further coefficients D_i, E_i, etc. and powers of λ suppressed incrementally. This structure is a nontrivial constraint on Δ itself as one easily finds from (10.9) that

$$\begin{aligned} \Delta &= J + \frac{S}{2J}\left(A_1\sqrt{\lambda} + A_2 + \frac{A_3}{\sqrt{\lambda}} + \dots\right) \\ &+ S^2\left(-\frac{A_1^2}{8J^3}\lambda - \frac{A_1A_2}{4J^3}\sqrt{\lambda} + \left[\frac{B_1}{2J} - \frac{A_2^2 + 2A_1A_3}{8J^3}\right]\right. \\ &+ \left.\left[\frac{B_2}{2J} - \frac{A_2A_3 + A_1A_4}{4J^3}\right]\frac{1}{\sqrt{\lambda}} + \dots\right). \end{aligned} \tag{10.10}$$

By definition the coefficients of S and S^2 are the slope and curvature functions respectively, so now we have their expansions at strong coupling in terms of A_i, B_i, C_i, etc. Since the S coefficient only contains the constants A_i, we can find all of their values by simply

[16] The generalization of (10.9) for $n > 1$ is not fully clear, as noted in [121].

expanding the slope function (7.35) at strong coupling. We get

$$A_1 = 2 \ , \ A_2 = -1 \ , \ A_3 = J^2 - \frac{1}{4} \ , \ A_4 = J^2 - \frac{1}{4} \dots \ . \tag{10.11}$$

Note that in this series the power of J increases by two at every other member, which is a direct consequence of omitting odd powers of Δ from (10.8). We also expect the same pattern to hold for the coefficients B_i, C_i, etc.

The curvature function written in terms of A_i, B_i, etc. is given by

$$\begin{aligned} \gamma_J^{(2)}(g) &= -\frac{2\pi^2 g^2 A_1^2}{J^3} - \frac{\pi g A_1 A_2}{J^3} - \frac{A_2^2 + 2A_1 A_3 - 4B_1 J^2}{8J^3} \qquad (10.12) \\ &- \frac{A_2 A_3 + A_1 A_4 - 2B_2 J^2}{16\pi g J^3} \\ &- \frac{A_3^2 + 2A_2 A_4 + 2A_1 A_5 - 4B_3 J^2}{128\pi^2 g^2 J^3} \qquad (10.13) \\ &- \frac{A_3 A_4 + A_2 A_5 + A_1 A_6 - 2B_4 J^2}{256\pi^3 g^3 J^3} + \mathcal{O}\left(\frac{1}{g^4}\right). \end{aligned}$$

The remaining unknowns here (up to order $1/g^4$) are B_1, B_2, which we expect to be constant due to the power pattern noticed above and B_3, B_4, which we expect to have the form $aJ^2 + b$ with a and b constant. These unknowns are immediately fixed by comparing the general curvature expansion (10.12) to the two explicit cases that we know for $J = 2$ and $J = 3$. We find

$$B_1 = 3/2 \ , \ B_2 = -3\,\zeta_3 + \frac{3}{8}, \tag{10.14}$$

and

$$B_3 = -\frac{J^2}{2} - \frac{9\,\zeta_3}{2} + \frac{5}{16} \ , \ B_4 = \frac{3}{16} J^2 (16\,\zeta_3 + 20\,\zeta_5 - 9) - \frac{15\,\zeta_5}{2} - \frac{93\,\zeta_3}{8} - \frac{3}{16}. \tag{10.15}$$

Having fixed all the unknowns we can write the strong coupling expansion of the curvature function for arbitrary values of J as

$$\begin{aligned} \gamma_J^{(2)}(g) &= -\frac{8\pi^2 g^2}{J^3} + \frac{2\pi g}{J^3} + \frac{1}{4J} + \frac{1 - J^2(24\,\zeta_3 + 1)}{64\pi g J^3} - \frac{8J^4 + J^2(72\,\zeta_3 + 11) - 4}{512 g^2 (\pi^2 J^3)} \\ &+ \frac{3\left(8J^4(16\,\zeta_3 + 20\,\zeta_5 - 7) - 16J^2(31\,\zeta_3 + 20\,\zeta_5 + 7) + 25\right)}{16384\pi^3 g^3 J^3} + \mathcal{O}\left(\frac{1}{g^4}\right) \end{aligned} \tag{10.16}$$

Expanding $\gamma_{J=4}^{(2)}$ defined in (A.17) at strong coupling numerically we were able to confirm the above result with high precision.

10.3 Anomalous dimension of short operators

In this section we will use the knowledge of slope functions $\gamma_J^{(n)}$ at strong coupling to find the strong coupling expansions of scaling dimensions of operators with finite S and J, in

particular we will find the three loop coefficient of the Konishi operator by utilizing the techniques of [90, 121]. What follows is a quick recap of the main ideas in these papers.

We are interested in the coefficients of the strong coupling expansion of Δ, namely

$$\Delta = \Delta^{(0)}\lambda^{\frac{1}{4}} + \Delta^{(1)}\lambda^{-\frac{1}{4}} + \Delta^{(2)}\lambda^{-\frac{3}{4}} + \Delta^{(3)}\lambda^{-\frac{5}{4}} + \dots \tag{10.17}$$

First, we use Basso's conjecture (10.9) and by fixing S and J we re-expand the square root of Δ^2 at strong coupling to find

$$\Delta = \sqrt{A_1 S}\,\sqrt[4]{\lambda} + \frac{\sqrt{A_1}\left(J^2 + A_2 S + B_1 S^2\right)}{2A_1\sqrt{S}}\,\frac{1}{\sqrt[4]{\lambda}} + \mathcal{O}\left(\frac{1}{\lambda^{\frac{3}{4}}}\right). \tag{10.18}$$

Thus we reformulate the problem entirely in terms of the coefficients A_i, B_i, C_i, etc. For example, the next coefficient in the series, namely the two-loop term is given by

$$\Delta^{(2)} = -\frac{\left(2A_2 + 4B_1 + J^2\right)^2 - 16A_1(A_3 + 2B_2 + 4C_1)}{16\sqrt{2}A_2^{3/2}}. \tag{10.19}$$

Further coefficients become more and more complicated, however a very clear pattern can be noticed after looking at these expressions: we see that the term $\Delta^{(n)}$ only contains coefficients with indices up to $n+1$, e.g. the tree level term $\Delta^{(0)}$ only depends on A_1, the one-loop term depends on A_1, A_2, B_1, etc. Thus we can associate the index of these coefficients with the loop level. Conversely, from the last section we learned that the letter of A_i, B_i, etc. can be associated with the order in S, i.e. the slope function fixed all A_i coefficients and the curvature function in principle fixes all B_i coefficients.

10.3.1 Matching with classical and semiclassical results

Looking at (10.18) we see that knowing A_i and B_i only takes us to one loop, in order to proceed we need to know some coefficients in the C_i and D_i series. This is where the next ingredient in this construction comes in, which is the knowledge of the classical energy and its semiclassical correction in the Frolov-Tseytlin limit, i.e. when $\mathcal{S} \equiv S/\sqrt{\lambda}$ and $\mathcal{J} \equiv J/\sqrt{\lambda}$ remain fixed, while S, J, $\lambda \to \infty$. Additionally we will also be taking the limit $\mathcal{S} \to 0$ in all of the expressions that follow. In particular, the square of the classical energy has a very nice form in these limits and is given by [45, 121]

$$\mathcal{D}^2_{\text{classical}} \;=\; \mathcal{J}^2 + 2\,\mathcal{S}\,\sqrt{\mathcal{J}^2+1} + \mathcal{S}^2\,\frac{2\mathcal{J}^2+3}{2\mathcal{J}^2+2} - \mathcal{S}^3\,\frac{\mathcal{J}^2+3}{8\left(\mathcal{J}^2+1\right)^{5/2}} + \mathcal{O}\left(\mathcal{S}^4\right), \tag{10.20}$$

where $\mathcal{D}_{\text{classical}} \equiv \Delta_{classical}/\sqrt{\lambda}$. The 1-loop correction to the classical energy is given by

$$\Delta_{sc} \simeq \frac{-\mathcal{S}}{2\left(\mathcal{J}^3+\mathcal{J}\right)} + \mathcal{S}^2\left[\frac{3\mathcal{J}^4+11\mathcal{J}^2+17}{16\mathcal{J}^3\left(\mathcal{J}^2+1\right)^{5/2}} - \sum_{\substack{m>0\\ m\neq n}} \frac{n^3m^2\left(2m^2+n^2\mathcal{J}^2-n^2\right)}{\mathcal{J}^3\left(m^2-n^2\right)^2\left(m^2+n^2\mathcal{J}^2\right)^{3/2}}\right] \tag{10.21}$$

(S, J)	$\lambda^{-5/4}$ prediction	$\lambda^{-5/4}$ fit	error	fit order
$(2, 2)$	$\frac{15\,\zeta_5}{2} + 6\,\zeta_3 + \frac{1}{2} = 15.48929958$	14.12099034	9.69%	6
$(2, 3)$	$\frac{15\,\zeta_5}{2} + \frac{63\,\zeta_3}{8} - \frac{619}{512} = 16.03417190$	14.88260078	7.74%	5
$(2, 4)$	$\frac{21\,\zeta_3}{2} + \frac{15\,\zeta_5}{2} - \frac{17}{8} = 18.27355565$	16.46106336	11.0%	7

Table 1: **Comparisons of strong coupling expansion coefficients for $\lambda^{-5/4}$ obtained from fits to TBA data versus our predictions for various operators.** The fit order is the order of polynomials used for the rational fit function (see [121] for details).

If the parameters $\mathcal{S}$ and $\mathcal{J}$ are fixed to some values then the sum can be evaluated explicitly in terms of zeta functions. We now add up the classical and the 1-loop contributions[17], take S and J fixed at strong coupling and compare the result to (10.9). By requiring consistency we are able to extract the following coefficients,

$$\begin{aligned}
A_1 &= 2, & A_2 &= -1 \\
B_1 &= 3/2, & B_2 &= -3\,\zeta_3 + \tfrac{3}{8} \\
C_1 &= -3/8, & C_2 &= \tfrac{3}{16}\,(20\,\zeta_3 + 20\,\zeta_5 - 3) \\
D_1 &= 31/64, & D_2 &= \tfrac{1}{512}(-4720\,\zeta_3 - 4160\,\zeta_5 - 2520\,\zeta_7 + 81)
\end{aligned}$$

As discussed in the previous section, we can in principle extract all coefficients with indices 1 and 2. In order to find e.g. B_3 we would need to extend the quantization of the classical solution to the next order. Note that the coefficients A_1, A_2 and B_1, B_2 have the same exact values that we extracted from the slope and curvature functions.

10.3.2 Result for the anomalous dimensions at strong coupling

The key observation in [121] was that once written in terms of the coefficients A_i, B_i, C_i, the two-loop term $\Delta^{(2)}$ only depends on $A_{1,2,3}$, $B_{1,2}$, C_1 as can be seen in (10.19). As discussed in the last section, the one-loop result fixes all of these constants except A_3, which in principle is a contribution from a true two-loop calculation. However we already fixed it from the slope function and thus we are able to find

$$\Delta^{(2)} = \frac{-21\,S^4 + (24 - 96\,\zeta_3)S^3 + 4\left(5J^2 - 3\right)S^2 + 8J^2S - 4J^4}{64\sqrt{2}\,S^{3/2}}. \tag{10.22}$$

Now that we know the strong coupling expansion of the curvature function and thus all the coefficients B_i, we can do the same trick and find the three loop strong coupling scaling dimension coefficient $\Delta^{(3)}$, which now depends on $A_{1;2;3;4}$, $B_{1,2,3}$, $C_{1,2}$, D_1. We find it to

[17] Note that they mix various orders of the coupling.

be

$$\Delta^{(3)} = \frac{187\,S^6 + 6\,(208\,\zeta_3 + 160\,\zeta_5 - 43)\,S^5 + \left(-146\,J^2 - 4\,(336\,\zeta_3 - 41)\right)S^4}{512\sqrt{2}\,S^{5/2}} + \\ + \frac{\left(32\,(6\,\zeta_3 + 7)\,J^2 - 88\right)S^3 + \left(-28\,J^4 + 40\,J^2\right)S^2 - 24\,J^4 S + 8\,J^6}{512\sqrt{2}\,S^{5/2}}, \quad (10.23)$$

for $S = 2$ it simplifies to

$$\Delta^{(3)}_{S=2} = \frac{1}{512}\left(J^6 - 20J^4 + 48J^2(4\zeta_3 - 1) + 64(36\,\zeta_3 + 60\,\zeta_5 + 11)\right) \quad (10.24)$$

and finally for the Konishi operator, which has $S = 2$ and $J = 2$ we get[18]

$$\Delta^{(3)}_{S=2,J=2} = \frac{15\,\zeta_5}{2} + 6\,\zeta_3 + \frac{1}{2}. \quad (10.25)$$

In order to compare our predictions with data available from TBA calculations [44], we employed Padé type fits as explained in [121]. The fit results are shown in table 1, we see that our predictions are within $\sim 10\%$ error bounds, which is a rather good agreement. However we must be honest that for the $J = 3$ and especially $J = 4$ states we did not have as many data points as for the $J = 2$ state and the fit is somewhat shaky. However we later compared the Konishi analytic prediction with our high-precision numerical solution of the QSC and found a perfect match (see the next part of this thesis).

10.4 BFKL pomeron intercept

The gauge theory operators that we consider here are of high importance in high energy scattering amplitude calculations, especially in the Regge limit of high energy and fixed momentum transfer [122, 123]. In this limit one can approximate the scattering amplitude as an exchange of effective particles, the so-called reggeized gluons, compound states of which are frequently called *pomerons*. When momentum transfer is large, perturbative computations are possible and the so-called 'hard pomeron' appears, the BFKL pomeron [124, 125, 126]. The BFKL pomeron leads to a power law behaviour of scattering amplitudes $s^{j(\Delta)}$, where $j(\Delta)$ is called the Reggeon spin and s is the energy transfer of the process. The remarkable connection between the pomeron and the operators we consider can be symbolically stated as

$$\text{pomeron} = \text{Tr}\left(Z\,\mathcal{D}^S_+\,Z\right) + \dots \quad (10.26)$$

[18] The ζ_3 and ζ_5 terms are coming from semi-classics and were already known before [94] and match our result.

where we are now considering twist two operators ($J = 2$) and the spin S can take on complex values by analytic continuation. The Reggeon spin $j(\Delta)$ (also refered to as a Regge trajectory) is a function of the anomalous dimension of the operator and is related to spin S as $j(\Delta) = S(\Delta) + 2$. Some of these trajectories are shown in figure 10.4. A very important quantity in this story is the BFKL intercept $j(0)$, which we consider next.

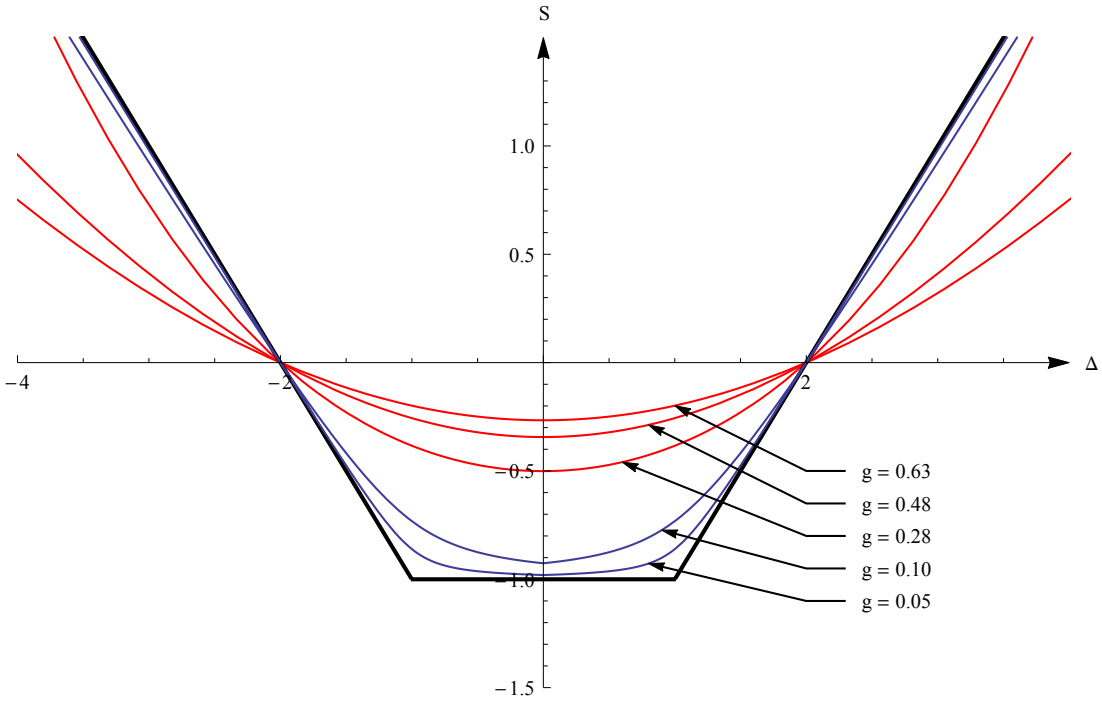

Figure 5: **The BFKL trajectories.** The BFKL trajectories $S(\Delta)$ at various values of the coupling. Blue lines are obtained using the known two loop weak coupling expansion [127, 128] and red lines are obtained using the strong coupling expansion [129, 130, 131].

One can also use the same techniques as in the previous section to calculate the strong coupling expansion of the BFKL intercept. As stated before, the intercept of a BFKL trajectory $j(\Delta)$ is simply $j(0)$ and we already wrote down an ansatz for $S(\Delta)$ in (10.8). The coefficients α_i, β_i, etc. are in one-to-one correspondence with the coefficients A_i, B_i etc. from (10.10), values of which we found in the previous sections. Plugging in their values we find

$$\alpha_1 = 1/2,\ \alpha_2 = 1/4,\ \alpha_3 = -1/16\ ,\ \alpha_4 = -\frac{3\zeta_3}{2} - \frac{1}{2}, \tag{10.27}$$

$$\alpha_5 = -\frac{9\zeta_3}{2} - \frac{361}{256},\ \alpha_6 = -\frac{39\zeta_3}{4} - \frac{511}{128} \tag{10.28}$$

$$\beta_3 = -3/16,\ \beta_4 = \frac{3\zeta_3}{8} - \frac{21}{64},\ \beta_5 = \frac{9\zeta_3}{8} - \frac{51}{128},\ \beta_6 = \frac{45\zeta_3}{8} + \frac{15\zeta_5}{16} + \frac{141}{512} \tag{10.29}$$

$$\gamma_5 = \frac{21}{128},\ \gamma_6 = -\frac{51\zeta_3}{64} - \frac{15\zeta_5}{64} + \frac{129}{256} \tag{10.30}$$

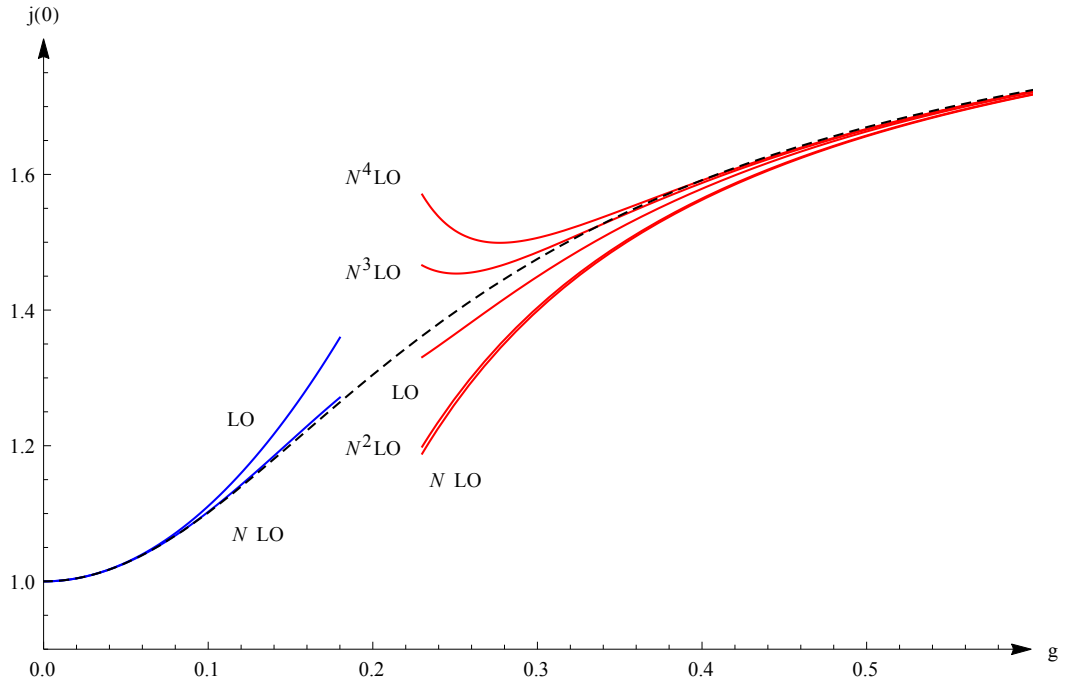

Figure 6: **The BFKL intercept.** The BFKL intercept $j(0) = 2 + S(0)$ dependence on the coupling constant g at two orders at weak coupling (blue lines), four orders at strong coupling (red lines) and a Padé type interpolating function in between (dashed line).

Furthermore, setting $\Delta = 0$ we find the intercept to be

$$\begin{aligned} j(0) = 2 + S(0) &= 2 - \frac{2}{\lambda^{1/2}} - \frac{1}{\lambda} + \frac{1}{4\,\lambda^{3/2}} + (6\zeta_3 + 2)\,\frac{1}{\lambda^2} \\ &+ \left(18\,\zeta_3 + \frac{361}{64}\right)\frac{1}{\lambda^{5/2}} + \left(39\,\zeta_3 + \frac{511}{32}\right)\frac{1}{\lambda^3} + \mathcal{O}\left(\frac{1}{\lambda^{7/2}}\right) \end{aligned} \tag{10.31}$$

The first four terms successfully reproduce known results [129, 130, 131] and the last two terms of the series are a new prediction (their derivation relies on the knowledge of the constants $B_{3,4;J=2}$ found in the last section). On Figure 10.4 we show plots of the intercept at weak and at strong coupling.

11 Conclusions

In this part we applied the recently proposed $\mathbf{P}\mu$-system of Riemann-Hilbert type equations to study anomalous dimensions in the $sl(2)$ sector of planar $\mathcal{N} = 4$ SYM theory. Our main result are the expressions (8.37), (8.38) and (A.17) for the curvature function $\gamma_J^{(2)}(g)$, i.e. the coefficient of the S^2 term in the anomalous dimension at small spin S. These results correspond to operators with twist $J = 2, 3$ and 4. Curiosly, we found that they involve essential parts of the BES dressing phase in the integral representation.

We derived these results by solving the $\mathbf{P}\mu$-system to order S^2 and they are exact at any coupling. While expansion in small S (but at any coupling) seems hardly possible to perform in the TBA approach, here it resembles a perturbative expansion – the $\mathbf{P}\mu$-system is solved order by order in S and the coupling is kept arbitrary.

For $J = 2$ and $J = 3$ our calculation perfectly matches known results to four loops at weak coupling. This includes in particular the leading finite-size correction at $J = 2$. At strong coupling we obtained the expansion of our results numerically, and also found full agreement with known predictions. This provides yet another check that our result incorporates all wrapping corrections. Going to higher orders in this expansion we were able to use the EZFace calculator [120] to fit the coefficients as linear combinations of ζ_3 and ζ_5 (and confirmed the outcome with high precision). By combining these coefficients with the other known results, we obtained the 3-loop coefficient in the Konishi anomalous dimension at strong coupling. This serves as a highly nontrivial prediction for a direct string theory calculation, which hopefully may be done along the lines of [48, 47]. Our results also predict the value of two new coefficients for the pomeron intercept at strong coupling.

Part III

Numerical solution of the spectral problem

In this part we discuss the efficient numerical method for solving the QSC, based on the paper [14].

12 Introduction

Even though many explicit analytic results are available both at strong and weak coupling, one important range of applications of the QSC that has remained unexplored for a significant time is the numerical investigation of the spectrum at finite coupling. Previous numerical methods based on TBA, even limited to a few operators[19], low precision and slow convergence rate gave, nevertheless, several highly important results, allowing, in particular, the first computation of the anomalous dimension of a nonprotected (Konishi) operator in a planar 4d theory at finite coupling [42]. The main goal of the present work is to remove the limitations of the previously known methods by developing an algorithm for a numerical solution of the QSC.

The low precision and performance of the TBA-like approach was mainly due to the complicated infinite system of equations and cumbersome integration kernels. The QSC includes only a few unknown functions and thus can be expected to give highly precise numerical results. However, the QSC equations are functional equations supplemented with some analyticity constraints of a novel type which makes it a priori not a trivial task to develop a robust numerical approach.

In this part, based on the paper [14], we propose an efficient method to solve the QSC numerically and illustrate our method by a few examples. Among the several equivalent formulations of the QSC we identified the equations which are best-suited for numerical solution[20]. We implemented our algorithm in *Mathematica* and were able to get a massive

[19] only for a few operators the complicated structure of the "driving terms" was deduced explicitly in a closed form. Even for those operators the driving terms may change depending on the value of the coupling.

[20] one may call this sub-system of equations as $\mathbf{P}\omega$-system, in contrast to previously used $\mathbf{P}\mu$-system or $\mathbf{Q}\omega$-system

increase in efficiency compared to the TBA or FiNLIE systems [42, 51, 44, 132]. With one iteration taking about 2 seconds we only need $2-3$ iterations (depending on the starting points) to reach at least 10 digits of precision. Quite expectedly, the precision gets lost for very large values of the 't Hooft coupling. Nevertheless, without any extra effort we reached $\lambda \sim 1000$ keeping a good precision, which should be more than enough for most practical goals.

Not only does our approach work for any finite length single trace operator and in particular for any value of the spin, it also works with minimal changes even away from integer quantum numbers! We demonstrate this in the particularly interesting case of the $\mathfrak{sl}(2)$ twist-2 operators. Their anomalous dimension analytically continued to complex values of the spin S is known to have a very rich structure, in particular the region $S \simeq -1$ is described by BFKL physics. As we show, within the framework of QSC it is not hard to specify any value of the Lorentz spin S as the conserved charges enter the equations through the asymptotics which can in principle take any complex values. Then we can compute the analytically continued scaling dimension Δ *directly* for complex S (or even interchange their roles and study S as a function of Δ). The result of this calculation can be seen on Fig. 12.

Let us stress that the algorithm is very simple and mainly consists of elementary matrix operations. As such it can be easily implemented on various platforms. In particular, we believe the performance could be increased by a few orders with a lower level, e.g. C++, implementation. In the presentation given here we mostly aim to demonstrate our algorithm, prototyped in *Mathematica*.

Finally, to improve the performance of our method we used the further simplification of the QSC obtained in [13], which allows us to eliminate auxiliary functions ω_{ij} from our algorithm and close the equations using Q-functions only (we demonstrate this for the $sl(2)$ sector states).

13 Description of the Method

As discussed before, the functions $\mathbf{P}_a$ and $\mathbf{P}_a$ carry complete information about the state and have only one cut, thus they can be parameterized as

$$\mathbf{P}_a(u) = \sum_{n=\tilde{M}_a}^{\infty} \frac{c_{a,n}}{x^n(u)} \,. \tag{13.1}$$

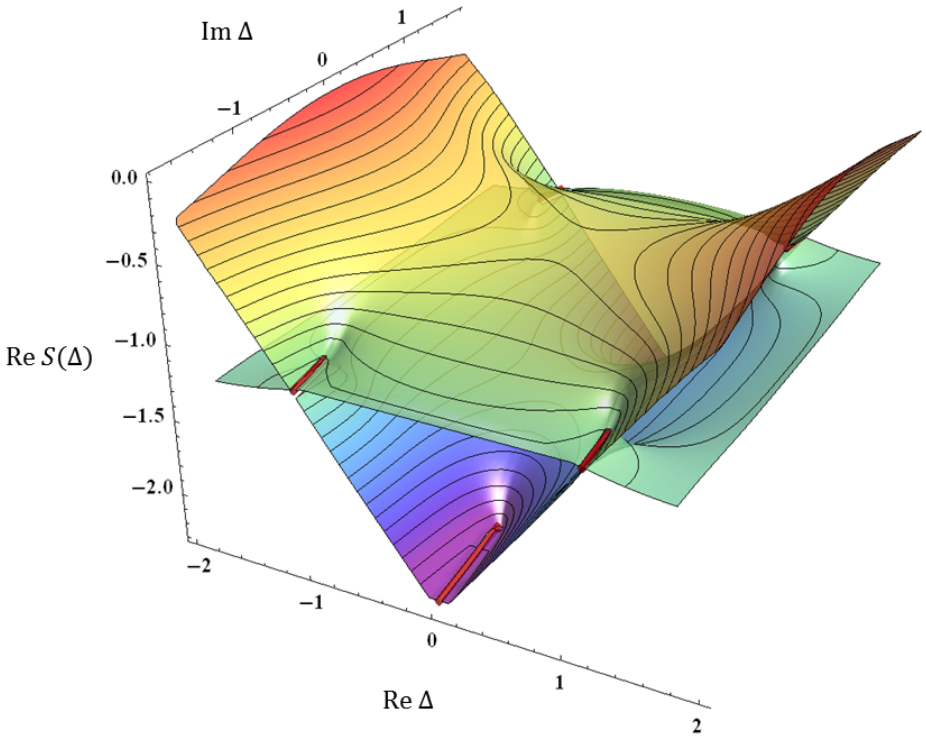

Figure 7: **Riemann surface of the function $S(\Delta)$ for twist-2 operators.** Plot of the real part of $S(\Delta)$ for complex values of Δ, generated from about 2200 numerical data points for $\lambda \approx 6.3$. We have mapped two Riemann sheets of this function. The thick red lines show the position of cuts. The upper sheet corresponds to physical values of the spin. Going through a cut we arrive at another sheet containing yet more cuts.

where $c+a, n$ are some unknown coefficients which are the main parameters in our numerics (we also have a similar parameterization for $\mathbf{P}^a$). This series is convergent everywhere on the upper sheet and also in an elliptic region around the cut on the next sheet (see Fig. 4.2).

The coefficients $c_{a,n}$ and corresponding coefficients $c^{a,n}$ of the expansion of $\mathbf{P}^a(u)$ need to be found. The constraint (4.21) fixes some of them (for example, we can use it to fix all $c_{1,n}$). The condition (4.27) gives the leading coefficients $c_{a,\tilde{M}_a}$. The remaining coefficients should be fixed from the analyticity constraints on $\mathbf{P}$'s as prescribed by QSC.

The main idea is to construct the functions $\mathcal{Q}_{a|i}$ by solving the equation

$$\mathcal{Q}_{a|i}(u+\tfrac{i}{2}) - \mathcal{Q}_{a|i}(u-\tfrac{i}{2}) = -\mathbf{P}_a(u)\mathbf{P}^b(u)\mathcal{Q}_{b|i}(u+\tfrac{i}{2}) \quad . \tag{13.2}$$

Then we can compute the $\mathbf{Q}_i$ via

$$\mathbf{Q}_i(u) = -\mathbf{P}^a(u)\ \mathcal{Q}_{a|i}(u+i/2)\ . \tag{13.3}$$

and we also find their analytic continuation around the branch point on the real axis from

$$\tilde{\mathbf{Q}}_i(u) = -\tilde{\mathbf{P}}^a(u)\ \mathcal{Q}_{a|i}(u + i/2) \tag{13.4}$$

$$\tilde{\mathbf{Q}}^i(u) = +\tilde{\mathbf{P}}_a(u)\ \mathcal{Q}^{a|i}(u + i/2) \tag{13.5}$$

Our parameterization for $\mathbf{P}_a$ covers a sufficient region to compute both $\mathbf{Q}_i$ and $\tilde{\mathbf{Q}}_i$ on the cut $[-2g, 2g]$. Then from the equation

$$\tilde{\omega}_{ij} - \omega_{ij} = \tilde{\mathbf{Q}}_i \mathbf{Q}_j - \mathbf{Q}_i \tilde{\mathbf{Q}}_j\ . \tag{13.6}$$

we can immediately reconstruct ω_{ij}! This is done by taking a simple integral transform of the r.h.s. (see below). This will allow us to close the equations.

The main step to be described is how to solve the equation on $\mathcal{Q}_{a|i}$. We will describe an algorithm which allows to solve it very efficiently and then find the coefficients $c_{a,n}$, which yields the solution of the QSC. We will also show that actually finding ω_{ij} is not necessary and we can close the system in terms of just $\mathbf{P}_a, \mathbf{Q}_i$ and $\mathcal{Q}_{a|i}$, thus speeding up the calculations.

13.1 Step 1: Solving the equation for $\mathcal{Q}_{a|i}$

As we explained above the quantity $\mathcal{Q}_{a|i}$ is at the heart of our procedure. In this section we will demonstrate how this set of 16 functions can be found for arbitrary $\mathbf{P}_a$ and $\mathbf{P}^a$. In this procedure the precise ansatz for $\mathbf{P}$ is not important. However, as we will see later, we should be able to compute $\mathbf{P}_a(u)\mathbf{P}^b(u)$ on the upper sheet for u with large imaginary part. Of course, having the ansatz in the form of a (truncated) series expansion (4.19) we can easily evaluate it everywhere on the upper sheet numerically very fast.

The process of finding $\mathcal{Q}_{a|i}$ is divided into two parts. Firstly, we find a good approximation for $\mathcal{Q}_{a|i}$ at some u with large imaginary part (in the examples we will need Im $u \sim 10 - 100$). At the next step we apply to this large u approximation of $\mathcal{Q}_{a|i}$ a recursive procedure which produces $\mathcal{Q}_{a|i}$ at $u \sim 1$.

Large u approximation. For Im $u \sim 10 - 100$ we can build the solution of (4.20) as a $1/u$ expansion. This is done by plugging the (asymptotic) series expansion of $\mathcal{Q}_{a|i}$ into (4.20):

$$\mathcal{Q}_{a|i}(u) = u^{\hat{M}_i - \tilde{M}_a} \sum_{n=0}^{N} \frac{B_{a|i,n}}{u^n}. \tag{13.7}$$

where N is some cutoff (usually $\sim 10-20$). This produces a simple linear problem for the coefficients $B_{a|i,n}$, which can be even solved analytically to a rather high order. The leading order coefficients of $\mathcal{Q}_{a|i}$ can be chosen arbitrarily. After that the linear system of equations becomes non-homogenous and gives a unique solution in a generic case.[21]

Finite u approximation. Once we have a good approximation at large u we can simply use the equation (4.20) to recursively decrease u. Indeed defining a 4×4 matrix

$$U_a{}^b(u) = \delta_a^b + \mathbf{P}_a(u)\mathbf{P}^b(u) \tag{13.8}$$

we have

$$\mathcal{Q}_{a|i}(u-\tfrac{i}{2}) = U_a{}^b(u)\mathcal{Q}_{b|i}(u+\tfrac{i}{2}). \tag{13.9}$$

Iterating this equation we get, in matrix notation

$$\mathcal{Q}_{a|i}(u-\tfrac{i}{2}) = [U(u)U(u+i)\dots U(u+iN)]_a{}^b\ \mathcal{Q}_{b|i}(u+iN+\tfrac{i}{2})\ . \tag{13.10}$$

For large enough N we can use the large u approximation (13.7) for $\mathcal{Q}_{b|i}$ in the r.h.s. As a result we obtain the functions $\mathcal{Q}_{a|i}$ for finite u with high precision.

13.2 Step 2: Recovering ω_{ij}

Now when we have a good numerical approximation for $\mathcal{Q}_{a|i}(u)$ we can compute $\mathbf{Q}_i$ and $\tilde{\mathbf{Q}}_i$ which through the discontinuity relation (4.33) will yield us ω_{ij}.

Let us also note that, as it was argued in our paper [13], one can in fact close the QSC equations without calculating ω_{ij} (this was shown explicitly for the symmetric $sl(2)$ sector states). This makes it possible to further speed up our numerical procedure as we will describe in detail in section 13.4. In the current section for completeness we will present the procedure without this shortcut, as for some applications it could turn out to be useful as well.

[21] The matrix of this system may become non-invertible unless some constraint (which is not hard to find) on the coefficients $c_{a,n}$ is satisfied. This constraint is fulfilled trivially for the even in the rapidity plane operators considered in the next section. There is also no such problem for the situation with generic twists (similar to $\beta-$ or γ-deformations, see the review [59]). Adding twists should correspond [53] to allowing exponential factors $e^{\alpha_a u}, e^{\beta_i u}$ in the asymptotics of $\mathbf{P}_a$ and $\mathbf{Q}_i$, making everything less degenerate and providing a useful regularization.

One can recover ω_{ij} from its discontinuity (4.30) modulo an analytic function using its spectral representation

$$\omega_{ij}(u) = \frac{i}{2}\int_{-2g}^{2g} dv \coth(\pi(u-v))\left[\tilde{\mathbf{Q}}_i(v)\mathbf{Q}_j(v) - \mathbf{Q}_i(v)\tilde{\mathbf{Q}}_j(v)\right] + \omega^0_{ij}(u) \tag{13.11}$$

where the "zero mode" $\omega^0_{ij}(u)$ is the analytic part of ω_{ij} — it has to be periodic, antisymmetric in i, j and should not have cuts. We will fix it below. We note that we only need to know values of $\mathbf{Q}$ and $\tilde{\mathbf{Q}}$ on the cut. In our implementation we use a finite number of sampling points on the cut given by zeros of Chebyshev polynomials. One can then fit the values of $\tilde{\mathbf{Q}}_i\mathbf{Q}_j - \mathbf{Q}_i\tilde{\mathbf{Q}}_j$ at those points with a polynomial times the square root $\sqrt{u^2-4g^2}$. After that we can use precomputed integrals of the form $\int_{-2g}^{2g}\coth(\pi(u_i-v))v^n\sqrt{v^2-4g^2}dv$ to evaluate (13.11) with high precision by a simple matrix multiplication, which produces the result at the sampling points u_A in an instant.

One more point to mention here is that in our implementation we only compute $\omega^{reg}_{ij} = \frac{1}{2}(\omega_{ij} - \tilde{\omega}_{ij})$ at the sampling points to avoid the problem of dealing with the singularity of the integration kernel. Note that ω^{reg}_{ij} can be used instead of ω_{ij} in the equations like (4.33), because the difference is proportional to $\mathbf{Q}_i\mathbf{Q}^i$ which is zero similarly to (4.21), as can be shown by combining (4.21) with (4.22), (4.24).

Finding zero modes. It only remains to fix $\omega^0_{ij}(u)$. First we notice that for all physical operators ω_{ij} should not grow faster than constant at infinity [53]. As the integral part of (13.11) does not grow either and since $\omega^0_{ij}(u)$ is i-periodic it can only be a constant. To fix this constant we use the following observation [53]: the constant matrix α^+_{ij} which ω_{ij} approaches at $u \to +\infty$ and the constant matrix α^-_{ij} which it reaches at $u \to -\infty$ are restricted by the quantum numbers [53]. To see this we can pick some point on the real axis far away from the origin and shift it slightly up into the complex plane, then from (4.33) we have

$$\omega_{ij}\mathbf{Q}^j(u+i0) = \alpha^+_{ij}\mathbf{Q}^j(u+i0) = \tilde{\mathbf{Q}}_i(u+i0) = \mathbf{Q}_i(u-i0). \tag{13.12}$$

Similarly for $-u$ we get

$$\alpha^-_{ij}\mathbf{Q}^j(-u+i0) = \mathbf{Q}_i(-u-i0). \tag{13.13}$$

Next, notice that since $\mathbf{Q}^j$ is analytic everywhere except the cut on the real axis, it can be replaced by its asymptotics above the real axis, i.e. $\mathbf{Q}^j(u+i0) \sim B^j u^{-\hat{M}_j}$, and also $\mathbf{Q}^j(-u+i0) \sim B^j u^{-\hat{M}_j} e^{-i\pi\hat{M}_j}$, as we find from the previous expression by a rotation by

π in the complex plane. As a result we get the asymptotics of $\mathbf{Q}_i$ at infinities and slightly below the real axis

$$\mathbf{Q}_i(u-i0) = \alpha_{ij}^{+} B^j u^{-\hat{M}_j} \ \ , \ \ \mathbf{Q}_i(-u-i0) = \alpha_{ij}^{-} B^j u^{-\hat{M}_j} e^{-i\pi\hat{M}_j} \ . \tag{13.14}$$

Using that they are related by the analytic continuation in the lower half plane the first equation also gives

$$\mathbf{Q}_i(-u-i0) = \alpha_{ij}^{+} B^j u^{-\hat{M}_j} e^{+i\pi\hat{M}_j} \ . \tag{13.15}$$

Combining this with (13.14) we get a relation between the constant asymptotics of ω at the two infinities

$$\alpha_{ij}^{+} = \alpha_{ij}^{-} e^{-2i\pi\hat{M}_j} \ . \tag{13.16}$$

At the same time from (13.11) we get

$$\alpha_{ij}^{\pm} = \pm I_{ij} + \omega_{ij}^{0} \ \ , \ \ I_{ij} \equiv \frac{i}{2} \int_{-2g}^{2g} dv \left[\tilde{\mathbf{Q}}_i(v) \mathbf{Q}_j(v) - \mathbf{Q}_i(v) \tilde{\mathbf{Q}}_j(v) \right], \tag{13.17}$$

which implies that

$$\omega_{kl}^{0} = -i I_{kl} \cot \pi \hat{M}_l. \tag{13.18}$$

We see that the zero modes can be also computed from the values of $\mathbf{Q}$ and $\tilde{\mathbf{Q}}$ on the cut.

Note also that the r.h.s. is not explicitly antisymmetric. Imposing the antisymmetry gives

$$I_{kl}(\cot \pi \hat{M}_l - \cot \pi \hat{M}_k) = 0, \tag{13.19}$$

so either $I_{kl} = 0$ or $\cot \pi \hat{M}_l = \cot \pi \hat{M}_k$. As Pf $\omega = 1$, all I_{kl} can not be equal to zero simultaneously. Having I_{kl} non-zero implies quantization of charges: for example, the choice $I_{12} \neq 0$ and $I_{34} \neq 0$, which is consistent with perturbative data, requires $\cot \pi \hat{M}_1 = \cot \pi \hat{M}_2$ and $\cot \pi \hat{M}_3 = \cot \pi \hat{M}_4$, and so S_1, S_2 have to be integer or half integer. In section 14 we will see how to relax this condition and do an analytic continuation in the spin S_1 to the whole complex plane.

13.3 Step 3: Reducing to an optimization problem

Having ω_{ij} and $\mathbf{Q}_{a|i}$ at hand we can try to impose the remaining equations of the QSC (4.33). We notice that there are two different ways of computing $\tilde{\mathbf{Q}}_i$, which should give the same result when we have a true solution: (4.25) and (4.33). Their difference, which at the end should be zero, is

$$F_i(u) = \tilde{\mathbf{P}}^a(u) \ \mathcal{Q}_{a|i}(u+i/2) + \omega_{ij}(u) \ \mathcal{Q}^{a|j}(u+i/2) \mathbf{P}_a(u) \ . \tag{13.20}$$

The problem is now to find $c_{a,n}$ for which $F_i(u)$ is as close as possible to zero. Here we have some freedom in how to measure its deviation from zero, but in our implementation we use the sum of squares of F_i at the sampling points u_A. Then the problem reduces to the classical optimization problem of the least squares type. In our implementation we found it to be particular efficient to use the Levenberg-Marquardt algorithm (LMA), which we briefly describe in the next section. The LMA is known to have a Q-quadratic convergence rate, which means that the error ϵ_n decreases with the iteration number n as fast as $e^{-c\,2^n}$. The convergence is indeed so fast that normally it is enough to do 2 or 3 iterations to get the result with 10 digits precision. We give some examples in the next section.

Levenberg-Marquardt algorithm Our problem can be reformulated as follows: given a vector function $f_i(c_a)$ of a set of variables c_a (which we can always assume to be real) find the configuration which minimizes

$$S(c_a) \equiv \sum_i |f_i(c_a)|^2 \ . \tag{13.21}$$

Assuming we are close to the minimum we can approximate f_i by a linear function:

$$f_i(\tilde{c}_a) \simeq f_i(c_a) + (\tilde{c}_a - c_a)J_{ai} \ \ , \ \ J_{ai} \equiv \partial_{c_a} f_i(c_a) \tag{13.22}$$

which gives the following approximation for $S(\tilde{c}_a)$:

$$S(\tilde{c}_a) = [f_i(c_a) + (\tilde{c}_a - c_a)J_{ai}]\left[\bar{f}_i(c_a) + (\tilde{c}_a - c_a)\bar{J}_{ai}\right] \tag{13.23}$$

The approximate position of the minimum is then at $\partial_{\tilde{c}_a} S = 0$ for which we get

$$J_{ai}\left[\bar{f}_i(c_a) + (\tilde{c}_a - c_a)\bar{J}_{ai}\right] + [f_i(c_a) + (\tilde{c}_a - c_a)J_{ai}]\,\bar{J}_{ai} = 0 \tag{13.24}$$

from which, in matrix notation,

$$\tilde{c} = c - (J\bar{J}^T + \bar{J}J^T)^{-1}(\bar{J}f + J\bar{f}) \ . \tag{13.25}$$

We see that for this method we should also know the derivatives of our $F_a(u)$ w.r.t. the parameters $c_{a,n}$, which in our implementation we find numerically by shifting a bit the corresponding parameter.

In some cases, when the starting points are far away from the minimum, the above procedure may start to diverge. In such cases one can switch to a slower, but more stable, gradient descent method for a few steps. The Levenberg-Marquardt algorithm provides a

nice way to interpolate between the two algorithms by inserting a positive parameter Λ into the above procedure,

$$c_{n+1} = c_n - (J\bar{J}^T + \bar{J}J^T + \Lambda I)^{-1}(\bar{J}f + J\bar{f}) \ . \tag{13.26}$$

The point is that for large Λ this is equivalent to the gradient descent method. Thus one can try to increase Λ from its zero value until $S(c_{n+1}) < S(c_n)$ and only then accept the new value c_{n+1}. This helps a lot to ensure stable convergence.

In the next section we demonstrate the performance of our numerical method by applying it to the twist-2 operators in $\mathfrak{sl}(2)$ sector.

13.4 Implementation for the $\mathfrak{sl}(2)$ Sector and Comparison with Existing Data

Although our method can be used for any state of the $\mathcal{N} = 4$ SYM theory, the examples we provide here are for states in the $\mathfrak{sl}(2)$ subsector. In this section we will discuss the physical operators which have integer spin, and demonstrate our numerical method in action for the Konishi operator. Then in section 14 we will show how the algorithm works for other states with S no longer an integer.

Improved implementation: skipping the computation of ω's. We have mentioned before that the simplification of the QSC achieved in [13] should allow to significantly improve the iterative procedure, as one can avoid calculating ω_{ij}. Here we present this improvement for symmetric states in the $sl(2)$ sector. Let us briefly recall the trick used in [13] to eliminate ω's. For the states we consider, each of the $\mathbf{P}_a(u)$ functions is either even or odd. Then, as follows from the 4th order finite difference eqation on $\mathbf{Q}_i$ with coefficients built from $\mathbf{P}$'s [22], $\mathbf{Q}_i(-u)$ satisfy the same finite difference equation as $\mathbf{Q}_i(u)$. Thus each of the former can be expressed as a linear combination of the latter with periodic coefficients:

$$\mathbf{Q}_i(u) = \Omega_i^j(u)\mathbf{Q}_j(-u) \ . \tag{13.27}$$

We work in the basis where $\mathbf{Q}_i$ have pure power-like asymptotics at large u, non-coinciding for general values of global charges. It is easy to see that at large u in this basis $\Omega_i^j(u)$ should be constant and diagonal. At the same time, (13.27) allows us to relate $\mathbf{Q}_i(-u)$ and $\tilde{\mathbf{Q}}_i$:

$$\tilde{\mathbf{Q}}_i(u) = \alpha_i^j \mathbf{Q}_j(-u), \quad \alpha_i^j = \omega_{il}\chi^{lk}\Omega_k^j, \tag{13.28}$$

[22] its explicit form is given e.g. in (3.2) of [72]

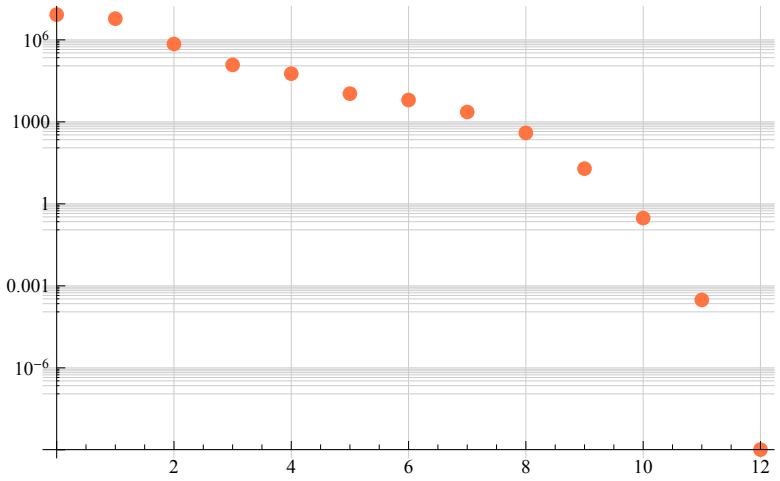

Figure 8: **Convergence of the algorithm.** The error ϵ_n as measured by the value of (13.21) reduces at the quadratic rate $\epsilon_n \sim e^{-c\,2^n}$ as a function of the iteration number. In most cases our program managed to find the solution from a very remote starting point. On the picture we started from all free parameters $c_{a,n}$ set to zero and with the initial value for the energy $\Delta_0 = 4.1$. After 12 iterations it correctly reproduced $\Delta = 4.4188599$ at $\lambda = 16\pi^2(0.2)^2 \simeq 31.6$. With each iteration taking about 1.5sec the whole procedure took about 20 sec on a Laptop with Intel i7 2.7GHz processor.

where χ is defined in (4.38). The functions $\mathbf{Q}_i(-u)$ and $\tilde{\mathbf{Q}}_i(u)$ have the same analytical properties, so α^i_j should be i-periodic and analytic. One should also take into account that only ω_{12} and ω_{34} are non-zero at infinity, thus many elements of α^j_i have to be zero. For indices 1 and 3 we finally get the key relations which appear to be sufficient to close the QSC equations:

$$\tilde{\mathbf{Q}}_1(u) = \alpha_{13}\mathbf{Q}_3(-u), \quad \tilde{\mathbf{Q}}_3(u) = \alpha_{31}\mathbf{Q}_1(-u) \tag{13.29}$$

Consistency of these two equations also implies that $\alpha_{13} = 1/\alpha_{31} \equiv \alpha$. Note that $\tilde{\mathbf{Q}}_1(u)$ can be also constructed as $\mathcal{Q}^+_{a|1}\mathbf{P}^a$. The equation above tells us that it should be proportional to $\mathbf{Q}_3(-u)$ with unknown constant of proportionality. This requirement can be also phrased as a minimization problem. For that let us evaluate the ratio $\tilde{\mathbf{Q}}_1(u)/\mathbf{Q}_3(-u)$ at sampling points u_k on the cut $[-2g, 2g]$ and compute its variance,

$$S(u) = \sum_{k=1}^{M} \left| \frac{\mathcal{Q}_{a|1}(u_k + i/2)\mathbf{P}^a(u_k)}{\mathbf{Q}_3(-u_k)} - B \right|^2 \tag{13.30}$$

where the constant B is the mean value,

$$B = \frac{1}{M}\sum_{k=1}^{M} \frac{\mathcal{Q}_{a|1}(u_k + i/2)\mathbf{P}^a(u_k)}{\mathbf{Q}_3(-u_k)} \tag{13.31}$$

On the true solution of the QSC this ratio is a constant so the variance should be zero, i.e. $S(u) = 0$. Thus our goal is to minimize the function $S(u)$, and for this we again use the Levenberg-Marquardt algorithm described above. This gives the desired numerical prediction for the coefficients $c_{a,n}$ parameterizing the **P**-functions.

The main performance gain stems from the fact that as we do not compute ω's, we no longer need to calculate the integrals (13.11) and (13.17). We expect this improved method to work for non left-right symmetric states as well, and details of this generalization will be presented elsewhere.

Implementation for Konishi Here we discuss the convergence on a particular example of the Konishi operator which corresponds to $S = 2, L = 2$. The reason we start from this operator is that it is very well studied both analytically at weak and strong coupling and also numerically. So we will have lots of data to compare with.

To start the iteration process described in the previous sections, we need some reasonably good starting points for the coefficients $c_{a,n}$. For the iterative methods, like, for instance, Newton's method, good starting points are normally very important. Depending on them the procedure may converge very slowly or even diverge. We made a rather radical test of the convergence of our method by setting all coefficients to zero, except the leading ones, which are fixed by the charges. For Δ we took the initial value 4.1 at the value of 't Hooft coupling $g = 0.2$. To our great surprise it took only 12 steps to converge from the huge value of $S(c_a) \sim 10^{+7}$ (defined in (28.16)) to $S(c_a) \sim 10^{-9}$. The whole process took about 20 seconds on a usual laptop (see Fig. 8), producing the value $\Delta = 4.4188599$, consistent with the best TBA estimates [42, 44].

After that we used the obtained coefficients as starting points for other values of the coupling to produce the Table 13.4. All the values obtained are consistent with the TBA results within the precision of the latter, being considerably more accurate at the same time.

The reason for such an excellent convergence is the Q-quadratic convergence rate of the algorithm we use. It means that the number of exact digits doubles with each iteration, or that the error decreases as $e^{-c\,2^n}$ at the step n, if the starting point is close enough. What is perhaps surprising is that the algorithm converges from a very remote starting point.

Another indicator of the convergence is the plot of $\tilde{\mathbf{Q}}$ computed in two different ways, i.e. (4.25) and (4.33). On the true solution of the QSC both should coincide. On Fig. 5 we show how fast the difference between them vanishes with iterations, i.e. how fast we

$\frac{\sqrt{\lambda}}{4\pi}$	$\Delta_{S=2}(\lambda)$	$\frac{\sqrt{\lambda}}{4\pi}$	$\Delta_{S=2}(\lambda)$
0.1	4.11550637794522105684004267185 1	0.2	4.41885988080235096225036287624 3
0.3	4.82694866228484230467128342527 1	0.4	5.27156518259589800822152854003 4
0.5	5.71272342478773903062696687597 3	0.6	6.13386281448869181959542576234 6
0.7	6.53160607785244019588655795369 0	0.8	6.90750420602456751582887278971 7
0.9	7.26416958743911277483963985391	1	7.60407071704738848334286555
1.1	7.92929426415684516321862641	1.2	8.24156344114770354267605 0
1.3	8.54230287229506674486342	1.4	8.8326999393163090494514
1.5	9.11375404891588560886	1.6	9.386314656368554140399
1.7	9.65111042653013781471	1.8	9.9087717085593508789
1.9	10.1598480131615473641	2	10.4048217434405061127
2.1	10.6441190951617575972	2.2	10.878118797537726796
2.3	11.107159189584305149	2.4	11.331544000504529107
2.5	11.551547111042160297	2.6	11.76741650605722239
2.7	11.97937757952067741	2.8	12.18763591669137588
2.9	12.3923796509149519	3	12.5937814717988565
3.1	12.7920003457144898	3.2	12.9871829973986392
3.3	13.1794651919629055	3.4	13.368972849208144
3.5	13.555823016292914	3.6	13.740124720157966
3.7	13.921979717391474	3.8	14.101483156227149
3.9	14.278724162943763	4	14.45378636296056
4.1	14.62674834530641	4.2	14.79768407780976
4.3	14.96666327925592	4.4	15.13375175384302
4.5	15.29901169250472	4.6	15.4625019450274
4.7	15.6242782663505	4.8	15.7843935399844
4.9	15.942897981092	5	16.099839321454

Table 2: Conformal dimension of Konishi operator

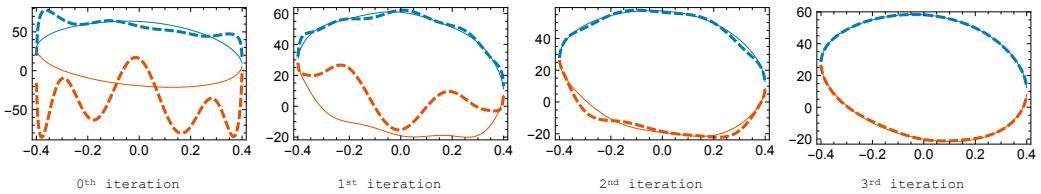

Figure 9: **Q-functions at the first several iterations.** Here we show how $\mathbf{Q}_3$ converges to the solution in just four iterations when calculating the Konishi anomalous dimension. At each picture solid and dashed blue lines show $\mathbf{Q}_3$ slightly below the cut calculated with (4.33) and (4.25) respectively, which should coincide on the solution. Red lines show the same slightly above the cut.

approach the exact solution of the QSC.

In the next section we discuss the analytic continuation in S away from its integer values. This is an important calculation which bring us to a highly accurate numerical estimate for the pomeron intercept at finite coupling — a quantity which can be studied exclusively by our methods.

14 Extension to Non-Integer Lorentz Spin

In this section we explain which modifications are needed in order to extend our method to non-integer values of spin S, and give two specific examples of calculations for such S.

14.1 Modification of the Algorithm for Non-Integer Spin

First we need to discuss how the procedure of fixing zero modes of ω's described in section 13.2 is modified for non-integer S. The main difference stems from the fact that analytic continuation to non-integer S changes the asymptotic behavior of ω_{ij} at large u, as described in [15, 72, 133]. While for integer S asymptotics of ω are constant, for non-integer S some components of ω have to grow exponentially. Without this modification the system has no solution: indeed, in section 13.3 we assumed constant asymptotics of all ω's and derived quantization condition for global charges.

A minimal modification would be to allow exponential asymptotics in one of the components of ω. In order to understand which of the components can it be, let us recall the

Pfaffian constraint satisfied by ω_{ij}

$$\operatorname{Pf}\omega = \omega_{12}\omega_{34} - \omega_{13}\omega_{24} + \omega_{14}^2 = 1. \tag{14.1}$$

First, it is clear ω_{14} alone can not have exponential asymptotics. Second, in the case of integer S both ω_{12} of ω_{34} are non-zero constants at infinity [72, 15]; then shifting S infinitesimally away from an integer we see that it would be impossible to satisfy the condition (14.1) if we allow one of them to have exponential asymptotics at infinity: this exponent will multiply the constant in the other one. So the only two possibilities left are ω_{13} and ω_{24}, which are both zeros at infinity for integer S. From perturbative data we know that it is ω_{24} which should have exponential asymptotics. Thus we formulate the "minimal" prescription for analytic continuation of Q-system to non-integer S: $e^{2\pi|u|}$ asymptotic has to be allowed in ω_{24}. This prescription was tested thoroughly on a variety of examples [134, 135, 72, 15, 133], but it would be interesting to derive it rigorously and generalize it to states outside of the $\mathfrak{sl}(2)$ sector. Of course, one can also consider adding exponents to more than one component of ω_{ij}: in this case the solution will not be unique. A complete classification of solutions of Q-system according to exponents in their asymptotics might be interesting. For example it is known that allowing for an exponent in some other components corresponds to the generalized cusp anomalous dimension [15, 12].

Because of the exponential asymptotics of ω_{24}, the argument in section 13.2, which fixes the zero modes of ω, has to be modified. First, formula (13.18) still holds true for $i = 1$ or $i = 3$, as ω_{24} does not enter anywhere in the derivation. Thus

$$\omega_{12} = -iI_{12}\cot\frac{\pi\,(S+\Delta)}{2},\ \omega_{34} = -iI_{34}\cot\frac{\pi\,(S-\Delta)}{2}. \tag{14.2}$$

Consequently, one can use (13.18) for both ω_{13} and ω_{31}, and reproduce the quantization condition (13.19) for global charges, which in this case implies that either $\Delta = 0$ or $\omega_{13} = 0$. Equation (13.18) can also be used for ω_{14} and ω_{23} (which are equal) and imposes that either $\Delta = 0$ or $\omega_{14} = 0$.

It remains to fix the zero mode in ω_{24}^0, for which we use an ansatz

$$\omega_{24}^0 = a_1 e^{2\pi u} + a_2 + a_3 e^{-2\pi u}. \tag{14.3}$$

The constants a_1, a_2, a_3 can be found from the Pfaffian constraint (14.1). To this end we expand the hyperbolic cotangent in (13.11) to get

$$\omega_{ij} = \omega_{ij}^0 + I_{ij} + 2e^{-2\pi u} I_{ij}^{+} + 2e^{-4\pi u} I_{ij}^{++} + \ldots,\ u \to +\infty, \tag{14.4}$$

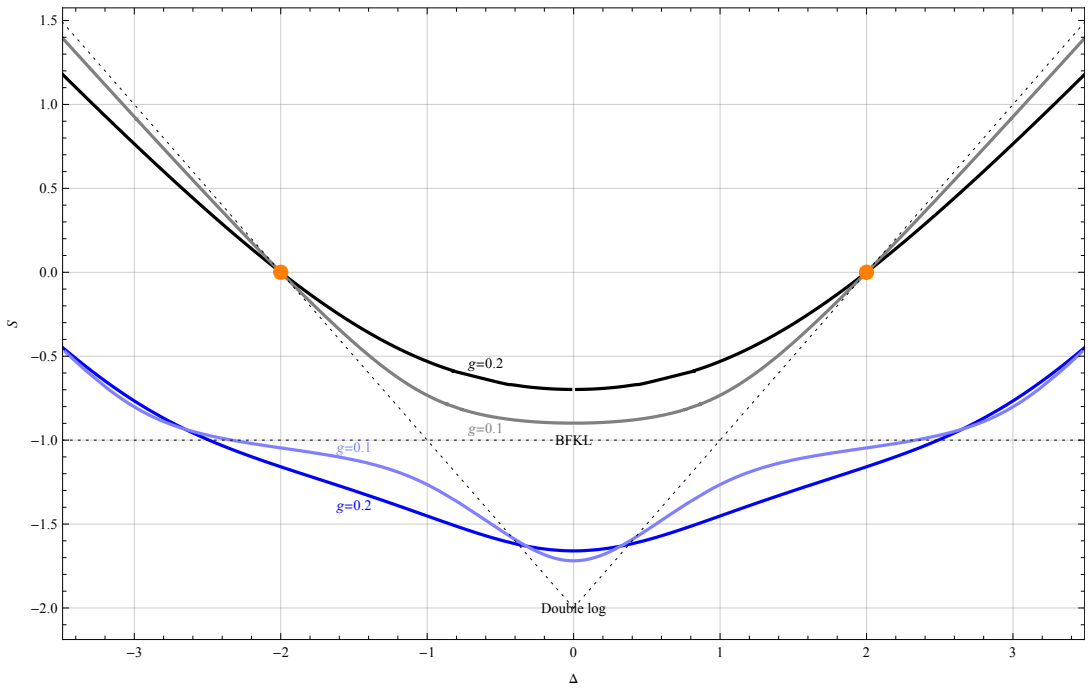

Figure 10: Section of the Riemann surface $S(\Delta)$ along Im $\Delta = 0$ for different values of coupling g. The upper two solid curves, shown in black and grey, represent the well-known BFKL eigenvalue as a function of Δ, whereas the lower two come from the unphysical sheet which can be accessed from the upper one by going through the cuts. The dashed line shows the zero-coupling limit of the curve. Orange dots mark BPS states $\mathrm{Tr}(ZZ)$.

where the terms of the expansion are integrals similar to I_{ij} with additional factors of $e^{2\pi u}$ or $e^{4\pi u}$ in the integrand[23]. Analogous expansion can be obtained at $u \to -\infty$. Then plugging these expansions into (14.1) we get formulas for the coefficients a_1, a_2, a_3. For example,

$$a_1 = 2i \frac{1 + \frac{I_{12} I_{34}}{4} \left(1 + i \cot \frac{\pi(\Delta+S)}{2}\right) \left(1 - i \cot \frac{\pi(\Delta-S)}{2}\right)}{I_{13}^{+}} \,. \tag{14.5}$$

With these modifications we can reconstruct all ω_{ij} including the zero modes and then proceed with our algorithm as in the case of integer S.

14.2 Exploring Complex Spin

In this section we briefly describe the results of our numerical exploration of $\Delta(S)$ as an analytic function of a complexified spin S. As explained in the previous section the generalization of our numerical method to arbitrary values of spin requires minimal modi-

[23] Actually, these integrals can be evaluated analytically in terms of Bessel functions

fications of our main code. Thus we are able to generate numerous values of the anomalous dimension for any S with high precision in seconds. In fact both S and Δ enter the QSC formalism on almost equal footing and we can also switch quite easily to finding S for given Δ. This is what is adopted in the vast literature on the subject and what we are going to consider below. This viewpoint is particular convenient due to the symmetry $\Delta \to -\Delta$ which makes the pictures particularly nice.

Starting from $S = 2$ (Konishi operator) we decreased the value of S or Δ in small steps using the solution at the previous step as a starting point for the next value. In this way we built the upper two curves on Fig. 10. Let us point out one curious technical problem – one can see for instance from (14.5) that the lines $S = \pm\Delta + \mathbb{Z}$ are potentially dangerous due to the divergence. In fact we found that near these dangerous points on the line the factor $I_{12}I_{34}$ also vanishes canceling the potential divergence. This however affect the convergence "radius" of our iterative procedure and we found it quite complicated to cross those lines, even though in very small steps we were able to reach close to them. The way out is to go around these lines in the complex plane Δ. To make sure there is no true singularity or branch point we also explored a big patch of the complex plane Δ, indeed finding some branch points, but deep inside the complex plane, having nothing to do with these lines. For example when $g = 0.2$ we found 4 closest branch points at roughly $\pm 1 \pm i$, see Fig. 12. By making an analytic continuation (described above) through those cuts we found another sheet of the Riemann surface $S(\Delta)$. On this sheet we have found four cuts: two are connecting it to the first sheet and two other ones, located symmetrically on the imaginary axis, lead to further sheets. We expect an infinite set of sheets hidden below and also more cuts on both sheets outside of the area that we have explored.

It is instructive to see how this Riemann surface behaves as $g \to 0$. First, the real parts of branch points on the physical sheet are very close to ± 1, but the imaginary part goes to zero. Thus at infinitely small g the cuts collide, isolating the region $|\Re\ \Delta| < 1$ from the rest of the complex plane. These two separated regions become then the areas of applicability of two different approximations: for $|\Re\ \Delta| > 1$ one can apply the usual perturbation theory and Beisert-Eden-Staudacher Asymptotic Bethe Ansatz, whereas the region $|\Re\ \Delta| < 1$ is described by BFKL approximation and so-called Asymptotic BFKL Ansatz [133].

The presence of the cut can be to some extent deduced from perturbative perspective in each region: in the regime of usual perturbation theory

$$\Delta(S) = 2 + S - 8g^2 H_S + \mathcal{O}(g^4), \tag{14.6}$$

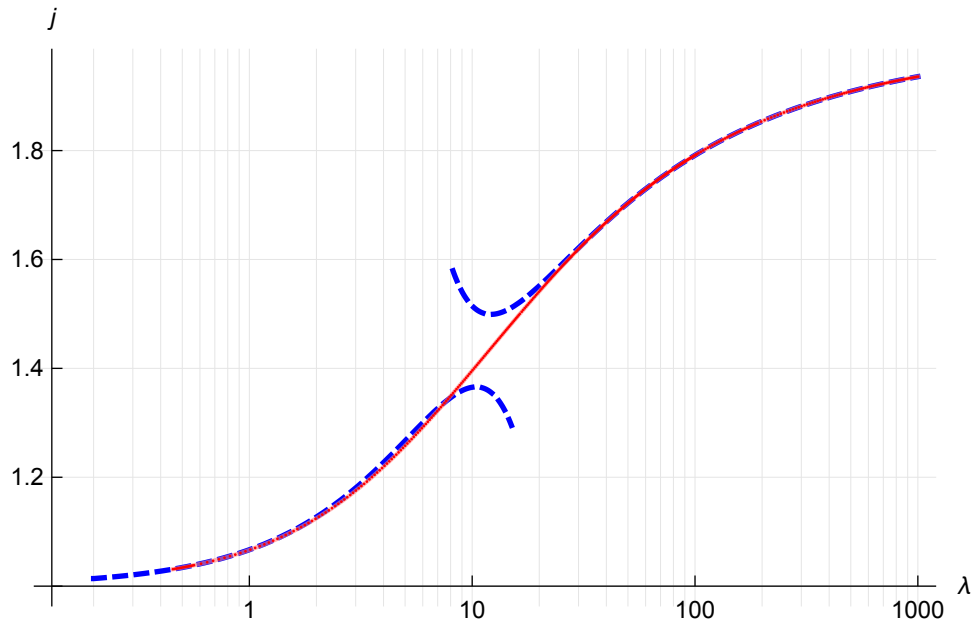

Figure 11: The BFKL intercept j as a function of coupling λ. The red solid line with tiny red dots is obtained by our numerical procedure. It interpolates perfectly between the known perturbative predictions (the blue dashed lines) at weak [128, 127] and strong coupling [129, 130, 131, 15].

where H_S is the harmonic number. It has poles for all negative integer values of S — these poles are weak-coupling remnants of the cuts we see at finite coupling. In the BFKL regime one should instead look at the leading order BFKL equation [136, 137, 128]

$$S(\Delta) = -1 + 4g^2 \left[\psi\left(\frac{1+\Delta}{2}\right) + \psi\left(\frac{1-\Delta}{2}\right) - 2\psi(1) \right] + \mathcal{O}(g^4) \,. \tag{14.7}$$

To make sense of this equation one has to take the limit $g \to 0$, $S \to -1$ so that the l.h.s stays finite. Then the ψ-functions in the r.h.s generate poles at odd values of Δ, which, again, are cuts degenerated at weak coupling.

Fig 10 represents a section of the Riemann surface by the plane $\Im\, u = 0$, i.e. dependence of S on Δ for real Δ, which, of course, consists of two curves, originating from the two sheets we explored. At weak coupling the upper curve becomes piecewise linear, approaching different parts of the dotted line: for $|\Delta| > 1$ it coincides with $S = \pm\Delta - 2$ and for $|\Delta| < 1$ it becomes $S = -1$. One could expect a similar piecewise linear behavior for the lower curve: it approaches $S = \pm\Delta - 2$ for $|\Delta| < 1$, approaches $S = 0$ in some region outside of $|\Delta| < 1$ and becomes a certain linear function even further away from $\Delta = 0$. It would be interesting to explore the complete analytic structure of this Riemann surface, and understand what describes its asymptotics when $g \to 0$. It should produce a

hierarchy of "Asymptotic Bethe Ansätze" each responsible for its own linear part of the limiting surface.

14.3 BFKL Pomeron Intercept

The pomeron intercept $j(\lambda)$ is a quantity which relates spectrum of single-trace operators and scaling of high energy scattering amplitudes in the Regge regime [124, 125, 126]. This regime is particularly interesting, since it establishes a connection between results in $\mathcal{N}=4$ SYM and multicolor QCD: the non-trivial leading order of so-called BFKL eigenvalue is the same in two theories, and in the higher orders $\mathcal{N}=4$ SYM is expected to reproduce at least the most complicated part of the QCD result.

Our goal is to demonstrate the universal power of our approach by giving an extremely precise numerical estimate for this important quantity at finite coupling in a wide range of couplings.

One defines the intercept as $j = S(\Delta = 0) + 2$, where S is the spin of the twist-2 operator such that $\Delta(S) = 0$. Having formulated the problem like this, we can in principle apply the algorithm described in section 13 to find the correct value of S, while keeping Δ at zero. However, one may already suspect that the point $\Delta = 0$ is special. Indeed, we know that for any solution of QSC there is always another one related by $\Delta \to -\Delta$ symmetry. At the level of $\mathbf{Q}_i$ functions this allows simultaneously interchanging $\mathbf{Q}_1 \leftrightarrow \mathbf{Q}_3$ and $\mathbf{Q}_2 \leftrightarrow \mathbf{Q}_4$ as one can see from the asymptotics. From this we see that at small Δ two different solutions of QSC (related by the symmetry) approach each other, making the convergence slow, exactly like Newton's method becomes inefficient for degenerate zeros. In other words, in the limit $\Delta \to 0$ the $\mathbf{Q}$'s related by the symmetry become linearly dependent in the leading order. Furthermore, since the matrix $\mathcal{Q}_{a|i}$ should stay invertible, the leading coefficients B_i of asymptotic expansion of $\mathbf{Q}_i$ diverge at $\Delta \to 0$.

The way out is to perform a linear transformation of $\mathbf{Q}$'s preserving the equations: it will replace two of them by linear combinations $\mathbf{Q}_3 - \gamma\mathbf{Q}_1$ and $\mathbf{Q}_4 + \gamma\mathbf{Q}_2$ with some coefficient γ, so that the divergent leading order cancels and the four functions $\mathbf{Q}_i$ become linearly independent.

For the gauge choice in which $B_1 = B_2 = 1$ the transformation acts on i-indices of

$\frac{\sqrt{\lambda}}{4\pi}$	$j(\lambda)$	$\frac{\sqrt{\lambda}}{4\pi}$	$j(\lambda)$
0.	1.000 000 000 000 000 000 0	0.1	1.101 144 978 997 772 874 8
0.2	1.301 794 032 258 782 208 7	0.3	1.470 445 240 989 187 630 6
0.4	1.587 128 066 254 129 730 4	0.5	1.666 438 709 974 061 852 3
0.6	1.721 917 842 815 631 353 9	0.7	1.762 239 296 816 453 814 3
0.8	1.792 626 253 069 403 59	0.9	1.816 252 952 807 284 11
1.	1.835 109 464 032 173 0	1.1	1.850 489 553 739 522 8
1.2	1.863 264 346 392 640 4	1.3	1.874 039 320 799 460
1.4	1.883 247 290 966 33	1.5	1.891 205 346 040 23
1.6	1.898 150 851 852 49	1.7	1.904 264 892 928 17
1.8	1.909 687 948 271 74	1.9	1.914 530 628 017 38
2.	1.918 881 187 304 9	2.1	1.922 810 887 750
2.2	1.926 377 890 67	2.3	1.929 630 129 41
2.4	1.932 607 459 1	2.5	1.935 343 287 2

Table 3: Numerical data for the pomeron intercept for various values of the 't Hooft coupling. All digits are expected to be significant but some additional tests are in progress, and will be reported in second version of this preprint.

Q-functions with a matrix[24].

$$H_i{}^j = \begin{pmatrix} 1 & 0 & 0 & 0 \\ 0 & 1 & 0 & 0 \\ -\gamma & 0 & 1 & 0 \\ 0 & \gamma & 0 & 1 \end{pmatrix}, \ \gamma = \frac{i(S-4)(S-2)S(S+2)}{16(S-1)^2\Delta}. \tag{14.8}$$

One can check that rotation by this matrix will render $\mathcal{Q}_{a|i}$ finite and linearly independent, and moreover, preserve relations (4.39). After this one can apply the standard procedure from section 13 with the only modification that the large u expansion of $\mathcal{Q}_{a|i}$ will contain $\log u/u^n$ terms in addition to the usual $1/u^n$.

Having done this, we can readily generate lots of numerical results. In particular we built numerically the function $j(\lambda)$ which interpolates perfectly between the weak and strong coupling predictions. We have found $j(\lambda)$ with high precision (up to 20 digits) for a wide range of 't Hooft coupling (going up to $\lambda \simeq 1000$). The results are also summarized in the Table 3.

Table 3 represents a small portion of all data we generated, which is available by

[24]This is a particular case of H-transformations described in section 4.1.3 of [53]

request. In particular we generated ~ 100 points with small g in the range $0.1 \ldots 0.017$ each with more than 20 digits precision. Fitting this data with powers of g^2 we found

$$j = 1 + 11.09035488895912 g^2 - 84.0785668075 g^4 - 2543.0481652 g^6 + 156244.8086 g^8$$

where the first 3 terms are known analytically from Feynman diagram perturbation theory calculations [128, 127] and their numerical values coincide in all digits with our prediction above. The last two terms give our numerical prediction for the numerical values of the NNLO and NNNLO BFKL pomeron intercept. Our fit also gives predictions for the higher corrections but with a smaller precision. In addition, we confirmed the analytic string coupling predictions for the intercept from [15] (our precision is sufficient at the moment to check all known coefficients except the last $\frac{1}{\lambda^3}$ term).

15 Conclusions and Future Directions

In this part we have demonstrated that in addition to their analytic power, the QSC equations can give highly precise numerical results at finite coupling. We develop a numerical procedure which applies to generic single trace operators and as such it is unique in its kind. Furthermore, the algorithm converges at a remarkably high rate which gives us access to high numerical precision results – up to 20 digits or even more in a few iterations.

The efficiency of our method is demonstrated on the example of $\mathfrak{sl}(2)$ sector operators. We also formulated how to extend our procedure to non-integer quantum numbers. We studied the twist-2 operators for complex values of the spin discovering a fascinating Riemann surface (see Fig.12). In addition we reformulated our equations to be directly applicable to the BFKL pomeron intercept and evaluated the intercept j with high precision of up to 20 significant figures. By fitting our data we also gave a prediction for the perturbation theory expansion

$$\begin{aligned} j(\lambda) &= 1 + 0.07023049277268284\ \lambda - 0.00337167607361\ \lambda^2 \\ &- 0.00064579607573\ \lambda^3 + 0.0002512619258\ \lambda^4 + \ldots \end{aligned} \tag{15.1}$$

reproducing correctly the first two nontrivial orders [128, 127] and giving a prediction for higher orders.

The range of possible applications of our method is vast. First, it is not limited solely to the $\mathfrak{sl}(2)$ sector of $\mathcal{N} = 4$ SYM, but is directly applicable to any single trace operators of the theory. It would be interesting to do an explicit example of a numerical calculation

with our algorithm outside of the $\mathfrak{sl}(2)$ sector. For example, the wider class of $\mathfrak{sl}(2,\mathbb{C})$ operators (identified in [133]), also exhibiting a BFKL regime, could be a good candidate to begin with. Third, it may be interesting to generalize our method to ABJM theory as well as to various integrable deformations of $\mathcal{N}=4$ SYM theory.

The numerical results could also be helpful for the analytical exploration of the spectrum – for instance, in such regimes as BFKL and at strong coupling, which remains almost unexplored, and various limiting cases of the generalized cusp. Furthermore, studying numerical results and the behavior of the generated Q-functions in various limits can reveal new analytically solvable regimes.

Part IV

BFKL Pomeron eigenvalue at next-to-next-to-leading order

The BFKL limit in $\mathcal{N}=4$ SYM corresponds to analytic continuation for $sl(2)$ sector operators to the singular value of the spin $S \to -1$ simultaneously with $g \to 0$. In this part, based on results of [13], we present a method which allows to compute the anomalous dimension in this highly nontrivial regime systematically from the QSC. In particular, we solve the longstanding open problem of computing the NNLO correction to the anomalous dimension.

16 Introduction

QCD is notorious for being hard to explore analytically: perturbative calculations become impossibly complex after first few loop orders. However, there are regimes in which one can probe all orders of perturbation theory analytically. The Balitsky-Fadin-Kuraev-Lipatov (BFKL) equation is applicable in processes like Deep Inelastic Scattering or hadronic dijet production, which are characterized by a presence of at least two widely separated energy scales. The large logarithm of ratio of these energy scales Δy enters into perturbative expansion, so in order to make sense of the perturbation theory one has to resum powers of Δy in every order of perturbation theory.

The most nontrivial part χ of the scattering amplitude [124, 125, 126] is the so-called BFKL eigenvalue [136, 137] which at LO reads

$$\chi^{LO}(\nu,n)=2\psi(1)-\psi\left(\frac{n+1+i\nu}{2}\right)-\psi\left(\frac{n+1-i\nu}{2}\right). \tag{16.1}$$

Here we focus on the case $n=0$. Taking into account the Next-to-Leading, Next-to-Next-to-Leading contributions, and the BFKL eigenvalue χ gets corrected by terms of order g^2, g^4 etc correspondingly. One often also introduces $j(i\nu)$, related to the BFKL eigenvalue as

$$\frac{j(i\nu)-1}{4g^2}=\chi^{\rm LO}(\nu,0)+g^2\chi^{\rm NLO}(\nu,0)+g^4\chi^{\rm NNLO}(\nu,0)+\dots\ .$$

The Next-to-Leading BFKL was obtained after 9 years of laborious calculations in [138, 139, 140, 128]; the result in modern notation is presented below in the text (16.2). The

corrections turned out to be numerically rather large compared to the LO, which makes one question the validity of the whole BFKL resummation procedure and its applicability for phenomenology.

This and other indications make it clear that just NLO may not be enough to match experimental predictions. It is important to understand the general structure of BFKL expansion terms and here we will study the NNLO BFKL eigenvalue in $\mathcal{N}=4$ SYM — a more symmetric analog of QCD. Notably, it was observed in [128] that the $\mathcal{N}=4$ SYM reproduces correctly the part of the QCD result with maximal transcendentality. In particular the LO coincides exactly in the two theories.

A technically convenient way to compute the Pomeron eigenvalue is due to the observation of [140] who reformulated the problem in terms of a certain analytical continuation of anomalous dimensions of twist-2 operators. Fortunately, in planar $\mathcal{N}=4$ SYM the problem of computing the anomalous dimensions is solved for finite coupling and any operator by the Quantum Spectral Curve (QSC) formalism [52, 53].

In order to obtain the BFKL eigenvalue in $\mathcal{N}=4$ SYM from the anomalous dimension of twist operators we consider the dimension $\Delta(S)$ of twist-two operator $\mathcal{O}=\mathrm{Tr}ZD_+^SZ$. The inverse function $S(\Delta)$ is known to approach -1 perturbatively for Δ in the range $[-1,1]$ and thus the map to the BFKL regime is given by $\Delta=i\nu$ and $j=2+S(\Delta)$. Then the goal is to compute $j(\Delta)$ as a series expansion in g^2. Indeed, from the QSC formalism it was shown in [72] that one reproduces correctly the LO (16.1). Here we use some shortcuts to the direct approach of [72] to push the calculation to NNLO order, which already gives useful new information about the QCD result.

An essential for us observation was made in [129][25] where it was pointed out that both LO and NLO results can be represented as a simple linear combination of the nested harmonic sums. Let us stress again that in our notation Δ is the full conformal dimension of the twist-two operator, related to the anomalous dimension γ as $\Delta=2+S+\gamma$. Then the expansion of $j(\Delta)$ can be written as

$$j(\Delta)=1+\sum_{\ell=1}^{\infty}g^{2\ell}\left[F_\ell\left(\frac{\Delta-1}{2}\right)+F_\ell\left(\frac{-\Delta-1}{2}\right)\right] \tag{16.2}$$

with the two first known orders given by [129]

$$\begin{aligned} F_1&=-4S_1 \\ \frac{F_2}{4}&=-\frac{3}{2}\zeta_3+\pi^2\ln 2+\frac{\pi^2}{3}S_1+2S_3+\pi^2S_{-1}-4S_{-2,1} \end{aligned} \tag{16.3}$$

[25] We are grateful to S. Caron-Huot for bringing our attention to this paper

where

$$S_{a_1,a_2,\ldots,a_n}(x) = \sum_{y=1}^{x} \frac{(\text{sign}\,(a_1))^y}{y^{|a_1|}} S_{a_2,\ldots,a_n}(y) \;\;,\;\; S(x) = 1\;.$$

We define harmonic sums for non-integer and negative arguments by the standard widely accepted prescription, namely analytical continuation from positive even integer values as in [141, 142, 143, 100]. These analytically continued sums, which we denote as $S_{a_1,a_2,\ldots}$, are denoted by $\bar{S}^+$ in [141], see e.g. Eq. (21) in that paper. A compatible but more general definition is given in [144].

We assume the NNLO order can also be written in this form. After that we only have to fix a finite number of coefficients which we do by expanding the QSC around some values of Δ where the result simplifies. Then we verify our result by comparing it with extremely high precision numerical evaluation proving this assumption to be correct.

17 Analytical Data from QSC

As we discussed before, the 4 functions $\mathbf{P}_a$ of the spectral parameter u which can be conveniently written as a convergent series expansion

$$\mathbf{P}_a(u) = \sum_{n=\tilde{M}_a}^{\infty} \frac{c_{a,n}}{x^n(u)} \;\;,\;\; x(u) = \frac{u + \sqrt{u-2g}\sqrt{u+2g}}{2g}\;.$$

We will follow the same approach as in the numerical algorithm, with the $\mathcal{Q}_{a|i}$ functions playing a central role. Let us describe the details of our analytical method. We will focus on some particular points $\Delta_0 = 1, 3, 5, 7$. It can be seen already from the LO (16.1) that the function $S(\Delta)$ is singular at these points, however the coefficients of the expansion are relatively simple and are given by ζ-functions. We will perform a double expansion first in g up to the order g^6 and then in $\delta = \Delta - \Delta_0$.

General iterative procedure for solving the QSC. We describe a procedure which for some given $\mathbf{P}_a$ (or equivalently $c_{a,n}$) takes as an input some approximate solution of (4.20) $\mathcal{Q}^{(0)}_{a|i}$ valid up to the order ϵ^n (where ϵ is some small expansion parameter) and produces as an output new $\mathcal{Q}_{a|i}$ accurate to the order ϵ^{2n}. The method is very general and in particular is suitable for perturbative expansion around any background.

Let dS be the mismatch in the equation (4.20), i.e.

$$\mathcal{Q}^{(0)}_{a|i}(u + \tfrac{i}{2}) - \mathcal{Q}^{(0)}_{a|i}(u - \tfrac{i}{2}) + \mathbf{P}_a \mathbf{P}^b \mathcal{Q}^{(0)}_{b|i}(u + \tfrac{i}{2}) = dS_{a|i}, \tag{17.1}$$

where $dS_{a|i}$ is small $\sim \epsilon^n$. We can always represent the exact solution in the form

$$\mathcal{Q}_{a|i}(u) = \mathcal{Q}^{(0)}_{a|i}(u) + b_i^{\ j}(u + \tfrac{i}{2})\ \mathcal{Q}^{(0)}_{a|j}(u) \tag{17.2}$$

where the unknown functions $b_i^{\ j}$ are also small. After plugging this ansatz into the equation (17.1) we get

$$\Big(b_i^{\ j}(u) - b_i^{\ j}(u+i)\Big)\ \mathcal{Q}^{+(0)}_{a|j} = dS_{a|i} + dS_{a|j} b_i^{\ j}\ . \tag{17.3}$$

Since $b_i^{\ j}$ is small it can be neglected in the r.h.s. where it multiplies another small quantity. Finally multiplying the equation by $\mathcal{Q}^{(0)a|k}$ we arrive at

$$b_i^k(u+i) - b_i^k(u) = -dS_{a|i}(u)\mathcal{Q}^{(0)a|k}\left(u + \tfrac{i}{2}\right) + \mathcal{O}(\epsilon^{2n})\ .$$

We see that the r.h.s. contains only the known functions dS and $\mathcal{Q}^{(0)}$ and does not contain b which means that the original 4th order finite difference equation is reduced to a set of independent 1st order equations! In most interesting cases the first order equation can be easily solved. After $\mathcal{Q}_{a|i}$ is found one can use (4.22) to find $\mathbf{Q}_i$.

Iterations at weak coupling. For our particular problem we will take either $\epsilon = g$ or $\epsilon = \delta$. Applying this procedure a few times we generate $\mathbf{Q}_i$ for sufficiently high order both in g and in δ. Finally, by "gluing" $\mathbf{Q}_i$ and $\tilde{\mathbf{Q}}_i$ on the cut we find $c_{a,n}$ and $S(\Delta)$ also as a double expansion.

For the above procedure we need the leading order $\mathcal{Q}^{(0)}_{a,i}$. One can expect that to the leading order in g the solution should be very simple - indeed the branch cuts collapse to a point making most of the functions polynomial or having very simple singular structure. Also one can use that to the leading order in g functions $\mathbf{P}_a$ are very simple and are already known from [72] for any Δ. By making a simple ansatz for $\mathbf{Q}_i$ we found for $\Delta_0 = 1$ to the leading order

$$\mathbf{Q}_1 \simeq u,\ \mathbf{Q}_2 \simeq 1/u,\ \mathbf{Q}_3 \simeq 1,\ \mathbf{Q}_4 \simeq 1/u^2\ . \tag{17.4}$$

For $\Delta_0 = 3, 5, \ldots$ the solution involves also the η-functions introduced in the QSC context in [109, 70]

$$\eta_{s_1,\ldots,s_k}(u) = \sum_{n_1 > n_2 \ldots n_k \geq 0} \frac{1}{(u+in_1)^{s_1}\ldots(u+in_k)^{s_k}}. \tag{17.5}$$

which are related in a simple way to the nested harmonic sums. For $\Delta = 3$ we found

$$\begin{aligned} &\mathbf{Q}_1 \simeq u^2,\ \mathbf{Q}_2 \simeq u^2\eta_{1,3} - i - \frac{1}{2u}, \\ &\mathbf{Q}_3 \simeq u^2\eta_{1,2} - iu - \frac{1}{2},\ \mathbf{Q}_4 \simeq u^2\eta_{1,4} - \frac{i}{u} - \frac{1}{2u^2}\ , \end{aligned} \tag{17.6}$$

which reflects the general structure of the expansion of $\mathbf{Q}_i$ around integer Δ's which contain only $\eta_{1,2},\ \eta_{1,3}$ and $\eta_{1,4}$ with polynomial coefficients. As it was explained in [109, 70] the η-functions are closed under all essential for us operations: the product of any two η-functions can be written as a sum of η-functions, and most importantly one can easily solve equations of the type

$$f(u+i) - f(u) = u^n \eta_{s_1,\dots,s_k} \tag{17.7}$$

for any integer n again in terms of a sum of powers of u multiplying η-functions (which we call η-polynomials). For example for $n=-1$ and $k=1,\ s_1=1$ we get $f=-\eta_2-\eta_{1,1}$ etc. Thus for these starting points we are guaranteed to get η-polynomials on each step of the general procedure described above.

Proceeding in this way we computed $\mathbf{Q}_i$ up to the order g^6 and δ^{10} for $\Delta=3,5,7$. After that we fix the coefficients in the ansatz for $\mathbf{P}_a$ from analyticity requirements described below.

Fixing remaining freedom. Here we will describe how to use $\mathbf{Q}_i$ found before to finally extract relation between S and Δ and the constants $c_{a,n}$. This is done by using a relation between $\mathbf{Q}_i$ and their analytical continuations $\tilde{\mathbf{Q}}_i$. On the one hand we have the relation (4.33). On the other hand we can use the $u\to -u$ symmetry[26] of the twist-2 operators to notice that $\mathbf{Q}_i(-u)$ should satisfy the same finite difference equation as $\mathbf{Q}_i(u)$ and thus we should have $\mathbf{Q}_i(u)=\Omega_i^j(u)\mathbf{Q}_j(-u)$ where $\Omega_i^j(u)$ is a set of periodic coefficients. As $\mathbf{Q}_i(u)$ has a power-like behavior at infinity, $\Omega_i^j(u)$ should not grow faster than a constant. Furthermore, since $\mathbf{Q}_i$ has a definite asymptotic (13.7) only diagonal elements of $\Omega_i^i(u)$ can be nonzero at infinity. Combining these relations we find

$$\tilde{\mathbf{Q}}_A(u) = \alpha_A^i \mathbf{Q}_i(-u)\ \ ,\ \ A=1,3\ , \tag{17.8}$$

where $\alpha_A^j=\omega_{Ai}\chi^{ik}\Omega_k^j$ are i-periodic (as a combination of i-periodic functions), analytic (as both $\tilde{\mathbf{Q}}_a(u)$ and $\mathbf{Q}_a(-u)$ should be analytic in the lower-half-plane) and growing not faster than a constant at infinity which implies that they are constants. Furthermore most of them are zero because only $\omega_{12},\ \omega_{34}$ and Ω_i^i are non-zero at infinity. Thus we simply get

$$\tilde{\mathbf{Q}}_1(u) = \alpha_{13}\mathbf{Q}_3(-u)\ \ ,\ \ \tilde{\mathbf{Q}}_3(u)=\alpha_{31}\mathbf{Q}_1(-u)\ . \tag{17.9}$$

Next we note that if we analytically continue this relation and change $u\to -u$ we should get an inverse transformation which implies $\alpha_{13}=1/\alpha_{31}\equiv\alpha$. The coefficient α depends on

[26] more generally one can also use complex conjugation symmetry

relative normalization of $\mathbf{Q}_1$ and $\mathbf{Q}_3$. Let us see how to use the identity (17.9) to constrain the constants $c_{a,i}$. We observed that all the constants are fixed from the requirement of regularity at the origin of the combinations $\mathbf{Q}_1 + \tilde{\mathbf{Q}}_1$ and $\frac{\mathbf{Q}_1 - \tilde{\mathbf{Q}}_1}{\sqrt{u^2-4g^2}}$, which now can be written as

$$\mathbf{Q}_1(u) + \alpha \mathbf{Q}_3(-u) = \text{reg} \ , \quad \frac{\mathbf{Q}_1(u) - \alpha \mathbf{Q}_3(-u)}{\sqrt{u^2-4g^2}} = \text{reg} \ .$$

This relation is used in the following way: one first expands in g the l.h.s. and then in u around the origin. Then requiring the absence of the negative powers will fix α, all the coefficients $c_{a,n}$, and the function $\Delta(S)$! So we can completely ignore ω_{ij}, $\mathbf{Q}_2$, and $\mathbf{Q}_4$ in this calculation. This observation can be used in more general situations and allows avoiding construction of ω_{ij}, and in particular can simplify the numerical algorithm of [14] considerably.

Constraints from poles. We use the procedure described above to compute the expansion of $S(\Delta)$ around $\Delta_0 = 3, 5, 7$. In particular for $\Delta = 5 + \epsilon$ we computed the first 8 terms

$$\begin{aligned} \chi^{\text{NNLO}} = & -\frac{1024}{\epsilon^5} + \frac{64\left(4\pi^2 - 33\right)}{3\epsilon^3} + \frac{16\left(-36\zeta_3 + 2\pi^2 + 31\right)}{\epsilon^2} \\ + & \frac{-288\zeta_3 + \frac{232\pi^4}{45} - 16\pi^2 - 296}{\epsilon} \\ & -\frac{2}{15}\left[20\left(4\pi^2 - 75\right)\zeta_3 + 6300\zeta_5 + \pi^4 - 215\pi^2 + 285\right] + \dots \ . \end{aligned} \tag{17.10}$$

The terms with ϵ, ϵ^2, and ϵ^3 which we also evaluated explicitly are omitted for the sake of brevity. We also reproduced expansions extracted from [71] for $\Delta = 1$. In our calculations we used several Mathematica packages for manipulating harmonic sums and multiple zeta values [107, 110].

18 The result

By observing (16.3) for LO and NLO we notice that the transcendentality of these expressions is uniform if one assigns to $S_{a_1,\dots,a_k}$ transcendentality equal to $\sum_{j=1}^{k} |a_j|$. The principal assumption of our calculation states that $F_3(x)$ can also be written as a linear combination of nested harmonic sums with coefficients made out of several transcendental constants $\pi^2, \log(2), \zeta_3, \zeta_5, \text{Li}_4\left(\frac{1}{2}\right), \text{Li}_5\left(\frac{1}{2}\right)$ of uniform transcendentality 5. The final basis obtained after taking into account the constants contains 288 elements.

Hence we build the linear combination of these basis elements with free coefficients and constrained them by imposing the expansion at $\Delta = 1, 3, 5, 7$ to match the results of

the analytic expansion of QSC (in particular, requiring (17.10)). This gave an overdefined system of linear equations for the unknown coefficients which happen to have a unique solution presented below:

$$\begin{aligned}\frac{F_3(x)}{256} &= -\frac{5S_{-5}}{8} - \frac{S_{-4,1}}{2} + \frac{S_1 S_{-3,1}}{2} + \frac{S_{-3,2}}{2} - \frac{5S_2 S_{-2,1}}{4} \\ &+\frac{S_{-4}S_1}{4} + \frac{S_{-3}S_2}{8} + \frac{3S_{3,-2}}{4} - \frac{3S_{-3,1,1}}{2} - S_1 S_{-2,1,1} \\ &+S_{2,-2,1} + 3S_{-2,1,1,1} - \frac{3S_{-2}S_3}{4} - \frac{S_5}{8} + \frac{S_{-2}S_1S_2}{4} \\ &+\pi^2\left[\frac{S_{-2,1}}{8} - \frac{7S_{-3}}{48} - \frac{S_{-2}S_1}{12} + \frac{S_1S_2}{48}\right] - \pi^4\left[\frac{2S_{-1}}{45} - \frac{S_1}{96}\right] \\ &+\zeta_3\left[-\frac{7S_{-1,1}}{4} + \frac{7S_{-2}}{8} + \frac{7S_{-1}S_1}{4} - \frac{S_2}{16}\right] \\ &+\left[2\mathrm{Li}_4\left(\tfrac{1}{2}\right) - \frac{\pi^2\log^2 2}{12} + \frac{\log^4 2}{12}\right](S_{-1} - S_1) \\ &+\frac{\log^5 2}{60} - \frac{\pi^2\log^3 2}{36} - \frac{2\pi^4\log 2}{45} - \frac{\pi^2\zeta_3}{24} + \frac{49\zeta_5}{32} - 2\mathrm{Li}_5\left(\tfrac{1}{2}\right)\ .\end{aligned} \tag{18.1}$$

The simplicity of the final result is quite astonishing: only 37 coefficients out of 288 turned out to be nonzero. Furthermore, they are significantly simpler than the coefficients appearing in the series expansion around the poles (17.10). These are all clear and expected indications of the correct result similar to what was observed in the usual perturbation theory [103]. In addition we also performed the numerical test described below.

19 Numerical tests

Using the method of [14] we evaluated 40 values of spin S for various values of the coupling g in the range $(0.01, 0.025)$ with exceptionally high 80 digits precision and then fit this data to get the following prediction for the N^{n}LO BFKL coefficients at the fixed value of $\Delta = 0.45$:

	value	error
N^{2}LO	10774.635818847176637957593127192456995929170948057653783424533229	10^{-61}
N^{3}LO	$-$366393.205205391703893790350747854454993553195933391916340383 6	10^{-56}
N^{4}LO	1.33273635568112691569404431036982856152194058897947687885 4 $\times 10^7$	10^{-51}
N^{5}LO	$-$4.92174013665791650091395555207507006072145095843655987 6 $\times 10^8$	10^{-47}

We found that our result (18.1) reproduces perfectly the first line in the table within the numerical error 10^{-61} which leaves no room for doubt in the validity of our result.

20 Summary

In this letter we have applied the Quantum Spectral Curve method [52, 53] to the calculation of the NNLO correction to the BFKL eigenvalue. We check our result numerically with 60 digits precision using the algorithm developed in [14] and gave numerical predictions for a few next orders. We also developed a general efficient analytic method suitable for systematic perturbative solution of QSC.

We hope that our findings could shed some light on the QCD counterpart of our result and resolve some mysteries shrouding the BFKL physics. Our method is in no way limited to NNLO: calculating further orders with our iterative algorithm seems to be just the question of computational time. The goal of this activity would of course be to understand the structure of the general term of BFKL expansion. The fact that our result turned our significantly simpler than one could expect looking at the initial basis asks of explanation.

Part V

Analytic solution of Bremsstrahlung TBA in the twisted case

In this part as well as the two following parts we will describe applications of the QSC to a nonlocal operator – a cusped Wilson line. The divergence in its expectation value is the famous generalized cusp anomalous dimension which it will be our goal to study. This part is devoted to describing the analytic solution of the TBA equations (which are the precursor to the QSC) in a near-BPS limit but to all loops, found in [16]. In the next two parts we will formulate the QSC for this observable at any values of the parameters and show that this leads to numerous new results in regimes that previously were impossibly difficult to study.

21 Introduction

The Y-system and TBA were originally presented for the spectrum of local operators. The same approach was shown in 2012 to be essential in understanding another kind of observable – the quark-antiquark potential on the three-sphere, or equivalently the generalized cusp anomalous dimension Γ_{cusp}. This quantity describes the divergence in the expectation value of a Wilson loop made of two lines forming a cusp,

$$\langle W \rangle \sim \left(\frac{\Lambda_{IR}}{\Lambda_{UV}} \right)^{\Gamma_{\text{cusp}}}, \tag{21.1}$$

with Λ_{UV} and Λ_{IR} being the UV and IR cutoffs [145]. The quantity Γ_{cusp} has been studied at weak and strong coupling (for some recent results see [146, 166, 175, 176, 171]), and is also related to a number of other observables, such as IR divergence in amplitudes and radiation power from a moving quark, see e.g. [147, 148, 149, 97]. The cusp anomalous dimension is a function of two angles, ϕ and θ, which describe the geometry of the Wilson line setup shown in Fig. 21 [150]. The first angle, ϕ, is the angle between the quark and antiquark lines at the cusp. The second angle, θ, arises because the locally supersymmetric Wilson lines considered here include a coupling to the scalar fields. As there are six real scalars in $\mathcal{N} = 4$ SYM the coupling can be defined by a unit vector $\vec{n}$ which gives a point on S^5. For the two lines we have two different vectors, $\vec{n}$ and $\vec{n}_\theta$, with θ being the angle

between them. Explicitly, we can write the cusped Wilson loop as

$$W_0 = \mathrm{P}\exp\int_{-\infty}^{0} dt\left[iA\cdot\dot{x}_q + \vec{\Phi}\cdot\vec{n}\,|\dot{x}_q|\right] \times \mathrm{P}\exp\int_{0}^{\infty} dt\left[iA\cdot\dot{x}_{\bar{q}} + \vec{\Phi}\cdot\vec{n}_\theta\,|\dot{x}_{\bar{q}}|\right], \tag{21.2}$$

where $\vec{\Phi}$ denotes a vector consisting of the six scalars of $\mathcal{N}=4$ SYM, while $x_q(t)$ and $x_{\bar{q}}(t)$ are the quark and antiquark trajectories (straight lines through the origin) which make up an angle ϕ at the cusp (see Fig.21).

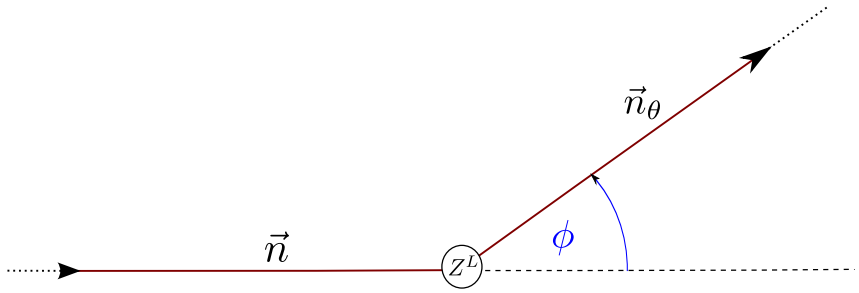

Figure 12: **The setup.** A Wilson line with a cusp angle ϕ and L scalar fields $Z=\Phi_1+i\Phi_2$ inserted at the cusp. Coupling of the scalar fields to the two half lines is defined by directions $\vec{n}$ and $\vec{n}_\theta$ in the internal space, with the angle θ between them.

A fully nonperturbative description for the value of Γ_{cusp} was obtained in a remarkable development by Drukker [64] and by Correa, Maldacena & Sever [63]. They proposed an infinite system of TBA integral equations which compute this quantity at arbitrary 't Hooft coupling λ and for arbitrary angles. In order to implement the TBA approach, the cusp anomalous dimension was generalized for the case when a local operator with R-charge L is inserted at the cusp (cf. Fig. 21):

$$W_L = \mathrm{P}\exp\int_{-\infty}^{0} dt\left(iA\cdot\dot{x}_q + \vec{\Phi}\cdot\vec{n}\,|\dot{x}_q|\right) \times Z^L \times \mathrm{P}\exp\int_{0}^{\infty} dt\left(iA\cdot\dot{x}_{\bar{q}} + \vec{\Phi}\cdot\vec{n}_\theta\,|\dot{x}_{\bar{q}}|\right). \tag{21.3}$$

Here $Z=\Phi_1+i\Phi_2$, with Φ_1 and Φ_2 being two scalars independent from $(\vec{\Phi}\cdot\vec{n})$ and $(\vec{\Phi}\cdot\vec{n}_\theta)$. The anomalous dimension $\Gamma_L(\phi,\theta,\lambda)$ corresponding to such Wilson loop is captured by the TBA equations exactly at any value of L. For $L=0$ the usual quark-antiquark potential is recovered. The number of field insertions plays the role of the system's volume in the TBA description, and $\Gamma_L(\phi,\theta,\lambda)$ is obtained as the vacuum state energy.

While the infinite system of these TBA equations is rather complicated, having the two angles as continuous parameters opens the possibility to look for simplifications in some limits where an exact analytical solution may be expected[27]. We will focus on the

[27] On the other hand, non-perturbative predictions from the spectral TBA have been mostly restricted to numerics [42, 44, 45, 46]; see also [43].

near-BPS limit when $\phi \approx \theta$. For $\phi = \theta$ the configuration is BPS and the anomalous dimension vanishes [151, 152][28]. The small deviations from this supersymmetric case are known to be partially under control: the cusp dimension at $L = 0$ was computed for $\phi \approx \theta$ analytically at any coupling in [147, 148] using results from localization methods [153, 154, 155, 156, 157, 158, 159, 160, 161, 162, 163]. The answer in the planar limit reads

$$\Gamma_{\rm cusp}(\phi,\theta,\lambda) = -\frac{1}{4\pi^2}(\phi^2-\theta^2)\frac{1}{1-\frac{\theta^2}{\pi^2}}\frac{\sqrt{\tilde\lambda}\, I_2\left(\sqrt{\tilde\lambda}\right)}{I_1\left(\sqrt{\tilde\lambda}\right)} + \mathcal{O}\left((\phi^2-\theta^2)^2\right), \quad \tilde\lambda = \lambda\left(1-\frac{\theta^2}{\pi^2}\right) \tag{21.4}$$

where I_n are the modified Bessel functions of the first kind. The existence of such explicit result suggests that the cusp TBA system should simplify dramatically when $\phi \approx \theta$. Even though the full set of TBA equations was simplified a bit in this limit as described in [63], the result is still an enormously complicated infinite set of integral equations. Remarkably, it turned out that these equations admit an exact *analytical* solution. It was obtained in [164] for the particular near-BPS configuration where $\theta = 0$ and ϕ is small. The result of [164] covers all values of L and λ and for $L = 0$ reproduces the localization result (21.4) in which θ should be set to zero.

We will show how to extend the results of [164] to the generic near-BPS limit. Thus, we consider the case when $\phi \approx \theta$, but θ is arbitrary and is an extra parameter in the result. We also filled some gaps in the previous derivation using the novel $\mathbf{P}\mu$-formulation [52]. We obtain an explicit expression valid for all values of θ, L and λ. For this we solve the Bremsstrahlung TBA analytically, following the strategy developed in [164]. Quite surprisingly the result for arbitrary θ is considerably simpler and takes the form

$$\Gamma_L(g) = \frac{\phi-\theta}{4}\partial_\theta \log\frac{\det \mathcal{M}_{2L+1}}{\det \mathcal{M}_{2L-1}}, \tag{21.5}$$

where we define an $N+1 \times N+1$ matrix

$$\mathcal{M}_N = \begin{pmatrix} I_1^\theta & I_0^\theta & \cdots & I_{2-N}^\theta & I_{1-N}^\theta \\ I_2^\theta & I_1^\theta & \cdots & I_{3-N}^\theta & I_{2-N}^\theta \\ \vdots & \vdots & \ddots & \vdots & \vdots \\ I_N^\theta & I_{N-1}^\theta & \cdots & I_1^\theta & I_0^\theta \\ I_{N+1}^\theta & I_N^\theta & \cdots & I_2^\theta & I_1^\theta \end{pmatrix} \tag{21.6}$$

and I_n^θ are

$$I_n^\theta = \frac{1}{2}I_n\left(\sqrt{\tilde\lambda}\right)\left[\left(\sqrt{\frac{\pi+\theta}{\pi-\theta}}\right)^n - (-1)^n\left(\sqrt{\frac{\pi-\theta}{\pi+\theta}}\right)^n\right]. \tag{21.7}$$

[28] Strictly speaking the BPS condition allows $\phi = -\theta$ in addition to $\phi = \theta$ but these two cases are trivially related.

At $L = 0$ we have reproduced in full the localization result (21.4). For $L > 0$ our result complements and generalizes the calculation of [164] as another integrability-based prediction for localization techniques. As in [164], the determinant expressions we got suggest a possible link to matrix models, which would be interesting to explore further.

22 TBA equations in the near-BPS limit

In this section we discuss the first simplification of the cusp TBA system in the near-BPS regime, when the two angles ϕ and θ are close to each other. Following [63] we will thus obtain a somewhat simpler, but still infinite, set of integral equations – the Bremsstrahlung TBA.[29]

Let us remind that the cusp TBA equations are very similar to those describing the spectrum of single trace operator anomalous dimensions. After subtracting the asymptotic large L solution, these two infinite sets of equations for the Y-functions $Y_{a,s}(u)$ become exactly the same. The integer indices (a, s) of the Y-functions take values in the infinite T-shaped domain familiar from the spectral TBA (see Fig. 22). The only difference is in an extra symmetry requirement for the Y-functions, and in the large L asymptotic solution[30].

The asymptotic solution encodes, in particular, the boundary scattering phase which has a double pole at zero mirror momentum. Due to this, the momentum-carrying functions $Y_{a,0}(u)$ have a double pole for $u = 0$. This greatly simplifies their dynamics in the near-BPS regime – only the residue at this pole is important and gives a non-vanishing contribution. This residue is small for $\phi \approx \theta$, and thus the structure of the expansion of the cusp TBA system in our case is very similar to what happens in the small angles regime discussed in detail in [63, 164].

We found it convenient to use a small expansion parameter

$$\epsilon \equiv (\phi - \theta) \tan \phi_0, \tag{22.1}$$

where[31] we denote $\phi_0 = (\phi + \theta)/2$. As in the small angles case, it is sufficient to keep only

[29] The authors of [63] obtained the Bremsstrahlung TBA equations for the generic case $\phi \approx \theta$, but the equations were given explicitly in [63] only for the small angles case so we will repeat the derivation here.

[30] The extra symmetry requirement in the cusp TBA reads $Y_{a,s}(u) = Y_{a,-s}(-u)$ but is irrelevant in our discussion as for our state all Y-functions are even.

[31] To shorten notation we will sometimes use θ instead of ϕ_0 in the text, on the understanding that equations containing θ are assumed to hold to the leading order in ϵ.

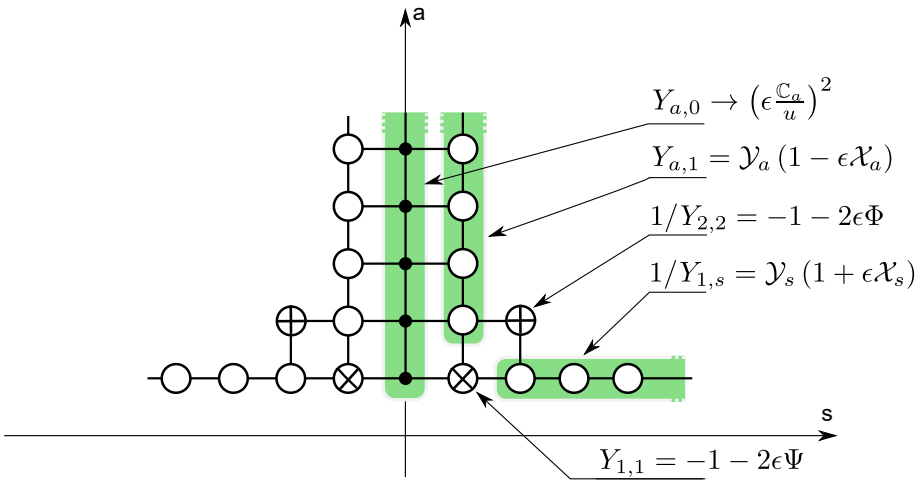

Figure 13: **The T-hook.** The indices (a, s) of Y-functions take values on the infinite T-shaped lattice in the figure. We also show the form of expansion in small ϵ for different groups of Y-functions. Notice that the momentum carrying Y-functions $Y_{a,0}$ are small in ϵ and enter the system only through the singularity at $u = 0$.

the leading orders in the expansion of the Y-functions, which are

$$Y_{a,1} = \mathcal{Y}_a\left[1 + \epsilon(\Omega_a - \mathcal{X}_a)\right],\ 1/Y_{1,s} = \mathcal{Y}_s\left[1 + \epsilon(\Omega_s + \mathcal{X}_s)\right], \tag{22.2}$$
$$Y_{1,1} = -1 - 2\epsilon\Psi,\ 1/Y_{2,2} = -1 - 2\epsilon\Phi,$$

while the residue of $Y_{a,0}$ reads

$$\lim_{u\to 0}\left(u^2 Y_{a,0}\right) = \left(\epsilon\,\mathbb{C}_a\right)^2. \tag{22.3}$$

This expansion (except for the Ω_a functions which will not enter our equations) is also shown in Fig. 22.

It is straightforward to plug these expansions into the cusp TBA system, and then simplify the equations a bit further using the same techniques as in the small angles case. The resulting set of Bremsstrahlung TBA equations reads:

$$\Phi - \Psi = \pi\mathbb{C}_a\hat{K}_a(u), \tag{22.4}$$
$$\Phi + \Psi = \mathbf{s} * \left[-2\frac{\mathcal{X}_2}{1+\mathcal{Y}_2} + \pi(\hat{K}_a^+ - \hat{K}_a^-)\mathbb{C}_a - \pi\delta(u)\mathbb{C}_1\right], \tag{22.5}$$
$$\log Y_{1,m} = \mathbf{s} * I_{m,n}\log\left(1 + Y_{1,n}\right) - \delta_{m,2}\mathbf{s}\hat{*}\left(\log\frac{\Phi}{\Psi} + \epsilon\left(\Phi - \Psi\right)\right) - \epsilon\pi\mathbf{s}\mathbb{C}_m, \tag{22.6}$$
$$\Delta_a = [\mathcal{R}_{ab}^{(10)} + \mathcal{B}_{a,b-2}^{(10)}]\hat{*}\log\frac{1+\mathcal{Y}_b}{1+A_b} + \mathcal{R}_{a1}^{(10)}\hat{*}\log\left(\frac{\Psi}{1/2}\right) - \mathcal{B}_{a1}^{(10)}\hat{*}\log\left(\frac{\Phi}{1/2}\right), \tag{22.7}$$
$$\mathbb{C}_a = (-1)^{a+1}a\frac{\sin a\theta}{\tan\theta}\left(\sqrt{1+\frac{a^2}{16g^2}} - \frac{a}{4g}\right)^{2+2L} F(a,g)e^{\Delta_a}, \tag{22.8}$$

where the kernels and conventions are the same as in [164] and are defined in Appendix B.1. The equation (22.6) for $Y_{1,m}$ should be understood to hold at orders $\mathcal{O}(\epsilon^0)$ and $\mathcal{O}(\epsilon^1)$ only. Notice that as in the small angles case the functions Ω_a from (22.2) have dropped out of the equations.

We see that our Bremsstrahlung TBA equations are almost the same as in [164]. However, importantly, the asymptotic condition at large real u is different:

$$1/Y_{1,m} \to \frac{\sin^2\theta}{\sin(m+1)\theta\sin(m-1)\theta}, \tag{22.9}$$

which should hold up to terms of order $\mathcal{O}(\epsilon)$ inclusive. Finally, the cusp anomalous dimension is determined by the double pole of momentum-carrying Y-functions:

$$\Gamma_L(g) = \epsilon\sum_{a=1}^{\infty}\frac{\mathbb{C}_a}{\sqrt{1+16g^2/a^2}}. \tag{22.10}$$

In the next section we will reduce this TBA system to a finite set of nonlinear equations.

23 FiNLIE

23.1 Twisted ansatz for T-functions

Our main task is to reduce the infinite set of equations (22.6) for the functions $Y_{1,m}$. In order to do this we use its relation to the Y-system and Hirota equations in the horizontal right wing of the T-hook. Indeed, from the integral form of (22.6) and the analyticity of the kernels it is clear that $Y_{1,m}(u)$ are analytic and regular in the strip $|\Im\, u| < \frac{m-1}{2}$. Then for $m > 2$ the equation (22.6) can be rewritten as the Y-system functional equation

$$\log\left(Y^+_{1,m}Y^-_{1,m}\right) = \log\left(1+Y_{1,m-1}\right)\left(1+Y_{1,m+1}\right). \tag{23.1}$$

This set of functional equations can be solved by switching to the so-called T-functions according to

$$1/Y_{1,m} = \frac{T^+_{1,m}T^-_{1,m}}{T_{1,m+1}T_{1,m-1}} - 1. \tag{23.2}$$

In terms of T-functions the Y-system equation becomes the Hirota equation in the horizontal strip, for which the general solution is known [51, 165] and involves only two unknown functions which we denote Q_1 and Q_2:

$$T_{1,s} = C\begin{vmatrix} Q_1^{[s]} & \bar{Q}_1^{[-s]} \\ Q_2^{[s]} & \bar{Q}_2^{[-s]} \end{vmatrix}. \tag{23.3}$$

In this way we are able to replace the infinite set of Y_m functions ($m = 2, 3, \dots$) by two functions $Q_1(u)$ and $Q_2(u)$. Now the problem is reduced to finding an ansatz for the functions Q_1, Q_2 entering (23.3). The main requirement for this ansatz is that the $Y_{1,m}$ generated by (23.2), (23.3) should have the correct asymptotics at large real u given by (22.9). For small angles the asymptotics is $\frac{1}{m^2-1}$ and the corresponding ansatz for the Q-functions is known [164]. Here we present an ansatz which works also in a deformed case with nontrivial twists.

The ansatz also has to ensure the correct analytical properties of the Y-functions which are dictated by the integral equations (22.6). First of all, the $Y_{1,m}$ functions should be analytic inside the strip $|\text{Im } u| < \frac{m-1}{2}$ and even as functions of u. The term with $\delta_{m,2}$ in (22.6) can be reproduced if $Y_{1,2}(u)$ has branch cuts starting at $u = i/2 \pm 2g$ and $u = -i/2 \pm 2g$.

Our proposal for Q-functions meeting these requirements is:

$$Q_1 = \bar{Q}_1 = e^{+\theta(u - i\mathcal{G}(u))}, \tag{23.4}$$

$$Q_2 = \bar{Q}_2 = e^{-\theta(u - i\mathcal{G}(u))}, \tag{23.5}$$

where $\mathcal{G}(u)$ should be a function with a branch cut on the real axis in order to satisfy the properties of T-functions listed above. Note that the asymptotics (22.9) of Y-functions is automatically satisfied for any $\mathcal{G}(u)$ decaying at infinity. Finally, as $T_{1,s}$ are even and real functions (to ensure the same properties for Y-functions), $\mathcal{G}(u)$ should be odd and imaginary.

With this choice of Q_1 and Q_2 we can calculate $T_{1,s}$ from (23.3) where for consistency with [164] in the small angle limit we choose $C = \frac{1}{2i \sin\theta}$

$$T_{1,s} = \frac{\sin(s - \mathcal{G}^{[s]} + \mathcal{G}^{[-s]})\theta}{\sin\theta}. \tag{23.6}$$

Discontinuity of the function $\mathcal{G}$ can be found from the equation analogous to (23.1) for $m = 2$ [51]. It reads

$$\frac{T_{1,1}^{++} T_{1,1}^{--}}{T_{1,1}^{+-} T_{1,1}^{-+}} = r, \quad \text{where } r = \frac{1 + 1/Y_{2,2}}{1 + Y_{1,1}} \tag{23.7}$$

and we denoted

$$T^{+\pm}(u) = T(u + i/2 \pm i0) \qquad \text{and} \qquad T^{-\pm}(u) = T(u - i/2 \pm i0)\,. \tag{23.8}$$

More explicitly, using the formula (23.6) for $T_{1,1}$ one can write

$$r = \frac{\sin\left(1 - \mathcal{G}^{[+2]} + \mathcal{G} - \rho/2\right)\theta \sin\left(1 + \mathcal{G}^{[-2]} - \mathcal{G} - \rho/2\right)\theta}{\sin\left(1 - \mathcal{G}^{[+2]} + \mathcal{G} + \rho/2\right)\theta \sin\left(1 + \mathcal{G}^{[-2]} - \mathcal{G} + \rho/2\right)\theta}, \tag{23.9}$$

where $\mathcal{G}(u)$ is the average of $\mathcal{G}$ on both sides of the cut if u is on the cut, and it is equal to $\mathcal{G}(u) + \rho(u)/2$ away from the cut. This allows to deduce the discontinuity of the function $\mathcal{G}$ with one real Zhukovsky cut in terms of a combination (23.7) of "fermionic" Y-functions $Y_{1,1}$ and $Y_{2,2}$.

Finally, for small θ the combinations $Q_1 \pm Q_2$ obtained from our ansatz nicely match[32] (up to overall factors) the Q-functions in the small angles case [164], where $Q_1 = 1$ and $Q_2 = -iu - \mathcal{G}(u)$.

23.2 Expansion in the near-BPS case

The ansatz presented in the previous subsection is valid for a general, not necessarily near-BPS situation. Here we will apply it to the case of $\phi \approx \theta$ (i.e. small ϵ).

As we have seen above, the solution for Y-functions is completely defined by a single function $\mathcal{G}(u)$, which we will call the resolvent. For our goals we only need to know $\mathcal{G}$ up to the linear in ϵ terms inclusive. Our proposal for the resolvent is

$$\mathcal{G}(u) = \frac{1}{2\pi i} \int_{-2g}^{2g} dv \frac{\rho(v)}{u-v} + \epsilon \sum_{a \neq 0} \frac{b_a}{u - ia/2} \,. \tag{23.10}$$

The first term creates a short branch cut[33] in $\mathcal{G}(u)$, which translates into the branch cuts of $\mathcal{Y}_m$. The discontinuity of the resolvent across this cut is the density ρ:

$$\rho(u) = G(u - i0) - G(u + i0). \tag{23.11}$$

The second term in (23.10) produces poles at $\pm i/2$ with residues proportional to ϵ in Y-functions, which account for the term $\epsilon\pi\mathbf{s}\mathbb{C}_m$ in (22.6).

One can see that the properties of $T_{1,m}$ being real and even imposes the following constraints on the density and poles: ρ should be even and real as a function with a long cut, while $b_a = b_{-a}$ and $b_a = -b_a^*$.

Most of the equations are already expanded in ϵ, so it is convenient to introduce expanded to the leading order versions of the quantities above. The leading order part of the resolvent is[34]

$$G(u) = \frac{1}{2\pi i} \int_{-2g}^{2g} dv \frac{\rho(v)}{u-v}. \tag{23.12}$$

[32] As $T_{1,s}$ are given by a determinant, we are free to replace $Q_{1,2}$ by their linear combinations

[33] i.e. a cut from $-2g$ to $2g$.

[34] The density ρ contains both the leading order in ϵ part and the linear correction, however, here we will never need to deal with this correction. Hence, we will denote the full density and its leading order part by the same letter ρ hoping that this will not cause any confusion.

We also introduce the leading order T-functions $\mathcal{T}_m$ related to the leading order Y-functions as

$$\mathcal{Y}_m = \frac{\mathcal{T}_m^+ \mathcal{T}_m^-}{\mathcal{T}_{m+1}\mathcal{T}_{m-1}} - 1. \tag{23.13}$$

Explicitly, the leading order part of (23.6) gives

$$\mathcal{T}_s = \frac{\sin\left(s - G^{[s]} + G^{[-s]}\right)\phi_0}{\sin\phi_0}. \tag{23.14}$$

23.3 Final reduction to FiNLIE

We now use the ansatz that we discussed above and finalize the reduction of the original Bremsstrahlung TBA system to a finite set of equations. Skipping the intermediate steps which are covered in [16] we find that the FiNLIE equations read:

$$\eta \frac{\sin\theta\rho}{\sin\theta} = -\sum_a \pi \mathbb{C}_a \hat{K}_a, \tag{23.15}$$

$$\eta \frac{\cos\theta\rho\cos\left(2 - G^+ + G^-\right)\theta - \cos\left(2G - G^+ - G^-\right)\theta}{\sin\theta\sin\left(2 - G^+ + G^-\right)\theta} =$$

$$= \mathbf{s} * \left[-2\frac{\mathcal{X}_2}{1+\mathcal{Y}_2} + \pi(\hat{K}_a^+ - \hat{K}_a^-)\mathbb{C}_a - \pi\delta(u)\mathbb{C}_1\right], \tag{23.16}$$

$$\mathbb{C}_a = (-1)^a a \mathcal{T}_a(0) \left(\sqrt{1 + \frac{a^2}{16g^2}} - \frac{a}{4g}\right)^{2+2L} \times \tag{23.17}$$

$$\exp\left[\tilde{K}_a \hat{*} \log\left(\eta \frac{\sinh 2\pi u}{2\pi u}\right)\right].$$

A clarification of notation used here and the kernels can be found in the Appendix B.1.[35]

24 Solving the FiNLIE: analytical ansatz

In the previous sections we presented the FiNLIE - a system of equations for $\mathbb{C}_a, \rho, \eta$. Following the spirit of [164], in order to solve it we should analyse the analytical properties of η and ρ as functions in the whole complex plane. We parametrize these functions in terms of auxiliary Bethe roots, for which we will obtain a set of Bethe equations. Then we solve them using Baxter equation techniques and obtain the result for the anomalous dimension $\Gamma_L(g)$.

[35] Strictly speaking these equations are also supplemented with several additional constraints which may be found in full detail in [16].

For the sake of readability we will not cover all steps of this calculation which are described in full detail in [16]. The main outcome is that the system reduces to a Baxter-like equation for several functions encoding the auxiliary Bethe roots x_k:

$$\mathbf{Q}_+(x) = \prod_{k\neq 0} \frac{x_k - x}{x_k} \ , \quad \mathbf{Q}_-(x) = \mathbf{Q}_+(-x) \tag{24.1}$$

Introducing

$$\mathbf{T}(x) = e^{+2g\theta x} x^{L+1} \mathbf{Q}_-(x) + (-1)^L \frac{e^{-2g\theta/x}}{x^{L+1}} \tilde{\mathbf{Q}}_+(x). \tag{24.2}$$

which encodes the whole set of auxiliary Bethe roots x_k, we will call $\mathbf{T}(x)$ the Baxter function. T

$$\mathbf{T}(-1/x) = -\mathbf{T}(x) \tag{24.3}$$

At large u one can show that

$$\mathbf{Q}_\pm(1/x) \to 1 \tag{24.4}$$

while

$$\mathbf{Q}_\pm \sim \tilde{C} \frac{\sinh 2\pi u}{2\pi u}, \ u \to +\infty \ . \tag{24.5}$$

Therefore the second term in (24.2) is suppressed compared to the first one and the asymptotics of the whole expression at large x is $\mathbf{T}(x) \sim x^L e^{2g(\pi+\theta)x}$. Then from (24.3) we can find the asymptotics of $\mathbf{T}(x)$ at $x \to 0$, and combining all these analytical properties together we can fix $\mathbf{T}$ uniquely to be

$$\mathbf{T}(x) = \sinh(2\pi u) e^{2g\theta(x-1/x)} P_L(x), \tag{24.6}$$

where $P_L(x)$ should be a rational function with behavior $\sim x^L$ at infinity. Since $\mathbf{T}(x)$ should not have singularities apart from $x = 0$ and $x = \infty$, the function P_L must be a polynomial in x and $1/x$. Moreover, (24.3) means that $P_L(-1/x) = P_L(x)$ and hence we can write

$$P_L(x) = C_1 x^L + C_2 x^{L-1} \cdots + (-1)^L C_1 x^{-L}. \tag{24.7}$$

To find $\mathbf{T}(x)$ explicitly it only remains to determine the coefficients C_i. This is straightforward to do by imposing the condition that the r.h.s. of (24.6) does not contain powers of x from $-L$ to L in its Laurent expansion (as follows from (24.2)) which must be the case since $\mathbf{Q}_-$ is regular at the origin.

Finally, and most importantly, one can show that the energy is given by

$$\Gamma_L(g) = -2(\phi - \theta) g \left[-\frac{C_2}{2C_1} + \frac{c}{2} + g\theta \right], \tag{24.8}$$

where c is the leading expansion coefficient of $\mathbf{Q}_\pm$:

$$\mathbf{Q}_\pm(x) \simeq 1 \mp cx \ , \ x \to 0. \tag{24.9}$$

Notice that the coefficients C_1, C_2 are also encoded in $\mathbf{Q}_\pm$: from (24.2), (24.6) we find

$$\mathbf{Q}_\pm(x) \simeq \sinh(2\pi u) \left[\frac{C_1}{x} \pm \frac{2g\theta C_1}{x^2} \mp \frac{C_2}{x^2} + \dots \right] \ , \ x \to \infty \, . \tag{24.10}$$

Now we have all the necessary tools to obtain the energy explicitly using the Baxter equation.

24.1 The $L = 0$ case

Let us first discuss the $L = 0$ case, because it is technically simpler. The function $P_L(x)$ from (24.6) is then just a constant,

$$P_L(x) = C_1. \tag{24.11}$$

To fix it we need to know the expansion of (24.6) in powers of x. Using that the exponent of $x + 1/x$ is a generating function for the modified Bessel functions of the first kind, $e^{2\pi g(x+1/x)} = \sum_{n=-\infty}^{\infty} I_n(4\pi g) x^n$, we get the expansion

$$\sinh\left(2\pi g(x + 1/x)\right) e^{2g\theta(x-1/x)} = \sum_{n=-\infty}^{+\infty} I_n^\theta x^n, \tag{24.12}$$

where I_n^θ are the "deformed" Bessel functions

$$I_n^\theta = \frac{1}{2} I_n \left(4\pi g \sqrt{1 - \frac{\theta^2}{\pi^2}} \right) \left[\left(\sqrt{\frac{\pi + \theta}{\pi - \theta}} \right)^n - (-1)^n \left(\sqrt{\frac{\pi - \theta}{\pi + \theta}} \right)^n \right]. \tag{24.13}$$

Below we will omit the argument of I_n, always assuming it to be the same as in (24.13).

The expansion (24.12) allows us to write the Baxter function (24.6) as

$$\mathbf{T}(x) = e^{+2g\theta x} x \mathbf{Q}_-(x) + \frac{e^{-2g\theta/x}}{x} \mathbf{Q}_+(1/x) = C_1 \sum_{n=-\infty}^{+\infty} I_n^\theta x^n.$$

We can now find $\mathbf{Q}_-$ as the regular part of the Laurent expansion of $\mathbf{T}$:

$$\mathbf{Q}_-(x) = C_1 \frac{e^{-2g\theta x}}{x} \sum_{n=1}^{+\infty} I_n^\theta x^n. \tag{24.14}$$

From (24.1) we see that $\mathbf{Q}_\pm(0) = 1$, so setting $x = 0$ in the last equation we fix C_1 as

$$C_1 = \frac{\sqrt{\pi^2 - \theta^2}}{\pi I_1}. \tag{24.15}$$

Since $L = 0$ we have $C_2 = 0$, while the coefficient c in (24.9) is read off from (24.14):

$$c = -2g\theta + \frac{2\theta}{\sqrt{\pi^2 - \theta^2}} \frac{I_2}{I_1} . \tag{24.16}$$

Then from (24.8) we get the energy

$$\Gamma_L = -2(\phi - \theta) \frac{\theta g}{\sqrt{\pi^2 - \theta^2}} \frac{I_2\left(\tilde{\lambda}^{1/2}\right)}{I_1\left(\tilde{\lambda}^{1/2}\right)}, \ \tilde{\lambda} = (4\pi g)^2 \left(1 - \tfrac{\theta^2}{\pi^2}\right) . \tag{24.17}$$

Remarkably, this is precisely the localization result of [147]! This is the first successful check of our construction.

24.2 Non-zero L

Let us now find the explicit expression for the energy at any L.

First we need to compute the coefficients C_k, using the equation (24.6). From (24.2) we see that the left hand side of (24.6) should not contain terms with powers of x from $-L$ to L, and also the coefficient of the x^{L+1} term should be 1. After we expand the right hand side according to (24.12) this condition generates $2L + 1$ equations for $2L + 1$ variables C_k:

$$\begin{cases} \sum\limits_{k=-L}^{L} I^{\theta}_{m-k} C_{k+L+1} = 0, \ m = -L+1 \dots L, \\ \sum\limits_{k=-L}^{L} I^{\theta}_{m-k} C_{k+L+1} = 1, \ m = L+1. \end{cases} \tag{24.18}$$

This linear system can be formulated in matrix form:

$$(\mathcal{M}_{2L})_{ik} C_{k+L+1} = \delta_{i,L+1}, \tag{24.19}$$

where

$$\mathcal{M}_N = \begin{pmatrix} I^{\theta}_1 & I^{\theta}_0 & \cdots & I^{\theta}_{2-N} & I^{\theta}_{1-N} \\ I^{\theta}_2 & I^{\theta}_1 & \cdots & I^{\theta}_{3-N} & I^{\theta}_{2-N} \\ \vdots & \vdots & \ddots & \vdots & \vdots \\ I^{\theta}_N & I^{\theta}_{N-1} & \cdots & I^{\theta}_1 & I^{\theta}_0 \\ I^{\theta}_{N+1} & I^{\theta}_N & \cdots & I^{\theta}_2 & I^{\theta}_1 \end{pmatrix} . \tag{24.20}$$

By Cramer's rule we obtain the solution

$$C_k = \frac{\det \mathcal{M}^{(2L+1,k)}_{2L}}{\det \mathcal{M}_{2L}}, \tag{24.21}$$

where $\mathcal{M}_N^{(a,b)}$ is the matrix obtained from $\mathcal{M}_N$ by deleting a^{th} row and b^{th} column. Plugging these coefficients into $P_L(x)$ we can combine it into a determinant again:

$$P_L(x) = \frac{1}{\det \mathcal{M}_{2L}} \begin{vmatrix} I_1^\theta & I_0^\theta & \cdots & I_{2-2L}^\theta & I_{1-2L}^\theta \\ I_2^\theta & I_1^\theta & \cdots & I_{3-2L}^\theta & I_{2-2L}^\theta \\ \vdots & \vdots & \ddots & \vdots & \vdots \\ I_{2L}^\theta & I_{2L-1}^\theta & \cdots & I_1^\theta & I_0^\theta \\ x^{-L} & x^{1-L} & \dots & x^{L-1} & x^L \end{vmatrix} . \tag{24.22}$$

Notice that now from (24.6) we have the Baxter function $\mathbf{T}(x)$ in a fully explicit form. In particular, one can easily find the functions $\mathbf{Q}_\pm$ encoding the Bethe roots. Namely, $\mathbf{Q}_-$ is the regular part of the Laurent expansion of $\mathbf{T}(x)$,

$$\mathbf{Q}_-(x) = x^{-L-1} e^{-2g\theta x} \left[\mathbf{T}(x)\right]_+ , \tag{24.23}$$

while $\mathbf{Q}_+(x) = \mathbf{Q}_-(-x)$.

It remains to find c – the coefficient of expansion of $\mathbf{Q}_\pm$ which enters the expression for $\Gamma_L(g)$. Consider expansion of (24.6) around $x = 0$, taking into account the definition of $\mathbf{T}$ (24.2):

$$(1+2g\theta x+\dots)x^{L+1}(1+cx+\dots)+\text{negative powers} = \sum_{n=-\infty}^{+\infty} I_n^\theta x^n \sum_{k=-L}^{L} C_{k+L+1} x^k \tag{24.24}$$

Equating the coefficients of x^L on both sides we get

$$2g\theta + c = \sum_{k=-L}^{L} I_{L+2-k} C_{k+L+1} . \tag{24.25}$$

Plugging the solution for C_k into the right hand side of the last equation we see that it combines nicely into a ratio of two determinants, resulting in

$$c = -2g\theta + \frac{\det \mathcal{M}_{2L+1}^{(2L+1,2L+2)}}{\det \mathcal{M}_{2L}}. \tag{24.26}$$

The determinants $\det \mathcal{M}_N^{(a,b)}$ satisfy a number of useful identities which allow us to bring the expressions for c and C_1/C_2 to the following form:

$$c = -2g\theta + \frac{\det \mathcal{M}_{2L+1}^{(1,2)}}{\det \mathcal{M}_{2L+1}^{(1,1)}}, \;\; C_1/C_2 = \frac{\det \mathcal{M}_{2L}^{(1,2)}}{\det \mathcal{M}_{2L}^{(1,1)}}. \tag{24.27}$$

Finally we can plug (24.27) into (24.8) and write our main result for $\Gamma_L(g)$

$$\Gamma_L(g) = (\phi - \theta) g \left(r_{2L-1} - r_{2L}\right), \; r_N = \frac{\det \mathcal{M}_{N+1}^{(1,2)}}{\det \mathcal{M}_N}. \tag{24.28}$$

Using the identities for these determinants, we can represent it in a compact form. The final formula reads

$$\boxed{\Gamma_L(g) = \frac{\phi-\theta}{4}\partial_\theta \log \frac{\det \mathcal{M}_{2L+1}}{\det \mathcal{M}_{2L-1}}}\,. \tag{24.29}$$

This is our main result which was announced in the Introduction. As an example, for $L = 1$ it reduces to

$$\Gamma_1(g) = (\phi-\theta)g\frac{1}{I_1^\theta}\frac{\left(I_2^\theta\right)^3 - 2I_1^\theta I_2^\theta I_3^\theta + \left(I_1^\theta\right)^2 I_4^\theta}{\left(I_1^\theta\right)^2 - I_1^\theta I_3^\theta + \left(I_2^\theta\right)^2}, \tag{24.30}$$

while for higher values of L the expression becomes quite lengthy.

A form more suitable for some calculations is

$$\Gamma_L(g) = (-1)^{L+1}(\phi-\theta)g\frac{\det \mathcal{M}_{2L+1}^{(1,2L+2)}}{\det \mathcal{M}_{2L}}. \tag{24.31}$$

Notice that here the matrix in the numerator is just $\mathcal{M}_{2L}$ with all indices of deformed Bessel functions I_n^θ increased by 1.

The explicit result for the energy (24.29) concludes our analytical solution of the cusp TBA equations. In the next subsection we will describe several checks of the result.

24.3 Weak and strong coupling limit

While for $L = 0$ our result matches fully the prediction from localization, at nonzero L our result is new. Here we will show that it passes several nontrivial checks.

At strong coupling our computation should reproduce the energy of the corresponding classical string solution which was computed in [164] (see also [146] for relevant calculations at strong and at weak coupling). To do this we first expanded the energy at large g and fixed L for several first values of L. The dependence on L happened to be polynomial which allows us to easily extend the result to an arbitrary L:

$$\frac{\Gamma_L}{2(\phi-\theta)\theta} = -\frac{g}{\sqrt{\pi^2-\theta^2}} + \frac{6L+3}{8\left(\pi^2-\theta^2\right)} - \frac{3\left(\left(6L^2+6L+1\right)\pi^2 - 2\theta^2(L+1)L\right)}{128g\pi^2\left(\pi^2-\theta^2\right)^{3/2}} + \dots \tag{24.32}$$

To compare with the classical string energy we re-expanded this formula in the regime

when L and g are both large, but $\mathcal{L} = L/g$ is fixed. Then at leading order in g we found

$$\begin{aligned}\frac{\Gamma_L}{2(\phi-\theta)\theta} &= \left(-\frac{g}{\pi}+\frac{3L}{4\pi^2}-\frac{9L^2}{64g\pi^3}-\frac{5L^3}{256g^2\pi^4}+\frac{45L^4}{16384g^3\pi^5}\right) \\ &+ \theta^2\left(-\frac{g}{2\pi^3}+\frac{3L}{4\pi^4}-\frac{21L^2}{128g\pi^5}-\frac{L^3}{16g^2\pi^6}-\frac{105L^4}{32768g^3\pi^7}\right) \\ &+ \theta^4\left(-\frac{3g}{8\pi^5}+\frac{3L}{4\pi^6}-\frac{99L^2}{512g\pi^7}-\frac{3L^3}{32g^2\pi^8}-\frac{2085L^4}{131072g^3\pi^9}\right) \\ &+ \theta^6\left(-\frac{5g}{16\pi^7}+\frac{3L}{4\pi^8}-\frac{225L^2}{1024g\pi^9}-\frac{L^3}{8g^2\pi^{10}}-\frac{7905L^4}{262144g^3\pi^{11}}\right) \\ &+ \theta^8\left(-\frac{35g}{128\pi^9}+\frac{3L}{4\pi^{10}}-\frac{1995L^2}{8192g\pi^{11}}-\frac{5L^3}{32g^2\pi^{12}}-\frac{97425L^4}{2097152g^3\pi^{13}}\right),\end{aligned} \tag{24.33}$$

which perfectly matches the expansion of the classical string energy from [164]! Since the classical energy was derived without appealing to integrability, this matching is a direct test of our calculation for nonzero L.

Later on a curious symmetry of the Bremsstrahlung function we computed was found in [167] and revealed new structure in the strong coupling limit. The strong coupling regime was studied further in [168] where the matrix model representation of (24.31) led to a classical spectral curve which describes the scaling limit $L, g \to \infty,\ L \sim g$.

At weak coupling we can compare our result to the leading Luscher correction to the energy. This correction was computed, as well as shown to follow from the TBA equations, in [63], [64] for generic ϕ and θ. It was also reproduced in [166][36] by a direct perturbative calculation. When $\theta \sim \phi$ this Luscher correction reduces to

$$\Gamma_L = (\phi-\theta)g^{2L+2}\frac{(-1)^L(4\pi)^{1+2L}}{(1+2L)!}B_{1+2L}\left(\frac{\pi-\theta}{2\pi}\right)+\mathcal{O}(g^{2L+4}) \tag{24.34}$$

where B_{1+2L} are the Bernoulli polynomials. For $L = 0, 1, 2, 3, 4$ we have checked that this expression precisely coincides with the leading weak-coupling term of our result.

25 Conclusions

We have computed explicitly the generalized cusp anomalous dimension $\Gamma_L(g, \phi, \theta)$ in the near-BPS limit when $\phi \approx \theta$. We have thus extended the $\theta = 0$ calculation of [164] to the arbitrary θ case. Our result (24.29) is fully non-perturbative and covers generic values for three ($g,\ L$ and θ) out of four parameters in the cusp anomalous dimension.

Let us also mention that having the all-loop analytic solution of the TBA presented here allowed in [16] to understand in part how the original QSC can be adapted to this

[36] except for the overall coefficient which was not fixed in [166]

twisted case. A nice match was found between the Baxter equation and the equations of the QSC, in particular the function $P_L(x)$ featuring in our solution is naturally identified wth one of the **P**-functions of the QSC up to a simple prefactor. We will see how the near-BPS solution is reconstructed directly from the QSC in the next part.

At $L = 0$ our result matches an earlier localization calculation. For nonzero L it serves as a new integrability-based prediction for localization techniques, and is fully confirmed by nontrivial checks both at strong and at weak coupling.

Our result for Γ_L has a form of a logarithmic derivative of a ratio of determinants, which hints that it could be obtained as an expectation value of some quantity in a matrix model. As in the $\theta = 0$ case [164] we expect that matrix model techniques should be very useful to analyze the semiclassical expansion of our predictions at large L.

Part VI

QSC for the cusp anomalous dimension

In this part, based on [12], we will formulate the Quantum Spectral Curve capturing the generalized cusp anomalous dimension for arbitrary values of the parameters and at any coupling.We will provide numerous tests of the construction and use it to generate new results.

26 Introduction

In the previous part we have seen that the generalized cusp anomalous dimension (equivalently, the generalized quark-antiquark potential) is described by an infinite system of TBA/Y-system equations. We will show how to adapt the Quantum Spectral Curve approach to this observable. Instead of deriving the QSC from the TBA (which is how the original QSC was obtained in [52, 53]), we make a proposal based on available data and consistency of the equations, and confirm it by several highly nontrivial tests. We find that all functional equations of the QSC remain unchanged, but the asymptotics at large values of the spectral parameter, as well as some of the analyticity properties, should be modified. In particular some functions acquire exponential asymptotics $\sim e^{\pm\phi u}, e^{\pm\theta u}$, as expected by analogy with spin chain Q-functions in the presence of twisted boundary conditions. We also observed that rather subtle cancelations take place resulting in complicated constraints on subleading coefficients in the large u asymptotics of Q-functions. As an application we compute the subleading term (of order $(\phi-\theta)^2$) in the near-BPS expansion of $\Gamma_{\rm cusp}$ without scalar insertions, at any coupling and for any ϕ. Our explicit result (28.26) fully agrees with perturbative predictions.

We will discuss the modifications needed in the QSC, focussing on the vacuum state, i.e. with only Z fields inserted at the cusp, but keeping L arbitrary. Then we reconstruct the near-BPS solution at any θ and L, and for $L=0$ extend it to the next order in the near-BPS expansion. Next we describe a highly precise numerical method for solving the QSC equations and demonstrate it on several examples. After this we discuss the weak coupling solution at generic angles, and finally present conclusions.

27 Constructing the Quantum Spectral Curve

In this section we will discuss the modifications in the QSC which are needed to describe the generalized quark-antiquark potential. Below we will only discuss the vacuum state, i.e. the Wilson line with L scalar insertions at the cusp (the extension for more general insertions should be straightforward).

The Quantum Spectral Curve equations of [52, 53] in $\mathcal{N} = 4$ SYM can be deduced from the TBA equations or the corresponding T- and Y-systems with special analyticity assumptions. In our case the TBA equations for the generalised cusp are almost the same as the original TBA system. The Y-system and T-system equations are exactly the same as for the original problem. Thus it is natural to expect that the QSC equations should also be the same to a large extent. In the TBA there are only two important differences: the extra boundary dressing phase supplementing the BES phase, and the twists which appear as chemical potentials and introduce the angles ϕ, θ into the problem[37]. We do not derive the QSC from the Thermodynamic Bethe ansatz, rather we will put forward and motivate a proposal which is consistent with several highly nontrivial checks, leaving little doubt as to its correctness.

First, we expect to have the same set of Q-functions and auxiliary functions such as μ_{ab} as in the original problem. All of them will satisfy the same functional relations, for instance the $\mathbf{P}\mu$-system equations or the QQ-relations are unchanged. However some analyticity properties will change, as we will discuss below, and in particular the $\mathbf{P}$-functions acquire an extra cut going from $u = 0$ to infinity. In addition, the large u asymptotics clearly need to be modified. Indeed, the twists in the boundary conditions typically correspond to imposing exponential rather than powerlike asymptotics for the Q-functions (see e.g. [53] and references therein). In our case the angle θ is naturally related to the S^5 part of the geometry, which qualitatively corresponds to the $\mathbf{P}$-functions, so roughly speaking we expect $\mathbf{P}_a \sim e^{\pm\theta u}$ at large u. Similarly, the angle ϕ is associated to AdS_5 leading to $\mathbf{Q}_i \sim e^{\pm\phi u}$. This argument is also supported by the expectation that $\mathbf{P}$'s and $\mathbf{Q}$'s should be related in the classical limit to the quasimomenta for S^5 and AdS_5, correspondingly. Similarly, we expect that L should enter the power in the asymptotics of $\mathbf{P}$'s, while the power in the asymptotics of $\mathbf{Q}$'s should contain Δ.

[37] There is also an extra symmetry requirement on the Y-functions of the TBA, namely they should be invariant under the exchange of the two wings of the Y-system with a simultaneous reflection $u \to -u$, i.e. $Y_{a,s}(u) = Y_{a,-s}(-u)$, see [63, 64] for details.

In the original QSC proposal [53] some guidance to fix the powers in the asymptotics came from comparison with the Asymptotic Bethe ansatz (ABA) which can be reproduced from the QSC, and also with the classical spectral curve. For our problem the ABA is also available [63, 64], and another piece of information is the all-loop solution of the $\mathbf{P}\mu$ system to leading order in the near-BPS expansion, based on analytic solutions of the TBA [164, 52, 16]. In particular these solutions suggest that the large u asymptotics should contain half-integer powers coming from a $\sqrt{u}$ prefactor which the $\mathbf{P}$'s contain. However it turns out that there is an important subtlety – in the near-BPS limit the leading large u coefficient in $\mathbf{P}_3, \mathbf{P}_4$ vanishes, making it not straightforward to guess the correct asymptotics even knowing the all-loop result.

The available data indicates that, first, the boundary dressing phase leads to *exponential* rather than powerlike asymptotics in μ_{ab}. This was already observed in [52, 16]. More precisely, we should have

$$\omega^{12} \sim \text{const} \cdot e^{2\pi|u|},\ \omega^{13} \sim \text{const},\ \omega^{24} \sim \text{const}, \qquad u \to \infty \tag{27.1}$$

while other components of ω^{ij} become zero at infinity. This translates via (4.35) into $e^{\pm 2\pi u}$ asymptotics in some components of the μ_{ab} matrix.

It remains to fix the powers in the asymptotics of $\mathbf{P}$'s and $\mathbf{Q}$'s, and relate their large u expansion coefficients to the charges of the state. To do this we demanded consistency of the equations (4.20), (4.22) expanded at large u. This precisely follows the logic for the undeformed case, where e.g. the relations for leading coefficients of $\mathbf{P}$'s follow from the powers in the asymptotics of these functions once we require consistency of the fucntional equations (4.20), (4.22). However, our case turned out to be much more tricky, in particular since some of the twists are the same (e.g. two of the $\mathbf{P}_a$ functions scale with the same exponent $\sim e^{\theta u}$) there are many subtle cancellations at the first several orders. It was also convenient at intermediate steps to use (4.41) as well as the 4th order Baxter-type difference equation on $\mathbf{Q}_i$ with coefficients built from $\mathbf{P}_a, \mathbf{P}^a$ – this equation follows from (4.20), (4.22) (see [72] for details on its derivation). Finally, already the near-BPS solution suggests that not all four $\mathbf{P}_a$ are independent, e.g. $\mathbf{P}_1(u)$ is equal up to a constant to $\mathbf{P}_2(-u)$.

As a result, we found the following large u asymptotics:

$$\begin{aligned}
\mathbf{P}_1(u) &= C\epsilon^{1/2}\, u^{-1/2-L}\, e^{+\theta u} f(+u) \;\;,\;\; f(u) = 1 + a_1/u + a_2/u^2 + a_3/u^3 + \ldots \\
\mathbf{P}_2(u) &= C\epsilon^{1/2}\, u^{-1/2-L}\, e^{-\theta u} f(-u) \;, \\
\mathbf{P}_3(u) &= \frac{1}{C}\epsilon^{3/2}\, u^{+3/2+L}\, e^{+\theta u} g(+u) \;\;,\;\; g(u) = 1 + b_1/u + b_2/u^2 + b_3/u^3 + \ldots \\
\mathbf{P}_4(u) &= -\frac{1}{C}\epsilon^{3/2}\, u^{+3/2+L}\, e^{-\theta u} g(-u) \;.
\end{aligned} \tag{27.2}$$

Here L is the number of scalar insertions at the cusp, while the constant C is unfixed and can be set to 1 by the rescaling symmetry as discussed below (27.8), (27.9). The coefficients should satisfy

$$\epsilon^2 = \frac{i(\cos\theta - \cos\phi)^2}{2(L+1)\sin^2\theta} \;\;,\;\; a_1 - b_1 = -\frac{(L+1)(2\cos\theta\cos\phi + \cos 2\theta - 3)}{2\sin\theta(\cos\theta - \cos\phi)} \;. \tag{27.3}$$

The relation which includes $\Delta \equiv \Gamma_{\rm cusp}$ is more involved and we give its full form in Eq. (C.1), Appendix C.1. For $L = 0$ it reduces to

$$\begin{aligned}
\Delta^2 &= \frac{(\cos\theta - \cos\phi)^3}{\sin\theta\sin^2\phi}\left[-a_1 a_2 + a_1 b_2 - \frac{a_1}{\sin^2\theta} + a_1^2\frac{(1 - \cos\theta\cos\phi)}{\sin\theta(\cos\theta - \cos\phi)}\right. \\
&- \left. a_2\cot\theta + a_3 - b_3\right] \;.
\end{aligned} \tag{27.4}$$

We see that in contrast to the undeformed case we need to expand $\mathbf{P}$'s up to *fourth* order at large u to extract the conformal dimension! With these asymptotic constraints the $\mathbf{P}\mu$-system becomes a closed a set of equations fixing the cusp anomalous dimension.

Notice that the asymptotics of $\mathbf{P}_a$ contains half-integer powers of u. Thus $\mathbf{P}_a$ are not as regular as in the case of local operators and should necessarily have extra cuts. Thus we require the regularity on the plane with only Zhukovsky cuts not for $\mathbf{P}_a$ (or $\mathbf{Q}_i$) but for

$$\mathbf{p}_a \equiv \mathbf{P}_a/\sqrt{u}, \quad \mathbf{q}_i \equiv \mathbf{Q}_i/\sqrt{u} \;. \tag{27.5}$$

This is an important additional analyticity condition. Let us underline that the extra $\sqrt{u}$ factor in (27.5) is not e.g. an artefact of the weak coupling expansion. Its presence at finite coupling is a part of our proposal, already observed in [16] based on the near-BPS all-loop solution of the TBA. It is further confirmed here by numerical results at strong coupling and analytic solution at weak coupling (which are described below).

Alternatively to the $\mathbf{P}\mu$-system one can use the $\mathbf{Q}\omega$ system described in (4.33) which is also a closed set of equations provided the proper constraints at large u are imposed. In our case the leading asymptotics of $\mathbf{Q}_i$ are

$$\mathbf{Q}_1 \sim u^{1/2+\Delta} e^{u\phi}, \;\; \mathbf{Q}_2 \sim u^{1/2+\Delta} e^{-u\phi}, \;\; \mathbf{Q}_3 \sim u^{1/2-\Delta} e^{u\phi}, \;\; \mathbf{Q}_4 \sim u^{1/2-\Delta} e^{-u\phi} \;. \tag{27.6}$$

The coefficients in their large u expansion are constrained similarly to (27.2), (27.4), and in particular one can extract from them the R-charge L. We give the corresponding relations in Appendix C.2.

Finally, like in the $sl(2)$ sector of the original QSC we have

$$\mathbf{P}^1 = -\mathbf{P}_4 \ , \ \mathbf{P}^2 = +\mathbf{P}_3 \ , \ \mathbf{P}^3 = -\mathbf{P}_2 \ , \ \mathbf{P}^4 = +\mathbf{P}_1, \ \ \mu_{14} = \mu_{23} \tag{27.7}$$

due to which $\mathbf{P}^a\mathbf{P}_a = 0$ is satisfied automatically.

It is useful to note that there is a rescaling symmetry under which

$$\mathbf{P}_1 \to \alpha\mathbf{P}_1, \ \mathbf{P}_2 \to \alpha\mathbf{P}_2, \ \mathbf{P}_3 \to \alpha^{-1}\mathbf{P}_3, \ \mathbf{P}_4 \to \alpha^{-1}\mathbf{P}_4, \tag{27.8}$$

$$\mu_{12} \to \alpha^2\mu_{12}, \qquad \mu_{34} \to \alpha^{-2}\mu_{34} \tag{27.9}$$

while other μ_{ab} are not changed (α is a constant). In particular with this rescaling one can set to 1 the constant C appearing in (27.2). We also have the γ-symmetry transformation [15, 53] which reads

$$\mathbf{P}_3 \to \mathbf{P}_3 + \gamma\mathbf{P}_1, \ \mathbf{P}_4 \to \mathbf{P}_4 - \gamma\mathbf{P}_2, \tag{27.10}$$

$$\mu_{14} \to \mu_{14} - \gamma\mu_{12}, \ \mu_{34} \to \mu_{34} + 2\gamma\mu_{14} - \gamma^2\mu_{12} \tag{27.11}$$

with constant γ. With this transformation the coefficients in the asymptotics of $\mathbf{P}$'s will also change, e.g. for $L = 0$

$$b_2 \to b_2 + \frac{C^2\gamma}{\epsilon}, \ b_3 \to b_3 + \frac{C^2\gamma}{\epsilon}a_1, \ \dots \tag{27.12}$$

The formula (27.4) for Δ is invariant under this transformation, as it should be.

As discussed above, from (27.2) we see that when $\phi \to \theta$ the leading coefficient in $\mathbf{P}_3, \mathbf{P}_4$ is proportional to $(\phi - \theta)^{3/2}$ and thus is not visible at the leading order in the near-BPS expansion. The next coefficients $b_1, b_2, \dots$ will scale as $1/(\phi - \theta)$ and thus all $\mathbf{P}_a$ are of order $\sqrt{\phi - \theta}$, as expected from the solution found in [16]. We will reconstruct this solution in the next section.

The asymptotics discussed in this section constitute our main result. They provide the crucial boundary conditions, thus concluding the reduction of the infinite TBA system of [63, 64] to the finite set of QSC equations.

In the next sections we will demonstrate the usage of the QSC in several cases. We will compute at all loops the next-to-leading term in the near-BPS expansion, solve the equations numerically and also construct the leading weak coupling solution. All these calculations provide stringent tests of our proposal as well as giving new results.

28 Near-BPS solution

In this section we will describe the solution of the QSC in the near-BPS limit $\phi \to \theta$. We will first recover the leading order solution at arbitrary θ found in [16], and then extend it to the next order. This calculation is quite similar to the iterative solution of the QSC at small spin studied in [15]. The main outcome is a prediction for the value of Γ_{cusp} at order $(\phi-\theta)^2$ to all loops.

28.1 Leading order

In the limit $\phi \to \theta$ the generalized cusp anomalous dimension can be written as

$$\Delta = \frac{\cos\phi - \cos\theta}{\sin\phi}\Delta^{(1)}(\phi) + \left(\frac{\cos\phi - \cos\theta}{\sin\phi}\right)^2 \Delta^{(2)}(\phi) + \mathcal{O}((\phi-\theta)^3) \ . \tag{28.1}$$

The first coefficient, also known as the Bremsstrahlung function, was computed at any coupling in [147, 148] and later reproduced from integrability in [164, 16] by a direct analytic solution of the TBA in this limit. It reads

$$\Delta^{(1)}(\phi) = \frac{2\phi g}{\sqrt{\pi^2-\phi^2}} \frac{I_2\left(4\pi g\sqrt{1-\frac{\phi^2}{\pi^2}}\right)}{I_1\left(4\pi g\sqrt{1-\frac{\phi^2}{\pi^2}}\right)} \ . \tag{28.2}$$

In [16] the leading near-BPS solution was obtained from the TBA and linked to the $\mathbf{P}\mu$-system. Let us rederive this solution using solely the information coming from our asymptotics.

The key simplification is that $\mathbf{P}_a, \tilde{\mathbf{P}}_a \sim \sqrt{\phi-\theta}$ are small. This can be seen from our general asymptotics (27.2), (27.6), (C.3) where we have to send $\epsilon \sim \phi - \theta \to 0$ meaning that in the near-BPS limit we get

$$\mathbf{P}_1 \sim u^{-1/2-L}e^{+\theta u} \ , \ \mathbf{P}_2 \sim u^{-1/2-L}e^{-\theta u} \ , \ \mathbf{P}_3 \sim u^{1/2+L}e^{+\theta u} \ , \ \mathbf{P}_4 \sim u^{1/2+L}e^{-\theta u} \ , \tag{28.3}$$

and

$$\mathbf{Q}^1 \sim u^{-1/2-L}e^{-\theta u} \ , \ \mathbf{Q}^2 \sim u^{-1/2-L}e^{+\theta u} \ , \ \mathbf{Q}^3 \sim u^{1/2+L}e^{-\theta u} \ , \ \mathbf{Q}^4 \sim u^{1/2+L}e^{+\theta u} \ , \tag{28.4}$$

Notice that the leading coefficient in $\mathbf{P}_3$ and $\mathbf{P}_4$ tends to zero faster than the subleading ones since $a_1 - b_1 \sim 1/\epsilon$, which modifies the expected behaviour at infinity in this limit

(and similarly for $\mathbf{Q}_3, \mathbf{Q}_4$). Thus we can write the expansion of $\mathbf{P}$ and μ as

$$\mathbf{P}_a = \mathbf{P}_a^{(0)} + \mathbf{P}_a^{(1)} + \mathcal{O}((\phi-\theta)^{5/2}), \qquad \mu_{ab} = \mu_{ab}^{(0)} + \mu_{ab}^{(1)} + \mathcal{O}((\phi-\theta)^2) \tag{28.5}$$

where the scaling is

$$\mathbf{P}_a^{(0)} \sim (\phi-\theta)^{1/2},\ \mathbf{P}_a^{(1)} \sim (\phi-\theta)^{3/2}, \qquad \mu_{ab}^{(0)} \sim 1,\ \ \mu_{ab}^{(1)} \sim (\phi-\theta)\ . \tag{28.6}$$

From (4.30) we see that at leading order the discontinuity of μ_{ab} vanishes so $\mu_{ab}^{(0)}$ are periodic entire functions. To fix them we should look in more detail at the functions $Q_{a|i}$ and $Q_{ab|ij}$, using (4.35) and our prescription (27.1) which states in particular that $\omega^{12} \sim e^{2\pi|u|},\ u \to \infty$. For $\phi \simeq \theta$ the r.h.s. of (4.20) is small so $Q_{a|i}$ are periodic functions. At the same time their large u asymptotics should be consistent with that of $\mathbf{Q}_i$ and $\mathbf{P}_a$ from (28.3), (28.4), meaning that $Q_{a|i} \simeq u^{N_{ai}} e^{\psi_{ai} u}$ where ψ_{ai} can be equal to $\pm 2\theta$ or to 0 in our limit. From that we conlude that $Q_{a|i}$ must be constants. Moreover the relation

$$\mathbf{P}_a = -\mathbf{Q}^i Q^+_{a|i}\ , \tag{28.7}$$

together with (28.3), (28.4) means that the only nonzero constants are

$$Q_{a|i} = \begin{pmatrix} 0 & K_1 & 0 & 0 \\ K_2 & 0 & 0 & 0 \\ 0 & 0 & 0 & K_3 \\ 0 & 0 & K_4 & 0 \end{pmatrix}\ . \tag{28.8}$$

In other words $\mathbf{P}_a$ and $\mathbf{Q}_i$ are the same in this limit after a relabeling of their indices (up to a constant factor). This is indeed an expected feature for a BPS configuration where cancellation between S^5 and AdS_5 modes is taking place. Similarly, ω^{ij} and μ^{ab} should coincide after the same relabeling of indices.

Together with our requirement (27.1) this means that $\mu_{12} = B_0 + B_1 e^{2\pi u} + B_2 e^{-2\pi u}$, μ_{13} and μ_{24} are constants, while other μ_{ab} are zero. Note that since we should have a $u \to -u$ symmetry of the system, of course μ_{12} should be either even or odd which further constrains these constants. This leads to (see [12] for full details)

$$\mu_{12}^{(0)} = A\sinh(2\pi u),\ \mu_{13}^{(0)} = 1,\ \mu_{14}^{(0)} = 0,\ \mu_{24}^{(0)} = -1,\ \mu_{34}^{(0)} = 0 \tag{28.9}$$

where A is a constant. This also implies that at leading order

$$\omega^{12} = \text{const} \cdot \sinh(2\pi u)\ . \tag{28.10}$$

Therefore the equations on the $\mathbf{P}$'s to leading order take the form

$$\begin{aligned}
\tilde{\mathbf{P}}_1^{(0)} &= A\sinh(2\pi u)\mathbf{P}_3^{(0)} - \mathbf{P}_2^{(0)} \\
\tilde{\mathbf{P}}_2^{(0)} &= A\sinh(2\pi u)\mathbf{P}_4^{(0)} - \mathbf{P}_1^{(0)} \\
\tilde{\mathbf{P}}_3^{(0)} &= \mathbf{P}_4^{(0)} \\
\tilde{\mathbf{P}}_4^{(0)} &= \mathbf{P}_3^{(0)} \ .
\end{aligned} \tag{28.11}$$

To solve them let us first introduce some notation. We have a very useful expansion

$$\sinh(2\pi u)e^{+2g\theta(x-1/x)} = \sum_{n=-\infty}^{\infty} I_n^{+\theta} x^n \ , \tag{28.12}$$

where

$$I_n^\theta = \frac{1}{2} I_n\left(4\pi g\sqrt{1-\frac{\theta^2}{\pi^2}}\right)\left[\left(\sqrt{\frac{\pi+\theta}{\pi-\theta}}\right)^n - (-1)^n\left(\sqrt{\frac{\pi-\theta}{\pi+\theta}}\right)^n\right] \ , \tag{28.13}$$

with I_n being the modified Bessel function. By $x(u)$ we denote the usual Zhukovsky variable which resolves the cut $[-2g, 2g]$,

$$x + \frac{1}{x} = \frac{u}{g}, \quad |x| \geq 1 \ . \tag{28.14}$$

We also have

$$I_{-n}^\theta = I_n^{-\theta} = (-1)^{n+1} I_n^\theta \tag{28.15}$$

and let us introduce

$$S_+(x) \equiv \sum_{n=1}^{\infty} I_n^{+\theta} x^{-n} \ , \ \ S_-(x) \equiv \sum_{n=1}^{\infty} I_n^{-\theta} x^{-n} \ . \tag{28.16}$$

In this notation we have e.g.

$$S_+ + \tilde{S}_- = \sinh(2\pi u)e^{-2g\theta(x-1/x)} \tag{28.17}$$

(notice that applying the tilde amounts to flipping $x \to 1/x$). We see that S_+ is the part of the Laurent expansion of $\sinh(2\pi u)e^{-2g\theta(x-1/x)}$ containing negative powers of x. We can alternatively write it as a contour integral

$$S_+(x) = \frac{1}{2\pi i}\oint \frac{dy}{x-y}\sinh(2\pi g(y+1/y))e^{-2g\theta(y-1/y)} \tag{28.18}$$

where the contour goes counterclockwise around the unit circle.

Focussing on the case $L = 0$ we can now write the explicit solution of (28.11):[38]

$$\mathbf{P}_1^{(0)} = B\sqrt{A}\sqrt{u}\, e^{+g\theta(x-1/x)} \sum_{n=1}^{\infty} I_n^{+\theta} x^{-n} \tag{28.19}$$

$$\mathbf{P}_2^{(0)} = B\sqrt{A}\sqrt{u}\, e^{-g\theta(x-1/x)} \sum_{n=1}^{\infty} I_n^{-\theta} x^{-n} \tag{28.20}$$

$$\mathbf{P}_3^{(0)} = \frac{B}{\sqrt{A}}\sqrt{u}\, e^{+g\theta(x-1/x)} \tag{28.21}$$

$$\mathbf{P}_4^{(0)} = \frac{B}{\sqrt{A}}\sqrt{u}\, e^{-g\theta(x-1/x)} \tag{28.22}$$

where $B \sim \sqrt{\phi - \theta}$ is a constant fixed from asymptotics (27.2) as

$$B = \sqrt{\frac{-i(\phi-\theta)}{g I_1^{\theta}}}\ . \tag{28.23}$$

The constant A is arbitrary and is related to the constant C appearing in the asymptotics (27.2), so using the rescaling (27.8), (27.9) one can set either A or C to 1. One can check that this solution is fully consistent with the asymptotics (27.2), noting that, as discussed above, in (27.2) the leading coefficient in $\mathbf{P}_3, \mathbf{P}_4$ vanishes and all $b_i \sim 1/(\phi - \theta)$. This solution also reproduces via (27.4) the known result for Δ at the leading order in $(\phi - \theta)$,

$$\Delta = -2(\phi-\theta)\frac{\phi g}{\sqrt{\pi^2-\phi^2}} \frac{I_2\left(4\pi g\sqrt{1-\frac{\phi^2}{\pi^2}}\right)}{I_1\left(4\pi g\sqrt{1-\frac{\phi^2}{\pi^2}}\right)} + \mathcal{O}((\phi-\theta)^2)\ . \tag{28.24}$$

We also translated to our conventions the solution for any L constructed in [16] and we present it in appendix C.3. Remarkably, the result for $\Gamma_{\rm cusp}$ extracted from this solution via our asymptotic relations (27.2), (27.4) perfectly matches the known predictions from TBA found in [16] (we have checked this explicitly for the first several values of L). This is already a nontrivial check of the proposed large u asymptotics.

28.2 Next-to-leading order

Let us now discuss the solution of the $\mathbf{P}\mu$ system at the next order in $(\phi - \theta)$. The calculation is rather similar to the one discussed in part II for the small spin expansion, apart from several technical complications. While full details are given in [12], here we will only quote the final result for the anomalous dimension. To compare with the literature

[38] This solution is slightly different from the one described in [16], as e.g. the relations (27.7) between $\mathbf{P}^a$ and $\mathbf{P}_a$ that we use differ by a sign compared to those used in that paper. The solution given in [16] is of course also valid, in the conventions used in that work.

we found it convenient to bring our result to the form

$$\Delta = \frac{\cos\phi - \cos\theta}{\sin\phi}\Delta^{(1)}(\phi) + \left(\frac{\cos\phi - \cos\theta}{\sin\phi}\right)^2 \Delta^{(2)}(\phi) + \mathcal{O}((\phi-\theta)^3) \tag{28.25}$$

so that at each order we have a nontrivial function of ϕ . Our all-loop result reads

$$\begin{aligned}\Delta^{(2)}(\phi) &= -\frac{1}{2}\oint\frac{du_x}{2\pi i}\oint\frac{du_y}{2\pi i}u_x u_y \times \\ &\quad [D_+\Gamma_{+\phi}(u_x-u_y) + D_0\Gamma_0(u_x-u_y) + D_-\Gamma_{-\phi}(u_x-u_y)]\end{aligned} \tag{28.26}$$

where both integrals run clockwise around the cut $[-2g, 2g]$ and

$$\begin{aligned}D_+ &= \frac{iS_+(y)e^{-2g\phi x+2g\phi/x+2g\phi y-2g\phi/y}}{g^3 I_1^\phi} \\ &\times \left(-\frac{2S_+(y)}{gI_1^\phi} - \frac{2S_+(x)e^{4g\phi x-4g\phi/x}}{gI_1^\phi} + \frac{2y}{y^2-1} + \frac{2x}{x^2-1} + \frac{I_2^\phi x S_+(y)}{(I_1^\phi)^2(x^2-1)}\right) , \\ D_0 &= \frac{2iS_+(y)}{g^3 I_1^\phi}\left(\frac{S_+(x)}{gI_1^\phi} - \frac{I_2^\phi S_+(x)}{(I_1^\phi)^2(x^2-1)} - \frac{2x^2}{(x+1/x)(x^2-1)}\right) , \\ D_- &= \frac{iI_2^\phi}{g^3(I_1^\phi)^3}\frac{x(S_+(x))^2 e^{2g\phi x-2g\phi/x-2g\phi y+2g\phi/y}}{(x^2-1)}\end{aligned} \tag{28.27}$$

We recall that S_+ was defined in (28.16), and the kernels Γ entering (28.26) are given by

$$\Gamma_{-\theta}(u) = e^{-2\theta u}\sum_{n=1}^{\infty}\left[\frac{e^{-2in\theta}}{u+in} - \frac{e^{2in\theta}}{u-in}\right] , \tag{28.28}$$

$$\Gamma_{+\theta}(u) = e^{2\theta u}\sum_{n=1}^{\infty}\left[\frac{e^{2in\theta}}{u+in} - \frac{e^{-2in\theta}}{u-in}\right] . \tag{28.29}$$

Let us now discuss several checks of our main result (28.26) at weak coupling. It is straightforward to expand it for $g \to 0$ simply by expanding the integrand in (28.26) at weak coupling and taking the residue at $u_x, u_y = 0$. Then we can make a test against perturbative predictions known up to four loops. In general the structure at weak coupling is expected to be

$$\Delta = \sum_{n=1}^{\infty}\gamma_n(\theta,\phi)g^{2n} \tag{28.30}$$

with

$$\gamma_n(\theta,\phi) = \sum_{k=1}^{n}\left(\frac{\cos\phi-\cos\theta}{\sin\phi}\right)^k \gamma_n^{(k)}(\phi) . \tag{28.31}$$

Our all-loop result allows to compute all coeficients $\gamma_n^{(2)}(\phi)$ in this expansion. Notice that at each loop order only a finite number of terms in the near-BPS expansion contribute, e.g. the two-loop result is completely determined by the first two terms in (28.25). For arbitrary

ϕ and θ the anomalous dimension was computed directly up to two loops [169, 146] giving

$$\gamma_1^{(1)}(\phi) = 2\phi, \tag{28.32}$$

$$\gamma_2^{(1)}(\phi) = \frac{4}{3}\phi(\phi^2-\pi^2), \tag{28.33}$$

$$\gamma_2^{(2)}(\phi) = 2i\phi\left[\mathrm{Li}_2(e^{2i\phi})-\mathrm{Li}_2(e^{-2i\phi})\right]-2\left[\mathrm{Li}_3(e^{2i\phi})+\mathrm{Li}_3(e^{-2i\phi})\right]+4\zeta(3) \tag{28.34}$$

and in [170] this data was reproduced from the TBA. We found that the weak coupling expansion of our result perfectly matches the prediction (28.34).

The cusp anomalous dimension was also computed to four loops in [166, 171], giving a prediction for the coefficients $\gamma_3^{(2)}(\phi), \gamma_4^{(2)}(\phi)$ which our result should reproduce. Indeed we found a perfect match with the perturbative data. The predictions of [171] are written in terms of harmonic polylogarithms, but match the expansion of our result[39] which does not include more complicated functions than Li_n. At three loops our result gives

$$\begin{aligned}\gamma_3^{(2)}(\phi) &= 24\left[\mathrm{Li}_5(e^{-2i\phi})+\mathrm{Li}_5(e^{2i\phi})\right]-18i\phi\left[\mathrm{Li}_4(e^{2i\phi})-\mathrm{Li}_4(e^{-2i\phi})\right] \\ &-4\phi^2\left[\mathrm{Li}_3(e^{-2i\phi})+\mathrm{Li}_3(e^{2i\phi})\right]+\frac{4}{3}i(\pi-\phi)(\phi+\pi)\phi\left[\mathrm{Li}_2(e^{2i\phi})-\mathrm{Li}_2(e^{-2i\phi})\right] \\ &+\frac{8}{3}\left(\phi^2-\pi^2\right)\phi^2\left[\log(1-e^{2i\phi})+\log(1-e^{-2i\phi})\right]+8\left(\zeta(3)\phi^2-6\zeta(5)\right)\end{aligned} \tag{28.35}$$

while at four loops

$$\begin{aligned}\gamma_4^{(2)}(\phi) &= -280\left[\mathrm{Li}_7(e^{2i\phi})+\mathrm{Li}_7(e^{-2i\phi})\right]+190i\phi\left[\mathrm{Li}_6(e^{2i\phi})-\mathrm{Li}_6(e^{2i\phi})\right] \\ &+\left(44\phi^2+\frac{16\pi^2}{3}\right)\left[\mathrm{Li}_5(e^{2i\phi})+\mathrm{Li}_5(e^{-2i\phi})\right] \\ &+\frac{4}{3}i\phi\left(11\phi^2-17\pi^2\right)\left[\mathrm{Li}_4(e^{2i\phi})-\mathrm{Li}_4(e^{-2i\phi})\right] \\ &+\frac{8}{9}\left(18\phi^4-21\pi^2\phi^2+\pi^4\right)\left[\mathrm{Li}_3(e^{2i\phi})+\mathrm{Li}_3(e^{-2i\phi})\right] \\ &-\frac{4}{9}i\left(15\phi^5-22\pi^2\phi^3+7\pi^4\phi\right)\left[\mathrm{Li}_2(e^{2i\phi})-\mathrm{Li}_2(e^{-2i\phi})\right] \\ &+\frac{40}{9}\left(\phi^3-\pi^2\phi\right)^2\left[\log(1-e^{2i\phi})+\log(1-e^{-2i\phi})\right] \\ &+16\zeta(3)\phi^4-\frac{8}{3}\left(4\pi^2\zeta(3)+33\zeta(5)\right)\phi^2-\frac{16}{9}\left(\pi^4\zeta(3)+6\pi^2\zeta(5)-315\zeta(7)\right)\end{aligned} \tag{28.36}$$

In fact it is clear that at any loop order our result would generate Li_n at most. The reason is that when evaluating the integral (28.26) by residues the most complicated functions that can appear are the $\mathrm{Li}_n(e^{\pm 2i\phi})$ coming from expansion of the kernels (28.28), (28.29). As a further example we computed the novel five- and six-loop coefficients, given in Eq. (C.18) (Appendix C.4).

[39] we checked this numerically for some particular values of ϕ

Thus at weak coupling our result matches known predictions to four loops, which serves as a deep test of the proposed Quantum Spectral Curve equations and of our near-BPS calculation.

29 Numerical solution

The formulation of the problem in terms of the QSC allows for an efficient numerical analysis of Γ_{cusp} at finite coupling. A highly precise and fast converging numerical method for solving the original QSC for local operators was proposed in [14]. Here we will describe how to modify it in the present case, and then demonstrate several applications. We will focus on the case $L = 0$, but we expect the discussion in this section should be valid for general L with minor changes.

29.1 The numerical algorithm

We start in the same way as in the numerical solution of the QSC for local operators: we parameterize the P-functions in terms of unknown coefficients $c_{a,n}$ and build the $Q_{a|i}$ functions which allow to obtain $\mathbf{Q}_i, \tilde{b}Q_i$ on the cut $[-2g, 2g]$. The only difference is that all these functions have exponential asymptotics, but this is easily incorporated in the algorithm.

The most important step is to close the equations in terms of $\mathbf{Q}_i, \tilde{\mathbf{Q}}_i$ and find the free coefficients $c_{a,n}$. For that we use the very convenient trick proposed originally in [13]. Let us discuss it in some detail as this is a crucial part of the calculation. We start by noticing that $\mathbf{Q}_i(u)$ and $\mathbf{Q}_i(-u)$ should satisfy the same 4th order difference equation following from (4.20), (4.22) with coefficients built from $\mathbf{P}$-functions as the equation is symmetric under $u \to -u$. As we discussed in section 27, Eq. (27.5), it is simpler to work with

$$\mathbf{q}_i(u) = \mathbf{Q}_i(u)/\sqrt{u} \ . \tag{29.1}$$

Then we have $\mathbf{q}_i(u) = \Omega_i^j(u)\mathbf{q}_j(-u)$ where $\Omega_i^j(u)$ are some $i-$periodic functions. As $\mathbf{Q}_i$ have a definite asymptotics with prescribed exponential part (27.6), all $\Omega_i^j(u)$ become constant at large u and furthermore only a few of them are nonzero at infinity, namely $\Omega_2^1,\ \Omega_1^2,\ \Omega_3^4,\ \Omega_4^3$. We also know that $\tilde{\mathbf{q}}_i(u) = \omega_{ij}(u)\chi^{jk}\mathbf{q}_k(u)$ where ω_{ij} are i-periodic. Combining these relations we find

$$\tilde{\mathbf{q}}_m(u) = \alpha_m^i(u)\mathbf{q}_i(-u), \quad m = 1, 2, 3, 4 \tag{29.2}$$

where $\alpha^i_m = \omega_{mj}\chi^{jk}\Omega^i_k$ are i-periodic (being built from periodic functions) and moreover analytic since $\tilde{\mathbf{q}}_i(u)$ and $\mathbf{q}_i(-u)$ are analytic in the lower half-plane. In addition to this, most of the functions α^i_m are equal to zero, because according to our prescription (27.1) from section 27 the only nonzero components of ω_{ij} at infinity are $\omega_{34} \sim \text{const} \cdot e^{2\pi|u|}$ and $\omega_{13}, \omega_{24} \sim \text{const}$. Using also that most components of Ω^j_i are zero at large u we get from (29.2) the following equations (it's enough for us to consider only $\mathbf{q}_1, \mathbf{q}_4$)

$$\begin{aligned} \tilde{\mathbf{q}}_1(u) &= s_1\mathbf{q}_1(-u) \\ \tilde{\mathbf{q}}_4(u) &= (ae^{2\pi u} + be^{-2\pi u} + c)\mathbf{q}_1(-u) + s_4\mathbf{q}_4(-u) \end{aligned} \tag{29.3}$$

where s_1, s_4, a, b, c are constants, and moreover a and b are nonzero as Ω^1_2 and the exponential part of ω_{34} are nonzero at infinity. Applying tilde to the first equation we also get

$$\mathbf{q}_1(u) = s_1\tilde{\mathbf{q}}_1(-u) = (s_1)^2\mathbf{q}_1(u) \tag{29.4}$$

so $(s_1)^2 = 1$. Similarly from the second equation we find $(s_4)^2 = 1$ as well as

$$\begin{aligned} as_1 + bs_4 &= 0 \\ bs_1 + as_4 &= 0 \\ cs_1 + cs_4 &= 0\ . \end{aligned} \tag{29.5}$$

This system has two solutions: either

$$s_1 = s_4,\ a = -b,\ c = 0 \tag{29.6}$$

or

$$s_1 = -s_4,\ a = b, \quad \text{and } c \text{ is arbitrary.} \tag{29.7}$$

By comparing to the leading near-BPS solution where $\omega^{12} \propto \sinh(2\pi u)$ (see Eq. (28.10)), we see that the first option is the correct one. It remains only to fix the sign of s_1. For that let us consider the explicit solution (28.19)-(28.22) for $\mathbf{P}_a$ in the near-BPS limit. We see that for $\mathbf{p}_a = \mathbf{P}_a/\sqrt{u}$ we have

$$\tilde{\mathbf{p}}_3(u) = \mathbf{p}_3(-u) \tag{29.8}$$

As in the near-BPS limit we expect to identify $\mathbf{q}_1$ and $\mathbf{p}_3$, comparing this relation with the first equation in (29.3) we see that we should choose $s_1 = +1$.

In summary, we get a remarkably simple set of equations:

$$\tilde{\mathbf{q}}_1(u) = \mathbf{q}_1(-u) \tag{29.9}$$

$$\tilde{\mathbf{q}}_4(u) = A\sinh(2\pi u)\mathbf{q}_1(-u) + \mathbf{q}_4(-u) \tag{29.10}$$

where A is a constant and we recall that in our notation $\mathbf{q}_i(u) = \mathbf{Q}_i(u)/\sqrt{u}$. These are the key equations which are enough to close the system. Let us stress that they are exact and are not restricted to large u or near-BPS limit. In particular, similarly to [13] these equations should be useful for a systematic weak coupling solution. With this approach we can completely avoid computing ω_{ij} as we are able to close the system using various Q-functions only. Notice also that in [13] the resulting equations were similar but coefficients in the r.h.s. were all constant, while here we also have $\sinh(2\pi u)$.

Now, finally, as we know $\mathbf{Q}_i$ and $\tilde{\mathbf{Q}}_i$ on the cut, we can evaluate both sides of (29.9), (29.10) at sampling points u_k on the cut, and minimize the difference between them. More precisely, we can express the constant A from (29.10) as

$$A = \frac{\tilde{\mathbf{q}}_4(u) - \mathbf{q}_4(-u)}{\mathbf{q}_1(-u)\sinh(2\pi u)} \tag{29.11}$$

and we build a function which on the true solution of the QSC should be zero[40]:

$$F = \sum_k |\tilde{\mathbf{q}}_1(u_k) - \mathbf{q}_1(-u_k)|^2 + \mathrm{Var}\left[\frac{\tilde{\mathbf{q}}_4(u_k) - \mathbf{q}_4(-u_k)}{\mathbf{q}_1(-u_k)\sinh(2\pi u_k)}\right] \tag{29.12}$$

where Var denotes the variance, i.e. measures the deviation of the function from a constant [41]. Thus we have reduced the problem to minimization of F which is a function of our main parameters $c_{a,n}$. It's easy to see that F can be written as the norm of a $2N$-dimensional vector where N is the number of sampling points. Therefore to find its minimum we can use the iterative Levenberg-Marquardt algorithm (an improved version of Newton's method) as in [14]. It converges rather fast and robustly, giving the values of coefficients $c_{a,n}$. Now we can reconstruct the $\mathbf{P}$'s and compute the anomalous dimension from e.g. (27.4).

29.2 Results

Let us now present the numerical results we obtained. First, we have evaluated Γ_{cusp} for a wide range of the coupling from $g = 0$ up to $g = 0.85$ at fixed values of the angles $\phi = \pi/4$, $\theta = 4\pi/10$. The results are given in Table 4. A fit of our data at weak coupling

[40] As in (29.12) we have $\sinh(2\pi u_k)$ in denominator we should make sure the sampling points do not include $u_k = 0$. We choose N sampling points as $u_k = 2gz_k$ where z_k are zeros of the N-th Chebyshev polynomial $T_N(z)$.

[41] $\mathrm{Var}\,[f_k] = \sum_k |f_k - \hat{f}|^2$ where $\hat{f}$ is the average of all elements f_k.

g	$\Gamma_{\text{cusp}}(g)$	g	$\Gamma_{\text{cusp}}(g)$	g	$\Gamma_{\text{cusp}}(g)$	g	$\Gamma_{\text{cusp}}(g)$
0.0125	0.000138062	0.025	0.000550881	0.0375	0.0012344	0.05	0.00218203
0.0625	0.00338487	0.075	0.00483202	0.0875	0.00651094	0.1	0.00840784
0.1125	0.010508	0.125	0.0127963	0.1375	0.0152575	0.15	0.0178762
0.1625	0.0206379	0.175	0.0235283	0.1875	0.0265342	0.2	0.0296431
0.2125	0.0328434	0.225	0.0361248	0.2375	0.0394776	0.25	0.0428933
0.2625	0.0463641	0.275	0.0498834	0.2875	0.053445	0.3	0.0570437
0.3125	0.0606747	0.325	0.0643342	0.3375	0.0680183	0.35	0.0717242
0.3625	0.0754492	0.375	0.0791908	0.3875	0.0829471	0.4	0.0867164
0.4125	0.0904971	0.425	0.0942879	0.4375	0.0980876	0.45	0.101895
0.4625	0.10571	0.475	0.109532	0.4875	0.113359	0.5	0.117191
0.5125	0.121027	0.525	0.124868	0.5375	0.128713	0.55	0.132561
0.5625	0.136413	0.575	0.140267	0.5875	0.144124	0.6	0.147984
0.6125	0.151845	0.625	0.155709	0.6375	0.159575	0.65	0.163442
0.6625	0.167312	0.675	0.171182	0.6875	0.175054	0.7	0.178928
0.7125	0.182803	0.725	0.186679	0.7375	0.190556	0.75	0.194434
0.7625	0.198313	0.775	0.202193	0.7875	0.206074	0.8	0.209955
0.8125	0.213838	0.825	0.217721	0.8375	0.221605	0.85	0.22549

Table 4: Numerical data used for the plot in Fig. 29.2. We give the values of Γ_{cusp} at finite coupling for $\phi = \pi/4,\ \theta = 4\pi/10$. Precision is decreased to fit the page. The full data set is available as attachment to the arXiv submission.

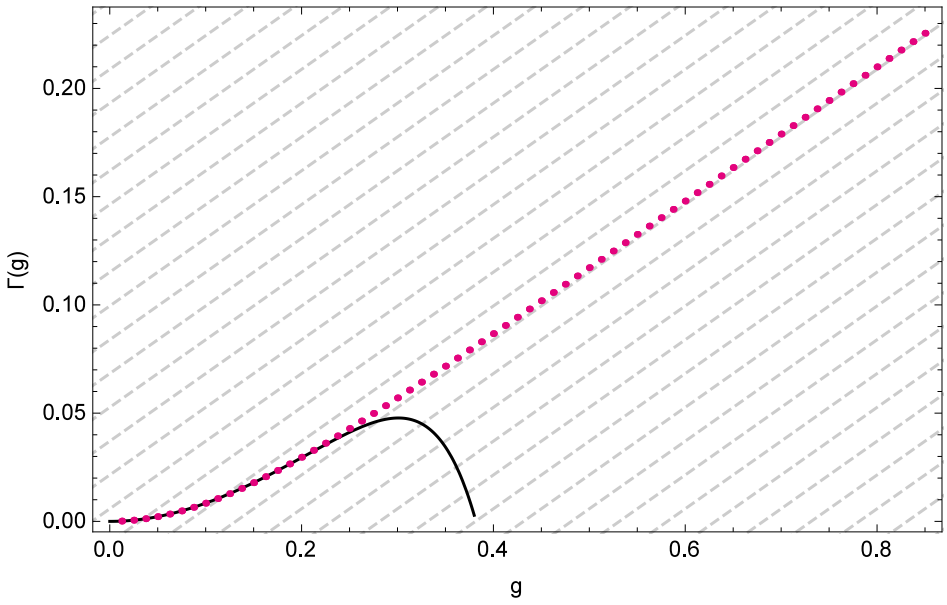

Figure 14: Numerically evaluated cusp anomalous dimension Γ_{cusp} for $\phi = \pi/4,\ \theta = 4\pi/10$ in a wide range of the coupling g. Solid line shows the 4-loop perturbation theory prediction of [169, 146, 166, 171]. Dashed lines indicate the leading strong coupling prediction for the slope of the function at $g \to \infty$.

gives

$$\begin{aligned}\Gamma_{\text{cusp}}\left(\phi=\frac{\pi}{4},\theta=\frac{4\pi}{10},g\right) &\simeq 0.884333160840179745804112 9816\, g^2 \\ &-4.700221937411277656828636 9\, g^4 + 37.481607207831059124394\, g^6 \\ &-321.37797809257617613\, g^8 + 2845.9019611906881\, g^{10} \\ &-25984.505154213\, g^{12} + \mathcal{O}(g^{14})\end{aligned} \tag{29.13}$$

which agrees with the analytical perturbative result of [169, 146, 166, 171] with $10^{-29}g^2 + 10^{-25}g^4 + 10^{-21}g^6 + 10^{-18}g^8$ error. The terms g^{10} and g^{12} above also give a numerical prediction for the five- and six-loop coefficients. One could try to get an analytic prediction for them by fitting the numerical data as a combination of some basis harmonic polylogarithms. This would require higher precision of course but should be possible to do (e.g. in [13] more than 60 digits of precision were reached).

At strong coupling only the leading classical result is known in explicit form at generic angles. It can be extracted from [146, 164] which gives the $\sim g$ coefficient. For $\phi = \frac{\pi}{4}$ and $\theta = \frac{4\pi}{10}$ it gives $\Gamma_{\text{cusp}}^{\text{classical}} \simeq 0.3122881g$. Fitting our data we get

$$\Gamma_{\text{cusp}}\left(\phi=\frac{\pi}{4},\theta=\frac{4\pi}{10},g\right) \simeq 0.3122892\, g - 0.0410591 + \frac{0.00073853}{g} + \mathcal{O}\left(\frac{1}{g^2}\right) \tag{29.14}$$

which agrees nicely with the AdS/CFT prediction. Let us mention that at strong coupling it requires some effort to get high precision since we need to keep many terms in the

expansion of the **P**'s in owers of x. It would be interesting to compare our result for the g^0 term with the 1-loop prediction of [146] which is written in an implicit form. One should also be able to derive the one-loop correction in a simpler and more general way by using the algebraic curve as in [31]. On Fig. 29.2 one can see that our data clearly interpolates between gauge and string theory results.

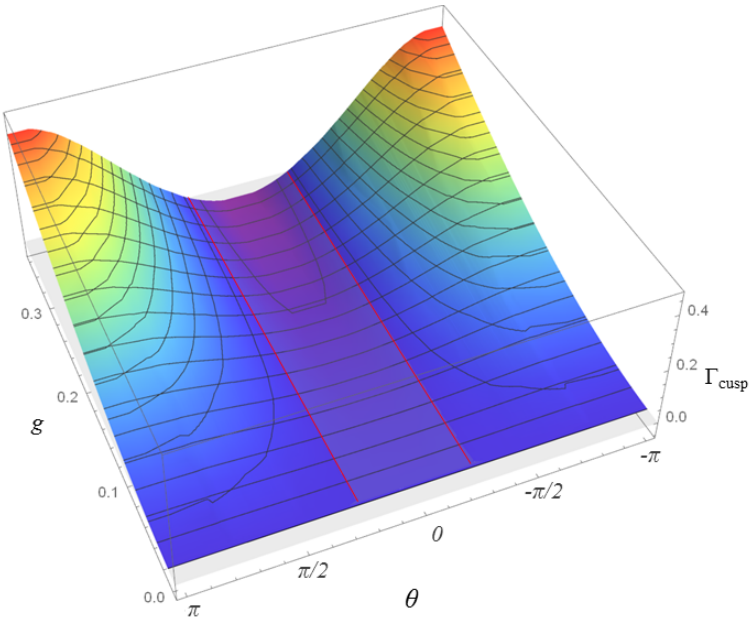

Figure 15: A 3d plot of Γ_{cusp} at fixed $\phi = \pi/4$ in a range of values of the coupling g and the angle θ, generated from ~ 800 data points. We also added a semi-transparent purple plane located at $\Gamma_{\text{cusp}} = 0$, and two red lines corresponding to the BPS configuration $\theta = \pm\phi$ for which $\Gamma_{\text{cusp}} = 0$ (i.e. $\theta = \pm\pi/4$ in our case).

In addition, on Fig. 29.2 we show our numerical data for the generalized cusp anomalous dimension at $\phi = \pi/4$ for various values of θ and of the coupling. One can clearly see in particular the straight lines corresponding to the BPS regime $\phi = \theta$ when Γ_{cusp} is zero. We covered the full range of θ from $-\pi$ to π, and on the plot one can see that as expected Γ_{cusp} is a smooth and 2π-periodic function of this angle, invariant under $\theta \to -\theta$.

30 Weak coupling solution

In section 28 we constructed the solution of the QSC in the near-BPS limit $\phi - \theta \to 0$. In this section we will describe the solution for *arbitrary* angles, at leading order in g. We will discuss the case $L = 0$.

At weak coupling the cuts degenerate into poles, but the singular part is typically suppressed by the coupling so one could expect $\mathbf{P}_a$ to be regular at leading order. However the asymptotics (27.2) mean that we have to allow a $1/\sqrt{u}$ singularity in $\mathbf{P}_1, \mathbf{P}_2$. This leads to the ansatz

$$\begin{aligned} \mathbf{P}_1 &= C_1 \frac{e^{\theta u}}{\sqrt{u}}, \qquad \mathbf{P}_2 = C_2 \frac{e^{-\theta u}}{\sqrt{u}}, \\ \mathbf{P}_3 &= e^{\theta u}(C_3 u^{3/2} + C_4 u^{1/2}), \qquad \mathbf{P}_4 = e^{-\theta u}(C_5 u^{3/2} + C_6 u^{1/2}) \ . \end{aligned} \tag{30.1}$$

Then all the coefficients are completely fixed by asymptotics (up to a rescaling (27.8)), giving

$$\begin{aligned} \mathbf{P}_1 &= \sqrt{\epsilon} \frac{e^{\theta u}}{\sqrt{u}}, \qquad \mathbf{P}_2 = \sqrt{\epsilon} \frac{e^{-\theta u}}{\sqrt{u}}, \\ \mathbf{P}_3 &= \epsilon^{3/2} u^{3/2} e^{\theta u}(1 + b/u), \qquad \mathbf{P}_4 = -\epsilon^{3/2} u^{3/2} e^{-\theta u}(1 - b/u) \end{aligned} \tag{30.2}$$

where

$$b = \frac{2\cos\theta\cos\phi + \cos 2\theta - 3}{2\sin\theta(\cos\theta - \cos\phi)} \tag{30.3}$$

and ϵ is defined in (27.3).

Let us now discuss μ_{ab}. At leading order in the weak coupling expansion we expect that in the general expression

$$\mu_{ab} = \frac{1}{2} Q^{-}_{ab|ij} \omega^{ij} \tag{30.4}$$

only ω^{12} will contribute, in analogy with the undeformed QSC [52, 53, 70] as this also what happens in the asymptotic large L regime. Based on our large u prescription $\omega^{12} \sim e^{2\pi|u|}$ and the near-BPS solution (28.9), it is natural to take

$$\omega^{12} = \text{const} \cdot \sinh(2\pi u) \ . \tag{30.5}$$

In fact, for computing higher orders in the weak coupling expansion it should be better to completely avoid calculating ω^{ij} and apply instead the equations (29.9), (29.10) we used in the numerics. For the functions $Q_{ab|12}$ we can make an ansatz as polynomials whose degree is determined by the asymptotics of $Q_{ab|12}$, times $e^{\pm 2\theta u}$ in accordance with

asymptotics again. Also, we expect that those of the functions $Q_{ab|12}$ which do not have exponential asymptotics should be either even or odd. Thus we use the following ansatz:

$$\{\mu^+_{12},\mu^+_{13},\mu^+_{14},\mu^+_{24},\mu^+_{34}\} = \tag{30.6}$$

$$\sinh(2\pi u)\Big\{D_1,\ e^{2\theta u}(D_2+uD_3),\ D_4u^2+D_5,$$
$$e^{-2\theta u}(D_6+uD_7),\ D_8u^4+D_9u^2+D_{10}\Big\}\ .$$

To fix the constants D_i appearing here we use the difference equation on μ_{ab} following from the $\mathbf{P}\mu$-system equations:

$$\mu^{++}_{ab}-\mu_{ab}=\mu_{ac}\mathbf{P}^c\mathbf{P}_b-\mu_{bc}\mathbf{P}^c\mathbf{P}_a \tag{30.7}$$

where $\mathbf{P}^a$ are related to $\mathbf{P}_a$ by (27.7). This equation fixes all the constants except one, and we get

$$\{\mu^+_{12},\mu^+_{13},\mu^+_{14},\mu^+_{24},\mu^+_{34}\} =$$
$$R\sinh(2\pi u)\left\{-\frac{\sin\theta}{\epsilon},\frac{e^{2\theta u}}{2}(2u-\cot\theta),\frac{\sin\theta}{4}\left(-\frac{2}{\sin^2\theta}+4u^2+1\right),\right.$$
$$\left.-\frac{1}{2}e^{-2\theta u}(\cot\theta+2u),\frac{1}{16}\left(4u^2+1\right)^2\epsilon\sin\theta\right\}\ . \tag{30.8}$$

Going to higher orders in g (see below) we also found that the constant R and ω^{12} scale as $\sim 1/g^2$.

The $\mathbf{Q}$-functions can be found from the 4th order Baxter equation on $\mathbf{Q}_i$ with coefficients built from $\mathbf{P}_a$ (see [72] for its derivation). They turn out to be written in terms of generalized η-functions defined as

$$\eta^{z_1,\dots,z_k}_{s_1,\dots,s_k}(u)\equiv\sum_{n_1>n_2>\dots>n_k\geq 0}\frac{z_1^{n_1}\dots z_k^{n_k}}{(u+in_1)^{s_1}\dots(u+in_k)^{s_k}} \tag{30.9}$$

For the case when all twists z_i are equal to 1 such functions already appeared in the weak coupling calculations of [109, 70]. Importantly, all operations needed for the iterative procedure of [13] (e.g. expressing the product as a linear combination or solving equations of the kind $f(u+i)-f(u)=\eta^{z_1,\dots,z_k}_{s_1,\dots,s_k}(u)$) can be carried out for these functions as we describe in Appendix C.5.

In terms of η-functions we found the following four linearly independent solutions of the fourth order Baxter equation:

$$\begin{aligned}
\mathbf{Q}_1 &= \sqrt{u}e^{u\phi}, \qquad (30.10)\\
\mathbf{Q}_2 &= \sqrt{u}e^{-u\phi},\\
\mathbf{Q}_3 &= \frac{e^{u\phi}(\sin\phi+iu(\eta^z_1-\eta^1_1)(\cos\theta-\cos\phi))}{\sqrt{u}(\cos\phi-\cos\theta)},\\
\mathbf{Q}_4 &= \frac{e^{-u\phi}(-\sin\phi+iu(\eta^{\bar z}_1-\eta^1_1)(\cos\theta-\cos\phi))}{\sqrt{u}(\cos\phi-\cos\theta)}
\end{aligned}$$

where $z = e^{2i\phi}, \bar{z} = e^{-2i\phi}$. The true $\mathbf{Q}$-functions should be identified with appropriate linear combinations of these four solutions.

To fix the anomalous dimension Γ_{cusp} one needs to go to higher orders in g. This can be done using the iterative algorithm of [13] for which $\mathbf{P}_a$ and $\mathbf{Q}_i$ we have found serve as a starting point. Notice that the weak coupling algorithm of [70] is not directly applicable in our situation, as all $\mathbf{P}_a$ are of the same order $\sim g^0$ and none of them are small at weak coupling. In particular, none of the five independent equations among (30.7) decouple from the rest at leading order. However the universal iterative method of [13] works well, and we used it to compute the $\mathbf{P}$- and $\mathbf{Q}$-functions at higher orders[42]. In particular we reproduced the one-loop prediction

$$\Gamma_{\text{cusp}} = 2g^2 \frac{\cos\phi - \cos\theta}{\sin\phi}\phi + \mathcal{O}(g^4) \tag{30.11}$$

directly at any ϕ and θ. The details of this calculation will be presented elsewhere. Using this method it is certainly possible to also reach much higher loops.

31 Conclusions

In this part we have presented the modifications needed in the Quantum Spectral Curve to describe the generalized cusp anomalous dimension. We showed that the main new ingredient of the boundary TBA formulation – the boundary reflection phase [63, 64] – is mapped to a simple modification of the ω^{12} asymptotics. In addition, the analytical properties of the key functions $\mathbf{P}_a(u)$ and $\mathbf{Q}_i(u)$ have to be modified, namely we require regularity in u on the defining sheet (except for the branch cut) once these functions are divided by $\sqrt{u}$, as described by Eq. (27.5).

Our proposal is consistent with the known near-BPS solution, and we also computed the subleading term in the near-BPS expansion at any coupling. The result matches perfectly the known perturbative predictions, providing a deep test of the QSC for this model.

Curiously, our modification of the asymptotics for the component ω^{12} of the periodic anti-symmetric matrix ω^{ij} is very similar to that needed for the analytic continuation in Lorentz spin for the twist-2 local operators where the ω^{13} asymptotics was relaxed to be exponentially large [15, 72, 14]. It seems to be a common feature of non-local operators.

[42] To simplify intermediate expressions we used several Mathematica packages [107, 110]

It would be interesting to classify all consistent asymptotics of this kind and find the corresponding integrable observables.

The drastic simplification of the TBA we have achieved calls for a systematic exploration of Γ_{cusp} in various regimes, with the hope of revealing new structures. It would be also interesting to explore the connection to the supersymmetric hydrogenlike bound states of massive W-bosons in $\mathcal{N} = 4$ SYM [172].

While a numerical solution of the TBA is additionally complicated by the infinite sums which diverge for real ϕ and θ [170], the simple high-precision numerical method of [14] for the QSC is applicable almost directly. Computing Γ_{cusp} numerically in a wide range of the coupling we found perfect interpolation between gauge theory and string theory predictions.

Part VII

Quark-antiquark potential

In this part we present the results of [11] where the QSC was used to explore the flat space quark-antiquark potential in a variety of regimes.

32 Introduction

One of the first predictions of AdS/CFT was the strong coupling limit of the potential between two heavy charged particles or "quarks" which is represented by a pair of anti-parallel Wilson lines separated by distance r [173, 155]. The potential is inversely proportional to the separation r due to conformal symmetry of the theory, with the strength of the interaction depending on the gauge coupling g_{YM}. In the planar limit $N_c \to \infty$ the potential is a highly non-trivial function of the 't Hooft coupling $\lambda = g_{YM}^2 N_c$,

$$V(\lambda, r) = -\frac{\Omega(\lambda)}{r} \ . \tag{32.1}$$

Currently the function $\Omega(\lambda)$ is known at 3 loops at weak coupling [173, 174, 146, 166, 175, 177, 178] and at one loop at strong coupling [179, 180, 181, 182]. In fact even at low orders the weak coupling expansion is rather involved and requires using a nontrivial low-energy effective theory. One can further generalize this observable by introducing an extra parameter θ, which may be associated with relative flavors of the particles. The particle flavor enters through the unit vector $\vec{n}$ in the expression for the Maldacena-Wilson line

$$\text{Pexp}\left[\int (iA_\mu \dot{x}^\mu + \vec{\Phi}\cdot\vec{n}\,|\dot{x}|)\right] \ . \tag{32.2}$$

The parameter θ is the angle between these vectors $\vec{n}$ for the two antiparallel lines. The expectation value of the pair of the Maldacena-Wilson lines is related to the potential as

$$\langle W \rangle \simeq e^{\frac{T\Omega(\lambda,\theta)}{r}} \tag{32.3}$$

where $T \gg r$ is the extent of the lines.

In this part we study this important quantity $\Omega(\lambda, \theta)$ intensively using the integrability-based Quantum Spectral Curve method introduced for local operators in [53, 52] and generalized for a subclass of Wilson lines in [12], as described above. We show how the results of [12] can be used to get a closed system of equations describing $\Omega(\lambda, \theta)$ exactly in the whole range of the parameters λ and θ. We find the analytic weak coupling expansion

up to 7 loops and also build a numerically-exact function interpolating from weak to strong coupling regime. Finally, we study analytically the limit $\theta \to i\infty$ (with $\lambda e^{-i\theta}$ fixed) to all orders in the 't Hooft coupling[43]. We demonstrate how the Schrödinger equation arising from resummation of the ladder diagrams in this limit appears from the Quantum Spectral Curve.

33 Quantum Spectral Curve for the quark–anti-quark potential

The configuration of two anti-parallel Wilson lines is closely related to a configuration where two straight lines meet at a cusp where they form an angle ϕ [150]. Indeed, the two setups are linked by the plane to cylinder transformation where the cusp point is mapped to infinity. In this picture the distance between the lines is given by $r = \phi - \pi$. When ϕ tends to π the curvature of the cylinder becomes irrelevant and one recovers the flat space quark–anti-quark potential.

In [146, 63, 64] it was shown that the anomalous dimension of the cusped Maldacena-Wilson line admits an integrability-based description in terms of an infinite system of integral equations (known as Thermodynamic Bethe Ansatz equations). This anomalous dimension depends on 3 parameters: θ, ϕ and the coupling $g = \frac{\sqrt{\lambda}}{4\pi}$. Subsequently a much simpler description in terms of the Quantum Spectral Curve (QSC) was found [12] which we use here.

In this section we will first introduce useful notation corresponding to a convenient normalization of the Q-functions, and then show what happens in the QSC when we take the singular limit $\phi \to \pi$.

[43] A similar limit in the γ-deformed SYM was recently considered in [183].

33.1 Notation and parameterisation of the Q-functions

It will be convenient to slightly change the notation compared to the previous part, namely after an appropriate $\alpha\beta$ rescaling we can write

$$\begin{aligned}
\mathbf{P}_1(u) &= +\epsilon\, u^{1/2}\, e^{+\theta u}\, \mathbf{f}(+u)\ , \\
\mathbf{P}_2(u) &= -\epsilon\, u^{1/2}\, e^{-\theta u}\, \mathbf{f}(-u)\ , \\
\mathbf{P}_3(u) &= +\epsilon\, u^{1/2}\, e^{+\theta u}\, \mathbf{g}(+u)\ , \\
\mathbf{P}_4(u) &= +\epsilon\, u^{1/2}\, e^{-\theta u}\, \mathbf{g}(-u)\ .
\end{aligned} \tag{33.1}$$

We have to impose $\mathbf{f} \simeq 1/u$ and $\mathbf{g} \simeq u$ for large u. For this normalization the prefactor ϵ is fixed to be

$$\epsilon = \sqrt{\frac{i}{2}}\, \frac{\cos\theta - \cos\phi}{\sin\theta}\ . \tag{33.2}$$

As $\mathbf{P}$'s have only one cut, $\mathbf{f}$ and $\mathbf{g}$ are regular function of the Zhukovsky variable $x(u)$ at least for $|x| > 1$. They can be written in terms of the Laurent expansion coefficients

$$\mathbf{f}(u) = \frac{1}{gx} + \sum_{n=1}^{\infty} \frac{g^{n-1} A_n}{x^{n+1}}\ \ ,\ \ \mathbf{g}(u) = \frac{u^2 + B_0 u}{gx} + \sum_{n=1}^{\infty} \frac{g^{n-1} B_n}{x^{n+1}}\ . \tag{33.3}$$

The first few coefficients encode the information about the AdS charges and twists, i.e. Δ and ϕ, via the relations [12]

$$A_1 g^2 - B_0 = -\frac{2\cos\theta\cos\phi + \cos(2\theta) - 3}{2\sin\theta(\cos\theta - \cos\phi)}\ , \tag{33.4}$$

$$\begin{aligned}
\Delta^2 &= \frac{(\cos\theta - \cos\phi)^3}{\sin\theta \sin^2\phi} \left[A_3 g^6 + \frac{A_1^2 g^4 (1 - \cos\theta\cos\phi)}{\sin\theta(\cos\theta - \cos\phi)} - A_2 g^4 \cot\theta \right. \\
&\quad \left. - g^2 (B_0 + B_1 + \cot\theta) - A_1 g^2 \left(A_2 g^4 - 2g^2 + \frac{1}{\sin^2\theta} \right) \right]\ .
\end{aligned} \tag{33.5}$$

We also note that the coefficients A_n and B_n are real and scale at weak coupling as $\mathcal{O}(g^0)$. Their leading weak coupling behavior can be deduced from [12] and is given in Appendix D.1.

Let us also write out explicitly the 4th order finite difference equation for $\mathbf{Q}_i$ with the coefficients built from $\mathbf{P}_a$, which follows from the QQ-relations (4.20) and (4.22):

$$\begin{aligned}
\mathbf{Q}_i^{[+4]} D_0 &- \mathbf{Q}_i^{[+2]} \left[D_1 - \mathbf{P}_a^{[+2]} \mathbf{P}^{a[+4]} D_0 \right] + \mathbf{Q}_i \left[D_2 - \mathbf{P}_a \mathbf{P}^{a[+2]} D_1 + \mathbf{P}_a \mathbf{P}^{a[+4]} D_0 \right] \\
&- \mathbf{Q}_i^{[-2]} \left[\bar{D}_1 + \mathbf{P}_a^{[-2]} \mathbf{P}^{a[-4]} \bar{D}_0 \right] + \mathbf{Q}_i^{[-4]} \bar{D}_0 = 0
\end{aligned} \tag{33.6}$$

Here $D_n, \bar{D}_n$ are some nice combinations of $\mathbf{P}$'s given in Appendix D.2. As a 4th order equation it has 4 independent solutions which are precisely the $\mathbf{Q}_i$. Let us remind that the relations (33.5) and (33.4) imply the following large u asymptotics for $\mathbf{Q}_i$

$$\mathbf{Q}_1 \sim u^{1/2+\Delta} e^{u\phi},\ \mathbf{Q}_2 \sim u^{1/2+\Delta} e^{-u\phi},\ \mathbf{Q}_3 \sim u^{1/2-\Delta} e^{u\phi},\ \mathbf{Q}_4 \sim u^{1/2-\Delta} e^{-u\phi}\ . \tag{33.7}$$

This is in fact how (33.5) and (33.4) were derived. Those 4 distinguished asymptotics allow to choose the basis of solutions $\{\mathbf{Q}_i\}$ uniquely up to a normalization. The functions $\mathbf{Q}_i$ are analytic in the upper half plane and have a cut $[-2g, 2g]$ on the real axis as well as more cuts below (as can be deduced from the equation (33.6)). A non-trivial new condition, which in fact allows to close the equations and fix the coefficients A_n and B_n uniquely, concerns the behavior of $\mathbf{Q}_i$ on the cut $[-2g, 2g]$. To describe it we introduce

$$\mathbf{q}_i = \mathbf{Q}_i u^{-1/2} \tag{33.8}$$

and denote by $\tilde{\mathbf{q}}_i$ the analytic continuation of $\mathbf{q}_i$ under the cut on the real axis. Then according to [12]

$$\tilde{\mathbf{q}}_1(u) = \mathbf{q}_1(-u) \tag{33.9}$$

$$\tilde{\mathbf{q}}_2(u) = \mathbf{q}_2(-u) \tag{33.10}$$

$$\tilde{\mathbf{q}}_3(u) = a_1 \sinh(2\pi u)\mathbf{q}_2(-u) + \mathbf{q}_3(-u) \tag{33.11}$$

$$\tilde{\mathbf{q}}_4(u) = a_2 \sinh(2\pi u)\mathbf{q}_1(-u) + \mathbf{q}_4(-u)\ . \tag{33.12}$$

It was noticed in [12] that it is sufficient to impose the first two equations in (33.9) only.

In the next section we discuss what happens in the singular limit $\phi \to \pi$ and derive a closed system of equations describing directly the potential $\Omega(\lambda, \theta)$.

33.2 QSC for the quark–anti-quark potential

We will focus on the particularly important limit $\phi \to \pi$ when the Wilson line with a cusp is related to a pair of anti-parallel lines. In this limit we expect the anomalous dimension Δ to diverge as

$$\Delta = -\frac{\Omega(\lambda)}{\pi - \phi} + \mathcal{O}((\pi - \phi)^0) \tag{33.13}$$

where $\Omega(\lambda)$ is a positive quantity (for real θ). As the anomalous dimension diverges we should expect a drastic change in the large u asymptotics of $\mathbf{Q}_i$, which for finite Δ is given by (33.7). To get some intuition about what happens we take $\phi = \pi - \epsilon$ with ϵ being small, so the asymptotics becomes

$$\mathbf{q}_1 \sim e^{\pi u} \exp\left[-u\epsilon - \frac{\Omega}{\epsilon}\log u\right]\ . \tag{33.14}$$

We see that the last term in the second factor explodes for u fixed and the asymptotics does not make sense. What happens is that the subleading coefficients become bigger in this limit in order to make the result finite. However, if we scale u to infinity while sending

$\epsilon \to 0$ we should be able to suppress the subleading in $1/u$ terms. The guiding principle is to try to balance the two terms in the square brackets, which is the case for $u \sim \Omega/\epsilon^2$ (treating $\log u$ as a constant compared to $\sqrt{u}$) or in other words for $\epsilon = c\sqrt{\Omega}/\sqrt{u}$ this results in

$$\log \mathbf{q}_1 \sim +\pi u - c\sqrt{\Omega u} + \mathcal{O}(u^0) \,. \tag{33.15}$$

The positive constant c cannot be determined from this heuristic argument and it will be shown below to be equal to $\sqrt{8}$. Similar considerations for $\mathbf{q}_2, \mathbf{q}_3$ and $\mathbf{q}_4$ lead to

$$\log \mathbf{q}_2 \sim -\pi u + ic\sqrt{\Omega u} + \mathcal{O}(u^0) \,, \tag{33.16}$$

$$\log \mathbf{q}_3 \sim +\pi u - ic\sqrt{\Omega u} + \mathcal{O}(u^0) \,, \tag{33.17}$$

$$\log \mathbf{q}_4 \sim -\pi u + c\sqrt{\Omega u} + \mathcal{O}(u^0) \,. \tag{33.18}$$

To get the precise value of the coefficient c and derive the asymptotics rigorously, we have to analyze the limit of $\mathbf{P}_a$ when $\phi \to \pi$. One could expect that $\mathbf{P}_a$ behave smoothly in this limit as they describe the S^5 part which is relatively isolated from the twist ϕ in AdS_5. It can be also seen from (33.4) and (33.5) that we can consistently assume the coefficients A_n and B_n in $\mathbf{P}$'s to remain finite when $\phi \to \pi$, giving

$$\epsilon = \sqrt{\frac{i}{2}\frac{\cos\theta + 1}{\sin\theta}} \;, \quad B_0 = A_1 g^2 - \frac{2 - \cos\theta}{\sin\theta} \,, \tag{33.19}$$

$$\begin{aligned} \Omega^2 = {} & \frac{g^2 \cot^3\frac{\theta}{2}}{2} \big[2\sin\theta \left(A_3 g^4 \sin\theta - A_2 g^2 \cos\theta - B_1 \sin\theta - 2\cos\theta + 2\right) \\ & + 2A_1^2 g^2 \sin\theta + A_1 \left(-2A_2 g^4 \sin^2\theta - g^2 \cos(2\theta) + g^2 - 2\right)\big] \,. \end{aligned} \tag{33.20}$$

This allows to find the asymptotics of $\mathbf{q}_i$ using the 4th order Baxter equation (33.6) in which we expand the coefficients at large u. The expressions we get are lengthy, and for illustration purposes let us drop some of the terms which do not affect the leading asymptotics, leaving the following equation:

$$\begin{aligned} & \mathbf{q}(u)\left(\frac{-\frac{2\Omega^2}{3} - 1}{u^2} + 1\right) + \left(-\frac{2}{3u^2} + \frac{i}{3u} + \frac{2}{3}\right)\mathbf{q}(u+i) + \left(-\frac{1}{6u^2} + \frac{i}{6u} + \frac{1}{6}\right)\mathbf{q}(u+2i) \\ & + \left(-\frac{2}{3u^2} - \frac{i}{3u} + \frac{2}{3}\right)\mathbf{q}(u-i) + \left(-\frac{1}{6u^2} - \frac{i}{6u} + \frac{1}{6}\right)\mathbf{q}(u-2i) = 0 \,. \end{aligned}$$

While the coefficients in this equation are simple, the asymptotics of its four solutions is quite nontrivial. It turns out to have indeed the form anticipated above in (33.15) as we get

$$\mathbf{q}_i = M_i u^{1/4} e^{\pm\pi u + \alpha_i\sqrt{u}} \left(1 + \mathcal{O}(1/u)\right) \tag{33.21}$$

where

$$\alpha_1 = -\sqrt{8\Omega}, \;\; \alpha_2 = +i\sqrt{8\Omega}, \;\; \alpha_3 = -i\sqrt{8\Omega}, \;\; \alpha_4 = +\sqrt{8\Omega} \,. \tag{33.22}$$

Expanding the Baxter equation to higher orders in u and keeping all the terms, we found the following expansion for the solution:

$$\mathbf{q}_i = M_i u^{1/4} e^{\pm\pi u + \alpha_i \sqrt{u}} \left(1 + \sum_{n=1}^{\infty} \frac{d_n}{(\alpha_i)^n u^{n/2}}\right) \tag{33.23}$$

This rather surprising asymptotics is a key result which supplements the QSC functional equations.

A natural way to fix the normalization of $\mathbf{Q}_i$ (which we will use here, e.g. in Appendix D.4) is to impose that the matrix $Q_{a|i}$ preserves the constant matrix χ^{ab}, i.e.

$$Q_{a|i}\chi^{ab}Q_{b|j}\chi^{jk} = \delta_i^k \tag{33.24}$$

This leads to

$$iM_1M_4 = M_2M_3 = \sqrt{2}\frac{\cos^4(\theta/2)}{\Omega^{3/2}} \ . \tag{33.25}$$

We conclude that the quark–anti-quark potential is described by QSC with a novel type of asymptotics of the Q-functions containing non-integer powers of the spectral parameter u in the exponent. These asymptotics together with the general relations from the previous section form a closed system of equations applicable at all values of the coupling g and the twist θ.

Despite the anomalous dimension Δ of the cusped Wilson line being infinite at $\phi = \pi$, we managed to reformulate the QSC equations in such a way that they only include the finite residue $\Omega(\lambda, \theta)$ and got rid of the auxiliary parameter ϕ completely. In the following sections we will solve these equations both analytically at weak coupling to a high order and numerically in a wide range of the coupling. We will be also able to demonstrate how in a special limit the QSC reduces to the Schrödinger equation of [173, 166] resumming the ladder diagrams to all orders in perturbation theory.

34 Weak coupling

In this section we show how to solve the equations from the previous section perturbatively at weak coupling. We will see that the weak coupling limit is rather nontrivial and contains qualitatively new features compared to all other perturbative expansions of the Quantum Spectral Curve studied previously [52, 70, 13, 88].

34.1 Different scales and structure of the expansion

The weak coupling limit is more involved in the present case as it depends on the scaling of the spectral parameter u. The situation here is similar to the conventional perturbation theory where in order to compute the quark–anti-quark potential one has to work with an effective theory resumming soft contributions. We also note that the limits $\phi \to \pi$ and $g \to 0$ do not commute with each other and it is crucial to have a closed system of equations directly at $\phi = \pi$ in order to get a sensible weak coupling expansion.

Another key feature of the weak coupling calculation is that the limits $g \to 0$ and $u \to \infty$ do not commute. The reason for this is that Ω, appearing in the asymptotics (33.23), goes to zero as g^2. In this case one should expect the following three natural scales

$$\begin{aligned} &\text{scale 1} : u \to \infty \ \text{ before } \ g \to 0 \\ &\text{scale 2} : g \to 0 \ \text{ with } \ v \equiv 8u\,\Omega \ \text{ fixed} \\ &\text{scale 3} : g \to 0 \ \text{ then } u \to \infty \end{aligned}$$

In the scale 1 we are in the regime where the asymptotics (33.23) is still valid. The scale 2 is natural to consider as in the asymptotics (33.23) u appears in this combination with Ω. In the scale 3 we are in the usual perturbative regime of the QSC studied intensively in [52, 70, 13, 88] and we should expect the usual expansion of the Q-functions in terms of η-functions introduced in [109]. These η-functions are defined as[44]

$$\eta_{s_1,\dots,s_k}(u) = \sum_{n_1>n_2\dots n_k\geq 0} \frac{1}{(u+in_1)^{s_1}\dots(u+in_k)^{s_k}}\,. \tag{34.1}$$

At large u however these functions can only give terms of the type $u^n \log^m u$, which are very different from the scale 1. The intermediate scale 2 should match the two regimes corresponding to scales 1 and 3. This regime plays an important role as it allows to identify correctly $\mathbf{q}_1$ and $\mathbf{q}_2$ in the scale 3 and distinguish them from $\mathbf{q}_3$ and $\mathbf{q}_4$, for which the analyticity condition on the cut $[-2g, 2g]$ given by (33.9) is different.

Thus, before we can use (33.9) and fix the coefficients A_n and B_n in the expression for $\mathbf{P}_a$, we have to pass through the regime with finite $v \equiv 8\Omega u$. Fortunately, in this regime the finite difference equation (33.6) on $\mathbf{q}_i$ (related to $\mathbf{Q}_i$ via (33.8)) simplifies into a 4th order differential equation which we can solve systematically order by order in g. Its solution provides a bridge between scale 1 and scale 3 by interpolating between the exponential

[44] In some cases the sum could be divergent, we regularize it as in [109, 70] so that e.g. $\eta_1(u) = i\psi(-iu)$.

and power-like with logs asymptotics. We will first demonstrate this procedure at the leading order in the coupling and then present our result to a high order in perturbation theory[45].

To study the 2nd scale we start from the 4th order Baxter equation (33.6) and expand it at large u (notice that in the 2nd scale u is large as it is $\sim 1/g^2$). By doing this we obtain a finite difference equation of the form

$$\begin{aligned}&-\mathbf{q}_i(u)\left(1+\frac{C_0}{u^2}+\dots\right)+\frac{\mathbf{q}_i(u+2i)}{6}\left(1+\frac{i}{u}+\frac{C_2}{u^2}+\dots\right)\\&+\frac{2\mathbf{q}_i(u+i)}{3}\left(1+\frac{i}{2u}+\frac{C_1}{u^2}+\dots\right)+\frac{\mathbf{q}_i(u-2i)}{6}\left(1-\frac{i}{u}+\frac{\bar{C}_2}{u^2}+\dots\right)\\&+\frac{2\mathbf{q}_i(u-i)}{3}\left(1-\frac{i}{2u}+\frac{\bar{C}_1}{u^2}+\dots\right)=0\end{aligned} \tag{34.2}$$

where C_n and the sub-leading coefficients are some explicit combinations of A_n and B_n. Next we use that $u=v/(8\Omega)$ where $\Omega\sim g^2$ and introduce a smooth function $f(v)$ such that $\mathbf{q}(u)=e^{\pm\pi u}f(8\Omega u)$ to obtain

$$f^{(4)}+\frac{2f^{(3)}}{v}-\frac{f}{16v^2}+8\hat{g}^2\frac{f''}{v^2}+\mathcal{O}\left(g^4\right)=0 \tag{34.3}$$

where $\hat{g}=g\cos\left(\frac{\theta}{2}\right)$. Fortunately, we can solve this equation analytically! At the leading order in g its 4 independent solutions are given by four different types of Bessel functions,

$$\sqrt{v}\,K_1(\sqrt{v})\ \ ,\ \ \sqrt{v}\,Y_1(\sqrt{v})\ \ ,\ \ \sqrt{v}\,I_1(\sqrt{v})\ \ ,\ \ \sqrt{v}\,J_1(\sqrt{v})\,. \tag{34.4}$$

Next we notice that the first solution should be related to $\mathbf{q}_1$ simply because its large v asymptotics matches precisely the asymptotics (33.23) of $\mathbf{q}_1$:

$$f_1(v)\equiv\sqrt{v}\,K_1(\sqrt{v})\simeq\sqrt{\frac{\pi}{2}}\,\sqrt[1/4]{8\Omega u}\ \ e^{-\sqrt{8\Omega u}}\,. \tag{34.5}$$

We note that since this is one of the decaying "small" solutions this identification is non-ambiguous.

At the higher orders in g the equation (34.3) gets corrected. In general one would have to solve (34.3) using perturbation theory, involving Green's function and multiple integrations. However, we found a much simpler procedure, which works magically up to at least g^{10} order. Once can simply build an ansatz for the corrected solution as a linear combination of $v^{(1/2-m)}\partial_\nu^n K_\nu(\sqrt{v})|_{\nu=1}$ for integer m and n. So for instance at g^2 order we simply get

$$f_1(v)=\sqrt{v}\,K_1(\sqrt{v})-8\hat{g}^2\sqrt{v}\,K_1^{(1,0)}(\sqrt{v})+\mathcal{O}(g^4)\,. \tag{34.6}$$

[45] At high orders to simplify intermediate expressions we used the HPL Mathematica package [107] and the package for working with multiple zeta values provided with the paper [109].

Having an explicit form of the solution in the scale 2, we can get information about the behavior of $\mathbf{q}_1$ in the scale 3. For that we expand (34.6) at small v,

$$\begin{aligned} f_1(v) &= 1+\frac{1}{4}v\left(\log\frac{v}{4}+2\gamma-1\right)+\frac{1}{64}v^2\left(2\log\frac{v}{16}+4\gamma-5\right)+O\left(v^3\right) \\ &\quad +4\hat{g}^2\left(\log\frac{v}{4}+2\gamma\right) \quad +\hat{g}^2 v\left(\log\frac{v}{4}+2\gamma-2\right)+O\left(g^2v^2\right)+\mathcal{O}(g^4)\,. \end{aligned} \tag{34.7}$$

We see that this expansion, rewritten in terms of u gives the *large* u expansion of $\mathbf{q}_1$ in the scale 3. So the first line (originating from the leading order in g in (34.6)) gives the leading large u term to all orders in g in this scale, the second line in (34.7) gives the subleading in large u term to all orders in g etc. This information is essential for the correct identification of $\mathbf{q}_1$ in the scale 3.

Now let us finally describe the situation in the scale 3. In this scale the 4th order finite difference equation cannot be much simplified but it can be solved iteratively order by order in the coupling g using the highly universal procedure from [13]. For instance at the first two orders we start by finding 4 independent solutions for $q=\mathbf{q}\,e^{\pm\pi u}$,

$$\begin{aligned} q_I &= 1+g^2\left(4iu\,\eta_2\cos^2\frac{\theta}{2}+2\,\eta_1\cot^2\frac{\theta}{2}((u+i)\cos\theta+u-i)\right. \\ &\quad \left.+\frac{\cot^2\frac{\theta}{2}\left(2u^3\cos\theta+2u^3-2u-i\right)}{u}\right)\,, \\ q_{II} &= u\,, \\ q_{III} &= u^2\,, \\ q_{IV} &= 4\eta_1 u\cos^2\frac{\theta}{2}-\frac{i}{u}\,. \end{aligned} \tag{34.8}$$

However, to be able to use the key analyticity condition (33.9) we need to identify $\mathbf{q}_1$ (or $\mathbf{q}_2$). That is, we have to find a linear combination of $q_I,\dots,q_{IV}$ which matches (34.7) at large u. From this condition one finds uniquely

$$\mathbf{q}_1 = e^{\pi u}\left(A_I q_I + A_{II}q_{II}+A_{III}q_{III}+A_{IV}q_{IV}\right)+\mathcal{O}(g^4) \tag{34.9}$$

where

$$A_I = 1+\hat{g}^2\left(4\log(2\Omega)+2\csc^2\frac{\theta}{2}+i\frac{\Omega}{\hat{g}^2}+2\pi i-4+8\gamma\right) \tag{34.10}$$

$$A_{II} = 0+\Omega(2\log(2\Omega)+i\pi+4\gamma-2) \tag{34.11}$$

$$A_{III} = 0-\hat{g}^2\left(4\cot^2\frac{\theta}{2}\right) \tag{34.12}$$

$$A_{IV} = 0-\hat{g}^2\left(\csc^2\frac{\theta}{2}+\frac{i\Omega}{2\hat{g}^2}\sec^2\frac{\theta}{2}\right)\,. \tag{34.13}$$

In this way we deduce $\mathbf{q}_1$. This allows us to find $\tilde{\mathbf{q}}_1(u)=\mathbf{q}_1(-u)$ via (33.9). On the last step of the procedure we consider the combinations

$$\mathbf{q}_1(u)+\tilde{\mathbf{q}}_1(u)\;,\quad \frac{\mathbf{q}_1(u)-\tilde{\mathbf{q}}_1(u)}{\sqrt{u^2-4g^2}} \tag{34.14}$$

in which the cut on the real axis disappears. As at weak coupling the cuts manifest themselves as poles, thus the poles at the origin which are naturally present in $\mathbf{q}_1$ should cancel in these combinations [52]. This condition fixes the coefficients A_n and B_n and also the value of the energy at the given order in g. So, for instance, at the g^2 order we find the following expansion at the origin

$$\mathbf{q}_1(u) \simeq \left[1 + \pi u + \mathcal{O}(u^2)\right] - \Omega \left[-\frac{\sec^2 \frac{\theta}{2}}{2u} + \mathcal{O}(u^0)\right] + \mathcal{O}(g^4) \,. \tag{34.15}$$

Then regularity of the second combination in (34.14) relates the singular term proportional to Ω with the linear coefficient πu so that we get

$$\Omega = 4\pi g^2 \cos^2 \frac{\theta}{2} + \mathcal{O}(g^4) \,. \tag{34.16}$$

This perfectly matches the well known leading order result.

34.2 Expansion to high order in the coupling

The procedure described above allows to efficiently generate the quark–anti-quark potential expanded to very high orders in g. We have computed the expansion up to g^{14} order.

The result up to g^{10} order is shown below

$$\begin{aligned}
\frac{\Omega}{4\pi} &= \hat{g}^2 + \\
&\hat{g}^4\left[16L-8\right]+\\
&\hat{g}^6\left[128L^2+L\left(64+\frac{64\pi^2T}{3}\right)-112-\frac{8\pi^2}{3}+72T\zeta_3\right]+\\
&\hat{g}^8\left[\frac{2048L^3}{3}+\frac{1024}{3}\pi^2L^2T+2048L^2+LT\left(768\zeta_3+\frac{2176\pi^2}{3}\right)\right.\\
&+\left(-768-\frac{640\pi^2}{3}\right)L+T^2\left(128\pi^2\zeta_3-760\zeta_5\right)\\
&\left.+T\left(384\zeta_3-640\pi^2+\frac{32\pi^4}{9}\right)+\frac{1664\zeta_3}{3}+\frac{1216\pi^2}{9}-1280\right]+\\
&\hat{g}^{10}\left[\frac{8192L^4}{3}+\frac{8192}{3}\pi^2L^3T+\frac{57344L^3}{3}+\frac{2048}{9}\pi^4L^2T^2\right.\\
&+L^2T\left(3072\zeta_3+\frac{71680\pi^2}{3}\right)+\left(20480-\frac{19456\pi^2}{3}\right)L^2\\
&+LT^2\left(\frac{8704\pi^2\zeta_3}{3}-6400\zeta_5+\frac{2560\pi^4}{3}\right)\\
&+LT\left(12800\zeta_3-\frac{46592\pi^2}{3}-\frac{6656\pi^4}{45}\right)+L\left(\frac{26624\zeta_3}{3}-26624+\frac{38912\pi^2}{9}\right)\\
&+T^3\left(\frac{1792\pi^4\zeta_3}{45}-\frac{4928\pi^2\zeta_5}{3}+8624\zeta_7\right)\\
&+T^2\left(3392\pi^2\zeta_3+1248\zeta_3^2-4000\zeta_5-\frac{1024\pi^4}{3}-\frac{16\pi^6}{45}\right)\\
&+T\left(896\zeta_3+\frac{3392\pi^2\zeta_3}{3}+1600\zeta_5-\frac{10112\pi^2}{3}+\frac{1408\pi^4}{45}\right)\\
&\left.+6656\zeta_3+\frac{736\pi^4}{45}+\frac{5824\pi^2}{27}-\frac{37888}{3}\right]\ .
\end{aligned} \tag{34.17}$$

Here we use the following notation

$$\hat{g}\equiv g\cos\frac{\theta}{2}\ \ ,\ \ T\equiv\frac{1}{\cos^2\frac{\theta}{2}}\ \ ,\ \ L\equiv\log\sqrt{8e^{\gamma}\pi\hat{g}^2}\ . \tag{34.18}$$

In Appendix D.3 we also give the expression for the quite lengthy $\hat{g}^{12}$ and $\hat{g}^{14}$ orders. They are particularly interesting since at order $\hat{g}^{12}$ an irreducible multiple zeta value appears for the first time (namely, $\zeta_{6,2}$).

We notice that at the g^{2n+2} order the result is a nth order polynomial in L and T. The terms with the maximal power of L and the subleading in L terms have a very simple structure which can be summarized by the following formula

$$\frac{\Omega}{4\pi}=\sum_{n=0}^{\infty}\hat{g}^{2n+2}\frac{16^nL^n}{n!}\left(1+\frac{3n^2-5n}{4L}+\pi^2T\frac{n^2-n}{12L}+\mathcal{O}(1/L^2)\right)\ . \tag{34.19}$$

Our 7-loop result computed from the QSC is in perfect agreement with direct field theory perturbative calculations. The first three orders were known completely and

were computed in [173, 174, 146, 166, 175, 177, 178]. In addition, our formula (34.19) matches the all-orders prediction of [174] for the coefficients of the leading logarithmic terms $\hat{g}^{2n}\log^{n-1}\hat{g}$. We also reproduced[46] the result of [177] for the subleading logaithmic term at 4th nontrivial order (i.e. $\hat{g}^8\log^2\hat{g}$).

In the next section we will show that the terms which do not contain T can be captured by a much simpler set of equations.

35 Ladders limit of the quark–anti-quark potential

A remarkable special limit, revealing rich structures, is the "double scaling" limit when the twist $t = e^{i\theta/2}$ scales to zero as g. In this limit the effective coupling $\hat{g} = \frac{g}{2t}(1+t^2)$ and $\Omega(\hat{g})$ remain finite. It is expected that in this special case our system of equations can be solved exactly to all orders in $\hat{g}$ or at least simplified considerably. From the gauge theory side, only the ladder diagrams contribute in that limit. Their resummation is achieved by Bethe-Salpeter techniques which results in a Schrödinger equation [173, 166]

$$F''(z) + F(z)\left(\frac{4\hat{g}^2}{z^2+1} - \frac{\Omega^2}{4}\right) = 0\,, \tag{35.1}$$

whose ground state energy gives the quark–anti-quark potential $\Omega(\hat{g})$. Its expansion in small $\hat{g}$ should capture all terms in (34.17) without T to all orders in $\hat{g}$, as $T \to 0$ in this limit. Below we will demonstrate how this Schrödinger equation is encoded into the QSC.

35.1 Double scaling limit of the QSC

The main simplification in this limit occurs because $g \to 0$ and thus each of the cuts $[-2g, 2g]$ collapses into a point. In particular this implies that $\mathbf{f}(u)$ and $\mathbf{g}(u)$ from (33.1), as analytic functions everywhere except the cut, reduce to simple rational functions. Nevertheless, the result is a nontrivial function of the coupling $\hat{g}$ which resums the usual perturbative expansion. In this sense this setup reminds the BFKL limit of the QSC studied in [72, 13]. Special care should be taken with the exponents $e^{\pm\theta u}$ in $\mathbf{P}_a$ which give extra factors of t or $1/t$ each time we shift the argument u by $\pm i/2$. For this reason we have to keep terms up to order t^4 in $\mathbf{P}_a$. Assuming all the coefficients $A_n, B_n \sim 1$ (which

[46] Some of the perturbative field theory calculations discussed here were done for the special case $\theta = 0$ only.

we initially deduced from the weak coupling solution described in Sec. 34, and confirmed by self-consistency) we get

$$\begin{aligned}
\mathbf{f}(u) &= \frac{1}{u}+\frac{4\hat{g}^2t^2\left(A_1u+1\right)}{u^3}+\frac{8\hat{g}^2t^4\left(2\hat{g}^2\left(A_2u^2+2A_1u+2\right)-u^2\left(A_1u+1\right)\right)}{u^5}+\mathcal{O}(t^6)\\
\mathbf{g}(u) &= u-i+t^2\left[\frac{4\hat{g}^2\left(A_1u^2+B_1+u-i\right)}{u^2}+4i\right]+t^4\left[-\frac{8\hat{g}^2\left(A_1u^2+B_1+u-3i\right)}{u^2}\right.\\
&+ \left.\frac{16\hat{g}^4\left(A_1u^2+\left(B_2+2\right)u+2\left(B_1-i\right)\right)}{u^4}-2i\right]+\mathcal{O}(t^6)
\end{aligned}\tag{35.2}$$

We can also exclude B_1 using the expression for Ω (33.20),

$$B_1=2i+t^2\left(4A_1\hat{g}^2+4iA_2\hat{g}^2-\frac{i\Omega^2}{\hat{g}^2}-4i\right)+\mathcal{O}\left(t^4\right)\ .\tag{35.3}$$

Next we plug the expressions (35.2) into (33.6) and expand to the leading order in t. We notice that the dependence on all remaining A_n and B_n disappears and we simply get

$$\begin{aligned}
&\left(\frac{16\hat{g}^4}{u^3}+\frac{16\hat{g}^2}{u}-\frac{4\Omega^2}{u}+6u\right)q(u)\\
+\ &(u+i)q(u+2i)-\left(\frac{4\hat{g}^2(2u+i)}{u(u+i)}+4u+2i\right)q(u+i)\\
+\ &(u-i)q(u-2i)-\left(\frac{4\hat{g}^2(2u-i)}{u(u-i)}+4u-2i\right)q(u-i)=0
\end{aligned}\tag{35.4}$$

where $q(u)=\mathbf{Q}(u)e^{\pm\pi u}/\sqrt{u}$. A great simplification comes from the fact that this equation can be factorized into two second order equations! This allows to replace (35.4) by a pair of second order equations

$$\boxed{-2q(u)\left(2\hat{g}^2-\Omega u+u^2\right)+u^2q(u-i)+u^2q(u+i)=0}\tag{35.5}$$

and the second one related by $\Omega\to-\Omega$. By analyzing the large u asymptotics it is easy to see that the two solutions of (35.5) correspond to $\mathbf{Q}_1$ and $\mathbf{Q}_4$. To fix the conventions and normalizations we define

$$q_1\simeq\sqrt{\pi/2}\,\sqrt[1/4]{8\Omega u}\,e^{-\sqrt{8\Omega u}}\ ,\quad q_4\simeq\frac{1}{16i\pi\Omega^2t^4}\sqrt{\pi/2}\,\sqrt[1/4]{8\Omega u}\,e^{+\sqrt{8\Omega u}}\ ,\quad q_4(0)=0\tag{35.6}$$

where

$$q_1=e^{-\pi u}\mathbf{Q}_1/\sqrt{u}\ ,\quad q_4=e^{+\pi u}\mathbf{Q}_4/\sqrt{u}\,.\tag{35.7}$$

The relative coefficient in (35.6) is chosen in agreement with the canonical normalization (33.25). We also choose q_1 and q_4 to be regular in the upper half plane as usual. We see that (35.5) is invariant under complex conjugation, which implies that $\bar{q}_1$ and $\bar{q}_4$ are some

linear combinations of q_1 and q_4 with i-periodic coefficients

$$\bar{q}_1 = \Omega_1^1 q_1 + e^{-2\pi u}\Omega_1^4 q_4 \tag{35.8}$$

$$\bar{q}_4 = e^{+2\pi u}\Omega_4^1 q_1 + \Omega_4^4 q_4 \,. \tag{35.9}$$

Here Ω_i^j are some i-periodic functions for which notation is introduced in accordance with the general consideration from Appendix D.4. Knowing the analytical properties of q_1 and q_4, which follow from the equation (35.5), we can constrain the possible form of Ω_i^j. From the equation (35.5) we can see that q_1 should have double poles at $u = -2in$ for $n = 1, 2, \dots$ due to the u^2 factors in the equation. Similarly q_4 has simple poles at the same points due to the additional condition $q_4(0) = 0$ which softens the singularity. Furthermore, the complex conjugate functions $\bar{q}_1$ and $\bar{q}_4$ should have the same poles as q_1 and q_4 but in the upper half-plane instead of the lower half-plane. The poles of $\bar{q}_1$ in the upper half plane can only originate from $\Omega' s$ in the r.h.s. of (35.8). This implies that Ω_1^1 and Ω_1^4 can have at most 2nd order poles, similarly, Ω_4^1 and Ω_4^4 can only have simple poles. Next, if we expand (35.8) near $u = 0$ in order to cancel poles in the r.h.s. we must assume that Ω_1^1 has simple pole only as $\bar{q}_4(0) = 0$. Similarly Ω_4^1 should be regular. Finally, since for large u the asymptotics of q_1 does not contain periodic exponents due to the definition (35.6) we can write the following ansatz for $\Omega' s$ in terms of a few constants a_i:

$$\Omega_1^1 = \frac{a_1 + a_2 e^{2\pi u}}{e^{2\pi u} - 1} \;\;,\;\; \Omega_1^4 = \frac{a_3 e^{2\pi u} + a_0}{(e^{2\pi u} - 1)^2} \;\;,\;\; \Omega_4^1 = a_4 e^{-2\pi u} \;\;,\;\; \Omega_4^4 = \frac{a_5 + a_6 e^{2\pi u}}{e^{2\pi u} - 1} \tag{35.10}$$

We also note that $a_0 = 0$ since Ω_1^4 should be even as explained in (D.20). By comparing the large u asymptotics in the first equation of (35.8) at $u \to -\infty$ we can fix a_3 and get Ω_1^4

$$a_3 = 16\pi t^4 \Omega^2 \;\;,\;\; \Omega_1^4 = \frac{4\pi t^4 \Omega^2}{\sinh^2(\pi u)} \,. \tag{35.11}$$

This allows to close the equations. Indeed, by rewriting

$$\Omega_1^4 = \left[\frac{\tilde{\Omega}_1^4 + \Omega_1^4}{2}\right] - \left[\frac{\tilde{\Omega}_1^4 - \Omega_1^4}{2\sqrt{u^2 - 4g^2}}\right]\sqrt{u^2 - 4g^2} \tag{35.12}$$

so that the expressions in the square brackets are regular at the origin to all orders in g we see that the poles present in (35.11) can only originate from the last term. At the same time the last term can be written in terms of q and $\bar{q}$ using (D.20):

$$\left[\frac{\tilde{\Omega}_1^4 - \Omega_1^4}{2\sqrt{u^2 - 4g^2}}\right] = -\frac{u\bar{q}_1(-u)q_1(-u)e^{-2\pi u} - u\bar{q}_1(u)q_1(u)e^{+2\pi u}}{2u} + \mathcal{O}(g^2) = bu + \mathcal{O}(u^3) + \mathcal{O}(g^2) \tag{35.13}$$

which results in the following pattern of the leading singularities in Ω_1^4

$$\Omega_1^4 = \frac{2bg^4}{u^2} + \frac{4bg^6}{u^4} + \cdots + \text{less singular terms} \tag{35.14}$$

thus we can relate b to $\Omega(\hat{g})$ as

$$b = \frac{\Omega^2(\hat{g})}{8\pi\hat{g}^4} \tag{35.15}$$

or

$$\boxed{\frac{\Omega^2(\hat{g})}{8\pi\hat{g}^4} = \lim_{u\to 0} \frac{\bar{q}_1(u)q_1(u)e^{+2\pi u} - \bar{q}_1(0)q_1(0)}{u}\,.} \tag{35.16}$$

This condition together with the finite difference equation (35.5) allows to determine $\Omega(\hat{g})$. Namely, we have to find such value of the parameter Ω in the finite difference equation (35.5) for which its solution q_1 with the asymptotic (35.6), expanded at the origin, satisfies the condition (35.16). This type of problem can be easily solved numerically or perturbatively in $\hat{g}$.

To solve the system perturbatively we repeat basically the same steps as in the previous section, with an additional simplification that we do not have to tune any parameters in $\mathbf{P}_a$ except $\Omega(\hat{g})$, and that we only have to deal with the second order equation instead of the 4th order equation. This procedure, explained in detail in Sec. 34.1, leads to the following result

$$\begin{aligned}
&\frac{\Omega(\theta = i\infty)}{4\pi} = \hat{g}^2 + \\
&\hat{g}^4\left[16L - 8\right] + \\
&\hat{g}^6\left[128L^2 + 64L - 112 - \frac{8\pi^2}{3}\right] + \\
&\hat{g}^8\left[\frac{2048L^3}{3} + 2048L^2 - \left(768 + \frac{640}{3}\pi^2\right)L - 1280 + \frac{1216}{9}\pi^2 + \frac{1664}{3}\zeta_3\right] + \\
&\hat{g}^{10}\left[\frac{8192L^4}{3} + \frac{57344L^3}{3} + \left(20480 - \frac{19456\pi^2}{3}\right)L^2\right. \\
&-\left(26624 - \frac{38912\pi^2}{9} - \frac{26624\zeta_3}{3}\right)L \\
&\quad\left. -\frac{37888}{3} + \frac{5824\pi^2}{27} + 6656\zeta_3 + \frac{736\pi^4}{45}\right] + \\
&\hat{g}^{12}\left[\frac{131072L^5}{15} + \frac{327680L^4}{3} + \left(\frac{1048576}{3} - \frac{1097728\pi^2}{9}\right)L^3\right. \\
&\quad + L^2\left(\frac{212992\zeta_3}{3} + 81920 + 24576\pi^2\right) \\
&\quad + L\left(212992\zeta_3 - \frac{1515520}{3} + \frac{1776640\pi^2}{27} + \frac{39424\pi^4}{15}\right) \\
&\quad\left. + \frac{124928\zeta_5}{5} + \frac{106496\zeta_3}{3} + \pi^2\left(-\frac{93184\zeta_3}{9} - \frac{107008}{27}\right) - \frac{1159424\pi^4}{675} - \frac{295936}{3}\right]
\end{aligned} \tag{35.17}$$

where as before $L \equiv \log \sqrt{8e^{\gamma}\pi\hat{g}^2}$. We notice that all the terms in (34.17) without T are reproduced perfectly by the above expansion.

In the next section we will show how to rewrite this finite difference 'boundary' problem into a spectral problem of a Schrödinger equation by performing a kind of Mellin transformation.

35.2 Equivalence to the Schrödinger equation

The double scaling limit of the quark–anti-quark potential has a long history. In [173, 166] it was shown that in this limit only the ladder diagrams contribute and they can be resummed by a Bethe-Salpeter equation. This problem can be reformulated as a problem of finding the ground-state energy of the Schrödinger equation

$$F''(z) + F(z)\left(\frac{4\hat{g}^2}{z^2+1} - \frac{\Omega^2}{4}\right) = 0\ . \tag{35.18}$$

The Schrödinger wavefunction is linked to the solution of the Bethe-Salpeter equation. In this section we will show that this problem is equivalent to the second order finite difference equation arising from the QSC accompanied by the "quantization condition" at the origin (35.16).

Relating q-function to the wave function. First we relate the q-function q_1 with the solution of (35.18) decaying at $+\infty$. We assume that the solution decaying at $+\infty$ is normalized so that

$$F(z) \simeq e^{-\Omega z/2}\ . \tag{35.19}$$

Let us show that the solution q_1 of (35.5) is given by the following integral Mellin-like transformation

$$\frac{q_1(u)}{u} = 2\int_i^{+\infty} \frac{e^{-\frac{\Omega z}{2}}}{z^2+1}\left(\frac{z+i}{z-i}\right)^{iu} F(z)dz\ \ ,\ \ \mathrm{Im}\ u > 0\ . \tag{35.20}$$

To see that that the equation (35.5) is indeed satisfied we consider an integral of a total derivative:

$$2\int_i^{\infty} \partial_z\left(\left[(z^2+1)F'(z) + \frac{1}{2}F(z)(-4u+\Omega+\Omega z^2)\right]\frac{e^{-\frac{\Omega z}{2}}}{z^2+1}\left(\frac{z+i}{z-i}\right)^{iu}\right)dz \tag{35.21}$$

the boundary terms vanish for Im $u > 1$ and the integral is zero. At the same time evaluating the derivative and excluding the second derivative $F''(u)$ using (35.18) we get

$$\begin{aligned} 0 &= 2\int_i^\infty \left[(-4\hat{g}^2 + 2\Omega u - 2u^2) + u(u+i)\left(\frac{z-i}{z+i}\right) + u(u-i)\left(\frac{z+i}{z-i}\right)\right] \\ &\times \frac{F(z)e^{-\frac{\Omega z}{2}}}{z^2+1}\left(\frac{z+i}{z-i}\right)^{iu} dz \\ &= (-4\hat{g}^2 + 2\Omega u - 2u^2)\frac{q_1(u)}{u} + u(u+i)\frac{q_1(u+i)}{u+i} + u(u-i)\frac{q_1(u-i)}{u-i}\,, \end{aligned} \tag{35.22}$$

which shows that $q_1(u)$ defined by the integral (35.20) satisfies (35.5). At the same time it is easy to see by the saddle-point analysis that $F(z) \simeq e^{-\Omega z/2}$ implies the following large u asymptotics for q_1:

$$q_1(u) \simeq \sqrt{\pi/2}\,\sqrt[1/4]{8\Omega u}\, e^{-\sqrt{8\Omega u}}\,. \tag{35.23}$$

Note that this map from $F(z)$ to $q_1(u)$ is valid for any (positive) value of Ω. Clearly, we have to additionally impose the decay of $F(z)$ at $z \to -\infty$ to constrain Ω. At the same time from the QSC point of view we should impose on q_1 the condition (35.16) at the origin. Below we show that these two conditions are equivalent.

Equivalence of the two quantization conditions. We should relate the behavior of $q_1(u)$ near the origin with the normalizability of $F(z)$ as a solution of the Schrödinger equation. It is clear that the singularity in $q(u)/u$ around $u = 0$ is due to the divergence in the integral (35.20) near $z = i$. Therefore it is controlled by the behavior of $F(z)$ at $z = i$. So our problem seems to be rather nontrivial as we have to relate the values of F at large z with its behavior near $z = i$. In general that would be impossible to do without an explicit solution. However, we noticed an interesting duality of the equation which allows to do this.

The key observation is that for the normalizable $F(z)$ its Fourier image satisfies essentially the same differential equation. More precisely, defining $G(k)$ as

$$\frac{G(k)}{k^2+1} = \frac{\Omega^{3/2}}{8\hat{g}\sqrt{\pi}}\int_{-\infty}^{\infty} dz F(z) e^{ik\frac{\Omega}{2}z} \tag{35.24}$$

it is easy to see that $G(k)$ satisfies literally the same Schrödinger equation (35.18). Furthermore, $G(k)$ also decays exponentially at both infinitites as Fourier transform of a smooth function and is also smooth since F itself decays exponentially at both infinities. This means that F and G should in fact coincide up to a constant factor. To make the

symmetry more manifest we can write the relation (35.24) between F and G as

$$F(z)=\frac{2\hat{g}}{\sqrt{\pi\Omega}}\int\limits_{-\infty}^{\infty}dk\frac{G(k)}{k^2+1}e^{ik\frac{\Omega}{2}z}\ ,\quad G(k)=\frac{2\hat{g}}{\sqrt{\pi\Omega}}\int\limits_{-\infty}^{\infty}dz\frac{F(z)}{z^2+1}e^{ik\frac{\Omega}{2}z}\ . \tag{35.25}$$

We see that in the normalization (35.24)[47] we must have $G(z)=F(z)$, so that we get

$$F(k)=\frac{2\hat{g}}{\sqrt{\pi\Omega}}\int\limits_{-\infty}^{\infty}dz\frac{F(z)}{z^2+1}e^{ik\frac{\Omega}{2}z}\ . \tag{35.26}$$

This property of the solution $F(z)$ allows to bootstrap the behavior at infinity and near the branch point $z=i$. Let's assume that $F(z)$ has the following expansion near $z=i$:

$$F(z)=-\frac{iC}{2\hat{g}^2}+C(z-i)\log(iz+1)+\dots \tag{35.27}$$

which is obtained by solving the equation (35.18) in the vicinity of $z=i$. As $z=i$ is the closest to the real axis singularity of $F(z)$ it controls the large z behavior of $F(z)$

$$F(k)\simeq\frac{2\hat{g}}{\sqrt{\pi\Omega}}\int\limits_{-\infty}^{\infty}dw\frac{-\frac{iC}{2\hat{g}^2}}{w^2+1}e^{ik\frac{\Omega}{2}w}=\frac{-iC}{\hat{g}}\sqrt{\frac{\pi}{\Omega}}e^{-\frac{k\Omega}{2}} \tag{35.28}$$

next using the normalization (35.19) we find

$$C=i\frac{\hat{g}\sqrt{\Omega}}{\sqrt{\pi}}\ , \tag{35.29}$$

which fixes the expansion (35.27) near $z=i$. This allows to find the residue of $q_1(u)/u$ at the origin by plugging (35.27) into (35.20):

$$\frac{q_1(u)}{u}\simeq\frac{iCe^{-\frac{i\Omega}{2}}}{2\hat{g}^2u}=-\frac{1}{u}\frac{e^{-\frac{i\Omega}{2}}\sqrt{\Omega}}{2\hat{g}\sqrt{\pi}}\ . \tag{35.30}$$

In Appendix D.5 we describe how to use a similar technique to establish the subleading coefficient in u which then gives:

$$e^{2\pi u}q_1(u)\bar{q}_1(u)=-\frac{C^2}{4\hat{g}^4}-\frac{C^2\Omega}{8\hat{g}^6}u+\mathcal{O}(u^2)=\frac{\Omega}{4\pi\hat{g}^2}+\frac{u\Omega^2}{8\pi\hat{g}^4}+\mathcal{O}(u^2) \tag{35.31}$$

showing that the condition (35.16), coming from the depth of QSC, does hold! This finishes the proof of equivalence between the QSC and the Schrödinger equation in the ladders limit.

[47] There is a possibility that $G(z)=-F(z)$, however, it is easy to see that since $F(z)>0$ for real z so must be G

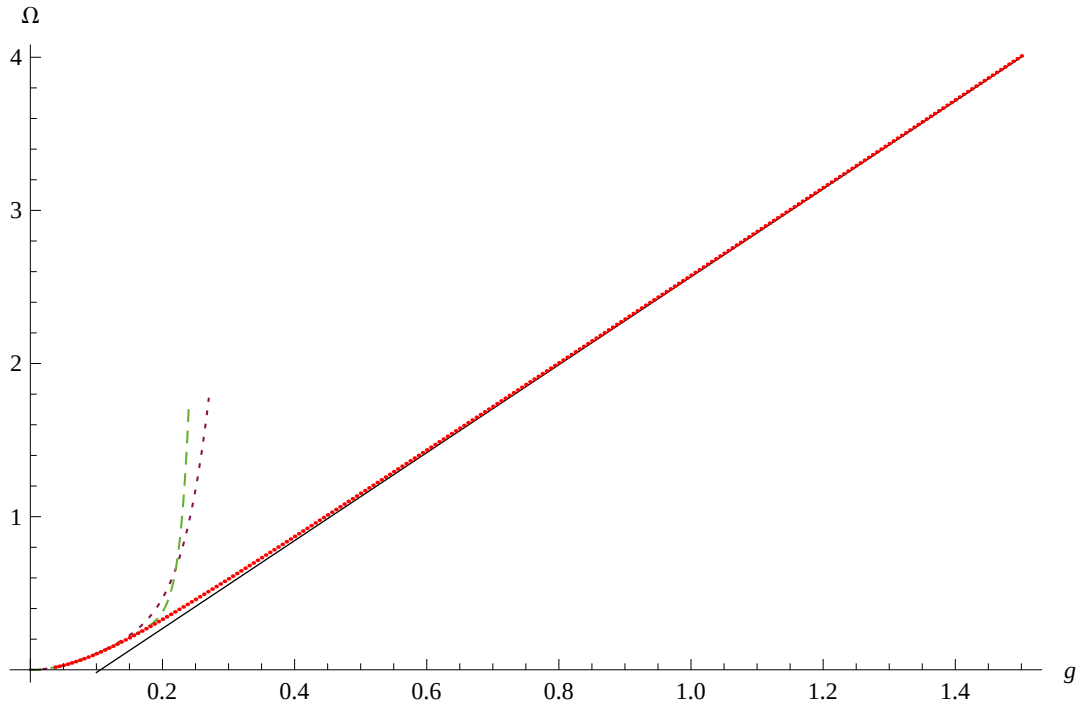

Figure 16: **Numerical results for the quark–anti-quark potential $\Omega(g)$ at $\theta = 0$.** Our numerical data points are shown in red, while the solid black line shows the strong coupling analytic prediction (36.1). The purple curve is the 3-loop weak coupling expansion, and the dashed green curve is our 7-loop perturbative result.

36 Numerical solution in a wide range of the coupling

The QSC can be very efficiently solved numerically with essentially arbitrary precision at finite values of the coupling and all other parameters. The general method, which is also applicable here, was developed in [14]. We have used it to generate numerical values for the quark–anti-quark potential in a wide range of the 't Hooft coupling with ~ 20 digits precision. Our method works well for arbitrary real θ, but we decided to focus on the case $\theta = 0$. Our numerical data is listed in Appendix D.6. A plot of our results is shown on Fig. 36.

Let us make a comparison with the known analytical predictions. At strong coupling the classical [179, 180] and 1-loop [181, 182] string theory results read

$$\Omega \simeq \frac{\pi(4\pi g + a_1)}{4K\left(\frac{1}{2}\right)^2} = 2.8710800442g - 0.3049193809\ . \tag{36.1}$$

At the same time a fit of our numerical data gives

$$\Omega = 2.8710800436g - 0.3049193819 + \frac{0.0100740}{g} + \frac{0.000381}{g^2} + \dots \tag{36.2}$$

which quite convincingly reproduces the first two known orders.

At weak coupling one can see on the plot that this expansion matches well our numerics. In addition, our analytic solution of the QSC at weak coupling described in Sec. 34 provides the expansion of Ω to first 7 loop orders presented in (34.17) and in Appendix D.3. Fixing a particular small value of the coupling $g = 0.0625$ we compared our numerical prediction $\Omega = 0.04472043670132964806$ at this point with the analytic weak coupling expansion. In Table 5 one clearly sees that including more and more orders in the expansion improves noticeably the agreement with our numerical result. This is a nice check of our weak coupling analytic prediction.

	$\Omega^{\text{perturbative}}$	$\Omega^{\text{numerical}}$	|difference|
1-loop	0.04908738521	0.04472043670	0.00436694851
2-loop	0.04487846353	0.04472043670	0.00015802682
3-loop	0.04473327069	0.04472043670	0.00001283399
4-loop	0.04471883557	0.04472043670	0.00000160113
5-loop	0.04472038490	0.04472043670	0.00000005179
6-loop	0.04472043227	0.04472043670	0.00000000442
7-loop	0.04472043747	0.04472043670	0.00000000076

Table 5: Comparison between the 7-loop weak coupling prediction and the numerical data for the quark–anti-quark potential at $g = 0.0625$.

37 Conclusion

In this part we demonstrated that the Quantum Spectral Curve approach allows to deeply explore the quark–anti-quark potential in a variety of settings. In particular, we generated highly precise numerical data at finite coupling interpolating extremely well between gauge theory and string theory predictions. Thus finally we are able to access on a fully nonperturbative level this observable which historically has been a milestone in the investigations of AdS/CFT.

The setup we study corresponds to a singular limit $\phi \to \pi$ of the cusp anomalous dimension which leads to a drastic change of Q-functions' asymptotics in the QSC. The asymptotics we found are of a novel type even for integrable systems with twisted boundary conditions. As this is yet another set of nontrivial asymptotics in the QSC, it is clearly

an important question how to classify all possible types of asymptotics. They should correspond to some kind of deformations and boundary problems for local or nonlocal observables likely including the setups studied in [65, 184]. Consistency of asymptotics with the functional QSC equations appears to be a highly nontrivial constraint giving hope for an exhaustive description.

Using the efficient iterative procedure of [13] we computed the weak coupling expansion of the potential to the 7th loop order. The perturbative expansion is known to be rather nontrivial and to be captured by an effective theory arising at low energy scales. Remarkably, we also observed the appearance of several distinct scales in the QSC which may be thought of as a counterpart to this effective field theory description. In the future it will be also interesting to apply the QSC to study the energies of hydrogen-like bound states in $\mathcal{N} = 4$ SYM [172] which are also related to a $\phi \to \pi$ limit. Moreover, our weak coupling results may be useful to establish connections with QCD, similarly to e.g. [185].

We also studied the double scaling limit when the twist θ in the scalar sector goes to $i\infty$. We showed how the Schrödinger equation arising on the field theory side from resummation of ladder diagrams is encoded in the QSC, with its wavefunction rather directly linked to the Q-functions. We believe that this approach should also apply to a similar double scaling limit of γ-deformed $\mathcal{N} = 4$ SYM recently proposed in [183], where the QSC has many common features with the one for the cusped Wilson lines setup [16, 12, 73][48]. This limit in the γ-deformed model was advocated in [183] to give a novel integrable 4d theory.

We also observed a peculiar duality of the Schrödinger equation with respect to Fourier transform, whose meaning in the QSC itself beyond this special limit calls for further clarification and might have something to do with dual conformal symmetry. Viewing the relation between the QSC and the Schrödinger equation as a kind of ODE/IM correspondence [189], it would be interesting to see what kind of generalization will take place at finite twist. Another important direction is to derive the Schrödinger equation of [166] in the ladders limit with generic ϕ.

Finally, as the ladders limit allows for a simpler access to the wrapping corrections, it could also serve as a useful ground to attempt a finite-size resummation of perturbation theory for 3-point correlators [190, 191, 192, 193, 58], using Q-functions as building blocks.

[48] The Y-system and TBA for the spectrum in the γ-deformed case were proposed earlier in [20, 186, 187, 188]

Part VIII

Conclusions and appendices

38 Summary and outlook

In this thesis we have described the Quantum Spectral Curve of AdS/CFT in application to a wide variety of problems. Numerical and analytical methods have been developed which make it possible to access the spectrum even in the extreme regimes which are far beyond the reach of previous techniques. Let us describe some of the possible directions for future work.

- While we have focused on exploration of the spectrum, we hope the results presented here could also be useful in application to correlation functions. The QSC construction provides exact Q-functions which serve as building blocks for wavefunctions in separated variables and with appropriate Sklyanin's measure should allow to reconstruct the correlator. The QSC and Sklyanin's separation of variables methods [54, 194] are naturally linked and their interplay would be very interesting to study. The many known solutions of the QSC, including those dicsussed in this thesis and in particular the all-loop solutions, should be very helpful in this problem. Also, as the ladders limit for the quark-antiquark potential allows for a simpler access to the wrapping corrections, it could also serve as a useful ground to attempt a finite-size resummation of perturbation theory for 3-point correlators [190, 191, 192, 193, 58], using Q-functions as building blocks.

- It is an important open problem to build a strong coupling analytic expansion. While we have seen that the QSC truly shines at weak coupling, at strong coupling we are still restricted to numerical data or re-expansions of near-BPS exact results.

- Further exploration of the BFKL and similar regimes with the hope of finding extra structures looks surely interesting.

- The double scaling limit in γ-deformed SYM, expected to lead to new 4d integrable QFTs [183], should be possible to study using the QSC, especially since a similar limit has been already understood for the quark-antiquark potential as described above in part VII [11].

- The deep origins of integrability on the gauge theory side remain mysterious, as all-loop integrability has been developed essentially by following the bootstrap program in the 2d string sigma model. Perhaps the QSC could shed light on this aspect by revealing hidden structures in perturbation theory. It would also be very interesting to explore links between the spectral problem and powerful methods developed in the context of amplitudes [195, 196, 197].

- It would be interesting to connect the AdS/CFT integrability with integrable systems linked with $\mathcal{N} = 2$ theories and AGT dualities (see e.g. [198]). In particular it might be possible to find a dual classical description of the AdS/CFT integrable system, in the spirit of classical/quantum dualities [199, 200, 201, 202].

- It should be possible to extend the QSC to various more involved deformations of $\mathcal{N} = 4$ SYM where a change in analytic structure would be expected [203, 204, 60]. We have also seen that e.g. the boundary dressing phase for the cusp setup corresponds to allowing exponential asymptotics in some parts of the QSC. It may be possible to classify all such asymptotics which would describe different boundary problems such as [65].

- Finally, it would be highly interesting to formulate the QSC for lower-dimensional AdS/CFT's (see e.g. [205, 206, 207, 208, 209]) and explore their rich properties and surprising features such as the appearance of massless modes.

A Appendices to part II

A.1 Summary of notation and definitions

Integral kernels

In order to solve for $\mathbf{P}_a^{(1)}$ in section 8.3 we introduce integral operators H and K with kernels

$$H(u,v) = -\frac{1}{4\pi i}\frac{\sqrt{u-2g}\sqrt{u+2g}}{\sqrt{v-2g}\sqrt{v+2g}}\frac{1}{u-v}dv, \tag{A.1}$$

$$K(u,v) = +\frac{1}{4\pi i}\frac{1}{u-v}dv, \tag{A.2}$$

which satisfy

$$\tilde{f}+f=h \ , \ f=H\cdot h \quad \text{and} \quad \tilde{f}-f=h \ , \ f=K\cdot h. \tag{A.3}$$

Since the purpose of H and K is to solve equations of the type A.3, H usually acts on functions h such that $\tilde{h} = h$, whereas K acts on h such that $\tilde{h} = -h$. On the corresponding classes of functions, provided also that the constant term in their Laurent expansion (denoted as $[h]_0$) is zero, H and K can be represented by kernels which are equal up to a sign

$$H(u,v) = -\frac{1}{2\pi i}\frac{1}{x_u - x_v}dx_v\Big|_{\tilde{h}=h}, \tag{A.4}$$

$$K(u,v) = \frac{1}{2\pi i}\frac{1}{x_u - x_v}dx_v\Big|_{\tilde{h}=-h}. \tag{A.5}$$

In order to be able to deal with series in half-integer powers of x in section 8.5 we introduce modified kernels:

$$H^* \cdot f \equiv \frac{x+1}{\sqrt{x}} H \cdot \frac{\sqrt{x}}{x+1} f, \tag{A.6}$$

$$K^* \cdot f \equiv \frac{x+1}{\sqrt{x}} K \cdot \frac{\sqrt{x}}{x+1} f. \tag{A.7}$$

Finally, to write the solution to equations of the type (8.5), we introduce the operator Γ' and its more symmetric version Γ

$$\left(\Gamma' \cdot h\right)(u) \equiv \oint_{-2g}^{2g} \frac{dv}{4\pi i} \partial_u \log \frac{\Gamma[i(u-v)+1]}{\Gamma[-i(u-v)]} h(v), \tag{A.8}$$

$$\left(\Gamma \cdot h\right)(u) \equiv \oint_{-2g}^{2g} \frac{dv}{4\pi i} \partial_u \log \frac{\Gamma[i(u-v)+1]}{\Gamma[-i(u-v)+1]} h(v). \tag{A.9}$$

A.2 NLO solution of $P\mu$ system at $J = 2$: details

In this appendix we will provide more details on the solution of the $\mathbf{P}\mu$-system and calculation of curvature function for $J = 2$ which was presented in the main text in section 8.1.

A.2.1 NLO corrections to μ_{ab}

Here we present some details of calculation of NLO corrections to μ_{ab} for $J = 2$ omitted in the main text. As described in section 8.2, $\mu_{ab}^{(1)}$ are found as solutions of (8.5) with appropriate asymptotics. The general solution of this equation consists of a general solution of the corresponding homogeneous equation (which can be reduced to one-parametric form (8.17)) and a particular solution of the inhomogeneous one. The latter can be taken to be

$$\mu_{ab}^{disc} = \Sigma \cdot \left(\mathbf{P}_a^{(1)} \tilde{\mathbf{P}}_b^{(1)} - \mathbf{P}_b^{(1)} \tilde{\mathbf{P}}_a^{(1)}\right). \tag{A.10}$$

One can get rid of the operation Σ, expressing μ_{ab}^{disc} in terms of Γ' and p'_a. This procedure is based on two facts: the definition (8.11) of p'_a and the statement that on functions decaying at infinity Σ coincides with Γ' defined by (8.9). After a straightforward but long calculation we find

$$\mu_{31}^{disc} = \epsilon^2 \Sigma \left(\frac{1}{x^2} - x^2 \right) = -\epsilon^2 \quad \left(\Gamma \cdot x^2 + p_2 \right), \tag{A.11}$$

$$\mu_{41}^{disc} = \epsilon^2 \left[-2I_1 p_1 - 4I_1 \Gamma \cdot x + \sinh(2\pi u) \left(\Gamma \cdot x^2 + p_0 \right) + \Gamma \cdot \sinh_- \left(x - \frac{1}{x} \right)^2 \right], \tag{A.12}$$

$$\mu_{43}^{disc} = -2\epsilon^2 \left[-2I_1 p_1 - 4I_1 \Gamma \cdot x + \sinh(2\pi u)(p_2 - p_0) + \Gamma \cdot \sinh_- \left(x - \frac{1}{x} \right)^2 \right], \tag{A.13}$$

$$\mu_{21}^{disc} = \epsilon^2 \left[2I_1 \Gamma \cdot x - \sinh(2\pi u) \; \Gamma \cdot x^2 - \Gamma \cdot \sinh_- \left(x^2 + \frac{1}{x^2} \right) \right], \tag{A.14}$$

$$\mu_{24}^{disc} = \epsilon^2 \left[2I_1 \Gamma \cdot \sinh_- \left(x + \frac{1}{x} \right) + I_1^2 p_0 + \right. \tag{A.15}$$

$$\left. + \sinh(2\pi u) \Gamma \cdot \sinh_- \left(x^2 - \frac{1}{x^2} \right) - \Gamma \cdot \sinh_-^2 \left(x^2 - \frac{1}{x^2} \right) \right]. \tag{A.16}$$

Here we write Γ and p_a instead of Γ' and p'_a taking into account the discussion between equations (8.22) - (8.27).

A.3 Result for $J = 4$

The final result for the curvature function at $J = 4$ reads

$$\gamma^{(2)}_{J=4} = \oint \frac{du_x}{2\pi i} \oint \frac{du_y}{2\pi i} \frac{1}{ig^2(I_3 - I_5)^3} \Bigg[\tag{A.17}$$
$$\frac{2\left(\mathrm{sh}^x_-\right)^2 y^4 \left(I_3\left(x^{10}+1\right) - I_5 x^2\left(x^6+1\right)\right)}{x^4\left(x^2-1\right)} - \frac{2\left(\mathrm{sh}^y_-\right)^2 x^4\left(y^8-1\right)\left(I_3 x^2 - I_5\right)}{\left(x^2-1\right)y^4} +$$
$$+ \frac{4\mathrm{sh}^x_- \mathrm{sh}^y_- \left(x^4y^4-1\right)\left(I_3 + I_3 x^6 y^4 - I_5 x^2\left(x^2y^4+1\right)\right)}{x^4\left(x^2-1\right)y^4}$$
$$+ \mathrm{sh}^y_- \left(\left(y^4+y^{-4}\right)x^{-1}\left(\left(I_1I_5 - I_3^2\right)\left(3x^4+1\right) - 2I_1I_3x^6\right) +\right.$$
$$+ \frac{2I_3x^2\left(I_5\left(x^2+1\right)x^2 + I_1\left(1-x^2\right)\right) - I_1I_5\left(x^2-1\right)^2 + I_3^2\left(-2x^6+x^4+1\right)}{x(x^2-1)} +$$
$$+ 2\left(y^3+y^{-3}\right)\frac{I_1I_3x^6 - I_1I_5x^4 - I_3^2\left(x^2-1\right)}{x^2-1} -$$
$$\left. -2I_3\left(y+y^{-1}\right)\frac{I_1\left(x^2-1\right) - I_3\left(x^6-x^2+1\right) + I_5\left(x^4-x^2+1\right)}{x^2-1}\right) +$$
$$+ \frac{4x^6y^2I_3\left(I_3^2 - I_1^2\right)}{x^2-1} + \frac{4xyI_1\left(I_3y^2+I_1\right)\left(I_3+I_5\right)}{x^2-1} +$$
$$\frac{2y^4\left(I_1+I_3\right)\left(I_1I_5 - I_3^2\right)}{x^2-1} - \frac{2y\left(y^2+1\right)\left(I_1+I_3\right)\left(I_1I_5 - I_3^2\right)}{x\left(x^2-1\right)} -$$
$$- \frac{2x^3y\left(I_1+I_3\right)\left(I_1\left(2I_3 + \left(3\,y^2+1\right)I_5\right) - I_3\left(2I_5y^2 + \left(y^2+3\right)I_3\right)\right)}{x^2-1}$$
$$+ \frac{2x^2y^4\left(-I_3^3 - I_1\left(3I_3+I_5\right)I_3 + I_1^2I_5\right)}{x^2-1}$$
$$+ \frac{2x^4y\left(I_1^2\left(2yI_5 - 2y^3I_3\right) - 2y\left(y^2+1\right)I_3^2I_5\right)}{x^2-1} +$$
$$\left. + \frac{4x^5yI_3\left(2I_1^2y^2 + I_3\left(I_5 - I_3\right)y^2 + I_1\left(I_3+I_5\right)\right)}{x^2-1}\right] \frac{1}{4\pi i}\partial_u \log\frac{\Gamma(iu_x - iu_y + 1)}{\Gamma(1 - iu_x + iu_y)}$$

where, similarly to $J = 2, 3$, the integrals go around the branch between $-2g$ and $2g$.

A.4 Weak coupling expansion – details

The expansion of our result for the slope-to slope function $\gamma^{(2)}_{J=2}$ to 10 loops reads:

$$
\begin{aligned}
\gamma^{(2)}_{J=2} &= -8g^2\zeta_3 + g^4\left(140\zeta_5 - \frac{32\pi^2\zeta_3}{3}\right) + g^6\left(200\pi^2\zeta_5 - 2016\zeta_7\right) \\
&+ g^8\left(-\frac{16\pi^6\zeta_3}{45} - \frac{88\pi^4\zeta_5}{9} - \frac{9296\pi^2\zeta_7}{3} + 27720\zeta_9\right) \\
&+ g^{10}\left(\frac{208\pi^8\zeta_3}{405} + \frac{160\pi^6\zeta_5}{27} + 144\pi^4\zeta_7 + 45440\pi^2\zeta_9 - 377520\zeta_{11}\right) \\
&+ g^{12}\Big(-\frac{7904\pi^{10}\zeta_3}{14175} - \frac{17296\pi^8\zeta_5}{4725} - \frac{128\pi^6\zeta_7}{15} - \frac{6312\pi^4\zeta_9}{5} \\
&\qquad -653400\pi^2\zeta_{11} + 5153148\zeta_{13}\Big) \\
&+ g^{14}\Big(\frac{1504\pi^{12}\zeta_3}{2835} + \frac{106576\pi^{10}\zeta_5}{42525} - \frac{18992\pi^8\zeta_7}{405} - \frac{16976\pi^6\zeta_9}{15} \\
&\qquad + \frac{25696\pi^4\zeta_{11}}{9} + \frac{28003976\pi^2\zeta_{13}}{3} - 70790720\zeta_{15}\Big) \\
&+ g^{16}\Big(-\frac{178112\pi^{14}\zeta_3}{382725} - \frac{239488\pi^{12}\zeta_5}{127575} + \frac{2604416\pi^{10}\zeta_7}{42525} + \frac{8871152\pi^8\zeta_9}{4725} \\
&\qquad + \frac{30157072\pi^6\zeta_{11}}{945} + \frac{8224216\pi^4\zeta_{13}}{45} - 133253120\pi^2\zeta_{15} \\
&\qquad +979945824\zeta_{17}\Big) \\
&+ g^{18}\Big(\frac{147712\pi^{16}\zeta_3}{382725} + \frac{940672\pi^{14}\zeta_5}{637875} - \frac{490528\pi^{12}\zeta_7}{8505} - \frac{358016\pi^{10}\zeta_9}{189} \\
&\qquad - \frac{37441312\pi^8\zeta_{11}}{945} - \frac{9616256\pi^6\zeta_{13}}{15} - \frac{16988608\pi^4\zeta_{15}}{3} \\
&\qquad +1905790848\pi^2\zeta_{17} - 13671272160\zeta_{19}\Big) \\
&+ g^{20}\Big(-\frac{135748672\pi^{18}\zeta_3}{442047375} - \frac{103683872\pi^{16}\zeta_5}{88409475} + \frac{1408423616\pi^{14}\zeta_7}{29469825} \\
&\qquad + \frac{2288692288\pi^{12}\zeta_9}{1403325} + \frac{34713664\pi^{10}\zeta_{11}}{945} + \frac{73329568\pi^8\zeta_{13}}{105} \\
&\qquad + \frac{305679296\pi^6\zeta_{15}}{27} + 121666688\pi^4\zeta_{17} - 27342544320\pi^2\zeta_{19} \\
&\qquad +192157325360\zeta_{21}\Big)
\end{aligned}
\tag{A.18}
$$

B Appendices to part V

B.1 Notation and conventions

In this appendix we summarized the notation which is used throughout part V. The basic definitions are in the first subsection, and the second one contains a glossary of integration kernels.

Basic notation

$$f^{[\pm a]} \equiv f(u \pm ia), \quad f^{\pm} \equiv f(u \pm i/2), \tag{B.1}$$

$$f^{[\pm 0]} = f(u \pm i0), \quad f^{\pm\pm} = f(u \pm i/2 \pm i0). \tag{B.2}$$

$$I_{m,n} \equiv \delta_{m+1,n} + \delta_{m-1,n}. \tag{B.3}$$

We also found it convenient to denote

$$T = e^{i\theta}, \; c_a = e^{2iG(ia/2)}, \; y_a = x(ia/2), \tag{B.4}$$

where G is the resolvent from (23.12).

Kernels in the TBA

We denote by $*$ the convolution over the full real axis from $-\infty$ to ∞, and by $\hat{*}$ the convolution over the range $-2g < u < 2g$.

Our definitions of the kernels coincide with the ones used in [63] and [164], and we summarize them below. Let us note that in some cases the "mirror" branch of x is used, for which $|x(u)| > 1$ for u in the upper half-plane, and $|x(u)| > 1$ for u in the lower half-plane (see [63]).

$$\mathbf{s}(u,v) = \frac{1}{2\cosh(\pi(u-v))}, \tag{B.5}$$

$$K_a(u,v) = \frac{2a}{\pi(a^2 + 4(u-v)^2)}, \tag{B.6}$$

$$\hat{K}_a(u) = \hat{K}_{y,a}(u,0) = \sqrt{\frac{4g^2-u^2}{4g^2+a^2/4}} K_a(u), \; \tilde{K}_a(u) = \sqrt{\frac{4g^2+a^2/4}{4g^2-u^2}} K_a(u), \tag{B.7}$$

$$K_{n,m}(u,v) = \sum_{j=-\frac{n-1}{2}}^{\frac{n-1}{2}} \sum_{k=-\frac{m-1}{2}}^{\frac{m-1}{2}} K_{2j+2k+2}(u,v), \tag{B.8}$$

$$K(u,v) = \frac{1}{2\pi i}\sqrt{\frac{4g^2-u^2}{4g^2-v^2}}\frac{1}{v-u}, \tag{B.9}$$

$$\log F_a(a,g) = \tilde{K}_a \hat{*} \log \frac{\sinh(2\pi u)}{2\pi u}\bigg|_{u=0}. \tag{B.10}$$

$$r(u,v) = \frac{x(u)-x(v)}{\sqrt{x(v)}},\ b(u,v) = \frac{1/x(u)-x(v)}{\sqrt{x(v)}}, \tag{B.11}$$

$$\mathcal{R}^{(ab)}_{nm} = \sum_{j=-\frac{n-1}{2}}^{\frac{n-1}{2}} \sum_{k=-\frac{m-1}{2}}^{\frac{m-1}{2}} \frac{1}{2\pi i}\frac{d}{dv}\log\frac{r(u+ia/2+ij, v-ib/2+ik)}{r(u-ia/2+ij, v+ib/2+ik)}, \tag{B.12}$$

$$\mathcal{B}^{(ab)}_{nm} = \sum_{j=-\frac{n-1}{2}}^{\frac{n-1}{2}} \sum_{k=-\frac{m-1}{2}}^{\frac{m-1}{2}} \frac{1}{2\pi i}\frac{d}{dv}\log\frac{b(u+ia/2+ij, v-ib/2+ik)}{b(u-ia/2+ij, v+ib/2+ik)}, \tag{B.13}$$

Given the definitions above one can prove the following identities (see [63]):

$$\mathcal{R}^{(10)}_{a1}(u,v) + \mathcal{B}^{(10)}_{a1}(u,v) = K_a(u,v), \tag{B.14}$$

$$\mathcal{R}^{(10)}_{a1}(u,v) - \mathcal{B}^{(10)}_{a1}(u,v) = K(u+ia/2,v) - K(u-ia/2,v), \tag{B.15}$$

$$\mathcal{R}^{(01)}_{1a}(u,v) + \mathcal{B}^{(01)}_{1a}(u,v) = K_a(u,v), \tag{B.16}$$

$$\mathcal{R}^{(01)}_{1a}(u,v) - \mathcal{B}^{(01)}_{1a}(u,v) = \hat{K}_{y,a}(u,v) = K(u,v-ia/2) - K(u,v+ia/2), \tag{B.17}$$

$$\mathcal{R}^{(01)}_{2n} = \frac{1}{2}\left(\hat{K}^+_n - \hat{K}^-_n + K^+_n + K^-_n\right) \tag{B.18}$$

$$\begin{aligned} \tilde{K}_{ab} &= \mathcal{R}^{(10)}_{ab} + \mathcal{B}^{(10)}_{ab-2} = \\ &= \frac{1}{2}\left(\tilde{K}^{[b-1]}_a - \tilde{K}^{[-b+1]}_a + K^{[b-1]}_a + K^{[-b+1]}_a\right) + \sum_{r=1}^{a} K_{b-a-3+2r} \end{aligned} \tag{B.19}$$

$$\begin{aligned} \hat{K}_{ba} &= \mathcal{R}^{(01)}_{ba} + \mathcal{B}^{(01)}_{b-2,a} = \\ &= \frac{1}{2}\left(\hat{K}^{[b-1]}_a - \hat{K}^{[-b+1]}_a + K^{[b-1]}_a + K^{[-b+1]}_a\right) + \sum_{r=1}^{a} K_{b-a-3+2r} \end{aligned} \tag{B.20}$$

C Appendices to part VI

C.1 The anomalous dimension from asymptotics

Here we present the explicit expression we got for the conformal dimension Δ in terms of the coefficients a_i, b_i in the large u expansion of the $\mathbf{P}$-functions (see Eq. (27.2)), for any L. It reads

$$\begin{aligned}
\Delta^2 &= -a_1\left[\frac{a_2(\cos\theta-\cos\phi)^3}{(L+1)\sin\theta\sin^2\phi}-\frac{b_2(\cos\theta-\cos\phi)^3}{(L+1)\sin\theta\sin^2\phi}+F(\theta,\phi,L)\right]\\
&- \frac{a_1^2(\cos\theta\cos\phi-1)(\cos\theta-\cos\phi)^2}{\sin^2\theta\sin^2\phi}+\frac{a_3(\cos\theta-\cos\phi)^3}{(L+1)\sin\theta\sin^2\phi}\\
&- \frac{a_2(\cos\theta-\cos\phi)^2(-2\cos\theta\cos\phi+(L+1)\cos 2\theta-L+1)}{2(L+1)\sin^2\theta\sin^2\phi}\\
&- \frac{b_3(\cos\theta-\cos\phi)^3}{(L+1)\sin\theta\sin^2\phi}+\frac{b_2L(\cos\theta\cos\phi-1)(\cos\theta-\cos\phi)^2}{(L+1)\sin^2\theta\sin^2\phi}\\
&+ \frac{(2L+1)L}{24\sin^2\theta\sin^2\phi}\Big[\cos\theta\,(\cos 3\phi-10\cos\phi)+\cos 3\theta\cos\phi+8\Big]-\frac{L(1-L)}{3}
\end{aligned} \tag{C.1}$$

where

$$\begin{aligned}
F(\theta,\phi,L) &= \frac{(\cos\theta-\cos\phi)}{4\sin^3\theta\sin^2\phi}\Big[-2(5L+4)\cos\theta\cos\phi+(L+2)\cos 2\phi+7L+4\\
&+ \cos 2\theta\,(2L\cos\theta\cos\phi+L\cos 2\phi-L+2)\Big]
\end{aligned} \tag{C.2}$$

C.2 Asymptotics of Q-functions

Similarly to the asymptotics of $\mathbf{P}_a$ given in (27.2) in the main text, we found that the asymptotics of $\mathbf{Q}_i$ have the form (with C an arbitrary constant)

$$\begin{aligned}
\mathbf{Q}_1(u) &\simeq C\epsilon'^{1/2}\,u^{1/2+\Delta}\,e^{+\phi u}F(+u)\ ,\quad F(u)=1+c_1/u+c_2/u^2+c_3/u^3+\ldots \qquad \text{(C.3)}\\
\mathbf{Q}_2(u) &\simeq C\epsilon'^{1/2}\,u^{1/2+\Delta}\,e^{-\phi u}F(-u)\\
\mathbf{Q}_3(u) &\simeq \frac{1}{C}\epsilon'^{3/2}\,u^{1/2-\Delta}\,e^{+\phi u}G(+u)\ ,\quad G(u)=1+d_1/u+d_2/u^2+d_3/u^3+\ldots\\
\mathbf{Q}_4(u) &\simeq -\frac{1}{C}\epsilon'^{3/2}\,u^{1/2-\Delta}\,e^{-\phi u}G(-u)
\end{aligned}$$

while $\mathbf{Q}$'s with upper and lower indices are related as in (27.7),

$$\mathbf{Q}^1=-\mathbf{Q}_4,\ \mathbf{Q}^2=+\mathbf{Q}_3,\ \mathbf{Q}^3=-\mathbf{Q}_2,\ \mathbf{Q}^4=+\mathbf{Q}_1 \tag{C.4}$$

The coefficients are constrained by

$$\epsilon'^2 = -\frac{i(\cos\theta-\cos\phi)^2}{2\Delta\sin^2\phi}\ ,\ \ c_1-d_1=-\frac{\Delta(2\cos\theta\cos\phi+\cos 2\phi-3)}{2\sin\phi(\cos\theta-\cos\phi)} \tag{C.5}$$

While Δ enters the powers in the asymptotics of $\mathbf{Q}_i$, the remaining conserved charge L is encoded in the large u expansion coefficients as

$$\begin{aligned} L(L+2) \quad &= c_2\left[\frac{d_1\csc^2\theta\csc\phi(\cos\phi-\cos\theta)^3}{\Delta}\right. \\ &\left.+\frac{(\Delta-1)\csc^2\theta\csc^2\phi(\cos\theta\cos\phi-1)(\cos\phi-\cos\theta)^2}{\Delta}\right] \\ &+\frac{c_3\csc^2\theta\csc\phi(\cos\theta-\cos\phi)^3}{\Delta}+\frac{d_3\csc^2\theta\csc\phi(\cos\phi-\cos\theta)^3}{\Delta} \\ &+d_1\left[\frac{d_2\csc^2\theta\csc\phi(\cos\theta-\cos\phi)^3}{\Delta}+F_1(\theta,\phi,\Delta)\right] \\ &+\frac{d_2\csc^2\theta\csc^2\phi(\cos\phi-\cos\theta)^2\left(\Delta\sin^2\phi+\cos\theta\cos\phi-1\right)}{\Delta} \\ &-d_1^2\csc^2\theta\csc^2\phi(\cos\phi-\cos\theta)^2(\cos\theta\cos\phi-1) \\ &+\frac{1}{24}\left[-(\Delta-1)(2\Delta-1)(\cos\theta-2)\cot^2\left(\frac{\theta}{2}\right)\sec^2\left(\frac{\phi}{2}\right)\right. \\ &-4(\Delta-1)(2\Delta-1)\cot\theta\csc\theta\cos\phi \\ &\left.+(\Delta-1)(2\Delta-1)(\cos\theta+2)\tan^2\left(\frac{\theta}{2}\right)\csc^2\left(\frac{\phi}{2}\right)+8((\Delta-3)\Delta-1)\right] \end{aligned} \tag{C.6}$$

where we denote

$$\csc\theta\equiv 1/\sin\theta,\quad \sec\theta\equiv 1/\cos\theta \tag{C.7}$$

and

$$\begin{aligned} F_1(\theta,\phi,\Delta) \quad &= \frac{1}{4}\csc^2\theta\csc^3\phi(\cos\theta-\cos\phi)\left[2\cos\theta\cos\phi((\Delta-1)\cos 2\phi-5\Delta+1)\right. \\ &\left.+\cos 2\theta((\Delta-1)\cos 2\phi+\Delta+1)-(\Delta-3)\cos 2\phi+7\Delta-3\right] \end{aligned} \tag{C.8}$$

C.3 The leading near-BPS solution at any L

Let us present explicitly the leading order near-BPS solution of the $\mathbf{P}\mu$ system at any L. It was constructed in [16] and below we write it in our conventions. Most importantly, imposing the asymptotics (27.2) and (27.3) we recovered from (27.4) the all-loop results of [16] for the near-BPS cusp anomalous dimension at nonzero L, providing a stringent test of the asymptotics we proposed[49].

The solution has the following form. First, the components of μ_{ab} are

$$\mu_{12}^{(0)}=A\sinh(2\pi u),\ \mu_{13}^{(0)}=(-1)^L,\ \mu_{14}^{(0)}=0,\ \mu_{24}^{(0)}=(-1)^{L+1},\ \mu_{34}^{(0)}=0 \tag{C.9}$$

[49] We checked the matching explicitly for the first several L's

Second, the **P**-functions read

$$\begin{aligned}
\mathbf{P}_1^{(0)} &= K\sqrt{A}\sqrt{u}e^{\theta u}\frac{\tilde{F}(x)}{x^{L+1}} \ , \\
\mathbf{P}_2^{(0)} &= K\sqrt{A}\sqrt{u}e^{-\theta u}\frac{\tilde{F}(-x)}{x^{L+1}} \ , \\
\mathbf{P}_3^{(0)} &= \frac{K}{\sqrt{A}}\sqrt{u}e^{g\theta(x-1/x)}P_L(x) \ , \\
\mathbf{P}_4^{(0)} &= (-1)^L\frac{K}{\sqrt{A}}\sqrt{u}e^{-g\theta(x-1/x)}P_L(-x) \ .
\end{aligned} \tag{C.10}$$

Here A is a constant which can be set to 1 via a rescaling (27.8), (27.9) while the constant $K \sim \sqrt{\theta-\phi}$ can be fixed from asymptotics (27.2), (27.3). The function $F(x)$ is a power series

$$F(x) = 1 + \sum_{n=1}^{\infty} f_n x^n \ , \tag{C.11}$$

which satisfies

$$e^{2g\theta x}x^{L+1}F(x) + (-1)^L e^{-2g\theta/x}x^{L+1}\tilde{F}(-x) = \sinh(2\pi u)e^{2g\theta(x-1/x)}P_L(x) \tag{C.12}$$

and is fixed as

$$F(x) = e^{-2g\theta x}x^{-L-1}\left[\sinh(2\pi u)e^{2g\theta(x-1/x)}P_L(x)\right]_+ \tag{C.13}$$

where $[f]_+$ denotes the part of the Laurent expansion of $f(x)$ with positive powers of x. Finally, the Laurent polynomial $P_L(x)$ reads

$$P_L(x) = \frac{1}{\det \mathcal{M}_{2L}}\begin{vmatrix} I_1^\theta & I_0^\theta & \cdots & I_{2-2L}^\theta & I_{1-2L}^\theta \\ I_2^\theta & I_1^\theta & \cdots & I_{3-2L}^\theta & I_{2-2L}^\theta \\ \vdots & \vdots & \ddots & \vdots & \vdots \\ I_{2L}^\theta & I_{2L-1}^\theta & \cdots & I_1^\theta & I_0^\theta \\ x^{-L} & x^{1-L} & \cdots & x^{L-1} & x^L \end{vmatrix} \tag{C.14}$$

where

$$\mathcal{M}_N = \begin{pmatrix} I_1^\theta & I_0^\theta & \cdots & I_{2-N}^\theta & I_{1-N}^\theta \\ I_2^\theta & I_1^\theta & \cdots & I_{3-N}^\theta & I_{2-N}^\theta \\ \vdots & \vdots & \ddots & \vdots & \vdots \\ I_N^\theta & I_{N-1}^\theta & \cdots & I_1^\theta & I_0^\theta \\ I_{N+1}^\theta & I_N^\theta & \cdots & I_2^\theta & I_1^\theta \end{pmatrix} . \tag{C.15}$$

Notice also that

$$P_L(1/x) = P_L(-x) \tag{C.16}$$

From this solution using (27.4) we recover the result of [16] for the cusp anomalous dimension,

$$\Gamma_{\text{cusp}} = L + \frac{\phi-\theta}{4}\partial_\theta \log\frac{\det \mathcal{M}_{2L+1}}{\det \mathcal{M}_{2L-1}} + \mathcal{O}((\phi-\theta)^2) \ . \tag{C.17}$$

C.4 Weak coupling predictions at five and six loops

From our all-loop result (28.26) it is straightforward to obtain a prediction for a part of the full anomalous dimension at five and six loops, namely for the coefficients $\gamma_5^{(2)}(\phi)$ and $\gamma_6^{(2)}(\phi)$ in (28.31). We found them to be

$$\begin{aligned}
\gamma_5^{(2)}(\phi) \quad &= 3360\left[\mathrm{Li}_9(e^{-2i\phi})+\mathrm{Li}_9(e^{2i\phi})\right]-2156i\phi\left[\mathrm{Li}_8(e^{2i\phi})-\mathrm{Li}_8(e^{-2i\phi})\right] \\
&-8\left(62\phi^2+15\pi^2\right)\left[\mathrm{Li}_7(e^{2i\phi})+\mathrm{Li}_7(e^{-2i\phi})\right] \\
&+\frac{20}{3}i\left(49\pi^2\phi-29\phi^3\right)\left[\mathrm{Li}_6(e^{2i\phi})-\mathrm{Li}_6(e^{-2i\phi})\right] \\
&-\frac{8}{3}\left(73\phi^4-87\pi^2\phi^2+6\pi^4\right)\left[\mathrm{Li}_5(e^{2i\phi})+\mathrm{Li}_5(e^{-2i\phi})\right] \\
&+\frac{4}{3}i\left(65\phi^5-94\pi^2\phi^3+29\pi^4\phi\right)\left[\mathrm{Li}_4(e^{2i\phi})-\mathrm{Li}_4(e^{-2i\phi})\right] \\
&-\frac{8}{9}(\pi-\phi)(\phi+\pi)\left(33\phi^4-31\pi^2\phi^2+2\pi^4\right)\left[\mathrm{Li}_3(e^{2i\phi})+\mathrm{Li}_3(e^{-2i\phi})\right] \\
&+\frac{32}{45}i\phi\left(7\pi^2-12\phi^2\right)\left(\pi^2-\phi^2\right)^2\left[\mathrm{Li}_2(e^{2i\phi})-\mathrm{Li}_2(e^{-2i\phi})\right] \\
&+\frac{32}{5}\phi^2\left(\phi^2-\pi^2\right)^3\left[\log(1-e^{2i\phi})+\log(1-e^{-2i\phi})\right] \\
&+\frac{16}{45}\left[83\zeta(3)\phi^6-15\left(8\pi^2\zeta(3)+31\zeta(5)\right)\phi^4\right. \\
&+3\left(9\pi^4\zeta(3)+85\pi^2\zeta(5)+930\zeta(7)\right)\phi^2 \\
&\left.-18900\zeta(9)+675\pi^2\zeta(7)+90\pi^4\zeta(5)+10\pi^6\zeta(3)\right]
\end{aligned} \tag{C.18}$$

and

$$\begin{aligned}
&\gamma_6^{(2)}(\phi) = -41580\left[\mathrm{Li}_{11}(e^{-2i\phi}) + \mathrm{Li}_{11}(e^{2i\phi})\right] \\
&+25704i\phi\left[\mathrm{Li}_{10}(e^{2i\phi}) - \mathrm{Li}_{10}(e^{-2i\phi})\right] \\
&+168(35\phi^2+12\pi^2)\left[\mathrm{Li}_9(e^{-2i\phi}) + \mathrm{Li}_9(e^{2i\phi})\right] \\
&-\frac{56}{3}i(241\pi^2\phi - 137\phi^3)\left[\mathrm{Li}_8(e^{2i\phi}) - \mathrm{Li}_8(e^{-2i\phi})\right] \\
&+\frac{8}{3}\left(943\phi^4 - 1150\pi^2\phi^2 + 91\pi^4\right)\left[\mathrm{Li}_7(e^{-2i\phi}) + \mathrm{Li}_7(e^{2i\phi})\right] \\
&-\frac{4}{9}i\left(2661\phi^5 - 3754\pi^2\phi^3 + 1077\pi^4\phi\right)\left[\mathrm{Li}_6(e^{2i\phi}) - \mathrm{Li}_6(e^{-2i\phi})\right] \\
&+\frac{8}{45}\left(-2299\phi^6 + 3970\pi^2\phi^4 - 1835\pi^4\phi^2 + 148\pi^6\right)F_5 \\
&-\frac{16}{45}i(\pi-\phi)\phi(\phi+\pi)\left(351\phi^4 - 449\pi^2\phi^2 + 154\pi^4\right)F_4 \\
&+\frac{8}{135}\left(639\phi^4 - 618\pi^2\phi^2 + 47\pi^4\right)\left(\pi^2-\phi^2\right)^2\left[\mathrm{Li}_3(e^{-2i\phi}) + \mathrm{Li}_3(e^{2i\phi})\right] \\
&+\frac{64}{135}i\phi\left(22\phi^2 - 15\pi^2\right)\left(\pi^2-\phi^2\right)^3\left[\mathrm{Li}_2(e^{2i\phi}) - \mathrm{Li}_2(e^{-2i\phi})\right] \\
&+\frac{1168}{135}\phi^2\left(\pi^2-\phi^2\right)^4\left[\log(1-e^{2i\phi}) + \log(1-e^{-2i\phi})\right] \\
&+\frac{752\zeta(3)\phi^8}{15} - \frac{16}{135}\left(970\pi^2\zeta(3) + 2493\zeta(5)\right)\phi^6 \\
&+\frac{16}{45}\left(208\pi^4\zeta(3) + 1130\pi^2\zeta(5) + 5175\zeta(7)\right)\phi^4 \\
&-\frac{16}{9}\left(2\pi^6\zeta(3) + 27\pi^4\zeta(5) + 414\pi^2\zeta(7) + 6615\zeta(9)\right)\phi^2 \\
&-\frac{8}{135}\left(94\pi^8\zeta(3) + 888\pi^6\zeta(5)\right. \\
&\left.+8190\pi^4\zeta(7) + 68040\pi^2\zeta(9) - 1403325\zeta(11)\right)
\end{aligned} \tag{C.19}$$

with

$$F_5 = \mathrm{Li}_5(e^{-2i\phi}) + \mathrm{Li}_5(e^{2i\phi}),\ \ F_4 = \mathrm{Li}_4(e^{2i\phi}) - \mathrm{Li}_4(e^{-2i\phi}) \tag{C.20}$$

C.5 Generalized η-functions

We found that the solution of the QSC for arbitrary angles at weak coupling involves the following generalized η functions

$$\eta^{z_1,\ldots,z_k}_{s_1,\ldots,s_k}(u) \equiv \sum_{n_1>n_2>\cdots>n_k\geq 0} \frac{z_1^{n_1}\ldots z_k^{n_k}}{(u+in_1)^{s_1}\ldots(u+in_k)^{s_k}} \tag{C.21}$$

which are a generalization of the multiple polylogarithms

$$\mathrm{Li}_{(s_1,\ldots,s_k)}(z_1,\ldots,z_k) = \sum_{n_1>n_2>\cdots>n_k\geq 1} \frac{z_1^{n_1}\ldots z_k^{n_k}}{n_1^{s_1}\ldots n_k^{s_k}} \tag{C.22}$$

For the case when all twists z_i are set to 1, the η-functions were encountered in the weak coupling computations of [109, 70]. In our calculation of $\Gamma_{\rm cusp}$ we had to deal with the case where twists are present. Below we summarize some useful relations analogous to those found in [109, 70].

Let us denote a solution of the equation

$$f(u+i)-f(u)=h(u) \tag{C.23}$$

as

$$f=\Sigma(h) \tag{C.24}$$

A useful property is

$$\eta^{Z,z}_{A,a}=Zz(\eta^{Z,z}_{A,a})^{[2]}+Z\frac{(\eta^{Z}_{A})^{[2]}}{u^a} \tag{C.25}$$

where A is a set of indices A_i and Z in the superscript is a set of twists Z_i, while z is a single complex number. The prefactor Z in the r.h.s. denotes the product $\prod_i Z_i$. Using this relation we find

$$\Sigma\left(\frac{z^{-iu}}{(u+in)^s}\right) = -z^{-iu}\eta^z_s(u+in) \tag{C.26}$$

$$\Sigma\left(\frac{z^{-iu}\eta^Z_S(u+in+i)}{(u+in)^s}\right) = -\frac{z^{-iu}}{Z}\eta^{Z(z/Z)}_{Ss}(u+in), \tag{C.27}$$

$$\begin{aligned}\Sigma\left[v^{-iu}u^a\eta^{Zz}_{Ab}(u+in)\right] &= \Sigma\left[\left(\frac{v}{zZ}\right)^{-iu}u^a\right](zZ)^{-iu}\eta^{Zz}_{Ab}(u+in) \\ &+ \Sigma\left[\Sigma\left[\left(\frac{v}{zZ}\right)^{-iu}u^a\right]^{[2]}(zZ)^{-iu}Z\frac{\eta^Z_A(u+in+i)}{(u+in)^b}\right]\end{aligned} \tag{C.28}$$

In these expressions $a,s=1,2,3,\ldots$ while n is arbitrary.

Finally we have the 'stuffle' relations which express a product of two η functions as a linear combination of some other η's. They are obtained by splitting the region of summation in the product of η functions and are directly analogous to those for polylogarithms or mutiple zeta values (see e.g. the pedagogical review [210] and references therein):

$$\eta^{\underline{z}}_{\underline{s}}\,\eta^{\underline{z}'}_{\underline{s}'}=\sum_{\underline{s}''}\eta^{\underline{z}''}_{\underline{s}''} \tag{C.29}$$

where in case two of the s indices are combined in the r.h.s. the corresponding twists are mutiplied, exactly as in the stuffle relations for polylogarithms. For example,

$$\eta^w_2\eta^z_3=\eta^{wz}_5+\eta^{w,z}_{2,3}+\eta^{z,w}_{3,2} \tag{C.30}$$

The operations described above are essential for the iterative procedure of [13] and should allow to run it to very high orders in the weak coupling expansion with any ϕ,θ.

D Appendices to part VII

D.1 Weak coupling limit of the coefficients

At weak coupling one can fix the values of the several leading coefficients A_n, B_n which parameterize the **P**-functions via (33.3). In order to do this we used the leading order weak coupling solution of the QSC constructed in [12]. With the $\mathbf{P}_a$ and μ_{ab} functions from that solution, one can build $\tilde{\mathbf{P}}_a = \mu_{ab}\chi^{bc}\mathbf{P}_c$ and compare the result with our ansatz (33.3) in which $\tilde{\mathbf{P}}_a$ is constructed by simply replacing $x \to 1/x$. For the case $\phi = \pi$ we found that

$$B_0 = \frac{\cos\theta - 2}{\sin\theta} + A_1 g^2 \tag{D.1}$$

and the remaining coefficients to the leading order are all fixed as

$$A_n = \frac{2^{n-1}\pi^n(1+(-1)^n)}{(n+1)!} + \mathcal{O}(g^2) \tag{D.2}$$

$$B_{2n} = \frac{(2\pi)^{2n-2}}{(2n-1)!} + \mathcal{O}(g^2) \ , \ n > 1 \tag{D.3}$$

$$B_{2n-1} = -\cot\theta\frac{(2\pi)^{2n-2}}{(2n-1)!} + \mathcal{O}(g^2) \ , \ n > 1 \tag{D.4}$$

$$B_1 = 2\tan\frac{\theta}{2} + \mathcal{O}(g^2) \tag{D.5}$$

$$B_2 = 0 + \mathcal{O}(g^2) \ . \tag{D.6}$$

D.2 Determinants entering the 5th order equation on $\mathbf{Q}_i$

The 4th order difference equation (33.6) on $\mathbf{Q}_i$ includes several determinants built out of the **P**-functions, which are defined as follows:

$$D_0 = \det \begin{pmatrix} \mathbf{P}^{1[+2]} & \mathbf{P}^{2[+2]} & \mathbf{P}^{3[+2]} & \mathbf{P}^{4[+2]} \\ \mathbf{P}^{1} & \mathbf{P}^{2} & \mathbf{P}^{3} & \mathbf{P}^{4} \\ \mathbf{P}^{1[-2]} & \mathbf{P}^{2[-2]} & \mathbf{P}^{3[-2]} & \mathbf{P}^{4[-2]} \\ \mathbf{P}^{1[-4]} & \mathbf{P}^{2[-4]} & \mathbf{P}^{3[-4]} & \mathbf{P}^{4[-4]} \end{pmatrix}, \tag{D.7}$$

$$D_1 = \det \begin{pmatrix} \mathbf{P}^{1[+4]} & \mathbf{P}^{2[+4]} & \mathbf{P}^{3[+4]} & \mathbf{P}^{4[+4]} \\ \mathbf{P}^{1} & \mathbf{P}^{2} & \mathbf{P}^{3} & \mathbf{P}^{4} \\ \mathbf{P}^{1[-2]} & \mathbf{P}^{2[-2]} & \mathbf{P}^{3[-2]} & \mathbf{P}^{4[-2]} \\ \mathbf{P}^{1[-4]} & \mathbf{P}^{2[-4]} & \mathbf{P}^{3[-4]} & \mathbf{P}^{4[-4]} \end{pmatrix}, \tag{D.8}$$

$$D_2 = \det \begin{pmatrix} \mathbf{P}^{1[+4]} & \mathbf{P}^{2[+4]} & \mathbf{P}^{3[+4]} & \mathbf{P}^{4[+4]} \\ \mathbf{P}^{1[+2]} & \mathbf{P}^{2[+2]} & \mathbf{P}^{3[+2]} & \mathbf{P}^{4[+2]} \\ \mathbf{P}^{1[-2]} & \mathbf{P}^{2[-2]} & \mathbf{P}^{3[-2]} & \mathbf{P}^{4[-2]} \\ \mathbf{P}^{1[-4]} & \mathbf{P}^{2[-4]} & \mathbf{P}^{3[-4]} & \mathbf{P}^{4[-4]} \end{pmatrix}, \tag{D.9}$$

$$\bar{D}_1 = \det \begin{pmatrix} \mathbf{P}^{1[-4]} & \mathbf{P}^{2[-4]} & \mathbf{P}^{3[-4]} & \mathbf{P}^{4[-4]} \\ \mathbf{P}^{1} & \mathbf{P}^{2} & \mathbf{P}^{3} & \mathbf{P}^{4} \\ \mathbf{P}^{1[+2]} & \mathbf{P}^{2[+2]} & \mathbf{P}^{3[+2]} & \mathbf{P}^{4[+2]} \\ \mathbf{P}^{1[+4]} & \mathbf{P}^{2[+4]} & \mathbf{P}^{3[+4]} & \mathbf{P}^{4[+4]} \end{pmatrix}, \tag{D.10}$$

$$\bar{D}_0 = \det \begin{pmatrix} \mathbf{P}^{1[-2]} & \mathbf{P}^{2[-2]} & \mathbf{P}^{3[-2]} & \mathbf{P}^{4[-2]} \\ \mathbf{P}^{1} & \mathbf{P}^{2} & \mathbf{P}^{3} & \mathbf{P}^{4} \\ \mathbf{P}^{1[+2]} & \mathbf{P}^{2[+2]} & \mathbf{P}^{3[+2]} & \mathbf{P}^{4[+2]} \\ \mathbf{P}^{1[+4]} & \mathbf{P}^{2[+4]} & \mathbf{P}^{3[+4]} & \mathbf{P}^{4[+4]} \end{pmatrix}. \tag{D.11}$$

D.3 Six and seven loop results at weak coupling

Using the QSC we have computed the weak coupling expansion of the quark–antiquark potential at the first seven nontrivial orders. The first five orders are given in the main text in (34.17). Here we present the rather bulky 6- and 7-loop results.

6-loop result. The term of order $\hat{g}^{12}$ in $\frac{\Omega}{4\pi}$ reads

$$
\begin{aligned}
&\frac{131072L^5}{15}+\frac{327680L^4}{3}+\frac{131072}{9}\pi^2L^4T+\frac{1048576L^3}{3}-\frac{1097728}{9}\pi^2L^3 \\
&+\frac{1163264}{3}\pi^2L^3T+\frac{32768}{9}\pi^4L^3T^2+81920L^2+24576\pi^2L^2+\frac{212992\zeta_3L^2}{3} \\
&-\frac{8192}{3}\pi^2L^2T+81920\zeta_3L^2T-\frac{77824}{5}\pi^4L^2T+\frac{475136}{9}\pi^4L^2T^2 \\
&+\left(\frac{65536}{3}\pi^2\zeta_3-5120\zeta_5\right)L^2T^2+-\frac{1515520L}{3}+\frac{1776640\pi^2L}{27}+212992\zeta_3L \\
&+\frac{39424\pi^4L}{15}-251904\pi^2LT+176128\zeta_3LT-\frac{16384}{27}\pi^4LT \\
&+\left(10240\zeta_5-\frac{71680}{9}\pi^2\zeta_3\right)LT-\frac{118784}{9}\pi^4LT^2+\left(\frac{573440}{3}\pi^2\zeta_3-99840\zeta_5\right)LT^2 \\
&+\left(3072\zeta_3^2+\frac{70912}{405}\pi^6\right)LT^2+\left(\frac{139264}{45}\pi^4\zeta_3-31232\pi^2\zeta_5+60928\zeta_7\right)LT^3 \\
&-\frac{295936}{3}-\frac{107008\pi^2}{27}+\frac{106496\zeta_3}{3}-\frac{1159424\pi^4}{675}+\left(\frac{124928\zeta_5}{5}-\frac{93184\pi^2\zeta_3}{9}\right) \\
&-\frac{1190528\pi^2T}{27}-19456\zeta_3T+\frac{3045376\pi^4T}{405}+\left(\frac{212992}{3}\pi^2\zeta_3+27648\zeta_5\right)T \\
&+\left(1536\zeta_3^2-\frac{14464\pi^6}{405}\right)T-\frac{50176}{3}\pi^4T^2-\left(\frac{172288}{3}\pi^2\zeta_3+24320\zeta_5\right)T^2 \\
&+\left(18816\zeta_3^2+\frac{17344\pi^6}{135}\right)T^2+\left(\frac{72704}{45}\pi^4\zeta_3+19136\pi^2\zeta_5-38976\zeta_7\right)T^2 \\
&+\left(\frac{228352}{45}\pi^4\zeta_3-\frac{107264}{3}\pi^2\zeta_5+43904\zeta_7\right)T^3 \\
&+\left(2496\zeta_{6,2}+\frac{20224}{3}\pi^2\zeta_3^2-31232\zeta_3\zeta_5+\frac{55304\pi^8}{42525}\right)T^3 \\
&+\left(-\frac{2560}{3}\pi^4\zeta_5+21504\pi^2\zeta_7-102816\zeta_9\right)T^4
\end{aligned}
\tag{D.12}
$$

At this order an irreducible multiple zeta value appears for the first time, given by $\zeta_{6,2}\simeq 0.017819740416836$.

7-loop result. The term of order $\hat{g}^{14}$ in $\frac{\Omega}{4\pi}$ is given by

$$\begin{aligned}
&\frac{1048576L^6}{45}+\frac{524288}{9}L^5\pi^2T+\frac{6815744L^5}{15}+\frac{262144}{9}L^4\pi^4T^2-65536L^4T\zeta_3+\frac{40632320}{9}L^4\pi^2T \\
&-\frac{15007744}{9}L^4\pi^2+2752512L^4+\frac{131072}{81}L^3\pi^6T^3+65536L^3\pi^2T^2\zeta_3+\frac{655360}{3}L^3T^2\zeta_5 \\
&+\frac{12255232}{9}L^3\pi^4T^2-\frac{64159744}{135}L^3\pi^4T-65536L^3T\zeta_3+\frac{13303808}{3}L^3\pi^2T+\frac{3407872L^3\zeta_3}{9} \\
&-\frac{11141120}{9}L^3\pi^2+\frac{15073280L^3}{3}+\frac{2080768}{45}L^2\pi^4T^3\zeta_3-\frac{499712}{3}L^2\pi^2T^3\zeta_5-129024L^2T^3\zeta_7 \\
&+32768L^2\pi^6T^3-\frac{2828288}{405}L^2\pi^6T^2-36864L^2T^2\zeta_3^2+\frac{11444224}{3}L^2\pi^2T^2\zeta_3+20480L^2T^2\zeta_5 \\
&+\frac{2351104}{3}L^2\pi^4T^2-\frac{7610368}{9}L^2\pi^2T\zeta_3-40960L^2T\zeta_5-\frac{27344896}{45}L^2\pi^4T+1671168L^2T\zeta_3 \\
&-3817472L^2\pi^2T+\frac{7221248L^2\pi^4}{45}+2555904L^2\zeta_3+\frac{17096704L^2\pi^2}{9}-\frac{6914048L^2}{3}+\frac{8192}{9}L\pi^6T^4\zeta_3 \\
&-\frac{133120}{3}L\pi^4T^4\zeta_5+369152L\pi^2T^4\zeta_7-628992LT^4\zeta_9+\frac{1176832L\pi^8T^3}{42525}+\frac{210944}{3}L\pi^2T^3\zeta_3^2 \\
&-71680LT^3\zeta_3\zeta_5+30720LT^3\zeta_{6,2}+\frac{7872512}{15}L\pi^4T^3\zeta_3-1899520L\pi^2T^3\zeta_5+867328LT^3\zeta_7 \\
&+\frac{212992}{27}L\pi^6T^3-\frac{1150976}{15}L\pi^4T^2\zeta_3+665600L\pi^2T^2\zeta_5-268800LT^2\zeta_7+\frac{2378752}{405}L\pi^6T^2 \\
&+43008LT^2\zeta_3^2+\frac{757760}{3}L\pi^2T^2\zeta_3-1587200LT^2\zeta_5-\frac{14838784}{9}L\pi^4T^2-\frac{2152448L\pi^6T}{2835} \\
&-163840LT\zeta_3^2+\frac{24051712}{9}L\pi^2T\zeta_3+364544LT\zeta_5+\frac{390412288}{405}L\pi^4T+2457600LT\zeta_3 \\
&-\frac{39706624}{9}L\pi^2T-\frac{5324800}{9}L\pi^2\zeta_3+\frac{1998848L\zeta_5}{5}-\frac{34199552L\pi^4}{225}+\frac{9797632L\zeta_3}{3} \\
&+\frac{61534208L\pi^2}{81}-\frac{23560192L}{3}-\frac{11264}{105}\pi^6T^5\zeta_5+\frac{73216}{5}\pi^4T^5\zeta_7-285120\pi^2T^5\zeta_9 \\
&+1271952T^5\zeta_{11}-\frac{10544\pi^{10}T^4}{93555}+\frac{91136}{9}\pi^4T^4\zeta_3^2-\frac{520832}{3}\pi^2T^4\zeta_3\zeta_5+179424T^4\zeta_5^2 \\
&+361088T^4\zeta_3\zeta_7+\frac{16768}{3}\pi^2T^4\zeta_{6,2}-26432T^4\zeta_{8,2}+\frac{65536}{45}\pi^6T^4\zeta_3-63488\pi^4T^4\zeta_5 \\
&+401408\pi^2T^4\zeta_7-508032T^4\zeta_9+\frac{5137792\pi^6T^3\zeta_3}{2835}-768T^3\zeta_3^3+30976\pi^4T^3\zeta_5 \\
&-\frac{941632}{3}\pi^2T^3\zeta_7+\frac{2211904T^3\zeta_9}{3}-\frac{142816\pi^8T^3}{14175}+\frac{1183232}{3}\pi^2T^3\zeta_3^2-337664T^3\zeta_3\zeta_5 \\
&+17664T^3\zeta_{6,2}-\frac{256000}{3}\pi^4T^3\zeta_3+\frac{1762304}{3}\pi^2T^3\zeta_5+367360T^3\zeta_7-\frac{446464}{45}\pi^6T^3 \\
&+\frac{2348512\pi^8T^2}{42525}-\frac{175360}{3}\pi^2T^2\zeta_3^2+\frac{76288}{3}T^2\zeta_3\zeta_5+26880T^2\zeta_{6,2}+\frac{6986752}{45}\pi^4T^2\zeta_3 \\
&+\frac{295424}{9}\pi^2T^2\zeta_5-611520T^2\zeta_7-\frac{1111552}{405}\pi^6T^2+225792T^2\zeta_3^2-\frac{2234624}{3}\pi^2T^2\zeta_3 \\
&-261120T^2\zeta_5+\frac{3700736\pi^4T^2}{27}-\frac{2342656}{135}\pi^4T\zeta_3+131584\pi^2T\zeta_5+33152T\zeta_7 \\
&+\frac{3462656\pi^6T}{2835}+165888T\zeta_3^2+\frac{3972608}{27}\pi^2T\zeta_3+387072T\zeta_5-\frac{222660352\pi^4T}{1215} \\
&-544768T\zeta_3+\frac{16618240\pi^2T}{81}-\frac{122624\pi^6}{945}+\frac{1384448\zeta_3^2}{9}+106496\pi^2\zeta_3+499712\zeta_5 \\
&+\frac{274300928\pi^4}{10125}-\frac{1384448\zeta_3}{3}-\frac{67858432\pi^2}{243}-\frac{4759552}{15}
\end{aligned} \tag{D.13}$$

where we have a new multiple zeta value $\zeta_{8,2} \simeq 0.004122469678399832224 0$.

D.4 Complex conjugation of the $\mathbf{Q}_i$ functions

Another set of useful relations concerns the expected symmetry of the QSC system under complex conjugation. Let's assume that under the complex conjugation the equation (33.6) remain invariant. In general this is true if

$$\bar{\mathbf{P}}_a = \lambda_a{}^b \mathbf{P}_b \ \ , \ \ \bar{\mathbf{P}}^a = \lambda^a{}_b \mathbf{P}^b \tag{D.14}$$

for some constant coefficients $\lambda_a{}^b$, such that $\lambda_a{}^b \lambda^a{}_c = -\delta^b_c$ (in our case $\lambda_a{}^b = -i\delta^b_a$). If this holds the complex conjugate $\bar{\mathbf{Q}}_i$ should give an alternative complete set of solutions of the finite difference equation (33.6), which should be related to the initial set as a linear combinations with some i-periodic coefficients

$$\bar{\mathbf{Q}}_i = \Omega_i{}^j \mathbf{Q}_j \ \ , \ \ \Omega_i{}^j(u+i) = \Omega_i{}^j(u) \ . \tag{D.15}$$

Those coefficients can be written in terms of $Q_{a|i}$ as

$$\Omega_i{}^j = -\bar{Q}_{a|i}(u - \tfrac{i}{2}) \lambda^a{}_b Q^{b|j}(u - \tfrac{i}{2}) \tag{D.16}$$

where $Q^{b|j} = -((Q_{b|j})^{-1})^{\mathrm{T}}$. We can easily check this is indeed true. We show that (D.15) holds:

$$\Omega_i{}^j \mathbf{Q}_j = -\bar{Q}_{a|i}(u - \tfrac{i}{2}) \lambda^a{}_b Q^{b|j}(u - \tfrac{i}{2}) \mathbf{Q}_j = -\bar{Q}_{a|i}(u - \tfrac{i}{2}) \lambda^a{}_b \mathbf{P}^b = -\overline{Q_{a|i}(u + \tfrac{i}{2}) \mathbf{P}^a} = \bar{\mathbf{Q}}_i \tag{D.17}$$

and also that the r.h.s. (D.16) is periodic:

$$\bar{Q}^+_{a|i} \lambda^a{}_b Q^{b|j+} = \overline{(Q^+_{a|i} - \mathbf{P}_a \mathbf{Q}_i)} \lambda^a{}_b (Q^{b|j-} + \mathbf{P}^b \mathbf{Q}^j) = \bar{Q}^-_{a|i} \lambda^a{}_b Q^{b|j-} \tag{D.18}$$

(we denoted $f^{\pm} = f(u \pm i/2)$). Finally we can find discontinuity of Ω using this identity

$$\tilde{\Omega}_i{}^j - \Omega_i{}^j = -\bar{Q}^-_{a|i} \lambda^a{}_b \left(\tilde{Q}^{b|j-} - Q^{b|j-} \right) = \bar{Q}^-_{a|i} \lambda^a{}_b \left(\tilde{\mathbf{P}}^b \tilde{\mathbf{Q}}^j - \mathbf{P}^b \mathbf{Q}^j \right) = -\bar{\tilde{\mathbf{Q}}}_i \tilde{\mathbf{Q}}^j + \bar{\mathbf{Q}}_i \mathbf{Q}^j \ . \tag{D.19}$$

We notice one more relation which we will use below. Consider Ω_1^4. Its discontinuity is due to (33.9)

$$\tilde{\Omega}_1^4(u) - \Omega_1^4(u) = u \bar{\mathbf{q}}_1(u) \mathbf{q}_1(u) - u \bar{\mathbf{q}}_1(-u) \mathbf{q}_1(-u) \tag{D.20}$$

from where we see that Ω_1^4 should be an even function.

D.5 Expansion of $q_1(u)$ at the origin

As discussed in the end of Sec 35.2, to demonstrate that the Schrödinger equation is encoded in the QSC we need to compute the expansion of $q_1(u)$ at the origin up to the term linear in u. Let us show how this can be done.

On the one hand, from the 2nd order difference equation (35.5) on q_1 we find that $q_1(0)$ and $q_1'(0)$ are related to its expansion at $u = -i$:

$$q_1(u) = \frac{4\hat{g}^2}{(u+i)^2} q_1(0) + \frac{4\hat{g}^2 q_1'(0) - 2q_1(0)\Omega}{u+i} + \mathcal{O}((u-i)^0) \ . \tag{D.21}$$

On the other hand, we can compute the expansion around $u = -i$ using the expression (35.20) for q_1 in terms of $F(z)$. In that expression the singularity of q_1 at $u = -i$ arises because the integrand is singular when $z = i$. In the vicinity of this point $F(z)$ is a linear combination of two solutions of the the Schrödinger equation, one of which is smooth at $z = i$ and the other one also includes terms of the type $(z-i)^n \log(iz+1)$ with $n \geq 1$. Solving the equation close to this point we find

$$F(z) = -\frac{iC}{2\hat{g}^2} + C(z-i)\log(iz+1) + iC_2(z-i) + \dots \ , \tag{D.22}$$

where the real[50] constant C_2 comes from the smooth solution and dots stand for more regular terms. Let us also note that the expression (35.20) is not applicable directly for Im $u < 0$ as the integrand is too singular near $z = i$. However, as we need only the coefficients of the double and the single pole at $u = -i$ in $q_1(u)$, we can modify (35.20) in a way which ensures convergence of the integral without changing these two coefficients:

$$2\int_i^\infty dz \frac{e^{-i\Omega/2}}{z^2+1}\left(\frac{z+i}{z-i}\right)^{iu}\left[\frac{iC}{2\hat{g}^2} + e^{-i\frac{z-\Omega}{2}}\left(-\frac{iC}{2\hat{g}^2} + C(z-i)\log(iz+1) + iC_2(z-i) + \dots\right)\right] . \tag{D.23}$$

We subtracted a part proportional to the integral

$$2\int_i^\infty dz \frac{1}{z^2+1}\left(\frac{z+i}{z-i}\right)^{iu} = \frac{1}{u} \ , \tag{D.24}$$

which does not affect the two coefficients we are after. From (D.23) we now find

$$q_1(u) = -\frac{2iCe^{-\frac{i\Omega}{2}}}{(u+i)^2} - \frac{e^{-\frac{i\Omega}{2}}\left(-\frac{iC\Omega}{2\hat{g}^2} - 2i\pi C - 2C - 2C\log 2 - 2iC_2\right)}{u+i} + \mathcal{O}((u-i)^0) \ . \tag{D.25}$$

Comparing this with (D.21) we get

$$q_1(0) = -\frac{iCe^{-\frac{i\Omega}{2}}}{2\hat{g}^2} \ , \tag{D.26}$$

[50] One can show that C_2 is real using the fact that $F(z)$ is a real and even function.

$$q_1'(0) = \frac{e^{-\frac{i\Omega}{2}}\left(4\hat{g}^2\left(iC_2 + C(1+i\pi+\log 2)\right) - iC\Omega\right)}{8\hat{g}^4} \ . \tag{D.27}$$

This finally allows to construct the combination $e^{2\pi u}q_1(u)\bar{q}_1(u)$ which we need. We observe that C_2 cancels out and we find

$$e^{2\pi u}q_1(u)\bar{q}_1(u) = -\frac{C^2}{4\hat{g}^4} - \frac{C^2\Omega}{8\hat{g}^6}u + \mathcal{O}(u^2) \ , \tag{D.28}$$

which is the key result used in (35.31) in the main text.

D.6 Numerical data

Here we present a part of our numnerical data for the quark–antiquark potential Ω at finite coupling g with zero twist $\theta = 0$. While the accuracy might vary slightly, we expect

all digits to be correct (with uncertanity in the last digit).

g	$\Omega(g)$	g	$\Omega(g)$
0	0	0.05	0.02937069654776
0.075	0.06265474565224	0.1	0.10511713720337
0.125	0.15465836443567	0.15	0.20955607216466
0.175	0.26845318866584	0.2	0.330312294925133
0.225	0.39435828555165	0.25	0.4600215248401101992
0.275	0.5268878004652301086	0.3	0.5946574683022822222
0.325	0.6631138101939375140	0.35	0.7320994342456940408
0.375	0.8014991401020814198	0.4	0.8712277052055592640
0.425	0.9412212786455914103	0.45	1.0114313519742950991
0.475	1.0818205391585539063	0.5	1.1523596132795935855
0.525	1.2230254118796313025	0.55	1.2937993424631526624
0.575	1.3646663040854278314	0.6	1.4356138993330072537
0.625	1.5066318508313724359	0.65	1.5777115633938239593
0.675	1.6488457911511407735	0.7	1.7200283813289496328
0.725	1.7912540747152853534	0.75	1.8625183485921063555
0.775	1.9338172918626574100	0.8	2.0051475048695944173
0.825	2.0765060183502537912	0.85	2.1478902273706390145
0.875	2.2192978370894877695	0.9	2.2907268179434612004
0.925	2.3621753683925865485	0.95	2.4336418837756454947
0.975	2.5051249301358780128	1.	2.5766232221146891288
1.025	2.6481356041939115734	1.05	2.7196610347092241265
1.075	2.7911985721684911266	1.1	2.8627473634963918184
1.125	2.9343066338961908685	1.15	3.0058756780749462488
1.175	3.0774538526229463147	1.2	3.1490405693740687669
1.225	3.2206352896028680533	1.25	3.2922375189379219065
1.275	3.3638468028903889215	1.3	3.4354627229126975867
1.325	3.5070848929154719081	1.35	3.5787129561817286982
1.375	3.6503465826264772085	1.4	3.7219854663574488362
1.425	3.793629323499052523	1.45	3.865277890247007235
1.475	3.936930921125622182	1.5	4.008588187423520918

References

[1] J. M. Maldacena, "The Large N limit of superconformal field theories and supergravity," Int. J. Theor. Phys. **38** (1999) 1113 [Adv. Theor. Math. Phys. **2** (1998) 231] [hep-th/9711200].

[2] S. S. Gubser, I. R. Klebanov and A. M. Polyakov, "Gauge theory correlators from noncritical string theory," Phys. Lett. B **428** (1998) 105 doi:10.1016/S0370-2693(98)00377-3 [hep-th/9802109].

[3] E. Witten, "Anti-de Sitter space and holography," Adv. Theor. Math. Phys. **2** (1998) 253 [hep-th/9802150].

[4] G. Moore, Visionary talk at Strings-2014 conference, Princeton

[5] J. A. Minahan and K. Zarembo, "The Bethe ansatz for N=4 superYang-Mills," JHEP **0303** (2003) 013 [hep-th/0212208].

[6] N. Beisert *et al.*, "Review of AdS/CFT Integrability: An Overview," Lett. Math. Phys. **99** (2012) 3 [arXiv:1012.3982 [hep-th]].

[7] O. Babelon, D. Bernard, M. Talon, "Introduction to Classical Integrable Systems", Cambridge University Press, 2007

[8] A. A. Belavin, A. M. Polyakov and A. B. Zamolodchikov, "Infinite Conformal Symmetry in Two-Dimensional Quantum Field Theory," Nucl. Phys. B **241** (1984) 333.

[9] A. B. Zamolodchikov and A. B. Zamolodchikov, "Factorized s Matrices in Two-Dimensions as the Exact Solutions of Certain Relativistic Quantum Field Models," Annals Phys. **120** (1979) 253.

[10] N. Seiberg and E. Witten, "Electric - magnetic duality, monopole condensation, and confinement in N=2 supersymmetric Yang-Mills theory," Nucl. Phys. B **426** (1994) 19 [Erratum-ibid. B **430** (1994) 485] [hep-th/9407087].

[11] N. Gromov and F. Levkovich-Maslyuk, "Quark–anti-quark potential in N=4 SYM," arXiv:1601.05679 [hep-th].

[12] N. Gromov and F. Levkovich-Maslyuk, "Quantum Spectral Curve for a Cusped Wilson Line in N=4 SYM," arXiv:1510.02098 [hep-th].

[13] N. Gromov, F. Levkovich-Maslyuk and G. Sizov, "Pomeron Eigenvalue at Three Loops in $\mathcal{N} = 4$ Supersymmetric Yang-Mills Theory," Phys. Rev. Lett. **115** (2015) 25, 251601 doi:10.1103/PhysRevLett.115.251601 [arXiv:1507.04010 [hep-th]].

[14] N. Gromov, F. Levkovich-Maslyuk and G. Sizov, "Quantum Spectral Curve and the Numerical Solution of the Spectral Problem in AdS5/CFT4," arXiv:1504.06640 [hep-th].

[15] N. Gromov, F. Levkovich-Maslyuk, G. Sizov and S. Valatka, "Quantum spectral curve at work: from small spin to strong coupling in $\mathcal{N} = 4$ SYM," JHEP **1407** (2014) 156 doi:10.1007/JHEP07(2014)156 [arXiv:1402.0871 [hep-th]].

[16] N. Gromov, F. Levkovich-Maslyuk and G. Sizov, "Analytic Solution of Bremsstrahlung TBA II: Turning on the Sphere Angle," JHEP **1310** (2013) 036 [arXiv:1305.1944 [hep-th]].

[17] M. Beccaria, F. Levkovich-Maslyuk, G. Macorini and A. A. Tseytlin, "Quantum corrections to spinning superstrings in AdS3 x S3 x M4: determining the dressing phase," JHEP **1304** (2013) 006 doi:10.1007/JHEP04(2013)006 [arXiv:1211.6090 [hep-th]].

[18] F. Levkovich-Maslyuk, "Numerical results for the exact spectrum of planar AdS4/CFT3," JHEP **1205** (2012) 142 doi:10.1007/JHEP05(2012)142 [arXiv:1110.5869 [hep-th]].

[19] M. Beccaria, F. Levkovich-Maslyuk and G. Macorini, "On wrapping corrections to GKP-like operators," JHEP **1103** (2011) 001 doi:10.1007/JHEP03(2011)001 [arXiv:1012.2054 [hep-th]].

[20] N. Gromov and F. Levkovich-Maslyuk, "Y-system and beta-deformed N=4 Super-Yang-Mills," J. Phys. A **44** (2011) 015402 [arXiv:1006.5438 [hep-th]].

[21] N. Gromov and F. Levkovich-Maslyuk, "Y-system, TBA and Quasi-Classical strings in AdS(4) x CP3," JHEP **1006** (2010) 088 [arXiv:0912.4911 [hep-th]].

[22] N. Tulyakov, F. Levkovich-Maslyuk, V. Samoilov, "Analytical Calculation of Atom Ejection from the Ni (111), Ni (001), and Au (001) Surfaces in Frames of a Three-Dimensional Model",

Journal of Surface Investigation. X-ray, Synchrotron and Neutron Techniques, 2011, Vol. **5**, p. 335.

[23] F. Levkovich-Maslyuk, "Two destructive effects of decoherence on Bell inequality violation", Phys. Rev. A **79**, 054101 (2009) [arXiv:0812.3736 [quant-ph]]

[24] J. A. Minahan, "Review of AdS/CFT Integrability, Chapter I.1: Spin Chains in N=4 Super Yang-Mills," Lett. Math. Phys. **99** (2012) 33 [arXiv:1012.3983 [hep-th]].

[25] M. F. Sohnius and P. C. West, "Conformal Invariance in N=4 Supersymmetric Yang-Mills Theory," Phys. Lett. B **100** (1981) 245.

[26] R. R. Metsaev and A. A. Tseytlin, "Type IIB superstring action in AdS(5) x S**5 background," Nucl. Phys. B **533** (1998) 109 [hep-th/9805028].

[27] A. A. Tseytlin, "Review of AdS/CFT Integrability, Chapter II.1: Classical AdS5xS5 string solutions," Lett. Math. Phys. **99** (2012) 103 [arXiv:1012.3986 [hep-th]].

[28] M. Magro, "Review of AdS/CFT Integrability, Chapter II.3: Sigma Model, Gauge Fixing," Lett. Math. Phys. **99** (2012) 149 [arXiv:1012.3988 [hep-th]].

[29] I. Bena, J. Polchinski and R. Roiban, "Hidden symmetries of the AdS(5) x S**5 superstring," Phys. Rev. D **69** (2004) 046002 [hep-th/0305116].

[30] N. Beisert, V. A. Kazakov, K. Sakai and K. Zarembo, "The Algebraic curve of classical superstrings on AdS(5) x S**5," Commun. Math. Phys. **263** (2006) 659 [hep-th/0502226].

[31] N. Gromov and P. Vieira, "The AdS(5) x S**5 superstring quantum spectrum from the algebraic curve," Nucl. Phys. B **789** (2008) 175 [hep-th/0703191 [HEP-TH]].

[32] C. Ahn and R. I. Nepomechie, "Review of AdS/CFT Integrability, Chapter III.2: Exact World-Sheet S-Matrix," Lett. Math. Phys. **99** (2012) 209 [arXiv:1012.3991 [hep-th]].

[33] P. Vieira and D. Volin, "Review of AdS/CFT Integrability, Chapter III.3: The Dressing factor," Lett. Math. Phys. **99** (2012) 231 [arXiv:1012.3992 [hep-th]].

[34] N. Beisert and M. Staudacher, "Long-range psu(2,2—4) Bethe Ansatze for gauge theory and strings," Nucl. Phys. B **727** (2005) 1 [hep-th/0504190].

[35] C. Sieg and A. Torrielli, "Wrapping interactions and the genus expansion of the 2-point function of composite operators," Nucl. Phys. B **723** (2005) 3 [hep-th/0505071].

[36] J. Ambjorn, R. A. Janik and C. Kristjansen, "Wrapping interactions and a new source of corrections to the spin-chain/string duality," Nucl. Phys. B **736** (2006) 288 doi:10.1016/j.nuclphysb.2005.12.007 [hep-th/0510171].

[37] A. B. Zamolodchikov, "Thermodynamic Bethe Ansatz in Relativistic Models. Scaling Three State Potts and Lee-yang Models," Nucl. Phys. B **342** (1990) 695.

[38] N. Gromov, V. Kazakov and P. Vieira, "Exact Spectrum of Anomalous Dimensions of Planar N=4 Supersymmetric Yang-Mills Theory," Phys. Rev. Lett. **103** (2009) 131601 [arXiv:0901.3753 [hep-th]].

[39] D. Bombardelli, D. Fioravanti and R. Tateo, "Thermodynamic Bethe Ansatz for planar AdS/CFT: A Proposal," J. Phys. A **42** (2009) 375401 [arXiv:0902.3930 [hep-th]].

[40] N. Gromov, V. Kazakov, A. Kozak and P. Vieira, "Exact Spectrum of Anomalous Dimensions of Planar N = 4 Supersymmetric Yang-Mills Theory: TBA and excited states," Lett. Math. Phys. **91** (2010) 265 [arXiv:0902.4458 [hep-th]].

[41] G. Arutyunov and S. Frolov, "Thermodynamic Bethe Ansatz for the AdS(5) x S(5) Mirror Model," JHEP **0905** (2009) 068 doi:10.1088/1126-6708/2009/05/068 [arXiv:0903.0141 [hep-th]].

[42] N. Gromov, V. Kazakov and P. Vieira, "Exact Spectrum of Planar $\mathcal{N} = 4$ Supersymmetric Yang-Mills Theory: Konishi Dimension at Any Coupling," Phys. Rev. Lett. **104** (2010) 211601 [arXiv:0906.4240 [hep-th]].

[43] G. Arutyunov, S. Frolov and A. Sfondrini, "Exceptional Operators in N=4 super Yang-Mills," JHEP **1209** (2012) 006 [arXiv:1205.6660 [hep-th]].

[44] S. Frolov, "Konishi operator at intermediate coupling," J. Phys. A **44** (2011) 065401 [arXiv:1006.5032 [hep-th]].

[45] N. Gromov, D. Serban, I. Shenderovich and D. Volin, "Quantum folded string and integrability: From finite size effects to Konishi dimension," JHEP **1108** (2011) 046 [arXiv:1102.1040 [hep-th]].

[46] S. Frolov, "Scaling dimensions from the mirror TBA," J. Phys. A **45** (2012) 305402 [arXiv:1201.2317 [hep-th]].

[47] R. Roiban and A. A. Tseytlin, "Semiclassical string computation of strong-coupling corrections to dimensions of operators in Konishi multiplet," Nucl. Phys. B **848** (2011) 251 [arXiv:1102.1209 [hep-th]].

[48] B. C. Vallilo and L. Mazzucato, "The Konishi multiplet at strong coupling," JHEP **1112** (2011) 029 [arXiv:1102.1219 [hep-th]].

[49] S. Frolov, M. Heinze, G. Jorjadze and J. Plefka, "Static gauge and energy spectrum of single-mode strings in AdS_5 x S^5," J. Phys. A **47** (2014) 085401 doi:10.1088/1751-8113/47/8/085401 [arXiv:1310.5052 [hep-th]].

[50] A. Cavaglia, D. Fioravanti and R. Tateo, "Extended Y-system for the AdS_5/CFT_4 correspondence," Nucl. Phys. B **843** (2011) 302 [arXiv:1005.3016 [hep-th]].

[51] N. Gromov, V. Kazakov, S. Leurent and D. Volin, "Solving the AdS/CFT Y-system," JHEP **1207** (2012) 023 [arXiv:1110.0562 [hep-th]].

[52] N. Gromov, V. Kazakov, S. Leurent and D. Volin, "Quantum Spectral Curve for Planar $\mathcal{N}$ = Super-Yang-Mills Theory," Phys. Rev. Lett. **112** (2014) 1, 011602 doi:10.1103/PhysRevLett.112.011602 [arXiv:1305.1939 [hep-th]].

[53] N. Gromov, V. Kazakov, S. Leurent and D. Volin, "Quantum spectral curve for arbitrary state/operator in AdS_5/CFT_4," JHEP **1509** (2015) 187 [arXiv:1405.4857 [hep-th]].

[54] E. K. Sklyanin, "Separation of variables - new trends," Prog. Theor. Phys. Suppl. **118** (1995) 35 doi:10.1143/PTPS.118.35 [solv-int/9504001].

[55] N. Gromov and P. Vieira, "Tailoring Three-Point Functions and Integrability IV. Theta-morphism," JHEP **1404** (2014) 068 [arXiv:1205.5288 [hep-th]].

[56] Y. Kazama, S. Komatsu and T. Nishimura, "Novel construction and the monodromy relation for three-point fuctions at weak coupling," arXiv:1410.8533 [hep-th].

[57] B. Basso, A. Sever and P. Vieira, "Spacetime and Flux Tube S-Matrices at Finite Coupling for N=4 Supersymmetric Yang-Mills Theory," Phys. Rev. Lett. **111** (2013) 9, 091602 [arXiv:1303.1396 [hep-th]].

[58] B. Basso, S. Komatsu and P. Vieira, "Structure Constants and Integrable Bootstrap in Planar N=4 SYM Theory," arXiv:1505.06745 [hep-th].

[59] K. Zoubos, "Review of AdS/CFT Integrability, Chapter IV.2: Deformations, Orbifolds and Open Boundaries," Lett. Math. Phys. **99** (2012) 375 [arXiv:1012.3998 [hep-th]].

[60] G. Arutyunov, M. de Leeuw and S. J. van Tongeren, "The exact spectrum and mirror duality of the $(AdS_5 \times S^5)_\eta$ superstring," Theor. Math. Phys. **182** (2015) 1, 23 [Teor. Mat. Fiz. **182** (2014) 1, 28] [arXiv:1403.6104 [hep-th]].

[61] T. Klose, "Review of AdS/CFT Integrability, Chapter IV.3: N=6 Chern-Simons and Strings on AdS4xCP3," Lett. Math. Phys. **99** (2012) 401 [arXiv:1012.3999 [hep-th]].

[62] A. Sfondrini, "Towards integrability for AdS3/CFT2," arXiv:1406.2971 [hep-th].

[63] D. Correa, J. Maldacena and A. Sever, "The quark anti-quark potential and the cusp anomalous dimension from a TBA equation," JHEP **1208** (2012) 134 [arXiv:1203.1913 [hep-th]].

[64] N. Drukker, "Integrable Wilson loops," JHEP **1310** (2013) 135 [arXiv:1203.1617 [hep-th]].

[65] Z. Bajnok, N. Drukker, A. Hegedus, R. I. Nepomechie, L. Palla, C. Sieg and R. Suzuki, "The spectrum of tachyons in AdS/CFT," JHEP **1403** (2014) 055 doi:10.1007/JHEP03(2014)055 [arXiv:1312.3900 [hep-th]].

[66] A. Chervov and D. Talalaev, "Quantum spectral curves, quantum integrable systems and the geometric Langlands correspondence," hep-th/0604128.

[67] B. Eynard and N. Orantin, "Invariants of algebraic curves and topological expansion," Commun. Num. Theor. Phys. **1** (2007) 347 doi:10.4310/CNTP.2007.v1.n2.a4 [math-ph/0702045].

[68] B. Eynard, "Topological expansion for the 1-Hermitian matrix model correlation functions," JHEP **0411** (2004) 031 doi:10.1088/1126-6708/2004/11/031 [hep-th/0407261].

[69] L. Freyhult, "Review of AdS/CFT Integrability, Chapter III.4: Twist States and the cusp Anomalous Dimension," Lett. Math. Phys. **99** (2012) 255 [arXiv:1012.3993 [hep-th]].

[70] C. Marboe and D. Volin, "Quantum spectral curve as a tool for a perturbative quantum field theory," Nucl. Phys. B **899** (2015) 810 doi:10.1016/j.nuclphysb.2015.08.021 [arXiv:1411.4758 [hep-th]].

[71] C. Marboe, V. Velizhanin and D. Volin, "Six-loop anomalous dimension of twist-two operators in planar $\mathcal{N} = 4$ SYM theory," JHEP **1507** (2015) 084 [arXiv:1412.4762 [hep-th]].

[72] M. Alfimov, N. Gromov and V. Kazakov, "QCD Pomeron from AdS/CFT Quantum Spectral Curve," JHEP **1507** (2015) 164 [arXiv:1408.2530 [hep-th]].

[73] V. Kazakov, S. Leurent and D. Volin, "T-system on T-hook: Grassmannian Solution and Twisted Quantum Spectral Curve," arXiv:1510.02100 [hep-th].

[74] A. Cavagli, D. Fioravanti, N. Gromov and R. Tateo, "Quantum Spectral Curve of the $\mathcal{N} = 6$ Supersymmetric Chern-Simons Theory," Phys. Rev. Lett. **113** (2014) 2, 021601 doi:10.1103/PhysRevLett.113.021601 [arXiv:1403.1859 [hep-th]].

[75] N. Gromov and P. Vieira, "The AdS(4) / CFT(3) algebraic curve," JHEP **0902** (2009) 040 doi:10.1088/1126-6708/2009/02/040 [arXiv:0807.0437 [hep-th]].

[76] N. Gromov and P. Vieira, "The all loop AdS4/CFT3 Bethe ansatz," JHEP **0901** (2009) 016 doi:10.1088/1126-6708/2009/01/016 [arXiv:0807.0777 [hep-th]].

[77] C. Ahn and R. I. Nepomechie, "N=6 super Chern-Simons theory S-matrix and all-loop Bethe ansatz equations," JHEP **0809** (2008) 010 doi:10.1088/1126-6708/2008/09/010 [arXiv:0807.1924 [hep-th]].

[78] D. Bombardelli, D. Fioravanti and R. Tateo, "TBA and Y-system for planar AdS(4)/CFT(3)," Nucl. Phys. B **834** (2010) 543 doi:10.1016/j.nuclphysb.2010.04.005 [arXiv:0912.4715 [hep-th]].

[79] A. Cavaglia, D. Fioravanti and R. Tateo, "Discontinuity relations for the AdS_4/CFT_3 correspondence," Nucl. Phys. B **877** (2013) 852 doi:10.1016/j.nuclphysb.2013.10.023 [arXiv:1307.7587 [hep-th]].

[80] N. Gromov and G. Sizov, "Exact Slope and Interpolating Functions in N=6 Supersymmetric Chern-Simons Theory," Phys. Rev. Lett. **113** (2014) 12, 121601 doi:10.1103/PhysRevLett.113.121601 [arXiv:1403.1894 [hep-th]].

[81] J. A. Minahan, O. Ohlsson Sax and C. Sieg, "Magnon dispersion to four loops in the ABJM and ABJ models," J. Phys. A **43** (2010) 275402 doi:10.1088/1751-8113/43/27/275402 [arXiv:0908.2463 [hep-th]].

[82] M. Leoni, A. Mauri, J. A. Minahan, O. Ohlsson Sax, A. Santambrogio, C. Sieg and G. Tartaglino-Mazzucchelli, "Superspace calculation of the four-loop spectrum in N=6 supersymmetric Chern-Simons theories," JHEP **1012** (2010) 074 doi:10.1007/JHEP12(2010)074 [arXiv:1010.1756 [hep-th]].

[83] T. McLoughlin, R. Roiban and A. A. Tseytlin, "Quantum spinning strings in AdS(4) x CP**3: Testing the Bethe Ansatz proposal," JHEP **0811** (2008) 069 doi:10.1088/1126-6708/2008/11/069 [arXiv:0809.4038 [hep-th]].

[84] O. Bergman and S. Hirano, "Anomalous radius shift in AdS(4)/CFT(3)," JHEP **0907** (2009) 016 doi:10.1088/1126-6708/2009/07/016 [arXiv:0902.1743 [hep-th]].

[85] M. C. Abbott, I. Aniceto and D. Bombardelli, "Quantum Strings and the AdS4/CFT3 Interpolating Function," JHEP **1012** (2010) 040 doi:10.1007/JHEP12(2010)040 [arXiv:1006.2174 [hep-th]].

[86] D. Astolfi, G. Grignani, E. Ser-Giacomi and A. V. Zayakin, "Strings in AdS4 x CP3: finite size spectrum vs. Bethe Ansatz," JHEP **1204** (2012) 005 doi:10.1007/JHEP04(2012)005 [arXiv:1111.6628 [hep-th]].

[87] C. Lopez-Arcos and H. Nastase, "Eliminating ambiguities for quantum corrections to strings moving in $AdS_4 \times \mathbb{CP}^3$," Int. J. Mod. Phys. A **28** (2013) 1350058 doi:10.1142/S0217751X13500589 [arXiv:1203.4777 [hep-th]].

[88] L. Anselmetti, D. Bombardelli, A. Cavagli and R. Tateo, "12 loops and triple wrapping in ABJM theory from integrability," arXiv:1506.09089 [hep-th].

[89] A. Cavagli, M. Cornagliotto, M. Mattelliano and R. Tateo, "A Riemann-Hilbert formulation for the finite temperature Hubbard model," JHEP **1506** (2015) 015 [arXiv:1501.04651 [hep-th]].

[90] B. Basso, "An exact slope for AdS/CFT," [arXiv:1109.3154 [hep-th]].

[91] B. Basso, "Scaling dimensions at small spin in N=4 SYM theory," arXiv:1205.0054 [hep-th].

[92] N. Gromov, "On the Derivation of the Exact Slope Function," JHEP **1302** (2013) 055 [arXiv:1205.0018 [hep-th]].

[93] M. Beccaria and A. A. Tseytlin, "More about 'short' spinning quantum strings," JHEP **1207** (2012) 089 [arXiv:1205.3656 [hep-th]].

[94] M. Beccaria, S. Giombi, G. Macorini, R. Roiban and A. A. Tseytlin, "'Short' spinning strings and structure of quantum $AdS_5 \times S^5$ spectrum," Phys. Rev. D **86** (2012) 066006 [arXiv:1203.5710 [hep-th]].

[95] M. Beccaria, C. Ratti and A. A. Tseytlin, "Leading quantum correction to energy of 'short' spiky strings," J. Phys. A **45** (2012) 155401 [arXiv:1201.5033 [hep-th]].

[96] A. Tirziu and A. A. Tseytlin, "Quantum corrections to energy of short spinning string in AdS(5)," Phys. Rev. D **78** (2008) 066002 [arXiv:0806.4758 [hep-th]].

[97] M. Kruczenski and A. A. Tseytlin, "Wilson loops T-dual to Short Strings," Nucl. Phys. B **875** (2013) 213 [arXiv:1212.4886 [hep-th]].

[98] A. V. Kotikov and L. N. Lipatov, "DGLAP and BFKL evolution equations in the N=4 supersymmetric gauge theory," hep-ph/0112346.

[99] A. V. Kotikov, L. N. Lipatov and V. N. Velizhanin, "Anomalous dimensions of Wilson operators in N=4 SYM theory," Phys. Lett. B **557** (2003) 114 [hep-ph/0301021].

[100] A. V. Kotikov, L. N. Lipatov, A. I. Onishchenko and V. N. Velizhanin, "Three loop universal anomalous dimension of the Wilson operators in N=4 SUSY Yang-Mills model," Phys. Lett. B **595** (2004) 521 [Erratum-ibid. B **632** (2006) 754] [hep-th/0404092].

[101] S. Moch, J. A. M. Vermaseren and A. Vogt, "The Three loop splitting functions in QCD: The Nonsinglet case," Nucl. Phys. B **688** (2004) 101 [hep-ph/0403192].

[102] M. Staudacher, "The Factorized S-matrix of CFT/AdS," JHEP **0505** (2005) 054 [hep-th/0412188].

[103] A. V. Kotikov, L. N. Lipatov, A. Rej, M. Staudacher and V. N. Velizhanin, "Dressing and wrapping," J. Stat. Mech. **0710** (2007) P10003 [arXiv:0704.3586 [hep-th]].

[104] Z. Bajnok, R. A. Janik and T. Lukowski, "Four loop twist two, BFKL, wrapping and strings," Nucl. Phys. B **816** (2009) 376 [arXiv:0811.4448 [hep-th]].

[105] T. Lukowski, A. Rej and V. N. Velizhanin, "Five-Loop Anomalous Dimension of Twist-Two Operators," Nucl. Phys. B **831** (2010) 105 [arXiv:0912.1624 [hep-th]].

[106] V. N. Velizhanin, "Twist-2 at five loops: Wrapping corrections without wrapping computations,"

[107] D. Maitre, "HPL, a mathematica implementation of the harmonic polylogarithms," Comput. Phys. Commun. **174** (2006) 222 [hep-ph/0507152]. • D. Maitre, "Extension of HPL to complex arguments," Comput. Phys. Commun. **183** (2012) 846 [hep-ph/0703052 [HEP-PH]].

[108] S. Leurent, D. Volin, Mathematica packages for working with zeta functions and FiNLIE-based weak coupling expansion. (http://people.kth.se/ dmytrov/konishi8.zip)

[109] S. Leurent and D. Volin, "Multiple zeta functions and double wrapping in planar $N = 4$ SYM," Nucl. Phys. B **875** (2013) 757 [arXiv:1302.1135 [hep-th]].

[110] J. Ablinger. A Computer Algebra Toolbox for Harmonic Sums Related to Particle Physics. Johannes Kepler University. Diploma Thesis. February 2009. arXiv:1011.1176 [math-ph]. • J. Ablinger. Computer Algebra Algorithms for Special Functions in Particle Physics. Johannes Kepler University. PhD Thesis. April 2012. • J. Ablinger, J. Blümlein and C. Schneider. Analytic and Algorithmic Aspects of Generalized Harmonic Sums and Polylogarithms. arXiv:1212.xxxx [math-ph]. • J. Ablinger, J. Blümlein and C. Schneider, "Harmonic Sums and Polylogarithms Generated by Cyclotomic Polynomials," J. Math. Phys. **52** (2011) 102301 [arXiv:1105.6063 [math-ph]]. • J. Blümlein. Structural Relations of Harmonic Sums and Mellin Transforms up to Weight w = 5. Comput. Phys. Commun. 180 (2009) 2218. [arXiv:0901.3106 [hep-ph]]. • E. Remiddi and J. A. M. Vermaseren. Harmonic polylogarithms. Int. J. Mod. Phys. A 15 (2000) 725. [hep-ph/9905237]. • J. A. M. Vermaseren. Harmonic sums, Mellin transforms and integrals. Int. J. Mod. Phys. A 14 (1999) 2037. [hep-ph/9806280].

[111] M. Beccaria, "Anomalous dimensions at twist-3 in the sl(2) sector of N=4 SYM," JHEP **0706** (2007) 044 [arXiv:0704.3570 [hep-th]].

[112] M. Beccaria, V. Forini, T. Lukowski and S. Zieme, "Twist-three at five loops, Bethe Ansatz and wrapping," JHEP **0903** (2009) 129 [arXiv:0901.4864 [hep-th]].

[113] V. N. Velizhanin, "Six-Loop Anomalous Dimension of Twist-Three Operators in N=4 SYM," JHEP **1011** (2010) 129 [arXiv:1003.4717 [hep-th]].

[114] M. Beccaria and G. Macorini, "On the one-loop curvature function in the $\sim\!\!\prec(2)$ sector of N=4 SYM," JHEP **1406** (2014) 141 doi:10.1007/JHEP06(2014)141 [arXiv:1404.0893 [hep-th]].

[115] M. Beccaria and F. Catino, "Sum rules for higher twist sl(2) operators in N=4 SYM," JHEP **0806** (2008) 103 [arXiv:0804.3711 [hep-th]].

[116] A. V. Belitsky, G. P. Korchemsky and R. S. Pasechnik, "Fine structure of anomalous dimensions in N=4 super Yang-Mills theory," Nucl. Phys. B **809** (2009) 244 [arXiv:0806.3657 [hep-ph]].

[117] N. Beisert, B. Eden and M. Staudacher, "Transcendentality and Crossing," J. Stat. Mech. **0701** (2007) P01021 [hep-th/0610251].

[118] N. Dorey, D. M. Hofman and J. M. Maldacena, "On the Singularities of the Magnon S-matrix," Phys. Rev. D **76** (2007) 025011 [hep-th/0703104 [HEP-TH]].

[119] N. Beisert, R. Hernandez and E. Lopez, "A Crossing-symmetric phase for AdS(5) x S**5 strings," JHEP **0611** (2006) 070 [hep-th/0609044].

[120] http://www.cecm.sfu.ca/projects/EZFace/index.html

[121] N. Gromov and S. Valatka, "Deeper Look into Short Strings," JHEP **1203** (2012) 058 [arXiv:1109.6305 [hep-th]].

[122] T. Regge, "Introduction to complex orbital momenta," *Nuovo Cim.* **14** (1959) 951.

[123] V. Gribov, "The theory of complex angular momenta: Gribov lectures on theoretical physics,".

[124] L. N. Lipatov, "Reggeization of the Vector Meson and the Vacuum Singularity in Nonabelian Gauge Theories," Sov. J. Nucl. Phys. **23** (1976) 338 [Yad. Fiz. **23** (1976) 642].

[125] E. A. Kuraev, L. N. Lipatov and V. S. Fadin, "The Pomeranchuk Singularity in Nonabelian Gauge Theories," Sov. Phys. JETP **45** (1977) 199 [Zh. Eksp. Teor. Fiz. **72** (1977) 377].

[126] I. I. Balitsky and L. N. Lipatov, "The Pomeranchuk Singularity in Quantum Chromodynamics," Sov. J. Nucl. Phys. **28** (1978) 822 [Yad. Fiz. **28** (1978) 1597].

[127] R. C. Brower, J. Polchinski, M. J. Strassler and C. -ITan, "The Pomeron and gauge/string duality," JHEP **0712**, 005 (2007) [hep-th/0603115].

[128] A. V. Kotikov and L. N. Lipatov, "DGLAP and BFKL equations in the N=4 supersymmetric gauge theory," Nucl. Phys. B **661**, 19 (2003) [Erratum-ibid. B **685**, 405 (2004)] [hep-ph/0208220].

[129] M. S. Costa, V. Goncalves and J. Penedones, "Conformal Regge theory," JHEP **1212**, 091 (2012) [arXiv:1209.4355 [hep-th]].

[130] A. V. Kotikov and L. N. Lipatov, "Pomeron in the N=4 supersymmetric gauge model at strong couplings," Nucl. Phys. B **874**, 889 (2013) [arXiv:1301.0882 [hep-th]].

[131] R. C. Brower, M. Costa, M. Djuric, T. Raben and C. -ITan, "Conformal Pomeron and Odderon in Strong Coupling," arXiv:1312.1419 [hep-ph].

[132] J. Balog and A. Hegedus, "Hybrid-NLIE for the AdS/CFT spectral problem," JHEP **1208** (2012) 022 [arXiv:1202.3244 [hep-th]].

[133] N. Gromov and G. Sizov, to appear

[134] R. A. Janik, "Twist-two operators and the BFKL regime - nonstandard solutions of the Baxter equation," JHEP **1311** (2013) 153 [arXiv:1309.2844 [hep-th]].

[135] N. Gromov, V. Kazakov, unpublished (2013)

[136] T. Jaroszewicz, "Gluonic Regge Singularities and Anomalous Dimensions in QCD," Phys. Lett. B **116** (1982) 291.

[137] L. N. Lipatov, "The Bare Pomeron in Quantum Chromodynamics," Sov. Phys. JETP **63** (1986) 904 [Zh. Eksp. Teor. Fiz. **90** (1986) 1536].

[138] V. S. Fadin and L. N. Lipatov, "BFKL pomeron in the next-to-leading approximation," Phys. Lett. B **429** (1998) 127 [hep-ph/9802290].

[139] M. Ciafaloni and G. Camici, "Energy scale(s) and next-to-leading BFKL equation," Phys. Lett. B **430** (1998) 349 [hep-ph/9803389].

[140] A. V. Kotikov and L. N. Lipatov, "NLO corrections to the BFKL equation in QCD and in supersymmetric gauge theories," Nucl. Phys. B **582** (2000) 19 [hep-ph/0004008].

[141] A. V. Kotikov and V. N. Velizhanin, "Analytic continuation of the Mellin moments of deep inelastic structure functions," hep-ph/0501274.

[142] D. I. Kazakov and A. V. Kotikov, "Total $\alpha^- s$ Correction to Deep Inelastic Scattering Cross-section Ratio, R = σ^-l / σ^-t in QCD. Gauge Invariance and Comparison With Experiment," Nucl. Phys. B **345** (1990) 299. doi:10.1016/0550-3213(90)90619-O

[143] C. Lopez and F. J. Yndurain, "Behavior at $x = 0, 1$, Sum Rules and Parametrizations for Structure Functions Beyond the Leading Order," Nucl. Phys. B **183** (1981) 157. doi:10.1016/0550-3213(81)90551-4

[144] J. Blumlein, "Structural Relations of Harmonic Sums and Mellin Transforms up to Weight w = 5," Comput. Phys. Commun. **180** (2009) 2218 [arXiv:0901.3106 [hep-ph]].

[145] A. M. Polyakov, "Gauge Fields as Rings of Glue," Nucl. Phys. B **164**, 171 (1980).

[146] N. Drukker and V. Forini, "Generalized quark-antiquark potential at weak and strong coupling," JHEP **1106** (2011) 131 [arXiv:1105.5144 [hep-th]].

[147] D. Correa, J. Henn, J. Maldacena and A. Sever, "An exact formula for the radiation of a moving quark in N=4 super Yang Mills," JHEP **1206** (2012) 048 [arXiv:1202.4455 [hep-th]].

[148] B. Fiol, B. Garolera and A. Lewkowycz, "Exact results for static and radiative fields of a quark in N=4 super Yang-Mills," JHEP **1205** (2012) 093 [arXiv:1202.5292 [hep-th]].

[149] B. Fiol, B. Garolera and G. Torrents, "Exact momentum fluctuations of an accelerated quark in N=4 super Yang-Mills," arXiv:1302.6991 [hep-th].

[150] N. Drukker, D. J. Gross and H. Ooguri, "Wilson loops and minimal surfaces," Phys. Rev. D **60**, 125006 (1999) [hep-th/9904191].

[151] K. Zarembo, "Supersymmetric Wilson loops," Nucl. Phys. B **643**, 157 (2002) [hep-th/0205160].

[152] N. Drukker and S. Kawamoto, "Small deformations of supersymmetric Wilson loops and open spin-chains," JHEP **0607** (2006) 024 doi:10.1088/1126-6708/2006/07/024 [hep-th/0604124].

[153] V. Pestun, "Localization of gauge theory on a four-sphere and supersymmetric Wilson loops," Commun. Math. Phys. **313** (2012) 71 doi:10.1007/s00220-012-1485-0 [arXiv:0712.2824 [hep-th]].

[154] V. Pestun, "Localization of the four-dimensional N=4 SYM to a two-sphere and 1/8 BPS Wilson loops," JHEP **1212** (2012) 067 doi:10.1007/JHEP12(2012)067 [arXiv:0906.0638 [hep-th]].

[155] J. K. Erickson, G. W. Semenoff and K. Zarembo, "Wilson loops in N=4 supersymmetric Yang-Mills theory," Nucl. Phys. B **582** (2000) 155 [hep-th/0003055].

[156] N. Drukker and D. J. Gross, "An Exact prediction of N=4 SUSYM theory for string theory," J. Math. Phys. **42** (2001) 2896 doi:10.1063/1.1372177 [hep-th/0010274].

[157] N. Drukker, "1/4 BPS circular loops, unstable world-sheet instantons and the matrix model," JHEP **0609** (2006) 004 doi:10.1088/1126-6708/2006/09/004 [hep-th/0605151].

[158] N. Drukker, S. Giombi, R. Ricci and D. Trancanelli, "On the D3-brane description of some 1/4 BPS Wilson loops," JHEP **0704** (2007) 008 doi:10.1088/1126-6708/2007/04/008 [hep-th/0612168].

[159] N. Drukker, S. Giombi, R. Ricci and D. Trancanelli, "More supersymmetric Wilson loops," Phys. Rev. D **76** (2007) 107703 doi:10.1103/PhysRevD.76.107703 [arXiv:0704.2237 [hep-th]].

[160] N. Drukker, S. Giombi, R. Ricci and D. Trancanelli, "Wilson loops: From four-dimensional SYM to two-dimensional YM," Phys. Rev. D **77** (2008) 047901 doi:10.1103/PhysRevD.77.047901 [arXiv:0707.2699 [hep-th]].

[161] A. Bassetto, L. Griguolo, F. Pucci and D. Seminara, "Supersymmetric Wilson loops at two loops," JHEP **0806** (2008) 083 doi:10.1088/1126-6708/2008/06/083 [arXiv:0804.3973 [hep-th]].

[162] S. Giombi, V. Pestun and R. Ricci, "Notes on supersymmetric Wilson loops on a two-sphere," JHEP **1007** (2010) 088 doi:10.1007/JHEP07(2010)088 [arXiv:0905.0665 [hep-th]].

[163] S. Giombi and V. Pestun, "Correlators of local operators and 1/8 BPS Wilson loops on S**2 from 2d YM and matrix models," JHEP **1010** (2010) 033 doi:10.1007/JHEP10(2010)033 [arXiv:0906.1572 [hep-th]].

[164] N. Gromov and A. Sever, "Analytic Solution of Bremsstrahlung TBA," JHEP **1211** (2012) 075 [arXiv:1207.5489 [hep-th]].

[165] N. Gromov, V. Kazakov, S. Leurent and Z. Tsuboi, "Wronskian Solution for AdS/CFT Y-system," JHEP **1101** (2011) 155 [arXiv:1010.2720 [hep-th]].

[166] D. Correa, J. Henn, J. Maldacena and A. Sever, "The cusp anomalous dimension at three loops and beyond," JHEP **1205**, 098 (2012) [arXiv:1203.1019 [hep-th]].

[167] M. Beccaria and G. Macorini, "On a discrete symmetry of the Bremsstrahlung function in N=4 SYM," JHEP **1307** (2013) 104 doi:10.1007/JHEP07(2013)104 [arXiv:1305.4839 [hep-th]].

[168] G. Sizov and S. Valatka, "Algebraic Curve for a Cusped Wilson Line," JHEP **1405** (2014) 149 doi:10.1007/JHEP05(2014)149 [arXiv:1306.2527 [hep-th]].

[169] Y. Makeenko, P. Olesen and G. W. Semenoff, "Cusped SYM Wilson loop at two loops and beyond," Nucl. Phys. B **748** (2006) 170 [hep-th/0602100].

[170] Z. Bajnok, J. Balog, D. H. Correa, A. Hegedus, F. I. Schaposnik Massolo and G. Zsolt Toth, "Reformulating the TBA equations for the quark anti-quark potential and their two loop expansion," JHEP **1403** (2014) 056 [arXiv:1312.4258 [hep-th]].

[171] J. M. Henn and T. Huber, "The four-loop cusp anomalous dimension from iterated Wilson line integrals," arXiv:1304.6418 [hep-th].

[172] S. Caron-Huot and J. M. Henn, "Solvable Relativistic Hydrogenlike System in Supersymmetric Yang-Mills Theory," Phys. Rev. Lett. **113** (2014) 16, 161601 [arXiv:1408.0296 [hep-th]].

[173] J. K. Erickson, G. W. Semenoff, R. J. Szabo and K. Zarembo, "Static potential in N=4 supersymmetric Yang-Mills theory," Phys. Rev. D **61**, 105006 (2000) doi:10.1103/PhysRevD.61.105006 [hep-th/9911088].

[174] A. Pineda, "The Static potential in N = 4 supersymmetric Yang-Mills at weak coupling," Phys. Rev. D **77** (2008) 021701 [arXiv:0709.2876 [hep-th]].

[175] D. Bykov and K. Zarembo, "Ladders for Wilson Loops Beyond Leading Order," JHEP **1209** (2012) 057 doi:10.1007/JHEP09(2012)057 [arXiv:1206.7117 [hep-th]].

[176] J. M. Henn and T. Huber, "Systematics of the cusp anomalous dimension," JHEP **1211** (2012) 058 doi:10.1007/JHEP11(2012)058 [arXiv:1207.2161 [hep-th]].

[177] M. Stahlhofen, "NLL resummation for the static potential in N=4 SYM theory," JHEP **1211** (2012) 155 doi:10.1007/JHEP11(2012)155 [arXiv:1209.2122 [hep-th]].

[178] M. Prausa and M. Steinhauser, "Two-loop static potential in $\mathcal{N} = 4$ supersymmetric Yang-Mills theory," Phys. Rev. D **88** (2013) 2, 025029 [arXiv:1306.5566 [hep-th]].

[179] J. M. Maldacena, "Wilson loops in large N field theories," Phys. Rev. Lett. **80** (1998) 4859 doi:10.1103/PhysRevLett.80.4859 [hep-th/9803002].

[180] S. J. Rey and J. T. Yee, "Macroscopic strings as heavy quarks in large N gauge theory and anti-de Sitter supergravity," Eur. Phys. J. C **22** (2001) 379 doi:10.1007/s100520100799 [hep-th/9803001].

[181] V. Forini, "Quark-antiquark potential in AdS at one loop," JHEP **1011** (2010) 079 [arXiv:1009.3939 [hep-th]].

[182] S. x. Chu, D. Hou and H. c. Ren, "The Subleading Term of the Strong Coupling Expansion of the Heavy-Quark Potential in a N=4 Super Yang-Mills Vacuum," JHEP **0908** (2009) 004 doi:10.1088/1126-6708/2009/08/004 [arXiv:0905.1874 [hep-ph]].

[183] O. Gurdogan and V. Kazakov, "New integrable non-gauge 4D CFTs from strongly deformed planar N=4 SYM," arXiv:1512.06704 [hep-th].

[184] Z. Bajnok and R. I. Nepomechie, "Wrapping corrections for non-diagonal boundaries in AdS/CFT," arXiv:1512.01296 [hep-th].

[185] A. Grozin, J. M. Henn, G. P. Korchemsky and P. Marquard, "The three-loop cusp anomalous dimension in QCD and its supersymmetric extensions," arXiv:1510.07803 [hep-ph].

[186] G. Arutyunov, M. de Leeuw and S. J. van Tongeren, "Twisting the Mirror TBA," JHEP **1102** (2011) 025 [arXiv:1009.4118 [hep-th]].

[187] C. Ahn, Z. Bajnok, D. Bombardelli and R. I. Nepomechie, "TBA, NLO Luscher correction, and double wrapping in twisted AdS/CFT," JHEP **1112** (2011) 059 doi:10.1007/JHEP12(2011)059 [arXiv:1108.4914 [hep-th]].

[188] M. de Leeuw and S. J. van Tongeren, "The spectral problem for strings on twisted AdS5 x S5," Nucl. Phys. B **860** (2012) 339 doi:10.1016/j.nuclphysb.2012.03.004 [arXiv:1201.1451 [hep-th]].

[189] P. Dorey, C. Dunning and R. Tateo, "The ODE/IM Correspondence," J. Phys. A **40** (2007) R205 doi:10.1088/1751-8113/40/32/R01 [hep-th/0703066].

[190] J. Escobedo, N. Gromov, A. Sever and P. Vieira, "Tailoring Three-Point Functions and Integrability," JHEP **1109** (2011) 028 doi:10.1007/JHEP09(2011)028 [arXiv:1012.2475 [hep-th]].

[191] N. Gromov and P. Vieira, "Quantum Integrability for Three-Point Functions of Maximally Supersymmetric Yang-Mills Theory," Phys. Rev. Lett. **111** (2013) 21, 211601 doi:10.1103/PhysRevLett.111.211601 [arXiv:1202.4103 [hep-th]].

[192] P. Vieira and T. Wang, "Tailoring Non-Compact Spin Chains," JHEP **1410** (2014) 35 doi:10.1007/JHEP10(2014)035 [arXiv:1311.6404 [hep-th]].

[193] J. Caetano and T. Fleury, "Three-point functions and $\mathfrak{su}(1|1)$ spin chains," JHEP **1409** (2014) 173 doi:10.1007/JHEP09(2014)173 [arXiv:1404.4128 [hep-th]].

[194] E. K. Sklyanin, "Quantum inverse scattering method. Selected topics," In: Quantum Group and Quantum Integrable Systems: Nankai Lectures on Mathematical Physics : Nankai Institute of Mathematics, China 2-18 April 1991 (World Scientific 1992), pp 63-97 [hep-th/9211111].

[195] A. Brandhuber, P. Heslop, G. Travaglini and D. Young, "Yangian Symmetry of Scattering Amplitudes and the Dilatation Operator in $N = 4$ Supersymmetric Yang-Mills Theory," Phys. Rev. Lett. **115** (2015) no.14, 141602 doi:10.1103/PhysRevLett.115.141602

[196] A. Brandhuber, B. Penante, G. Travaglini and D. Young, "Integrability and unitarity," JHEP **1505** (2015) 005 doi:10.1007/JHEP05(2015)005

[197] A. Brandhuber, B. Penante, G. Travaglini and D. Young, "Integrability and MHV diagrams in N=4 supersymmetric Yang-Mills theory," Phys. Rev. Lett. **114** (2015) 071602 doi:10.1103/PhysRevLett.114.071602 [arXiv:1412.1019 [hep-th]].

[198] N. A. Nekrasov and S. L. Shatashvili, "Quantization of Integrable Systems and Four Dimensional Gauge Theories," arXiv:0908.4052 [hep-th].

[199] A. Mironov, A. Morozov, Y. Zenkevich and A. Zotov, "Spectral Duality in Integrable Systems from AGT Conjecture," JETP Lett. **97** (2013) 45 [Pisma Zh. Eksp. Teor. Fiz. **97** (2013) 49] doi:10.1134/S0021364013010062 [arXiv:1204.0913 [hep-th]].

[200] A. Mironov, A. Morozov, B. Runov, Y. Zenkevich and A. Zotov, "Spectral Duality Between Heisenberg Chain and Gaudin Model," Lett. Math. Phys. **103** (2013) no.3, 299 doi:10.1007/s11005-012-0595-0 [arXiv:1206.6349 [hep-th]].

[201] Z. Tsuboi, A. Zabrodin and A. Zotov, "Supersymmetric quantum spin chains and classical integrable systems," JHEP **1505** (2015) 086 doi:10.1007/JHEP05(2015)086 [arXiv:1412.2586 [math-ph]].

[202] A. Alexandrov, V. Kazakov, S. Leurent, Z. Tsuboi and A. Zabrodin, "Classical tau-function for quantum spin chains," JHEP **1309** (2013) 064 doi:10.1007/JHEP09(2013)064 [arXiv:1112.3310 [math-ph]].

[203] G. Arutyunov, M. de Leeuw and S. J. van Tongeren, "The Quantum Deformed Mirror TBA II," [JHEP **1302** (2013) 012] [arXiv:1210.8185 [hep-th]].

[204] G. Arutyunov, M. de Leeuw and S. J. van Tongeren, "The Quantum Deformed Mirror TBA I," JHEP **1210** (2012) 090 [arXiv:1208.3478 [hep-th]].

[205] T. Lloyd, O. Ohlsson Sax, A. Sfondrini and B. Stefaski, Jr., "The complete worldsheet S matrix of superstrings on AdS3 x S3 x T4 with mixed three-form flux," Nucl. Phys. B **891** (2015) 570 doi:10.1016/j.nuclphysb.2014.12.019 [arXiv:1410.0866 [hep-th]].

[206] R. Borsato, O. Ohlsson Sax, A. Sfondrini and B. Stefaski, "The $\mathrm{AdS}_3 \times \mathrm{S}^3 \times \mathrm{S}^3 \times \mathrm{S}^1$ worldsheet S matrix," J. Phys. A **48** (2015) no.41, 415401 doi:10.1088/1751-8113/48/41/415401 [arXiv:1506.00218 [hep-th]].

[207] R. Borsato, O. Ohlsson Sax, A. Sfondrini, B. Stefaski and A. Torrielli, "The all-loop integrable spin-chain for strings on $\mathrm{AdS}_3 \times S^3 \times T^4$: the massive sector," JHEP **1308** (2013) 043 doi:10.1007/JHEP08(2013)043 [arXiv:1303.5995 [hep-th]].

[208] B. Hoare, A. Pittelli and A. Torrielli, "Integrable S-matrices, massive and massless modes and the AdS_2 * S2 superstring," JHEP **1411** (2014) 051 doi:10.1007/JHEP11(2014)051 [arXiv:1407.0303 [hep-th]].

[209] A. Prinsloo, V. Regelskis and A. Torrielli, "Integrable open spin-chains in AdS3/CFT2 correspondences," Phys. Rev. D **92** (2015) no.10, 106006 doi:10.1103/PhysRevD.92.106006 [arXiv:1505.06767 [hep-th]].

[210] C. Duhr, "Mathematical aspects of scattering amplitudes," arXiv:1411.7538 [hep-ph].